UNIVERSITY OF LONDON THESIS

Degree PHD Year 2008 Name of Author VASUDEVAN, SOJAN.

Utility of the Pareto-Front Approach in Elucidating Ship Requirements during Concept Design

by

Sojan Vasudevan

A thesis submitted for the degree of

Doctor of Philosophy

Department of Mechanical Engineering

UCL

2008

ProQuest LLC
789 East Eisenhower Parkway
P.O. Box 1346
Ann Arbor, MI 48106-1346

Declaration

I, Sojan Vasudevan, confirm that the work presented in this thesis is my own.

Where information has been derived from other sources, I confirm that this has been indicated in the thesis.

Signed:

Date: 04.04.'08

Abstract

Concept design is the initial stage of the ship design process during which design alternatives are developed to study their cost and performance trade-offs. Traditional design approaches are capable of exploring only a small region of the design space around a chosen parent. Alternative approaches have not received widespread acceptance because of their "black-box" nature, whereby they try to provide prescriptive solutions rather than assist the designer in comparing available design alternatives. This thesis proposes a new design approach that avoids these drawbacks.

Central to the proposed design approach is a multi-objective optimisation tool using genetic algorithms, capable of generating the 'Pareto-front' consisting of designs optimised to a set of objectives. The novelty in the proposed design approach lies in the analysis of the Pareto-front, which helps to provide design insights about the whole Pareto-front and about the individual designs.

This thesis describes and illustrates the proposed design approach with example ship designs. To demonstrate the approach, it is used to re-design three naval combatants that were originally designed using a traditional design approach. These applications illustrate how the analysis of the Pareto-front can potentially assist in the concept design process. For example, it may reveal interesting regions of the performance space, such as discontinuities. Multiple Pareto-fronts with varying constraints or design inputs may identify designs not traditionally examined. Such results may help the designer to have a more informed dialogue with the customer about the design requirements and the potential solutions. It is hoped that the transparent and interactive nature of the proposed design approach will make it useful to practising designers and thus improve the applicability of multi-objective optimisation during preliminary ship design. This may improve the quality of the ships designed, albeit within the limited objectives considered for optimisation, and reduce the total time taken for concept design.

Dedication

To my family, and to Krishnakumari teacher.

Table of Contents

APPENDICES

List of Figures

List of Tables

Acknowledgements

I would not be able to complete my research without the help of several people.

I owe particular thanks to my supervisors Professor Simon Rusling and Professor David Andrews. Professor Rusling was available whenever I needed him and I thank him for his advice, ideas and guidance, besides the patience to bear with my questions. This thesis would not have been possible without his enthusiasm and inspiration. Professor Andrews has provided advice and guidance to my research, first during the MPhil-PhD Transfer Interview and many times thereafter, especially in the final stages when my effort concentrated on how to convert the research work of three years into a document conforming to the requirements for a PhD thesis. I should also thank Mr. David Fellows for his comprehensive comments and advice during the MPhil-PhD Transfer Interview.

Many thanks to the rest of the staff in the Department of Mechanical Engineering, especially Colin, Tim, Tristan and David, for their advice and assistance throughout my stay at UCL, as well as for creating a friendly working environment.

I am grateful to the U.S. Office of Naval Research (ONR), and Dr. Kelly Cooper in particular, for funding this research through the Atlantic Center for Innovative Design and Control of Small Ships (ACCeSS) consortium. Thanks are also due to all the members of this consortium, especially Prof. Michael Bruno and Dr. Raju Datla at Stevens Institute of Technology (SIT) and Prof. Jennifer Waters at the United States Naval Academy (USNA), for their comments and suggestions at the start of my research. Special thanks to my ACCeSS colleagues and PhD candidates at SIT, Soma, Sreekanth and Michael, for the joint work initially carried out, resulting in a combined paper presented at the 2006 World Maritime Technology Conference.

Nomenclature

Δ	:	Displacement (t)
∇_{Gross}	:	Gross enclosed volume of a ship (m^3)
ρ	:	Overall density of the ship = Δ / ∇_{Gross}
2D	:	Two-dimensional
3D	:	Three-dimensional
AHP	:	Analytic Hierarchy Process
ANN	:	Artificial Neural Network
B	:	Breadth (m)
CAD	:	Computer Aided Design
C_B	:	Block coefficient (-)
CFD	:	Computational Fluid Dynamics
C_M	:	Midship area coefficient (-)
CODASID	:	Concordance and Discordance Analyses by Similarity to Ideal Designs
C_P	:	Prismatic coefficient (-)
D	:	Depth of the main hull (m)
dB	:	Change in breadth (m)
Design space	:	The set of all ship designs in terms of their physical characteristics (such as L, B, T, C_B and C_P)
dL	:	Change in length (m)

DOE	:	Design of Experiments
dofinf	:	Degree of infeasibility (-). A parameter used by the GA Tool as a measure of the feasibility of a design (see Appendix H.7)
dT	:	Change in draught (m)
EA	:	Evolutionary Algorithms
EP	:	Evolutionary Programs
ES	:	Evolution Strategies
Fn_∇	:	Froude-displacement number (-) $Fn_\nabla = \frac{V}{\sqrt{g\nabla^{1/3}}}$, where V is the ship speed in m/s and g is the acceleration due to gravity in m/s^2
GA	:	Genetic Algorithm
GA Tool	:	The GA-based design tool developed as part of this research, capable of generating the Pareto-front for a set of design requirements
GM	:	Transverse metacentric height
GP	:	Genetic Programming
ICCAS	:	International Conference on Computer Applications in Shipbuilding
IMDC	:	International Marine Design Conference
L	:	Length waterline (m)
Ⓜ	:	Circular $M = \frac{L}{\sqrt[3]{\nabla}}$ (-)
MAVT	:	Multi-Attribute Value Theory

MCDM	:	Multiple Criteria Decision Making
MOEA	:	Multi-Objective Evolutionary Algorithm
MOGA	:	Multi-Objective Genetic Algorithm
MOO	:	Multi-Objective Optimisation
NSGA	:	Nondominated Sorting Genetic Algorithm
NumGen	:	Number of generations (a parameter used by the GA Tool)
OMOE	:	Overall Measure of Effectiveness
OMOR	:	Overall Measure of Risk
Performance space	:	The set of all ship designs in terms of their performance characteristics (such as seakeeping, shaft power and cost)
PopSize	:	Population size (a parameter used by the GA Tool)
P_s	:	Shaft power (kW)
PSO	:	Particle Swarm Optimisation
pvf	:	Payload/volume fraction = V_{pay} / ∇_{Gross}
SA	:	Simulated Annealing
SDE	:	Ship Design Exercise (part of the MSc in Naval Architecture offered by the Department of Mechanical Engineering at UCL)
ss	:	Superstructure ratio (= volume of superstructure / volume of enclosed hull to the weatherdeck)
T	:	Draught (m)

TOPSIS	:	Technique for Order Preference by Similarity to Ideal Solution
TS	:	Tabu Search
UPC	:	Unit Procurement Cost
UTA	:	Utility Theory Additive
VEGA	:	Vector Evaluated Genetic Algorithm
V_{pay}	:	Payload volume (m^3)
W_{pay}	:	Payload weight (t)
WMTC	:	World Maritime Technology Conference

Preface

The work reported in this thesis was carried out by the candidate as part of a collaborative research programme undertaken by the Atlantic Center for Innovative Design and Control of Small Ships (ACCeSS).

ACCeSS is an international consortium of universities and industrial partners, funded by the United States Navy Office of Naval Research, under the auspices of the U.S. National Naval Responsibility on Naval Engineering Program (ONR contract number 527703-02). ACCeSS is aimed at promoting innovation in hull form design, ship performance analysis, and automation and control. It provides an environment for interaction among the participating organisations through joint research projects and student exchange programmes. There are three participating universities from the U.S.A.: Stevens Institute of Technology (SIT, Hoboken, New Jersey), United States Naval Academy (USNA, Annapolis, Maryland) and Webb Institute (Glen Cove, New York). UCL is the fourth participating university, and is the only non-U.S. university. The industrial partners are Lockheed Martin (Bethesda, Maryland), VT Shipbuilding (Portsmouth) and AMSEC LLC (formerly M. Rosenblatt & Son, New York).

The ACCeSS consortium has funded two PhD candidates at UCL. While the candidate worked on developing an innovative methodology for the concept design of ships, the second PhD candidate (Chee Kuang Tam) is working in the field of automation and control, trying to predict the optimum path of fast craft for navigation in littoral waters. The research at the U.S. universities, as part of the ACCeSS consortium, has focussed on hull form database development (mainly for planing hulls) and development of innovative tools based on artificial neural networks for hydrodynamic performance prediction. The industrial partners bring into the consortium the needs and perspectives of the industry. They provide expert advice and guidance to the university partners on the direction of the research.

The consortium met three times during the candidate's PhD duration – once in the USNA and twice in UCL. These meetings provided a forum where members could

present and discuss their work and obtain feedback from colleagues and experts in the consortium. The joint work carried out by the PhD candidates from UCL and SIT was presented at the 2006 World Maritime Technology Conference in London (see Appendix A).

1. Introduction

Concept design is the initial stage of the ship design process during which several design alternatives are considered to study their cost and performance trade-offs with the aim of elucidating design requirements [1,2]. This thesis identifies the drawbacks in the current approaches used for concept design of ships and proposes a new design approach that can potentially eliminate these drawbacks. The advantages of the proposed design approach are demonstrated through a series of examples, and its limitations are discussed.

1.1. Background – concept design of ships

The concept design process focuses on elucidating the design requirements by generating and evaluating alternative design solutions to reveal cost and performance trade-offs. Ideally, the concept design process should start with a clear statement of need by the customer. This would include payload and performance requirements as well as restrictions and constraints. However, especially for naval ships, many of these requirements cannot be specified meaningfully without some knowledge of the solution itself. This makes ship design a 'wicked problem' [3], implying that the main difficulty lies in formulating the design requirements, rather than finding design solutions that meet a specified set of requirements. Thus, the concept design stage of the ship design process becomes an iterative process, where a set of postulated requirements are used by the designer to generate design solutions, and the characteristics of these design solutions are used to elucidate and affirm the design requirements. This process of requirements elucidation takes place through the customer-designer dialogue to discuss and evaluate the cost and performance trade-offs among the design alternatives.

Concept design of ships is traditionally based on the basis ship method. Here the design process starts by identifying a basis (parent) ship, i.e., an existing design (or a class of similar designs) that closely matches the perceived performance requirements of the new design. The parent ship is then iteratively refined to obtain

a suitable compromise among the conflicting performance requirements. The designer's intuition and experience influence the choice of design parameters.

The parent ship method, with its dependence on past design data, is low risk and helps to ensure that the performance for the new design is well understood. However, there are two drawbacks to this method. Firstly, the characteristics of the new design are heavily dependent on the parent selected: the designer is able to explore only a small region of the design space around the parent ship, which prevents the discovery of suitable design alternatives that may lie further away in the design space. The second drawback is that only one ship is designed at a time, which makes it time-consuming for the designer to generate many design alternatives to demonstrate performance trade-offs. Modern design tools such as ASSET [4,5] and PASS [6,7] overcome this problem by automatically generating a number of designs by varying one or more design parameters. However, since they do not have the capability to direct the designs to the performance characteristics of interest, they tend to produce a large number of designs, many of them probably of little relevance to the designer.

Researchers have tried to improve upon the parent ship method by developing and adopting new design approaches. One of these approaches is the application of multi-objective optimisation, which tries to develop a number of optimal designs trading off desired performance characteristics such as cost, resistance and seakeeping capability. The set of optimal solutions is termed as the 'Pareto-front' [8]. Numerous applications of multi-objective optimisation in ship design are found in the recent literature [9-21]. These applications concentrate on generating the Pareto-front; the selection of suitable designs from the Pareto-front is either left to the discretion of the designer, or done using multiple criteria decision making (MCDM) techniques [22]. Such techniques tend to suggest prescriptive solutions; the designer gets little opportunity to examine the characteristics of the designs before choosing the most suitable ones. Due to this, multi-objective optimisation has been received with little enthusiasm by practising designers [1,23,Andrews's comments on 24].

1.2. Aim of the thesis

The aim of this thesis is to develop a new, transparent and interactive design approach based on multi-objective optimisation, identify its advantages and limitations, demonstrate it with specific examples, and compare the results with the traditional ship design methods. The term 'utility' in the title of the thesis denotes usefulness to designers rather than the technical meaning used in the context of Multiple Criteria Decision Making, as clarified in Section 2.6.7.

1.3. Scope of the thesis

The scope of this thesis is limited to the concept design phase of the ship design process and early stages of feasibility studies. The strengths of the proposed design approach lie in ab-initio concept design with freedom of choice for most design parameters, or in modifying a parent design where the scope for changes in major design parameters may be more limited. It may also be useful in the early stages of feasibility studies for minimising the changes required of major design parameters as a result of design modifications. However, the proposed design approach is not suitable for detailed design, where a particular design is developed to high levels of detail to enable production.

The proposed design approach is generic; it does not limit itself to any particular classes of ships (such as frigates or merchant ships) or types of ships (such as monohulls or catamarans). However, the examples used in the thesis to demonstrate the capabilities of the proposed design approach are monohull naval combatants (frigates and corvettes).

The proposed design approach is applicable equally to conventional ships as well as innovative designs, the proviso being that the performance analysis modules should be applicable for the type of ship being designed.

1.4. Design considerations

The concept design phase of the ship design process involves many interacting and interdisciplinary tasks, constraints and objectives. Not all of these are considered in the design applications demonstrated in this thesis. Some aspects have been simplified for demonstration of the utility of the proposed design approach without getting into too much of detail. These are described in the following subsections.

1.4.1. Design requirements

To start the ship design process, one needs to specify the payload requirements. For merchant ships, such as bulk carriers and tankers, the type and amount of cargo to be carried will be specified by the customer (either a fixed value, or a range of values within which to optimise the design). For passenger vessels and ferries, the payload would be the number of passengers, cars, trucks etc. For warships, however, the situation is more complex: the payload consists of the type of armament and the configuration of weapon systems selected, and many configurations may have to be evaluated before a final selection is made. However, for the demonstration of the proposed design approach, the payload requirements are simply defined in terms of the total payload weight and the total payload volume. No detailed payload distribution is considered, as might be required usually for warship design. Though this is a major simplification of the concept design stage, in practice it is considered adequate for the demonstration of the proposed design approach.

Apart from payload, the requirements include performance aspects such as top speed, cruising speed and range (endurance).

1.4.2. Design tasks

The major design tasks involved in the concept design stage include selection or determination of the following:

- The overall topology, i.e., the type of the ship such as monohull or trimaran;

- The overall size of the ship, in terms of displacement and gross enclosed volume;
- Main dimensions and coefficients of fineness;
- Resistance, speed and power estimate;
- The layout of the ship;
- The weight and space requirements of ship systems, as well as their centres of gravity;
- Trim and stability;
- Machinery selection – propulsion plant type, installed power, number of propulsors, auxiliary machinery, electricity generation etc;
- Manning.

Not all the tasks listed above are considered in the demonstration of the proposed design approach. The aspects that are not considered include:

- The layout of the ship;
- Centre of gravity estimates;
- Trim.

The layout of the ship is an important design aspect [25,26], which should be done taking into account the operational requirements, the customer's preferences, aesthetics etc. Such non-numerate design aspects are difficult to incorporate within the proposed design approach. Hence, the designer will have to produce and assess the layout for each design of interest while analysing the results.

The centre of gravity estimates and trim are not included in the demonstration of the proposed design approach in view of simplicity. It would not be difficult to

incorporate these within the proposed design approach if required; however, a preliminary layout will be essential to ensure that such estimates are sensible.

While demonstrating the proposed design approach, some design tasks have been dealt with in a simplistic manner compared to the design process in practice. The following are the simplified design tasks:

- Regression-based weight and volume estimates for ship systems [27,28]. Both the simpler equations for merchant ships and the more detailed formulations for frigate-like warships have been implemented;

- Resistance estimate based on the Holtrop method [29]. This was used initially in conjunction with the weight and volume estimates for merchant ships. It was later decided to continue using it for warship designs as well, instead of programming another more suitable method. It is believed that the qualitative comparison of design alternatives using this method will be sufficient to demonstrate the capabilities of the proposed design approach;

- Simple equations for the manning estimate and the endurance fuel estimate [28];

- Stability based on initial metacentric height. No detailed intact or damaged stability analyses have been incorporated;

- Simple weight and volume estimates [27,28] for machinery selection, as against a realistic machinery selection.

1.4.3. Design constraints

The design process involves a number of constraints such as the bounds for L/D, L/B and B/T (based on past experience) as well as constraints specific to the current design (such as low noise level and deep draught required by a hull-mounted sonar). A set of standard constraints (bounds for L/D, L/B, B/T etc) have been used for demonstration of the new approach. Additional constraints have been used

when appropriate, for example, while demonstrating the proposed design approach in comparison with a ship designed using a traditional design approach.

1.4.4. Design objectives

Design objectives are the characteristics used to evaluate the cost and performance of the design. They include minimisation or maximisation of various performance characteristics, or obtaining target values for them. Such aspects include build cost, operating cost, speed, seakeeping and manoeuvring. They could also include non-numerate aspects such as layout, aesthetics and risk.

The design objectives used for demonstration of the proposed design approach, and the means used to assess each objective, include:

- Shaft power: based on the Holtrop method [29];
- Total build cost: simple regression equations [27,28];
- Unit procurement cost: total build cost plus the cost of the combat system equipment for warships. This is used to compare the results of the proposed design approach with traditional design approaches. In this case, the cost of the combat system equipment is taken as a fixed value known from the existing ship design;
- Seakeeping: a simple measure of seakeeping, the Bales Rank [30,31] (see Appendix H.6.5), is used to estimate the seakeeping quality of ships. This has been used for its simplicity while demonstrating the proposed design approach.

Although the performance aspects have been limited to the above for the demonstration of the approach, it is possible to incorporate other suitable performance parameters as part of the design approach. However, this may be difficult for non-numerate design aspects such as aesthetics, layout and producibility.

1.5. Research methodology

The methodology followed for the present research can be divided into five stages.

The first stage of the research involved developing a multi-objective optimisation tool for concept design of ships. This design tool was developed in Matlab [32] using genetic algorithms (GA). With a set of design requirements, the GA-based design tool (hereafter referred to as the "GA Tool") develops a set of design solutions optimised to meet a set of user defined design criteria, known as the "Pareto-front". The GA Tool was tested and validated appropriately.

The second stage of the research involved developing suitable visualisation techniques to assist in the analysis of the Pareto-front. This was necessary because the performance space cannot be visualised by a simple two-dimensional plot when there are more than two objectives to consider. The design space, in any case, consists of a number of parameters, and the simple 2D-plots are of limited use. Hence, appropriate visualisation methods suitable for representing multi-dimensional data were developed.

The third stage of the research involved the analysis of the structure of the Pareto-front, both in the performance space and in the design space, in order to determine the types of design insights that can be derived. This involved examining the trends of design parameters and performance characteristics, exploring the design space and performance space around the designs of interest, and analysing the effects of varying design inputs and constraints on the characteristics of the Pareto-front.

The fourth stage of the research involved the formulation of the proposed design approach incorporating the capabilities of the GA Tool to generate Pareto-fronts and analyse them with the help of suitable visual representation.

The final stage of the research involved the demonstration of the capabilities of the proposed design approach using various design examples and by comparing the results with those obtained using traditional design approaches.

1.6. Structure of the thesis

The overall structure of the thesis is shown in Figure 1-1. The thesis is divided into ten chapters, followed by references and appendices, and Figure 1-1 shows the interconnection between chapters and appendices.

Chapter 1 discusses the general background to the thesis, the motivation for the research and the overall outline of the research approach.

Chapter 2 describes the different phases of the ship design process and reviews the current approaches for concept design of ships. The advantages and disadvantages of the current approaches are discussed. Multi-objective optimisation (MOO) is identified as a promising approach for further research.

Chapter 3 surveys the application of multi-objective optimisation in ship design. The difficulties involved in the use of multi-objective optimisation are identified. A novel idea to improve the use of multi-objective optimisation for concept design of ships is proposed.

Chapter 4 explains the proposed design approach and its implementation through a design tool developed as part of the research. The potential applications of the proposed design approach are identified.

Chapter 5 demonstrates the proposed design approach for a fictitious set of design requirements. Each step of the proposed design approach is described in detail. This is repeated for the types of applications identified in the previous chapter.

Chapter 6 demonstrates the advantages of the proposed design approach with three example designs – a large frigate, a small frigate and a corvette. The results from the proposed design approach are compared with the original designs that were designed using the traditional design approach, as followed by the MSc students at UCL during their Ship Design Exercise.

Chapter 7 reviews the proposed design approach based on the work described in the previous chapters. The advantages and limitations of the proposed design approach are discussed.

Chapter 8 identifies the work that needs to be done to convert the proposed design approach from an academic design research tool into a practical design approach used in the ship design industry.

The conclusions of the thesis are presented in Chapter 9.

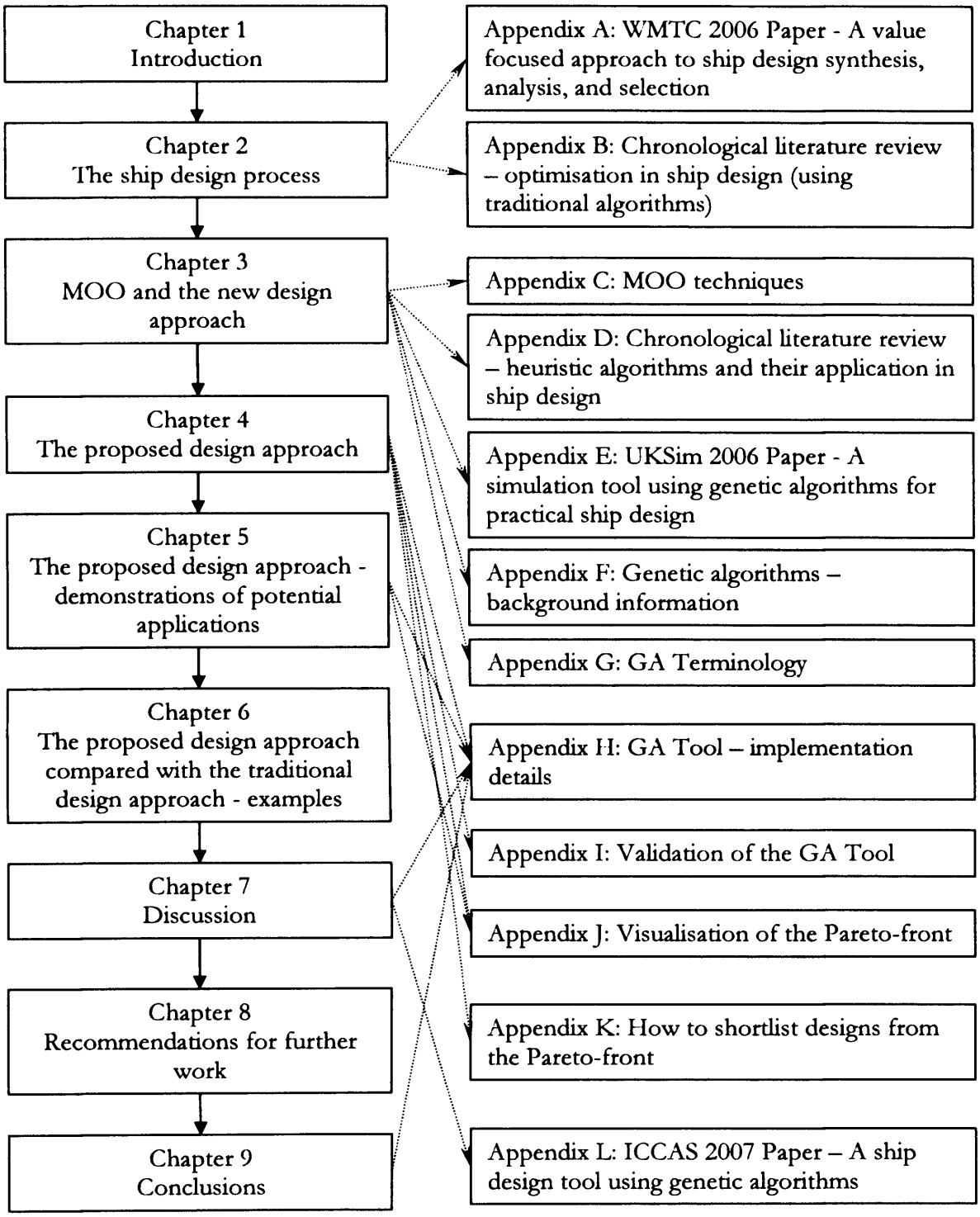

Figure 1-1: Overall structure of the thesis

2. The ship design process

This chapter provides an overview of the ship design process. Various approaches to ship design are examined and the most suitable among these approaches is selected for further study.

A diagram relating the sections within this chapter and relevant appendices is given in Figure 2-1. The chapter starts by describing the different stages in the overall ship design process. The concept design stage is identified as the focus of this thesis. Then the nature of the ship design process is discussed, with special emphasis on the concept design stage. This is followed by a description of the 'basis ship method', which is the traditional approach to the concept design of ships, and its limitations are discussed. The advent of computers has helped to improve the traditional ship design approach and to create new approaches for ship design. The characteristics of these alternative design approaches are considered, and their advantages and limitations are discussed. These considerations lead to the present research that focuses on improving the concept design stage by eliminating some of the limitations of the current design approaches.

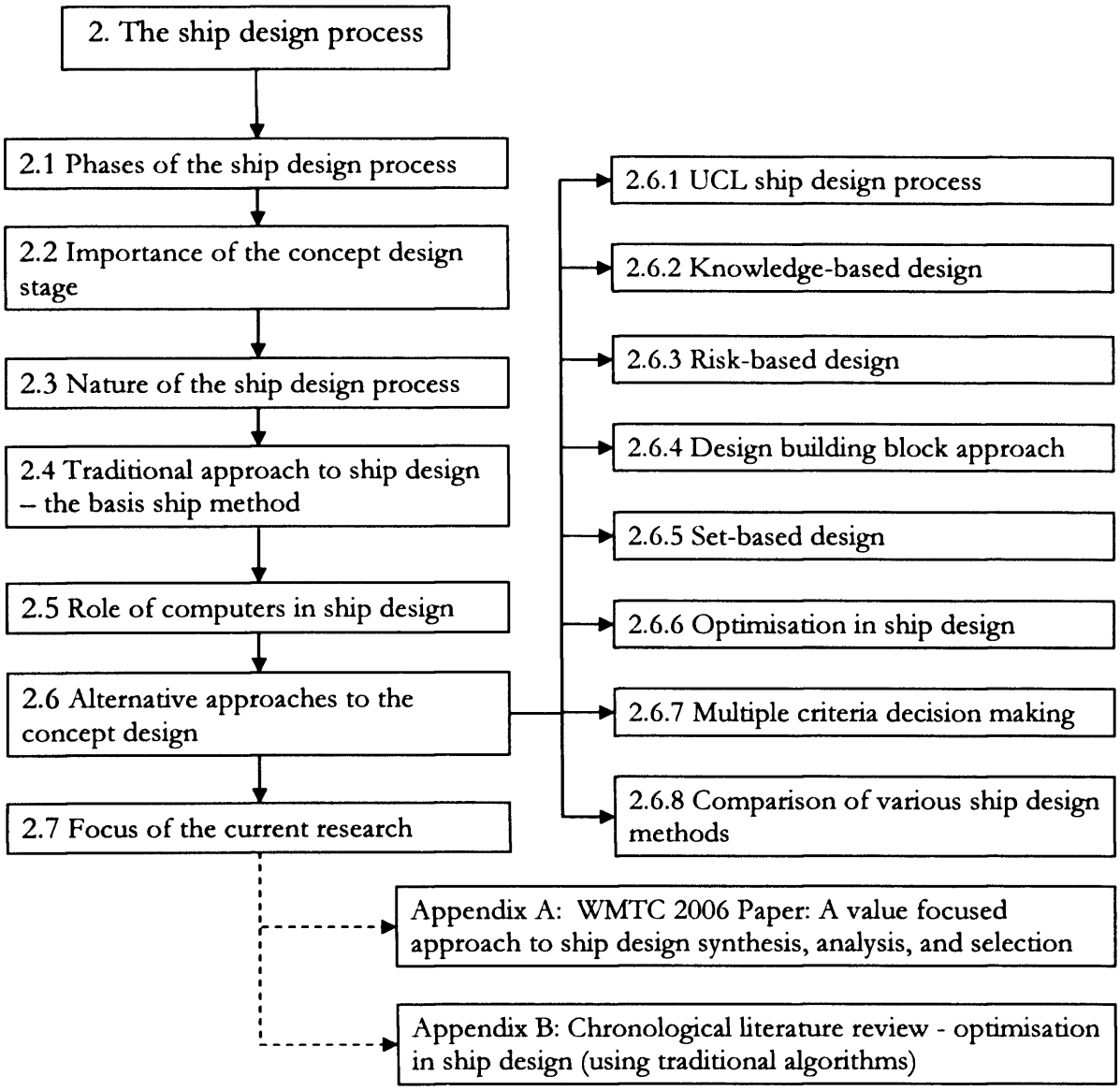

Figure 2-1: Outline of Chapter 2

2.1. Phases of the ship design process

Ship design may be defined as the activity involved in producing the drawings, specifications and other data needed to construct a ship [33]. The process involves integrating different disciplines of knowledge, taking appropriate decisions, making assumptions when required, and refining these decisions and assumptions when more information becomes available.

The design process can be divided into four stages [1,33-36]:

- concept design / requirement elucidation

- feasibility studies / preliminary design
- contract design
- detailed design

Concept design is the initial stage of the ship design process during which the designer develops several potential design solutions. The knowledge of the design solutions is used to guide in elucidating design requirements. The aim of this stage is to enable an informed dialogue with the customer about the ship requirements and choose the most suitable design solution (or a few promising designs – usually just one or two) for the next stage. During concept design, the emphasis is on comparing the relative merits of different design options; absolute accuracy for costing or performance analysis is less essential than good comparison indicators for trade-off studies.

The feasibility studies stage further develops the most promising design solutions chosen from the concept design stage. The designs are worked up to sufficient detail to assess their feasibility in terms of cost, performance, project time span and risk. One design solution is finalised to take forward to the next stage of the design process. Technical specifications for the chosen design are prepared describing its main characteristics.

The chosen design from the feasibility stage is further refined in the contract design stage to be the basis for shipbuilders to bid. The technical specifications are refined to be contractually binding and contract drawings are prepared.

The detailed design stage involves developing the Shipbuilder's Build Specification and working drawings for all components to enable building and in service maintenance of the ship.

In practice, there is no universal agreement on the number of design phases or their names. The term "concept design" often refers to the combination of concept design and feasibility studies mentioned above. Conversely, the term "feasibility study" is often used to mean concept design, whereas the term "preliminary design"

often refers to the first three stages mentioned above (mainly by the United States Navy). The intended meaning is often apparent from the context.

2.2. Importance of the concept design stage

Among the different phases of the ship design process, it is during the concept design stage that some of the most important decisions regarding the ship are made and where there is a high degree of flexibility to change the final cost of the built ship [1,37]. In contrast, the costs incurred and resources employed for concept design are only a small fraction of those required for the later design stages. This is illustrated in Figure 2-2 (from [1]).

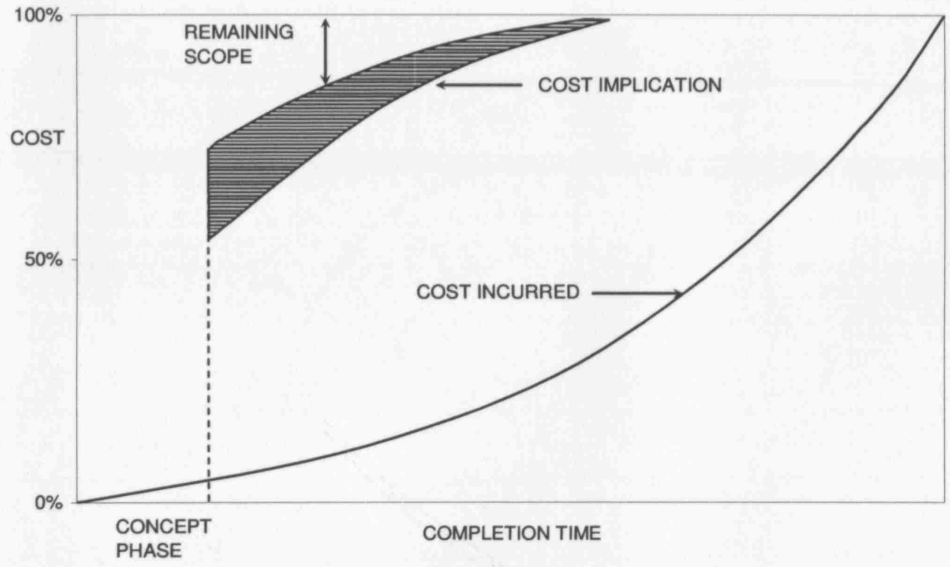

Figure 2-2: Importance of concept design [1]

Erikstad [23], from various sources, states that 60% to 80% of the total life cycle cost of a ship is determined during the early design stages. This is because all decisions taken in the later stages of the design process have to be made within the framework set during the early design stages, and hence they can have only limited influence on cost and overall performance of the ship. Looking at the design process from the point of view of design freedom, it is at the concept design stage that the designer has the highest degree of design freedom. This is because at the start of the design process, no decisions about the design have been made yet. Each

subsequent decision puts constraints on this freedom, until the design is completely defined [23].

The design freedom during the concept design stage of the ship design process, coupled with its influence on the final design outcome, indicates that if the concept design stage is improved, even at the expense of some additional resources, it could have major impact on improving the overall design in terms of bringing down the overall cost and improving the performance characteristics. Hence, this thesis focuses on the concept design stage of the ship design process.

2.3. Nature of the ship design process

Ship design, as well as the four design phases, is traditionally considered as sequential and iterative in nature. At any stage of the design process, the required information may be incomplete or unavailable. Despite this, decisions have to be made to make progress with the design, consequently forcing the designer to make various assumptions throughout the design process. The designer then has to revisit the earlier design stages when more knowledge is developed and more information becomes available. This sequential and iterative nature of the design process is traditionally represented as a design spiral, originally proposed by Harvey-Evans [38]. A sample design spiral from [33] is shown in Figure 2-3.

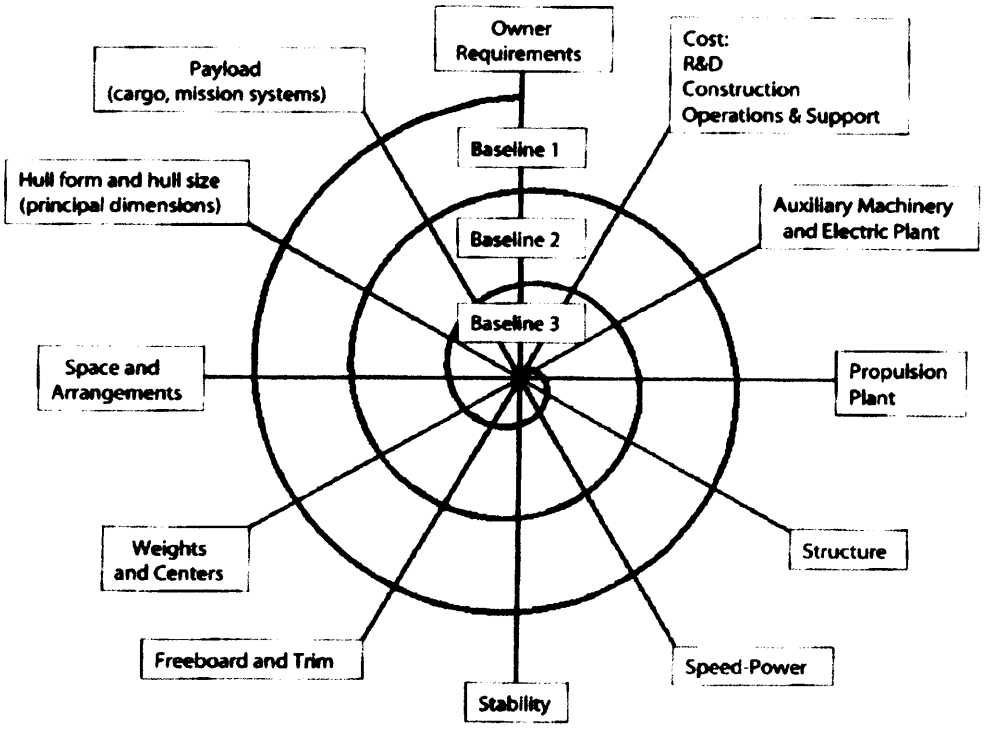

Figure 2-3: Traditional design spiral [33]

Andrews [39] added a third dimension to the design spiral. This 3D design spiral shows the effects of design constraints as fundamental to the progress of the design, apart from the technical issues. A cross section of the 3D spiral represents a snapshot of the design process at any instance. The 3D design spiral is shown in Figure 2-4.

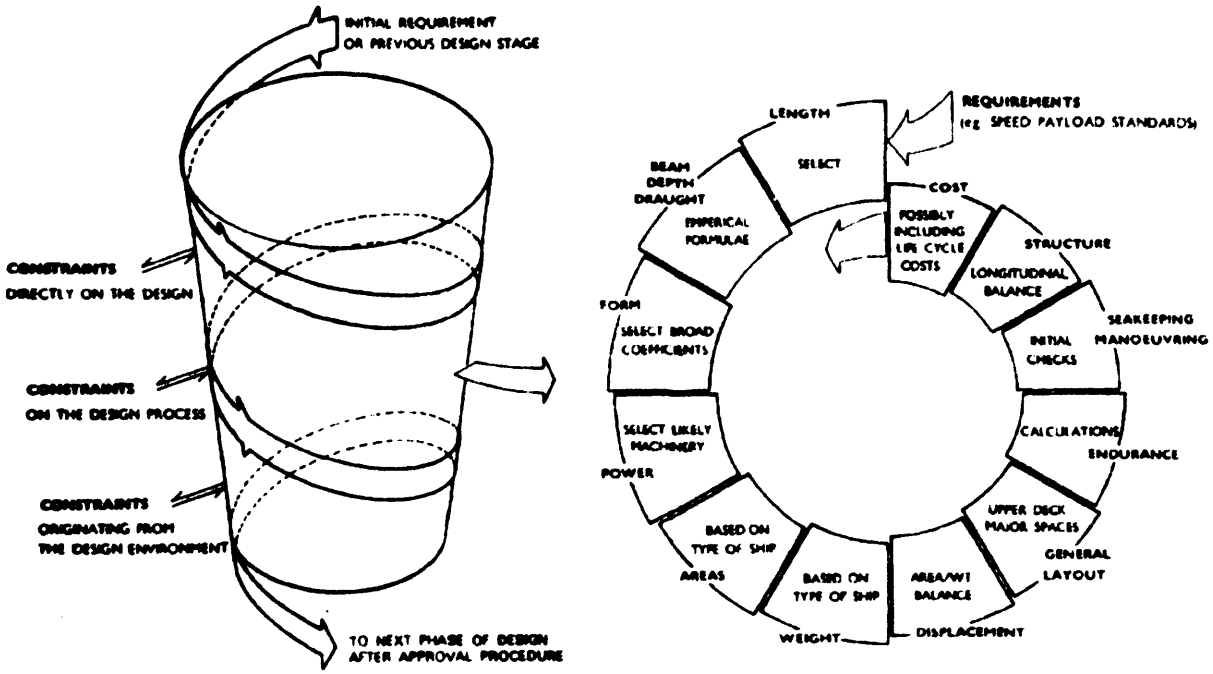

Figure 2-4: Andrews's 3D design spiral [39]

The complexity of the ship design process demands careful planning, organisation and management of the design process. Systems engineering (SE) is a notable approach in this context. It is a formal process for managing the design of complex systems to meet the required performance objectives within cost and schedule constraints. This is achieved by decomposing the total product into smaller sub-systems that are easily manageable. The objective is to optimise the overall system effectiveness, even though individual sub-systems may not all be optimal [33].

SE is sometimes claimed to be a general solution for producing any complex artefact; however, many practitioners have questioned its applicability to marine design [25]. In reality, SE is just a generalised model of the engineering process, which needs tailoring to be applicable to a particular product and project. Its original principles are heavily based on large software projects, for which the

hierarchical breakdown proved advantageous; it may not be applicable to the same extent in the case of ship design where interactions between various subsystems are more prominent [2,40,41]. Moreover, as van Griethuysen [40] points out, ships have always been designed and produced using a form of SE even though those particular words were rarely used. This is endorsed in [42], where the authors comment on a lecture on design at Norway's Institute of Technology as early as 1951. There the design task was attacked by decomposing it into a number of subtasks, which is the basic principle of SE.

One may conclude that careful application of SE would indeed benefit the ship designer (Gates's comments on [25]). It puts the focus on engineering as the creative heart of the management of projects. In this limited sense, SE can be of assistance to the designers - "a good servant but a poor master to the creative ship designer" [25].

2.4. Traditional approach to ship design – the basis ship method

The traditional design spiral, discussed in Section 2.3, suggests that the aim of the ship design process is to arrive at a single design solution. This approach to the design process may be classed as 'point-based design' [43]. Ship design using the basis or type ship method is an example of this approach.

The basis or type ship method is the traditional approach for ship design. From historic data, an existing successful design is selected as a 'basis ship' such that its performance characteristics are similar to the customer requirements as far as possible. Reliable design and performance data for the basis ship should be readily available. The data for the basis ship form the starting point in the design spiral. The design parameters are then suitably modified, guided by the designer's knowledge and intuition, in order to satisfy the customer requirements as far as possible.

An obvious drawback of the basis ship method is that if the customer requirements are significantly different from the ships for which data are available, a suitable basis ship cannot be chosen. Another disadvantage is that since this is a point-based design method there is no way for the designer to know how far from the

"optimum point" the final design lies: i.e., whether it is the best compromise considering all requirements and constraints. The third disadvantage is that this approach forces the designer to come up with a design similar to the basis ship: it explores the design space around the parent design; better design alternatives that may lie elsewhere in the design space, or totally different design options such as innovative design configurations, cannot be located using this method.

Similar to the basis ship approach is the design lane approach [36]. If the new design is to be similar to an existing class of vessels (say, a typical frigate or a container ship), a number of similar ships (instead of a single basis ship) can be analysed, usually using regression techniques, to estimate the design and performance parameters of the new ship.

2.5. Role of computers in ship design

The advent of computers has helped to improve the quality of designs and reduce the overall design time. This has been achieved by using computers for analysis, modelling and synthesis of designs.

Computers with their fast processing ability are ideally suited for numerically intensive analyses. Their aim is to speed up calculations that would take a lot of time when done manually. Thus, many tedious and repetitive design calculations have been computerised, such as resistance calculation, stability estimation and structural calculations. Most of the analyses, such as resistance estimation, involve regression analysis of historical design data [29]. Newer analysis tools are based on more sophisticated mathematical techniques, such as Artificial Neural Networks and Genetic Algorithms, which are capable of handling non-linear responses [44]. The outputs of the analyses are presented as tables or graphs. Other uses of computers in design analysis include Computational Fluid Dynamics (CFD) to calculate the effects of fluid flow such as wave resistance and Finite Element Analysis (FEA) to determine structural response to loading.

The second use of computers is in modelling the ship and its components using computer aided design (CAD) tools. One application of the initial CAD tools is to

generate simple drawings showing a visual description of the spatial configuration of the ship, such as a general arrangement. Another application is in the development of faired hull surfaces. Many modern CAD tools can store very detailed design information (e.g.: 3D product modelling) which can be interrogated to generate suitable drawings such as lines plan, general arrangement, structural plans and working drawings (e.g.: Tribon [45], Foran [46], CATIA [47], NAPA [48]).

The integration of modelling and analysis can significantly increase the utility of computers in ship design. For example, a graphical model (such as a three-dimensional wire-frame model of a ship) can be used to derive the necessary inputs for an analysis tool. The graphical model can be modified through a user interface so that any changes made to the model can be immediately analysed. Most modern CAD tools for ship design have this capability (e.g.: Tribon [45], Foran [46], Paramarine [49], CATIA [47], NAPA [48]). Some of these tools, such as Tribon and Foran, are mainly used for merchant ship design, for both concept design and later stages of the design process. Others, such as Paramarine, are aimed at the preliminary stages of warship design where the design space is more open.

Capabilities of computers have been used to develop design synthesis tools such as the US Navy's Advanced Surface Ship Evaluation Tool (ASSET) [4,5]. Such tools generally use approximate methods for analyses (such as weight and space estimates based on historic data), with limited capabilities for more detailed analyses. They have been useful in the concept design stage, for studying the cost-capability characteristics of competing designs [50].

2.6. Alternative approaches to the concept design of ships

The limitations of the traditional point-based design process forced naval architects to look at alternative ways of designing ships. The capabilities of computers for modelling, analysis, and synthesis heavily influenced these alternative approaches. They were also influenced by design theory and techniques developed and applied in other engineering fields. Andreasen [51] gives an outline of the development of general design methodology, explaining important approaches and methods. Hoset

and Erichsen [42] give a review of the books and papers during 1951 – 1995, dealing with general design theory applied in practical ship design. Comprehensive summaries of ship design methods can be found in the Design Methodology State of the Art Reports of IMDC 1997 [52] and IMDC 2006 [53]. The following sections discuss the modern approaches to ship design particularly relevant in the concept design stage.

2.6.1. UCL ship design process

The ship design process followed by the MSc students in UCL is largely based on the design spiral approach. However, it incorporates some limited design space exploration during concept design, thus improving upon the traditional point-based design.

The UCL concept design process is divided into two phases. The first phase is called 'Initial Sizing' and the second phase is called 'Parametric Survey' [35].

In the Initial Sizing phase, a ship is synthesised in terms of displacement, gross enclosed volume and preliminary dimensions to satisfy the payload, speed and other design requirements. This iterative process aims to balance the displacement and gross enclosed volume of the ship with the weight and space requirements of the components constituting the ship. The approach used simple weight and space algorithms based on past ship design data. This avoids first principle analysis at initial sizing and is adequate for the purposes of demonstrating the particular approach when multiple solutions are produced.

The process diagram for initial sizing, as adapted from [35], is shown in Figure 2-5.

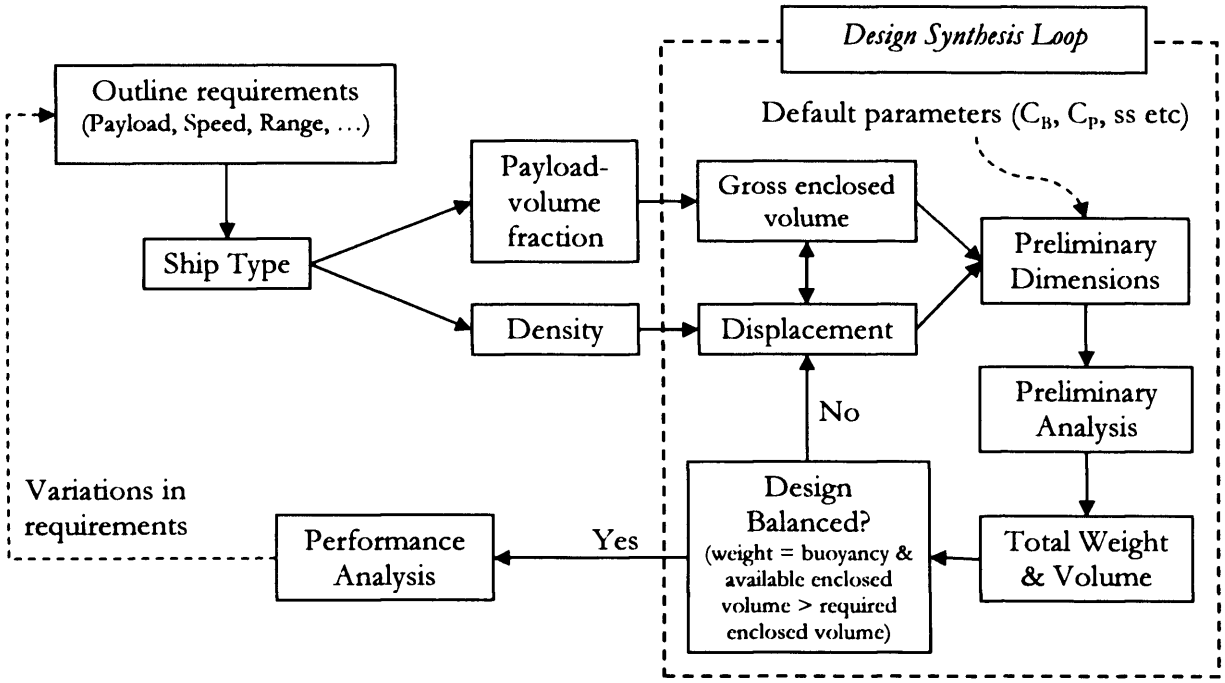

Figure 2-5: UCL initial sizing process

The Initial Sizing process starts with the payload, speed and other requirements. Depending on these, a suitable ship type is selected. The total volume and displacement are then estimated based on assumed values of payload-volume fraction (pvf) and overall ship density (displacement / gross enclosed volume) relevant to the chosen ship type. The loop starts with crude preliminary dimensions based on total volume and displacement, and assumed hull form parameters based on historic data. Preliminary analysis is then done to estimate the weights and volumes of individual systems and components. For a balanced design, the summation of the weights should be equal to the estimated displacement and the summation of volumes should be less than or equal to the estimated total volume. If these are not satisfied, the synthesis loop is continued with the newly obtained displacement and total volume. The iteration continues until a balanced design is obtained, the performance and cost of which is then estimated. The process is repeated for as many payload and performance variations as time permits to enable cost-benefit analysis. This helps to compare the performance characteristics of various design candidates thereby facilitating an informed dialogue with the customer. A potential design solution taking into account the outline requirements is chosen for the subsequent Parametric Survey phase.

The objective of the Parametric Survey phase is to modify the design solution in order to improve its performance characteristics, without compromising the payload capacity whilst still meeting the design constraints. This is done in two stages. In the first stage ('major parametric survey'), two major design parameters - depth (D) and superstructure ratio (ss) - are varied systematically, while keeping the other parameters constant. The range of technically feasible solutions are identified and compared. Among these, the most suitable solution is chosen by considering relevant performance characteristics and constraints. Keeping the corresponding values of depth and superstructure ratio constant, the second stage ('minor parametric survey') is carried out. Here the minor design parameters C_B and C_P are systematically varied. Again, the final choice among the design variations is made based on comparative costs and capabilities. Thus, the Parametric Survey phase is an optimisation process, albeit within a very restricted area of the design space and using very simplistic analysis.

Past design information relevant to the type of ship being designed is used to guide the designer during Initial Sizing. This is done by setting the values of various design parameters based on historic data and design curves (for example, the data and curves given in [54]). This ensures that the new design has reasonably good performance characteristics. The Parametric Survey phase then helps in refining the characteristics of the new design.

The UCL ship design process allows limited exploration of the design space and the corresponding performance space during the Parametric Survey phase. However, only a small region of the design space is explored around the initial design parameters assumed during Initial Sizing. Moreover, the design space exploration is limited to two parameters at a time (D and ss during the major parametric survey, followed by C_B and C_P during the minor parametric survey). It could be argued that a much wider region of the design space could be explored by considering simultaneous variation of all these four parameters. However, considering all such combinations simply means an exhaustive search of the design space. Such a search would require a large number of designs to be synthesised and analysed. Many of the designs would be infeasible or have very bad performance characteristics, which

means much of the design effort is spent in creating designs that will not be of any interest to the designer or the customer. Hence an exhaustive search of the design space is not done in practice; instead, the two-stage Parametric Survey phase is adopted, thereby accepting the limited exploration of the design space.

2.6.2. Knowledge-based design

Knowledge-based design is based on the concept that computers can be used to capture and utilise past design experience, which can then guide the designer while producing a new design by drawing upon relevant design knowledge. Knowledge-based systems store past design knowledge in a suitable database. Such design knowledge may include design practices for various types of ships, relevant design procedures and empirical formulae. The knowledge is represented in such a way that it is understandable to humans as well as computers [55]. The emphasis is on the explicit representation of knowledge independent from the methods using or operating upon this knowledge [23]. This is in contrast with the procedural algorithms used in traditional computer programs, which require that the knowledge be used in certain pre-specified sequences. For example, the expression $C_P = C_B / C_M$ when implemented in a traditional computer program would imply calculation of C_P for pre-specified values of C_B and C_M. In contrast, for a knowledge-based system, the same expression would imply calculation of any one of the three parameters when the other two are known.

Expert systems are an extension to knowledge-based systems, based on artificial intelligence [55]. They take the role of an experienced designer who gives his expert advice and opinion on a new design. They consist of a knowledge base, an inference engine and a user interface. The knowledge base incorporates human expertise. This can be done in three ways: using a set of rules [55], using descriptions of past designs [56], or by specifying explicit relationships among design parameters [57]. The inference engine identifies and extracts relevant knowledge depending on the features of the current design. This knowledge is then presented to the designer through the user interface.

Techniques such as artificial neural networks and relational databases are used in modelling knowledge-based systems [55,58]. Other modern techniques include semantic web technology instead of a relational database [59]. Semantic web technology is a knowledge-management framework, which is claimed to have better scalability and maintainability compared to relational databases. It is an extension of the current web that enables "computers and people to work in cooperation". Recent research on expert systems has focussed on 'case-based reasoning' where the system recognises features in the current design similar to particular solutions existing in the database and provides advice accordingly [60].

Example applications of knowledge-based and expert systems for ship design include basic design [59], concept design [61] and structural design [62]. Combining knowledge-based and expert systems with parametric CAD modelling systems has also been demonstrated [63]. Other applications include coupling of expert systems with multi-objective optimisation methods (see Section 2.6.6), as demonstrated in [64-67].

Expert systems have the capability to store and retrieve past design knowledge from different experts and hence have the potential to be more knowledgeable than an experienced designer. They help to guide the designer using the historic data in their databases. Hence they can be very useful to design a ship based on past design information [55]. However, there are many disadvantages to expert systems. When explicit relationships between different design parameters are specified, they provide the flexibility to allow the calculation of any unknown parameter from any starting point. However, the data used is only that which can be readily manipulated in direct numerical format. This implies that such systems disguise the extent to which subjective judgments are built into the data [1]. Moreover, the reliance on specific rules and past design data would lead to traditional designs, and may not be suitable for innovative designs. This is because the explicit design rules based on type ships limit the scope of their application, thus reducing the possibility for innovation. Furthermore, technical decisions that are inherent in any design, but do not directly result from explicit rules, are difficult to be incorporated. In addition, if descriptions of past designs are stored in the knowledge base, difficulties arise about which

characteristics need to be stored and how they should be represented. This is because the inference engine should be capable of recognising features in the new design and relate them to the characteristics stored in the database. This means that the development of new designs is influenced by the structure of the knowledge base.

2.6.3. Risk-based design

Risk-based design (RBD) is based on the principle that shipping operations are risky and hence ships should be designed with this in mind [53]. The aim of RBD is the prevention or reduction of risk to life, property and the environment [68-71]. Traditionally, risk has been treated as a constraint on the design process, imposed by rules and regulations. In contrast, RBD systematically integrates risk analysis as an objective in the design process, in addition to standard design objectives such as speed and seakeeping. Current RBD research focuses on collision and grounding, crashworthiness, damaged stability and survivability, fire/smoke and evacuation, and system and component redundancies etc. If relevant performance analysis methods are available, risk can be used as an additional objective during concept design, and hence can be used in conjunction with design methods using multi-objective optimisation (see Section 2.6.6).

Vassalos describes a European thematic framework established for "Design for Safety" [68,69], targeted towards safer design of ro-ro and passenger ferries and harmonising safety standards. The aim of the framework is to move from the current prescriptive and deterministic safety standards to performance-based probabilistic standards based on a comprehensive assessment of the risks involved and risk mitigation measures and their implications on cost and benefit. Another recent application of RBD is a European Commission project aimed at developing a rational basis for the design, operation and regulation of oil tankers [72].

RBD involves the following steps [69]:

- identify the risk events (e.g.: collision)

- estimate frequency - assess the probability of the risk events (e.g.: based on historical data)

- analyse consequences - estimate the cost of the consequences (e.g.: fatalities per ship year)

- identify risk control options to improve undesirable risks (e.g.: subdivision improvements, collision avoidance measures, alternative layouts to improve evacuation etc)

- analyse cost-effectiveness for each risk control option (e.g.: improved subdivision would require increased cost, the benefit being a reduction in fatalities)

- choose the most cost-effective solution, considering cost and other design objectives

This shows that RBD by itself is not a new design approach: it simply advocates that risk be treated as an objective of the design process. In other words, risk becomes a design aspect to be traded off, similar to cost and various performance criteria. Thus, when carrying out concept design, the designer may choose to incorporate relevant risks among the design objectives and develop suitable trade-off solutions.

2.6.4. Design building block approach

Traditional design synthesis is essentially numeric in nature, ignoring the spatial and stylistic aspects of the design. This can be misleading, especially for novel designs and for configuration-driven designs such as aircraft carriers and cruise liners. Andrews [73] argued that this traditional process should be replaced with an integrated synthesis procedure driven by the spatial and stylistic aspects. This concept was developed into a new design paradigm called the design building block approach (DBB) [25,74,75]. In this approach, the designer considers various architectural elements representing payload, combat systems, mobility and other functions in discrete blocks. The blocks can be placed together / juxtaposed in whatever way the designer wishes. Each building block can be assigned

characteristics such as weight, space, personnel, electrical power requirements and textual tags. The arrangement and positioning of the building blocks together determines the overall configuration of the ship, which can then be examined for feasibility and performance measures. With the recent advances in computer graphics, the notion of design building blocks offers significant advantages for concept design of ships. A single computer model that combines the traditional numerical description of the ship with interactive graphical building blocks can represent a more holistic view of the ship.

Following this concept, a new software program called SURFCON was developed [76]. It forms part of the established ship design suite of Paramarine [49]. Using SURFCON, the design is developed by assembling a number of design building blocks, around which a hull form is wrapped, whereby the usual naval architectural analysis such as resistance and seakeeping can be carried out. The open nature of the objects contained within the software means that SURFCON is not a "black-box" system. Andrews has demonstrated several successful applications of SURFCON, for example, for the design of a multirole frigate and an offshore support vessel [76].

The Design Building Block approach allows early introduction of configuration into the design process, resulting in the ability to analyse critical design aspects early in the design process. It is useful during the concept design of configuration-driven ships, for example, to compare different topologies. This is especially relevant for innovative ship design, where there is no parent ship commensurate with the design requirements and the overall configurational style is initially unknown. In such cases, the DBB approach would help to identify the important design drivers and the relationship between different aspects of the design, thus assisting in designer decision making. The flexible nature of the DBB approach, combined with its emphasis on interactive graphical display, helps in exploring design options and assessing the resulting configurations. Its usefulness has also been demonstrated in incorporating production issues earlier in the design process, thereby reducing the overall design cost and the project time span [75-77].

The strengths of the DBB approach lie in its ability to assess different topologies early in the design process. This makes it very useful for the design of innovative and configuration-driven ships where major changes in topology and layout have a large impact on capability. Though it can be used as a creative exploration approach for the design of other ship types, its benefits may be less apparent while exploring cost-capability trade-offs for ships with less emphasis on topological variations.

The DBB approach is not readily amenable to numerical parametric survey of a single configuration, such as assessing the effect of varying underwater hull form coefficients or other design parameters. This is because of the difficulties involved in working up the details of building blocks for each design option [77]. However, it may provide useful guidance to the parametric survey with internal arrangement issues if these are significant design drivers.

2.6.5. Set-based design

Set-based design (SBD) provides an alternative approach to improve the traditional point-based design process. It is based on the "design bounding" approach developed by Lamb [78]. In contrast to point-based design, it starts with broad sets for design parameters. A number of alternative feasible designs are created to reveal trade-offs between conflicting design requirements. The sets are gradually narrowed until a more global "optimum" is revealed and refined. Set-based design does not use any optimisation algorithms to try to find a unique optimum solution. Instead, it finds a number of feasible solutions and presents them to the designer, along with their performance characteristics and design parameters, from which a selection can be made. Set-based design has been shown to produce better designs in shorter time, albeit in an academic environment [79,80].

The set-based design has some advantages over the traditional point-based design methods. In the traditional design process, the designer has no way of knowing, other than from experience, whether the single ship that is designed is a good solution. In contrast, set-based design generates many alternative acceptable solutions with different characteristics. The designer can evaluate them and compare

their characteristics. There is no optimisation attempted and the whole design process is transparent.

The main drawback of the set-based design is that it aims at generating many feasible design solutions without directing them towards relevant performance characteristics. For example, if the design problem is not severely constrained, the design process could generate a number of feasible solutions with widely varying performance characteristics. It is left to the designer to sift through all such designs and find the solutions of interest, which could be a tedious and time-consuming process. It is however possible to use techniques such as Multiple Criteria Decision Making to assist in this process.

2.6.6. Optimisation in ship design

The inability of point-based design methods to obtain a globally optimal solution prompted researchers to examine the application of formal optimisation methods in ship design. The earliest works were done in the 1960s using single-objective optimisation techniques [81-84]. These techniques can produce good designs if there is a well-defined measure of merit for optimisation, such as the minimisation of resistance. However, in practice, there is often no single measure of merit, and the designer has then to combine multiple disparate objectives into an overall measure of merit. Multiple Criteria Decision Making (MCDM) techniques help to achieve this. Examples of such applications in the context of ship design can be found in [22,85-93]. However, designers remain sceptical of the idea of combining multiple disparate objectives into a single measure of merit for complex multi-role vessels [1].

Introduction of multi-objective optimisation techniques removed the need for forming a single measure of merit. These techniques generate the so-called "Pareto front", i.e., the set of optimal trade-off solutions. Most such methods are based on heuristic techniques such as Genetic Algorithms [94-97]. Despite the fact that they tend to be computationally expensive, they are being increasingly used by

researchers for optimisation in many fields. Numerous applications of these techniques in ship design have been found in the recent literature [5,10-17,98-103].

Multi-objective optimisation has been criticised for its inability to handle non-numerate aspects of the design problem, thereby ignoring wider issues such as spatial disposition and stylistic aspects. According to Erikstad [23], "there seems to be a mismatch between the *actual* design problem, as seen from the practising designers' point-of-view, and the idealised *representation* of the problem required by the optimisation-based design tool". Another difficulty with multi-objective optimisation is in selecting a preferred solution from the Pareto-front. The use of MCDM techniques to achieve this has had only limited success. More importantly, optimisation methods usually lack transparency and consequently they are unable to provide useful insights into the design process. This has caused them to be labelled as black-box solutions unacceptable to practising designers [1,23].

2.6.7. Multiple criteria decision making

Multiple criteria decision making methods are a useful partner to optimisation methods. They have two primary uses. The first one is to formulate a reliable measure of merit (sometimes referred to as OMOE – overall measure of effectiveness [11,93]) that can be used for single objective optimisation. The second use is as a post-processor after multi-objective optimisation to select the best trade-off design from the Pareto-front [22,53].

The measure of merit is formed by combining multiple design objectives with suitable weightings for each objective to form an overall measure of effectiveness (OMOE) [104-107]. The formulation of weightings can be quite complex, taking into account various aspects of each objective such as the subjective preferences of experts and decision makers. The analytic hierarchy process (AHP) developed by Saaty is popular in formulating weightings [108,109]. Many researchers have applied MCDM techniques to formulate an OMOE in the context of ship design, and used it in conjunction with suitable optimisation techniques [22,85-93].

As a post-processor to multi-objective optimisation, MCDM techniques are used to rank the set of Pareto-optimal solutions. For example, Dalton et al show how MCDM techniques can be used in conjunction with genetic algorithms for multi-objective optimisation [110]. MCDM techniques useful in this context include [110,111]:

- UTA (Utility Theory Additive): The term 'utility' in the title of the thesis is used in the general sense of usefulness to designers. However, 'utility' in the context of MCDM refers to the quantification of the decision maker's subjective preferences among candidate solutions. UTA uses subjective ranking of alternative designs and constructs a value function based on linear programming.

- TOPSIS (Technique for Order Preference by Similarity to Ideal Solution): one among the Pareto-optimal designs is chosen as the preferred solution such that it has the shortest Euclidean distance from the ideal solution on the multi-dimensional performance space. The ideal solution is the set of ideal performance values as specified by the designer or experts.

- CODASID (Concordance and Discordance Analyses by Similarity to Ideal Designs): uses a decision matrix to generate a preference order for a set of designs based on a preference concordance index, an evaluation concordance index and a discordance index to provide independent measures for ranking designs. It requires the designer to assign weightings and preferences among objectives.

MCDM methods require hierarchical decomposition of the total system. Sceptics are concerned about the designer having to give numerical weightings to many parameters, especially because most of them represent disparate quantities and include subjective preferences. As Andrews [1] states, the process of assigning weightings ignores the "complex interactions and synergies among the parameters". Though MCDM techniques such as TOPSIS and CODASID have been used in

conjunction with multi-objective optimisation techniques to select the best trade-off solutions, they are not without their weaknesses. For example, TOPSIS has been criticised to be overly sensitive to subjective weighting factors and for its tendency to choose extreme solutions or designs with overall good average performance. CODASID is seen to overcome some of these problems, though it is more complex to implement [110,111].

2.6.8. Comparison of various ship design methods

From the description of the modern alternative approaches to ship design described in the preceding subsections, the underlying thrust is seen to be on the following aspects:

1. how to improve the quality of the designs, i.e., obtain the best trade-off solutions considering all requirements and constraints;

2. how to reduce the time taken for the design process;

3. how to incorporate traditionally neglected features earlier in the design process.

Risk-based design and design building blocks belong to the third category. Risk-based design incorporates risk as an objective in the design process, in addition to the other usual objectives. Apart from this, it does not modify the underlying design process. The Design Building Block approach incorporates spatial and stylistic aspects early in the design process. This is especially useful for configuration-driven designs.

The UCL ship design process belongs to the first category. It provides a slight improvement to the traditional basis ship approach, in that it offers scope for limited design space exploration during the parametric survey stage, thus taking one step towards design optimisation. Knowledge-based systems and expert systems formalise the basis-ship method by collecting expert design knowledge in a database or similar system, which can be suitably retrieved to assist in a new design. The

underlying design method is not significantly different from the traditional point-based method. They may also be considered to be in the first category.

Set-based design helps to keep various trade-off solutions open much longer than is done traditionally. It follows the approach of rejecting infeasible solutions rather than trying to use any kind of optimisation. Thus, it helps in wider exploration of the design space, thereby generating a number of alternative design solutions. It is claimed that set-based designs can produce better designs in shorter time. Consequently, it falls into categories 1 and 2 mentioned above.

Multi-objective optimisation methods are also capable of wider exploration of the design space and generating a number of good trade-off solutions in shorter time (categories 1 and 2 mentioned above). However, they are generally considered as "black boxes" in that they do not provide the designers with relevant design insights; hence, designers remain unable or unwilling to use them in practice.

2.7. Focus of the current research

From the discussion in the previous section, one may conclude that set-based design and multi-objective optimisation are two methods that seem suitable for the generation of good trade-off solutions during concept design while reducing the time taken for the design process as well. Multi-objective optimisation may be preferable because it is possible to direct the design effort towards "Pareto-optimal" solutions, whereas set-based design makes only the simple distinction between feasible and infeasible solutions. Thus, it was decided to examine multi-objective optimisation in more detail to identify areas for improvement, emphasising its application for ship design, especially in avoiding the "black-box" nature of optimisation-based methods. The concept was presented to the members of the ACCeSS consortium in a joint meeting at the United States Naval Academy in May 2005. To illustrate the potential of the concept, a single-objective optimisation tool was developed. The use of this tool was demonstrated in conjunction with a performance analysis tool using artificial neural networks developed by the PhD

candidates at Stevens Institute of Technology (USA). A joint paper based on this concept was presented at the WMTC 2006 conference (see Appendix A).

A chronological review outlining the history of the use of traditional optimisation techniques in ship design is given in Appendix B. All the applications are found to be single-objective. When multiple objectives are considered, they need to be combined into a single measure of merit using appropriate weightings. The weighting for each objective is decided based on its perceived importance in relation to the other objectives. Thus, the weightings are rather subjective, depending on the designer's experience, the customer's preferences or the experts' opinions. Therefore, traditional optimisation algorithms are not suitable for solving multi-objective problems without resorting to such arguable weightings. The characteristics of multi-objective optimisation, the methods used for solving it, and its potential utility for concept design of ships are discussed in the next chapter, leading to the proposed design approach.

3. Multi-objective optimisation and the new design approach

The previous chapter identified multi-objective optimisation (MOO) as a promising area of research into ship design methods. This chapter examines the concept of MOO in more detail, identifies the weaknesses in its current applications, and proposes a new design approach that extends its use in preliminary ship design.

A diagram relating various sections within this chapter and relevant appendices is given in Figure 3-1. Firstly, the concept of optimality in the context of MOO is explained and the methods employed to generate optimal solutions are outlined. Then the applications of multi-objective optimisation in ship design are discussed. Areas for improvement in these applications are then discussed: MOO in ship design is usually carried out from a hydrodynamic point of view, keeping the displacement constant and ignoring the overall design synthesis process that would ensure a feasible ship satisfying the design requirements; the choice of designs for the next stage of the design process may not be straightforward; the "black box" nature of MOO makes the interpretation of the results difficult. These limitations restrict the use of MOO in practical ship design. A new design approach is proposed, which aims to overcome these limitations. The anticipated advantages and potential applications of the proposed design approach are presented.

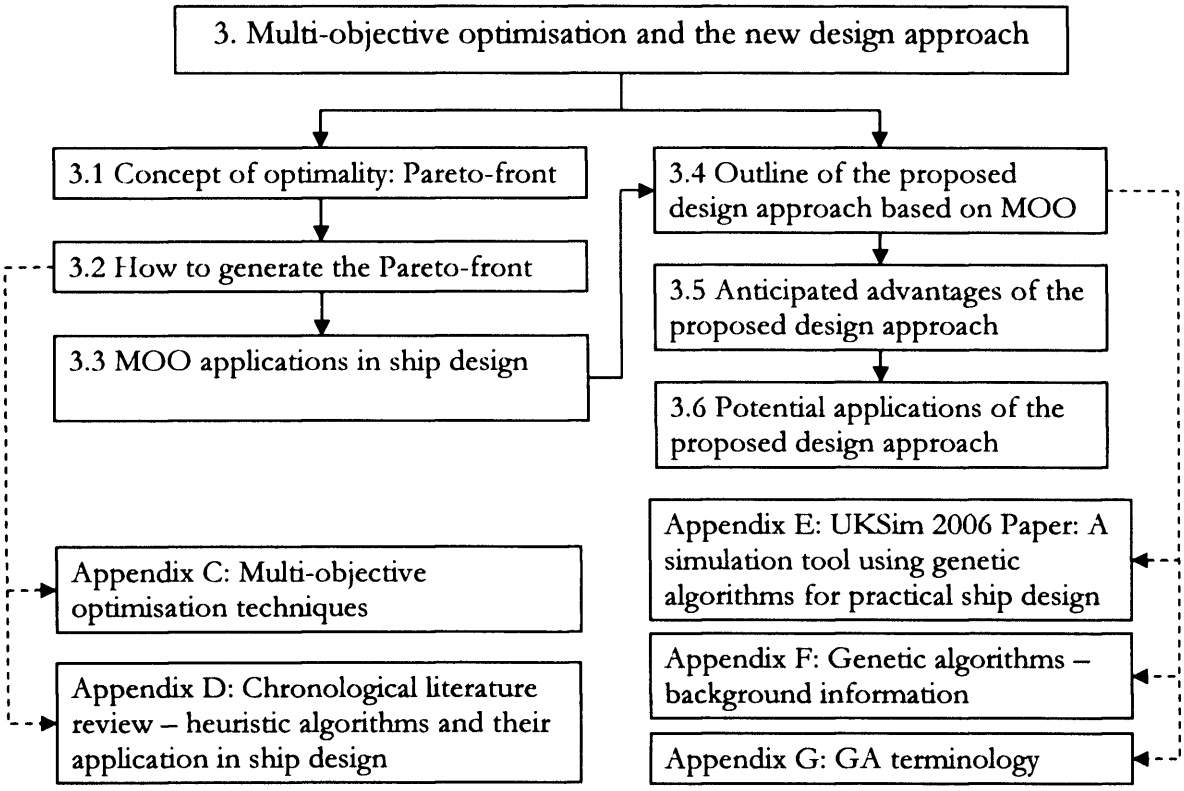

Figure 3-1: Outline of Chapter 3

3.1. Concept of optimality: Pareto-front

Multi-objective optimisation is characterised by not having a unique solution, but a set of solutions taking into account all objectives. Such solutions are termed as "Pareto-optimal solutions" or "nondominated solutions". A solution is Pareto-optimal if it cannot be improved in any objective without worsening at least one other objective [8]. The set of Pareto-optimal solutions is characterised by the Pareto-front, a hyper-surface in the n-dimensional performance space defined by all Pareto-optimal points (where n is the number of objectives). The primary aim of MOO is to locate the Pareto-front effectively and efficiently. For example, consider Figure 3-2, which shows the results of a two-objective optimisation problem - maximise Overall Measure of Effectiveness (OMOE) and minimise cost. The curve represents the best OMOE possible for a given cost. The OMOE of any solution lying in the thin region of the curve can be achieved at a lower cost, by another solution lying in the thick region of the curve. Thus, the solutions on the thin region are not Pareto-optimal, and the thick region represents the Pareto-front.

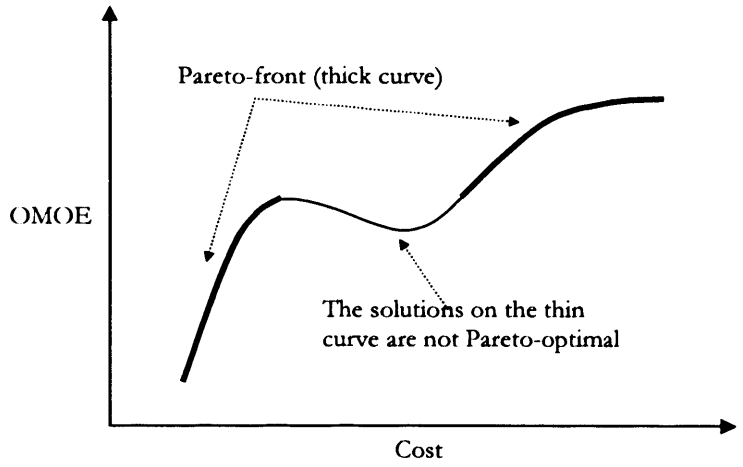

Figure 3-2: Definition of the Pareto-front for two objectives

3.2. How to generate the Pareto-front

The most popular methods for generating the Pareto-front are based on heuristic approaches, as opposed to traditional pattern-search or gradient-based optimisation methods. There are a number of heuristic techniques based on the analogy with natural evolution. Collectively, they are known as 'Evolutionary Algorithms' [112-114]. They include Genetic Algorithms, Evolution Strategies, Genetic Programming and Evolutionary Programming. These techniques are similar to one another in principle, but differ in details of their implementation. The common underlying idea is that the environmental pressure on a population of individuals causes natural selection causing an increase in fitness of the population with time. The evolution is characterised by various genetic operators.

Other popular heuristic optimisation methods include Particle Swarm Optimisation, Simulated Annealing and Tabu Search. Particle swarm optimisation is based on the social interactive and co-operative behaviour of groups of organisms, such as flocking birds [115,116]. Simulated Annealing is based on the analogy with statistical mechanics [44,117]. Tabu Search is similar to gradient search methods, but with memory of good and bad solutions [44]. More details of these MOO techniques and comparison of their characteristics are given in Appendix C. A chronological literature review of the development of the heuristic techniques for general multi-

objective optimisation and their application in ship design can be found in Appendix D.

3.3. MOO applications in ship design

Most of the literature on the application of MOO in ship design is limited to two objectives. Maximisation of overall measure of effectiveness (OMOE) and minimisation of cost are generally the two objectives. The OMOE in this case is formulated either as a simple weighted sum or based on more complex Multiple Criteria Decision Making (MCDM) techniques such as Analytic Hierarchy Process (see Section 2.6.7). Examples of two-objective optimisation problems in ship design are found in [5,10-12,16,17,100,102]. They demonstrate the application of MOO in ship design; however, from the point of view of practical ship design, it would be more desirable to generalise the method by considering all objectives individually, thus avoiding the need to formulate an OMOE. One of the reasons behind using just two objectives is the need for meaningful interpretation and visual representation of the results. For two objectives, the results are simple to show in a 2-D graph and the trade-off between the two objectives can easily be examined. This becomes difficult for a higher number of objectives.

There have been a few instances in recent literature that consider more than two objectives. For example, Peri and Campana [15] simultaneously minimised three objectives: resistance, heave motion and pitch motion. Olcer et al [14] maximised three objectives: maximum allowable wave height satisfying the damage stability criteria, KG limiting value satisfying the damage stability criteria and cargo capacity. Hutchinson and Sen [89] used multiple objectives related to the recent probabilistic stability standards. Moreover, there has been an EU initiative (FANTASTIC) with the aim of improving ship design, which focussed on multi-objective optimisation methods among other things [101,118-120]. These attempts suggest that there might be potential for successful application of MOO for ship design.

The following subsections highlight the limitations of the current MOO applications in ship design and thus try to identify areas for improvement.

3.3.1. Incorporating design synthesis within MOO

MOO in ship design is generally carried out from a hydrodynamic point of view, varying the main design parameters (L, B, T, C_B ...) while keeping the displacement constant. Although this is a logical approach from the point of view of hydrodynamics, it is of limited use for practising designers. For example, two ships having the same displacement but different main particulars cannot, in general, have the same payload capacity, and hence are not directly comparable [121,122]. Thus, it is imperative that a design synthesis module be made part of the optimisation procedure to better ensure that the generated designs satisfy the payload and other requirements, as well as various constraints such as the bounds for L/D. It will then be more likely that the resulting designs are realistic and comparable with one another. A few papers have included a design synthesis module within the optimisation procedure [5,10,11,17,98,102,123].

3.3.2. Selection of the best trade-off solution from the Pareto-front

MOO generates a set of 'optimal' trade-off solutions forming the Pareto-front. The next step is to compare the Pareto-designs and choose one (or a few) for feasibility studies and detailed design. Some authors have used MCDM techniques for selecting the most suitable trade-off solution [14,87,110]. Such techniques have been criticised as rather mechanistic and incapable of providing design insights. Practitioners remain critical of the need to assign consistent weightings to disparate objectives [1]. Other researchers simply leave the choice of the best trade-off solution to the designer [16,124].

3.3.3. "Black-box"

Sophisticated optimisation techniques often present the designer with 'black box' solutions [1]. A black box solution is one from which the user gets little insight into the underlying processes: the user has no option but to trust their outputs. The lack of transparency and control over the optimisation process makes the interpretation of the results difficult. Consequently, the designer gets little wisdom about the design drivers or technical risks. Optimisation techniques that suggest a prescriptive

optimum solution leave no room for the designer to modify or improve the solution based on his/her experience [23]. This, coupled with the lack of evidence of past successful industrial applications of optimisation techniques, makes the designer feel sceptical about using the results of such optimisation.

3.3.4. Summary – MOO in ship design

The discussion above shows that substantial research has been carried out on the application of MOO in ship design. However, the research seems to focus on generating the Pareto-front and not on fully utilising it. The only perceived use of the Pareto-front seems to be in selecting the 'best trade-off' solution, which is either left to the designer's discretion or achieved using MCDM methods. The former is evidently unsatisfactory and the latter has been criticised for being too mechanistic – such approaches choose a design based on a pre-specified 'ideal' solution without considering the design parameters of the chosen design either in isolation or in relation to the surrounding designs. This lack of transparency and the inability to provide design insights from the Pareto-front suggest most MOO applications are consequently 'black box' solutions.

It should be possible to achieve better utilisation of the Pareto-front and enable better understanding about the structure of the whole Pareto-front as well as about individual Pareto-designs, for both the design space and the performance space. This should make the designer feel more confident in using MOO in practice. The current proposal focuses on this aspect of MOO, and is presented in the next section.

3.4. Outline of the proposed design approach based on MOO

Having identified the drawbacks of the current applications of MOO, the current proposal is a new ship design approach based on MOO. This approach uses the Pareto-front to derive design insights during the concept design stage. This is achieved by analysing the structure of the whole Pareto-front and by examining individual designs of interest in further detail. This proposed design approach will help the designer to have a more informed dialogue with the customer and, in

particular, to clarify the design requirements. A preliminary demonstration of this concept was presented at the UKSim2006 conference, illustrating a preliminary ship design tool using multi-objective genetic algorithms (MOGA) developed in Matlab. This paper is included at Appendix E.

The steps involved in the proposed design approach are as follows:

1. Specify outline or preliminary design requirements: These include input parameters such as payload weight and payload volume, design parameters such as the number of decks and block coefficient, design objectives such as minimisation of cost and maximisation of seakeeping capability, and constraints such as the allowable bounds for L/D and B/T. Each design parameter is usually specified by a lower bound and an upper bound (e.g.: payload volume = [2000 to 2500]) rather than using a fixed value, as is the case in the traditional design approaches. It is, however, possible to fix the value of any parameter, if desired.

2. Generate the Pareto-front: The Pareto-front is generated using a software tool developed by the candidate based on genetic algorithms. This GA Tool takes the design requirements as input and generates the Pareto-front consisting of design solutions with 'optimal' performance characteristics. A design synthesis module has been incorporated within the tool to ensure that the generated designs are realistic. More information on genetic algorithms, such as their advantages, the details of genetic operators used, how they are applied for multi-objective optimisation etc are described in Appendix F. Technical terms that usually arise in the context of genetic algorithms are defined in Appendix G.

3. Analyse the Pareto-front: The aim of this step is to derive possible design insights about the Pareto-front as a whole, as well as about individual designs. The analysis is carried out by visual and numerical examination of the performance space and the design space. Suitable visualisation methods have been implemented to assist in this process. The analysis helps in understanding the trends of performance characteristics and design

parameters, exploring the structure of the Pareto-front to locate discontinuities or irregularities, examining the robustness of individual designs and identifying the relative importance of various design constraints.

4. Re-generate the Pareto-front with revised constraints: The analysis of the Pareto-front in the previous step identifies the relative importance of various design constraints considered. The important constraints may then be relaxed suitably and the Pareto-front re-generated. The comparison between the old and new Pareto-fronts would indicate the potential improvements.

5. Re-generate the Pareto-front with revised design inputs: Some of the design inputs used may be revised and the Pareto-front re-generated. This would help to establish if any gain in performance could be gained by modifying the design inputs.

6. Discuss the results with the customer: The analysis of the structure of the Pareto-front could reveal interesting trends of design parameters and performance characteristics. The subsequent steps could also identify the effects of varying design constraints and design inputs. These can then be discussed with the customer to clarify the design requirements and make appropriate modifications.

7. Repeat the above steps, if required, with the modified design requirements.

8. Select the most appropriate solution(s) to take forward to the next stage of the design process.

The proposed design approach as outlined above is discussed in more detail in Chapter 4.

3.5. Anticipated advantages of the proposed design approach

The proposed design approach, with its focus on deriving design insights by appropriate analyses of the Pareto-front, brings an openness to the MOO process. It does not try provide prescriptive solutions; instead it provides guidance to the designer based on the analysis of the Pareto-front. This open and interactive nature of the approach, as opposed to the 'black box' nature of the current MOO methods, is expected to be attractive and useful to practising designers.

3.6. Potential applications of the proposed design approach

The proposed design approach is primarily aimed at the concept design phase of the ship design process, to generate and compare potential design alternatives. In addition, it can be used to modify a parent design to improve its performance. A third possible application would be in the early stages of feasibility studies to handle design changes, which could reduce the demand for modifications to the most important design parameters.

The next chapter describes the proposed design approach and explains how it can be used for the three potential applications just listed.

4. The proposed design approach

The previous chapter introduced the proposed design approach. This chapter describes it in more detail. Each stage of the proposed design approach is explained. Finally, three potential applications of the proposed design approach are discussed. A diagram relating various sections within this chapter and relevant appendices is given in Figure 4-1.

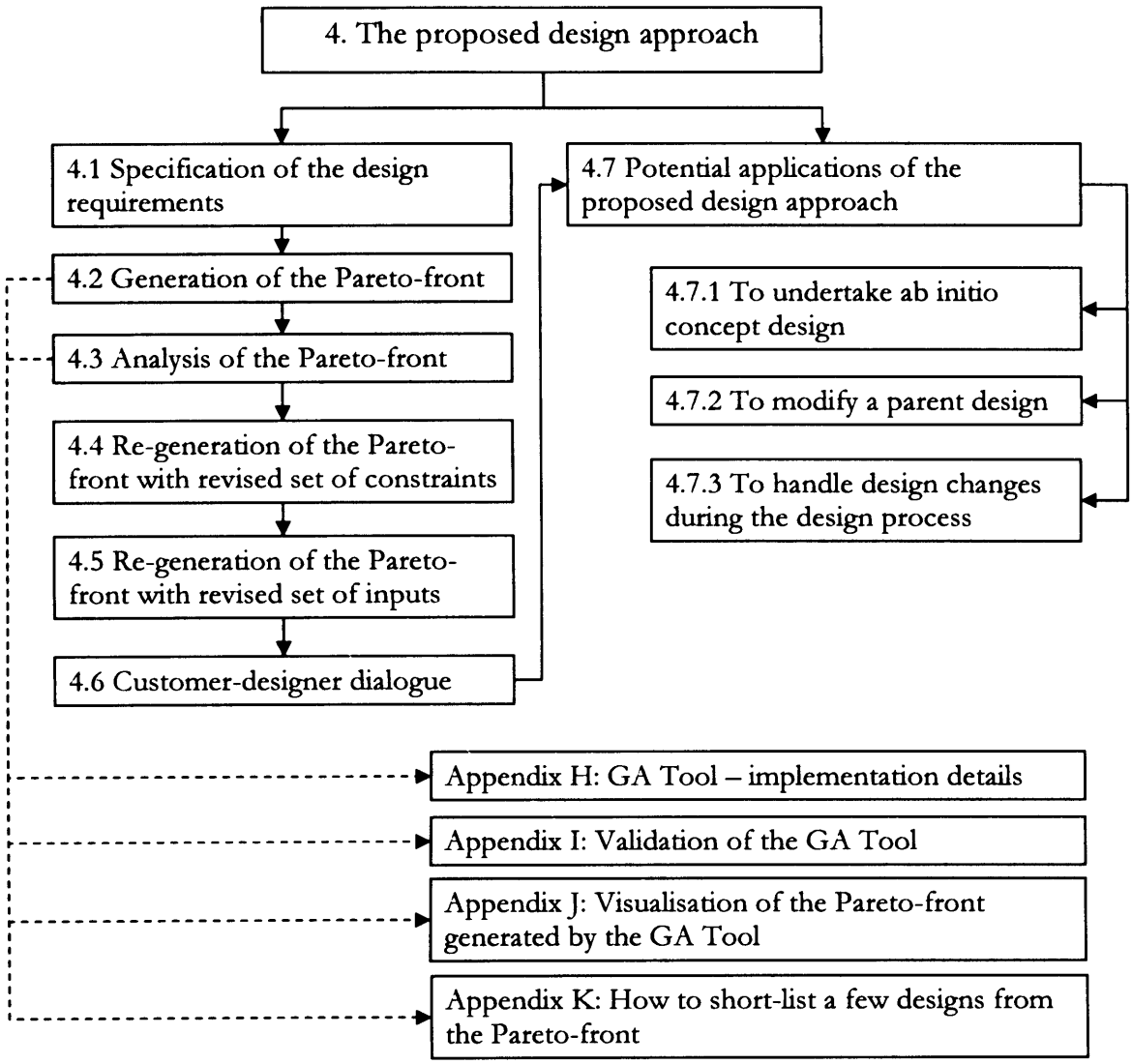

Figure 4-1: Outline of Chapter 4

The steps involved in the proposed design approach were outlined in Section 3.4, and are shown in Figure 4-2. Each step is explained in the following subsections.

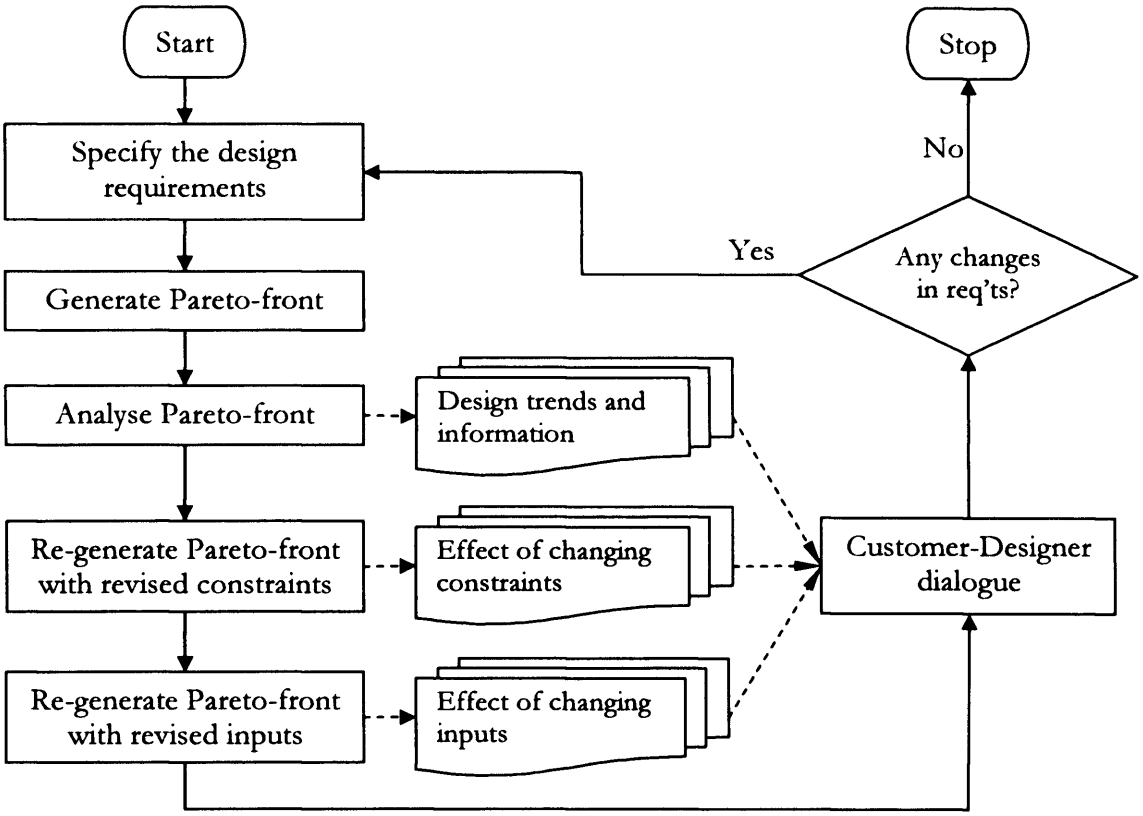

Figure 4-2: The proposed design approach

4.1. Specification of the design requirements

The first stage in the proposed design approach is to specify outline or preliminary design requirements. Such requirements include cargo or payload details, speed, endurance, area of operations and any special constraints (such as maximum length due to dock restrictions). To start with, the cargo or payload requirements have to be converted to the total payload weight and the total payload volume. For warships, this implies the total weight and volume required by the combat system equipment.

The design requirements can be divided into inputs, constraints and objectives. Some of these may be specified by the customer (such as the payload and speed requirements), whereas others may be decided by the designer (such as the

acceptable range of values for L/D. A set of typical design requirements, split into customer and designer requirements, is given in Table 4-1.

Table 4-1: A set of typical design requirements

	Design inputs	Design constraints	Design objectives
Customer requirements	Payload weight Payload volume Maximum speed Endurance speed Range	Draught limitations (due to area of operations) Length limitations (due to length of dock etc) Customer's budget Operable seastate	Minimise build cost Minimise operating costs Maximise seakeeping capability
Designer requirements	Number of decks, or main hull depth Superstructure ratio C_B C_P Complement	Bounds of typical design ratios such as L/B, L/D, B/T, Ⓜ Minimum draught (slam limit, propeller immersion etc) Stability requirements Freeboard requirements	Satisfy stability requirements Achieve acceptable manoeuvring characteristics

In traditional design approaches, the design inputs generally are specified constant – for example, a fixed value of payload volume is used to design a ship. However, in the proposed design approach, most of the design inputs are given a range of values rather than a fixed value. For example, payload volume = [2000 to 2500], implying that the design is free to have any value in this range.

The set of design inputs that are capable of taking a range of values are termed design variables. A set of design variables, along with the fixed design inputs, can be used to synthesise a unique ship. The design variables that are currently used in the proposed design approach are:

- Main hull depth (D)
- Payload / Volume Fraction (pvf)

- Overall density (ρ)
- Superstructure ratio (ss)
- Block coefficient (C_B)
- Prismatic coefficient (C_P)
- Transverse Metacentric height (GM)
- Payload weight (W_{pay})
- Payload volume (V_{pay})

Among these design variables, pvf and ρ are not 'independent' – their initial values are used only to begin the design synthesis process, and they get modified during design synthesis to achieve the weight and space balances. Similarly, GM is usually estimated during design synthesis to achieve adequate stability, in which case it is also a dependent variable. The remaining design variables are called 'independent design variables'.

4.2. Generation of the Pareto-front

The second step in the proposed design approach is to generate the Pareto-front. A GA Tool capable of multi-objective optimisation using genetic algorithms is currently implemented for this purpose. Once the design requirements are specified, the design tool is executed to generate the Pareto-front. The tool starts with a set of random ship designs forming the 'initial population'. After evaluating their performance and ranking them, genetic algorithms modify the best of these designs using genetic operators, resulting in an 'offspring population' with, usually, better performance characteristics. The offspring population replaces the initial population and the genetic operators are applied again. As iterations ('generations') progress, the population approaches the Pareto-front. The characteristics of the ships on the Pareto-front, consisting of their design parameters (such as L, B, T, C_B and C_P) and their performance characteristics (such as build cost and seakeeping index) are

stored numerically as well as graphically. Further details of the implementation of the GA Tool are given in Appendix H. The GA Tool User Guide [125], along with the accompanying CD containing source code and examples, provides further guidance on using the GA Tool.

Since the design tool was independently developed by the candidate, its capability to generate the true Pareto-front had first to be established. A number of tests, involving both mathematical test functions and ship design examples, were carried out to validate the GA Tool. The results from these tests are summarised in Appendix I.

4.3. Analysis of the Pareto-front

The analysis of the Pareto-front is the heart of the proposed design approach. It involves studying the trends in performance characteristics and design parameters, exploring the structure of the Pareto-front to locate discontinuities or irregularities, examining the robustness of individual designs, identifying the relative importance of various constraints and inputs etc.

Suitable methods for the visual representation of results are necessary to assist in analysing the Pareto-front. This is especially important when there are more than two objectives, in which case the performance space cannot be visualised by a simple two-dimensional plot. The design space, in any case, consists of a number of parameters, and simple 2D-plots are of limited use. Instead, appropriate visualisation methods suitable for representing multivariate data are used. Details of these methods are discussed in Appendix J.

The steps involved in the analysis of the Pareto-front are shown in Figure 4-3. Each step is described in the following subsections.

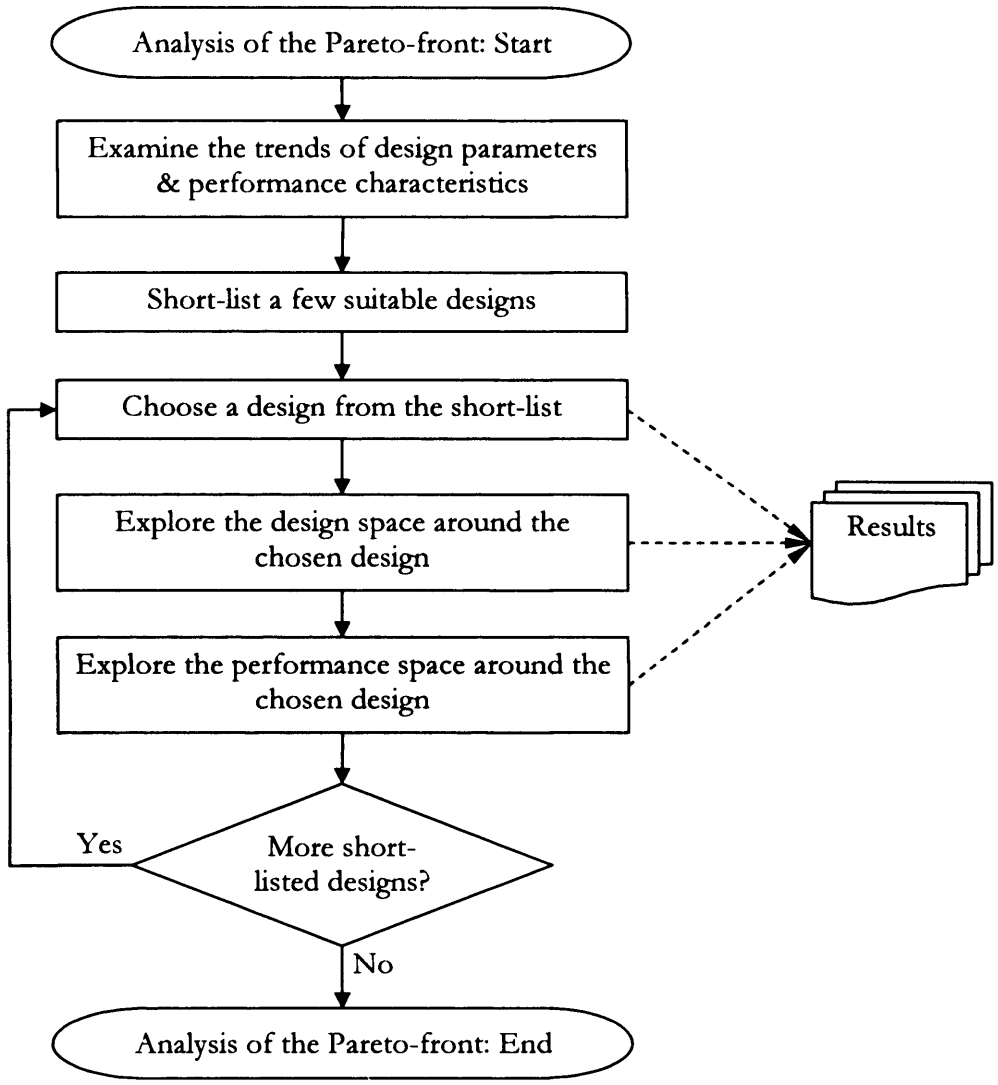

Figure 4-3: The steps involved in the analysis of the Pareto-front

4.3.1. Examination of the trends of design parameters and performance characteristics

The first step in the analysis of the Pareto-front is to examine the whole Pareto-front in the design space as well as in the performance space to identify the general trends of the design parameters against the performance characteristics, such as the variation in length required to get better seakeeping. A 'colour diagram' representation has been found useful in spotting these trends (see Appendix J.6). In this representation, the performance characteristics and the design parameters of interest are tabulated such that each row corresponds to one ship design and each column represents one design parameter or performance characteristic. The

variation of colours along each column shows the trends of that parameter, with blue representing low values and red representing high values. A sample colour diagram, consisting of 181 designs on the Pareto-front, is shown in Figure 4-4. The minimum and maximum values for each column are shown at the bottom of the table to indicate the range of variations of each parameter.

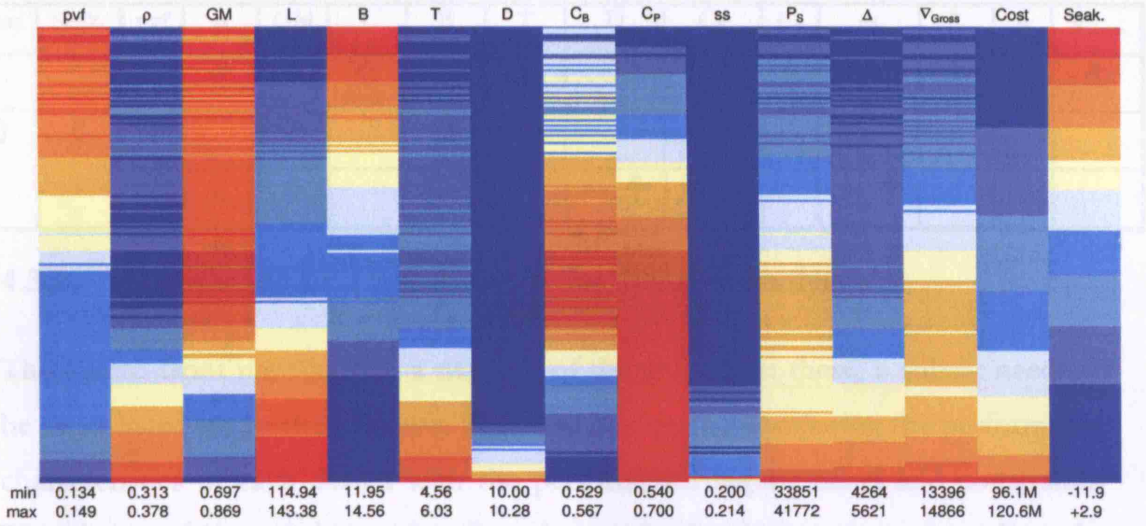

Figure 4-4: A sample colour diagram showing variation in design parameters and performance characteristics for a Pareto-front consisting of 181 designs

The last two columns represent the two objectives: cost and seakeeping. The designs on the Pareto-front have been sorted in the increasing order of the first objective (cost, in this case). Hence, moving from the top of the colour diagram to the bottom, cost varies from blue to red (i.e., it increases), while seakeeping changes from red to blue (hence, it decreases, i.e. improves). The colour variations in the other columns indicate the associated changes in design parameters. For example, looking at the first column (pvf), the colour varies from red to blue. This indicates that designs with low cost and bad seakeeping (i.e., designs near the top of the table) have relatively high values of pvf (red colour). Moving down the table, pvf changes from red to blue, indicating that as cost increases and seakeeping improves, pvf reduces. Similarly, each column can be studied and the trends examined. The general trends of all parameters can be tabulated, for example, as shown in Table 4-2. The table shows how each parameter changes when cost increases (or, equivalently, seakeeping improves). The parameters that show an increasing trend are shown in the first row; those that show a decreasing trend is shown in the second row; those

that show little variations or irregular trends are shown in the third row. Bold arrows (⇧,⇩) indicate strong trends compared to the normal arrows (↑,↓). When a parameter remains constant, or when the trends are unclear or irregular, it is indicated by '↔'.

Table 4-2: Trends of the design parameters in relation to the performance characteristics, for the colour diagram shown in Figure 4-4

Cost	Seak.	pvf	ρ	GM	L	B	T	D	C_B	C_P	ss	P_s	Δ	∇_{Gross}
			↑		⇧		↑			⇧		↑	↑	↑
⇧	⇩	↓		↓		⇩								
								↔,↑	↑,↓		↔,↑			

4.3.2. Short-listing of a few designs for detailed analyses

The Pareto-front may contain a number of designs. From these, a subset needs to be short-listed for further analysis. This may be done by comparing the performance characteristics of each design with the performance requirements and constraints. The characteristics of the surrounding designs in the design space, as well as the performance space, may also be taken into account. This process of short-listing designs is somewhat subjective: the designer's judgement plays a large part in the number of designs short-listed as well as the choice of designs. For example, suppose the customer has specified a seakeeping requirement, but the Pareto-front indicates that the corresponding cost is much higher than the customer's budget. In this case, the designer may decide to choose one design at the customer's budget (which has less seakeeping quality than desired), another design with the required seakeeping quality (but at a much higher cost), and one or two additional designs as a compromise between cost and seakeeping. These may be sufficient if the trends of design parameters and performance characteristics, as seen from the colour diagram, are fairly regular. However, in some cases, the Pareto-front may show discontinuities or non-linearities (for example, as seen in Section 6.2.3). Different visualisation schemes may help to spot such discontinuities in the Pareto-front. Such designs may not usually be robust, where a non-robust design occurs when any small changes in one or more design variables may result in rather large changes in performace. However, there could be exceptions. For instance, the designs S34 and

S35 discussed in Section 6.2.3 (see Table 6-11) are both robust designs (which can be verified using design space exploration), though they lie on either side of a discontinuity in the Pareto-front. In such cases, the designer may find it advantageous to include the designs surrounding the discontinuities in the short-list to analyse them further.Moreover, sometimes the detailed analysis of the short-listed designs may reveal additional information about the structure of the Pareto-front that may prompt the designer to add more designs to the short-list and analyse them in detail. In summary, the process of short-listing designs from the Pareto-front is not straightforward. Further information on this can be found in Appendix K.

After the short-listing process, each design in the short-list is analysed in detail, as explained in the following subsections.

4.3.3. Exploration of the design space around each design in the short-list

For each short-listed design, the nearby design space is explored by varying one independent design variable at a time to study its effect on the objectives as well as ship particulars. The results are presented as sensitivity plots, showing the variation in performance and ship particulars against each design variable.

The procedure for design space exploration is similar to the Parametric Survey that follows the Initial Sizing process in the UCL MSc Ship Design Procedure (see Section 6.1.1). First, one of the independent design variables is chosen (i.e., D, ss, C_B, C_P, W_{pay} or V_{pay}). These variables are considered independent in terms of the UCL design synthesis. The value of the chosen design variable is varied within a short range (typically $\pm 10\%$). Corresponding ships are synthesised and their performance analysed. Then, variations in performance and ship particulars are plotted against this design variable. The plots would also indicate if any of the customer / designer constraints were violated.

As an example, consider the sample sensitivity plot for the design variable C_B shown in Figure 4-5. The original short-listed design is the middle one in the x-axis, with $C_B = 0.587$. There are two designs with lower values of C_B, and two designs with

higher values of C_B. The other independent design variables D, ss, C_P, W_{pay} and V_{pay} are the same for all five designs.

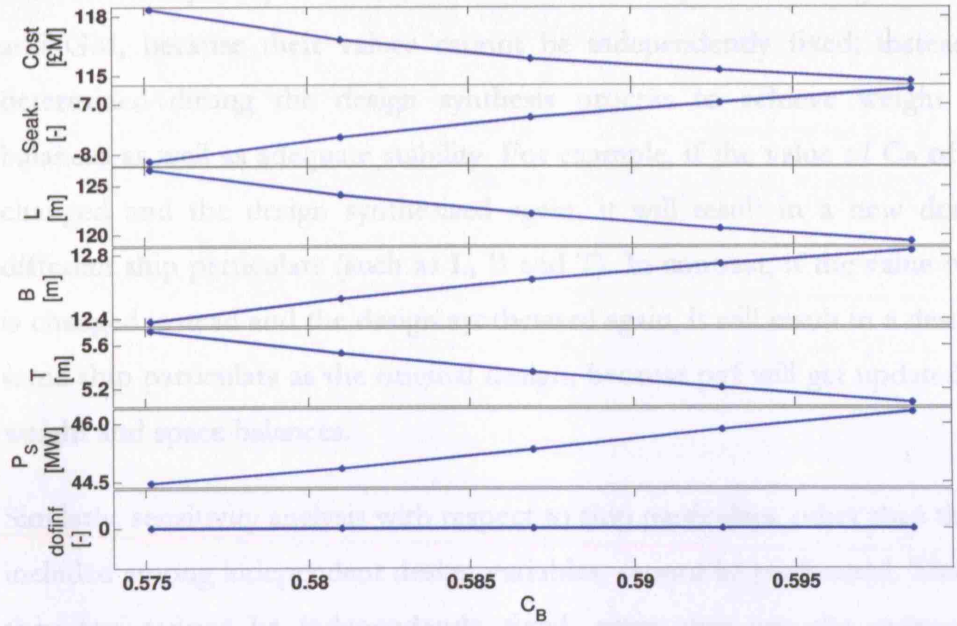

Figure 4-5: A sample sensitivity plot - C_B

The y-axis shows the variation against C_B of the two objectives, Cost and Seakeeping, (the latter expressed as the 'negative Bales Rank', as explained in Section 5.1.2) and relevant ship particulars (L, B, T and P_s) as well as a parameter named 'dofinf'. This parameter requires some explanation. It is used in the GA Tool to represent the 'degree of infeasibility' of a design. If dofinf = 0, the design does not violate any constraints; if dofinf > 0, one or more constraints have been violated. The value of dofinf is used within the GA Tool to penalise the objectives appropriately while calculating fitness values of a design: the higher the dofinf, the greater the penalty, which helps the genetic algorithms to distinguish between 'good' and 'bad' designs. More details on this are given in Appendix H.7.

Figure 4-5 shows that increase in C_B is beneficial for cost, but worsens seakeeping. When C_B increases, L and T decrease, while B and P_s increase. The parameter 'dofinf' remains zero for all five designs, indicating that none of the five designs violate any constraints; i.e., small variations in C_B do not cause infeasibility.

Similarly, variations with respect to the other independent design variables (D, ss, C_P, W_{pay} and V_{pay}) can also be plotted and the general trends observed. However, such sensitivity analysis cannot be done for the 'dependent' design variables pvf, ρ and GM, because their values cannot be independently fixed; instead, they are determined during the design synthesis process to achieve weight and space balances as well as adequate stability. For example, if the value of C_B of a design is changed and the design synthesised again, it will result in a new design having different ship particulars (such as L, B and T). In contrast, if the value of pvf alone is changed instead and the design synthesised again, it will result in a design with the same ship particulars as the original design, because pvf will get updated to achieve weight and space balances.

Similarly, sensitivity analysis with respect to ship particulars, other than those already included among independent design variables, cannot be performed. This is because they too cannot be independently fixed, since they are the output of design synthesis. For example, sensitivity analysis against L cannot be done because L is not an input to the design synthesis process, but an output of the process. Hence, variation in L can be observed only by changing an independent design variable (D, ss, C_P etc), and then synthesising a new design.

Exploration of the design space helps the designer to get some understanding of the region around the short-listed design in the following ways:

1. To check if small variations in any independent design variable will cause large variations in other design parameters or performance characteristics. A design whose performance characteristics are relatively insensitive to small changes in any independent design variable can be considered robust. Choosing such a design over a less robust one will ensure that if some design parameters change later in the design process, the performance characteristics will not be too adversely affected.

2. To verify if small variations in any design variable will cause infeasibility or constraint violation. For example, suppose the L/D of the short-listed design

has a value near its upper bound. In this case, if a decrease in D corresponds to an increase in L, it might violate the L/D constraint, which can be identified from the sensitivity plots. A design that causes infeasibility or constraint violation may be less preferable over another design that stays well within the constraint bounds.

3. To examine whether small variations in any design variable will result in a design with better overall performance characteristics. This is important because genetic algorithms cannot guarantee convergence to the true Pareto-front; hence there is always a low probability that small variations in one or more design variables may result in an improved design.

4.3.4. Exploration of the performance space around each design in the short-list

For each short-listed design, the local performance space is explored by choosing a few designs in its neighbourhood. The slopes along each objective are examined. This may be rather trivial when there are just two objectives, because the slopes are clearly visible in a 2D-plot. However, it can be useful when there are more objectives to consider, by providing the designer with a sense of the "fitness landscape" around the chosen design, i.e., the local shape of the Pareto-front in the performance space.

The procedure adopted for performance space exploration is as follows. First, the Pareto-front is filtered by specifying appropriate lower and/or upper bounds for each objective. This is to focus on a small region in the performance space around the short-listed design. Now the designs within this small region are sorted in the ascending order of one objective (say, Obj-K). Suppose the short-listed design is n^{th} in the sorted list; then, designs n-2, n-1, n, n+1 and n+2 are selected. Each objective is plotted against the design number (n-2, n-1, ..., n+2). The shapes of the plots indicate the local slopes of the Pareto-front along Obj-K.

This process may be repeated by again filtering the Pareto-front appropriately and sorting it with respect to another objective (say Obj-M). If the short-listed design is

p^{th} in the sorted list, designs p-2, p-1, p, p+1 and p+2 are chosen. (Note that these designs may be different from those obtained for Obj-K). Again, each objective is plotted against design number (p-2, p-1, …, p+2) to get the local slopes of the Pareto-front along Obj-M. This process can be repeated for all the objectives.

Exploration of the performance space helps in the following ways:

1. To check if the short-listed design lies near a cliff or on a plateau. Such discontinuities are easy to spot when there are just two objectives, such as the "jump" near the middle of the Pareto-front shown in Figure 4-6. However, when there are more objectives, such discontinuities are impossible to spot by visual examination of the whole n-dimensional Pareto-front. The local slopes plots are helpful in such circumstances.

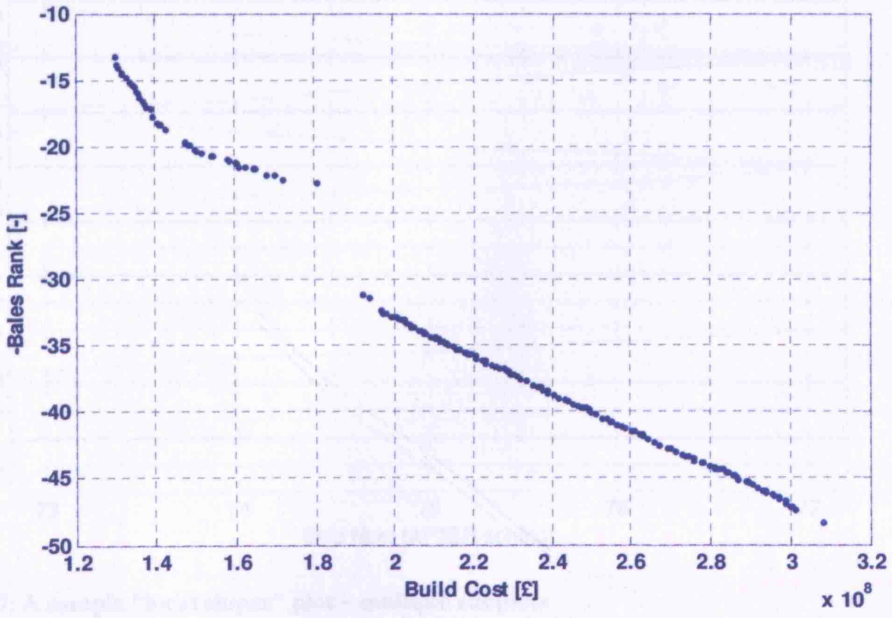

Figure 4-6: A Pareto-front showing discontinuity

2. To examine the design space of the surrounding designs to find out if there are any large differences in design parameters. In general, designs having similar performance will have similar design parameters as well. In other words, they lie close together in the performance space as well as design space. However, there may be cases when designs lying close together in the performance space may come from different regions of the design space.

Such cases are interesting because similar performance can be achieved by ships having rather different design parameters: the designer is given the freedom to compare the design parameters of these ships and choose the one that is most suitable in terms of design aspects other than the specific performance characteristics considered in the Pareto-front analysis.

An example of local slopes plots for two objectives is shown in Figure 4-7. The short-listed design is number 75. The two designs each to its left and right are the ones surrounding the short-listed design, arranged in the ascending order of UPC. The corresponding ship particulars are shown in each sub-plot. It is seen that the ship particulars follow a regular pattern.

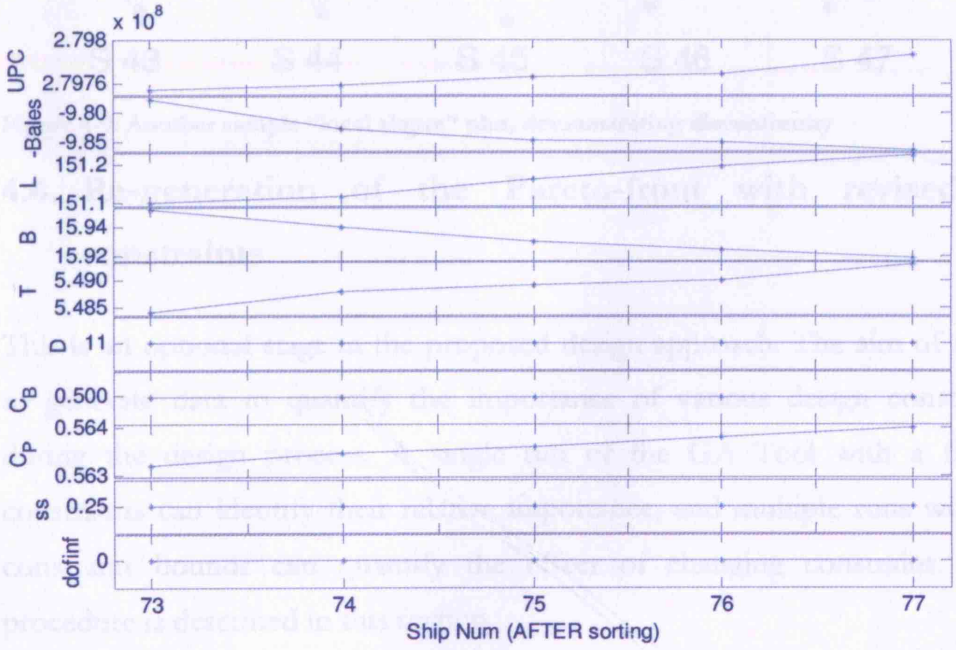

Figure 4-7: A sample "local slopes" plot – multiple subplots

Sometimes it is better to look at the results in the form of star plots, for example, as shown in Figure 4-8. Each "star" represents one ship design, and each "spoke" within a star represents one design parameter or performance characteristic. The length of the spoke is proportional to the value of the parameter relative to other designs: the longer a spoke the larger the value of the parameter. Thus, star plots provide a quick qualitative comparison of many designs. For more details of star plots and their uses, see Appendix J.7.

Figure 4-8: A sample "local slopes" plot – star plots

In Figure 4-8, the five designs seem rather similar, indicating that there are no large variations in design parameters. If there were any large changes in design parameters, it would be easy to spot them from star plots. An example for this is shown in Figure 4-9, where S46 and S47 are clearly different from S43, S44 and S45.

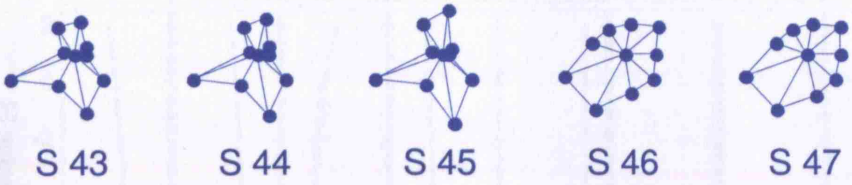

Figure 4-9: Another sample "local slopes" plot, demonstrating discontinuity

4.4. Re-generation of the Pareto-front with revised set of constraints

This is an optional stage in the proposed design approach. The aim of this stage is to generate data to quantify the importance of various design constraints used during the design process. A single run of the GA Tool with a fixed set of constraints can identify their relative importance, and multiple runs with different constraint bounds can quantify the effect of changing constraint levels. The procedure is described in this section.

A fixed set of design constraints are used during one run of the GA Tool. These constraints include both the bounds of the design variables (such as D and C_B) and the bounds of the soft constraints (such as L/B and B/T). After generating the Pareto-front, one can look at the corresponding constraints plot to identify the important constraints. An example constraints plot is shown in Figure 4-10. The plot shows the actual values of the design constraints (the blue data points) for all designs on the Pareto-front. The lower and upper bounds of each constraint are

included for comparison: these are the vertical black and red dashed lines at the left and right sides of each subplot.

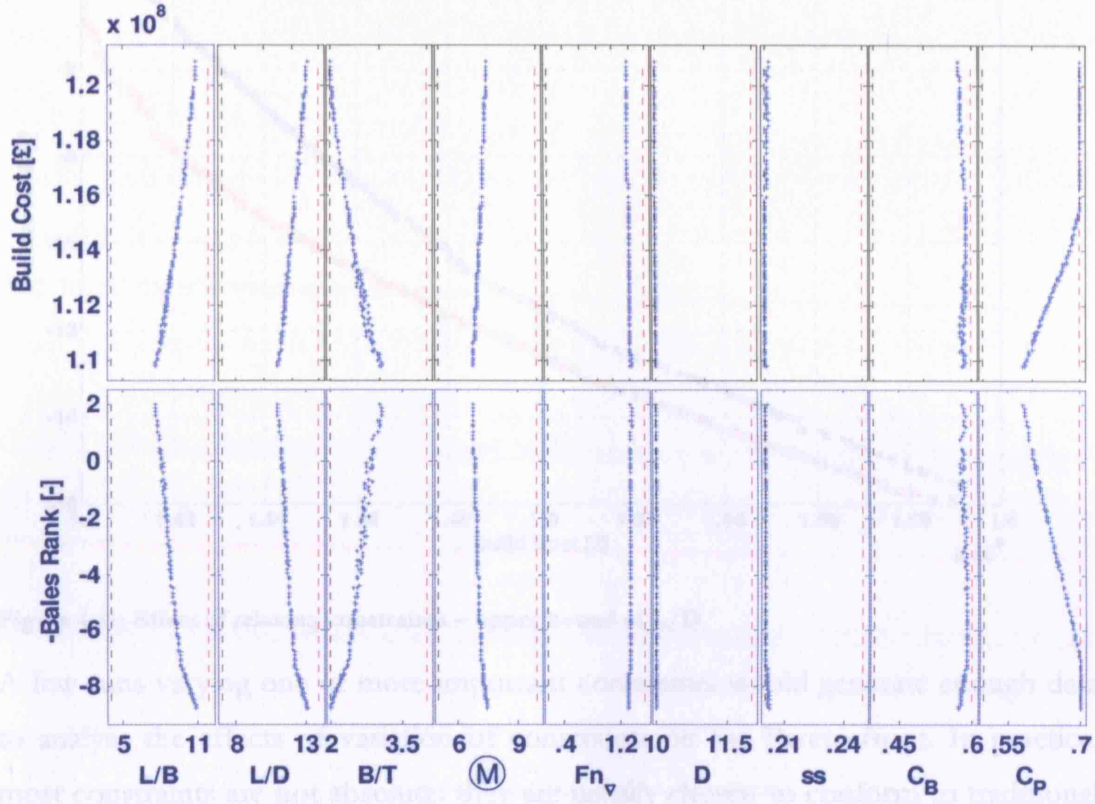

Figure 4-10: A sample constraints plot

From the constraints plot, it is seen that the values of D are close to its lower bound throughout the Pareto-front. Hence, relaxing it should certainly help in improving the Pareto-front. On the other hand, Ⓜ (circular M) remains well within its bounds; hence relaxing them is unlikely to have any effect on the Pareto-front. Similar conclusions can be reached regarding the other constraints.

After examining constraints plots, the designer may decide to find out how much improvement in the Pareto-front can be obtained by relaxing some constraints. Thus, the GA Tool is re-run after relaxing one or more constraints. An example demonstrating the improvement in a Pareto-front obtained by relaxing the upper bound of L/D is shown in Figure 4-11.

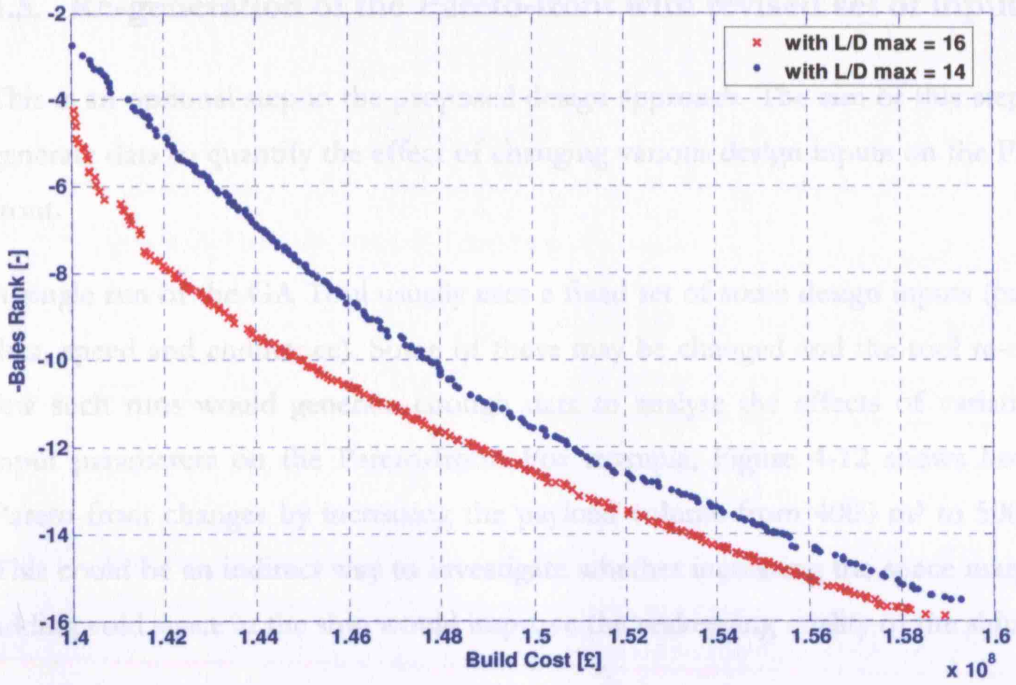

Figure 4-11: Effect of relaxing constraints – upper bound of L/D

A few runs varying one or more important constraints would generate enough data to analyse the effects of variation of constraints on the Pareto-front. In practice, most constraints are not absolute: they are usually chosen to conform to traditional ship shapes and proven hull forms, or to ensure validity of the performance analysis methods used. In such cases, it may be possible to relax their bounds if necessary. If some of them result in substantial improvement of the Pareto-front in the region of interest, the designer may think of measures that would allow the concerned constraint to be relaxed if practical, in consultation with the customer. For example, if relaxing L/D slightly can cause a large improvement in performance, it may be possible to improve structural design to allow unusually high L/D and achieve this performance. (In this case, the Pareto-front will have to be re-generated after modifying the weight estimate algorithms within the GA Tool to reflect the new structural design). In summary, multiple runs with varying constraint bounds are useful to quantify their effect on the quality of the Pareto-front.

4.5. Re-generation of the Pareto-front with revised set of inputs

This is an optional step in the proposed design approach. The aim of this step is to generate data to quantify the effect of changing various design inputs on the Pareto-front.

A single run of the GA Tool usually uses a fixed set of some design inputs (payload data, speed and endurance). Some of these may be changed and the tool re-run. A few such runs would generate enough data to analyse the effects of variation of input parameters on the Pareto-front. For example, Figure 4-12 shows how the Pareto-front changes by increasing the payload volume from 4000 m^3 to 5000 m^3. This could be an indirect way to investigate whether increasing the space margin or adding void space in the ship would improve the seakeeping quality of the ship.

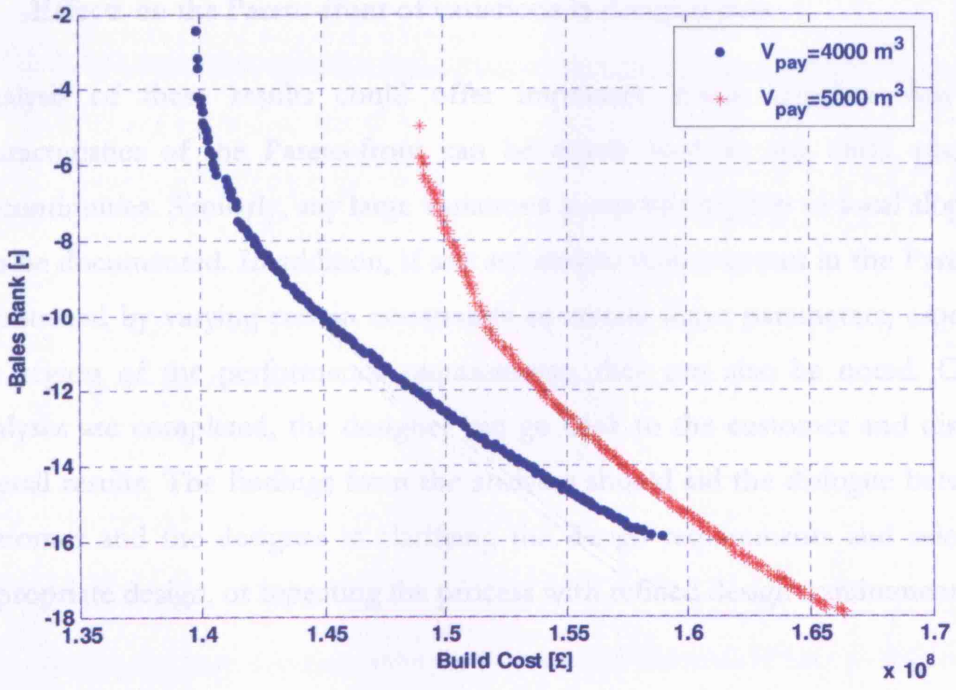

Figure 4-12: Effect of varying design inputs - payload volume

4.6. Customer-designer dialogue

The tasks listed in the previous subsections generate numerous results, such as:

- The Pareto-front of the original run (both in the performance space and the design space) and the set of short-listed designs
- Results of exploring the design space around each short-listed design (sensitivity plots)
- Results of exploring the performance space around each short-listed design (local slopes plots)
- Effects on the Pareto-front of variations in design constraints
- Effects on the Pareto-front of variations in design inputs

Analysis of these results could offer important design insights. Any special characteristics of the Pareto-front can be noted, such as any cliffs, plateaus or discontinuities. Similarly, any large variations in sensitivity plots or local slopes plots can be documented. In addition, if any substantial improvement in the Pareto-front is obtained by varying certain constraints or certain input parameters, especially in the region of the performance requirements, they can also be noted. Once the analyses are completed, the designer can go back to the customer and discuss the overall results. The findings from the analyses should aid the dialogue between the customer and the designer in clarifying the design requirements and selecting an appropriate design, or repeating the process with refined design requirements.

4.7. Potential applications of the proposed design approach

There seem to be three potential applications for the proposed design approach. Firstly, it can be used to generate design options during the concept design stage. Secondly, it can be used to modify a parent design aiming to improve its performance. Thirdly, it can be used in the early stages of feasibility studies to handle design changes that demand modifications to important design parameters. These three uses are explained and demonstrated in the following subsections.

4.7.1. To undertake ab initio concept design

The aim of the concept design stage is to generate potential design options based on an outline or preliminary set of design requirements and use the results to elucidate the design requirements with the customer. Using the GA Tool, the concept design process can be carried out in three phases:

- In the first phase, the GA Tool is used to generate the Pareto-front for a postulated set of design requirements. The Pareto-front is then examined to identify the most suitable designs, which are then analysed further.

- In the second phase (which is optional), one or more design constraints are relaxed with a view to identifying those constraints that most severely restrict the Pareto-front.

- In the third phase (which is also optional), one or more input parameters are changed in order to identify their effects on the Pareto-front.

See Section 5.1 for a demonstration of the application of the proposed design approach for ab initio concept design.

4.7.2. To modify a parent design

Sometimes a design may already exist and the aim may be to find possible improvements in performance with minor modifications in design parameters. The

process is essentially the same as for ab initio concept design, except for the narrower ranges for the design variables. See Section 5.2 for an example.

4.7.3. To handle design changes during the design process

Very often, the design chosen at the end of the concept design stage may require changes during the post-concept or early feasibility stages. Changes may be needed because of design issues (such as the changes required by more detailed and accurate design calculations). At other times, the customer may ask for changes, such as an increase in top speed or reduction in cost. Usually, the later such changes are identified, the more expensive they are to carry out. Besides, it may not be obvious which design parameters need to be changed to get the desired results without adversely affecting other design aspects. Ideally, the desired outcome should be achieved with minimal modifications to important design parameters. The GA Tool can be used to study this, though its utility will be limited as design departure increases in depth.

As an example scenario, consider a design for which the detailed damage stability analysis showed that the stability is insufficient. One way to remedy this problem (apart from changing the subdivision and compartment layout) is to increase the beam. The designer would like to achieve the required increase in beam with minimal change in length so that the main deck layout would not be affected. Minimal change in draught could also be preferred, say, to avoid repeating the structural analysis. Traditionally, this would be a tedious process involving trial and error taking up a lot of time for re-design and analysis. Using the GA Tool, this scenario can be studied by using target values for length and draught as additional objectives. This will generate many design options that can be examined and the most suitable can be one chosen. A demonstration of similar scenarios is given in Section 5.3.

Having examined the proposed design approach and identified its potential applications, the next chapter demonstrates these applications with three examples with fictitious sets of design requirements.

5. The proposed design approach – demonstrations of potential applications

The last chapter described the proposed design approach and identified three potential applications for it. This chapter demonstrates how the proposed design approach can be used for these three potential applications. Fictitious sets of design requirements are used for demonstration. A diagram relating various sections within this chapter and relevant appendices is shown in Figure 5-1.

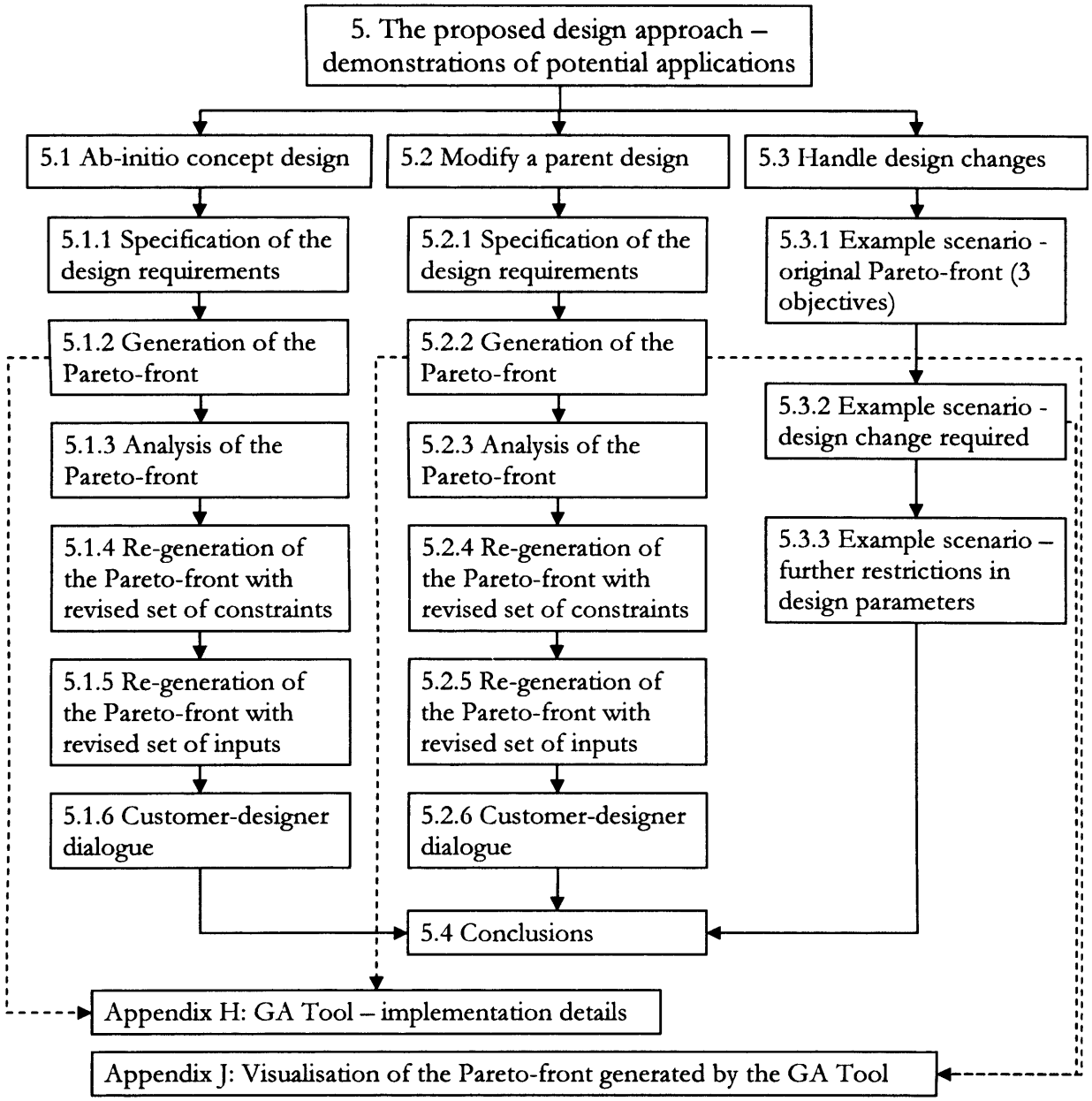

Figure 5-1: Outline of Chapter 5

5.1. Application of the proposed design approach for ab-initio concept design

This section will demonstrate the application of the proposed design approach for concept design. A two-objective problem is considered with a fictitious set of design requirements. The step-by-step design process is described in the following subsections.

5.1.1. Specification of the design requirements

The design requirements considered for this demonstration are summarised below. Some of the values are admittedly not typical and are probably beyond the usual limits; this has been done to demonstrate some key characteristics of Pareto-fronts relevant in the context of the proposed design approach.

design inputs

- Payload weight 1000 t
- Payload volume 3000 m^3
- Maximum speed 30 kn
- Endurance speed 18 kn
- Endurance 5000 nm

design objectives

- Minimise build cost (preferably, below £140M)
- Maximise seakeeping capability

The constraints used for the current run are given in Table 5-1. This constraints set is identified as 'C01'. (More constraint sets will be dealt with later in Section 5.1.3). Design variables should preferably lie within the constraint bounds.

Table 5-1: Design constraints considered

Constr. ID		D	ss	C_B	C_P	B/T	L/B	L/D	Ⓜ
C01	min	10	0.20	0.40	0.50	2	4	7	5
	max	12	0.25	0.60	0.70	4	12	14	10

5.1.2. Generation of the Pareto-front

The design requirements were used as input to the GA Tool. The standard set of GA parameters was used (see Appendix H). Minimisation of build cost was selected as the first objective. Maximisation of Bales Rank, which represents a figure of merit for the overall seakeeping quality of a ship, was selected as the second objective. Since the GA Tool treats all objectives to be minimised, the minimisation of the negative of Bales Rank is done instead of the maximisation of Bales Rank.

The Pareto-front resulting from this set of input data is shown Figure 5-2. Five separate runs are shown, each run for 500 generations. All the five runs, R1 to R5, converge to the same Pareto-front, except for a little scatter at each end.

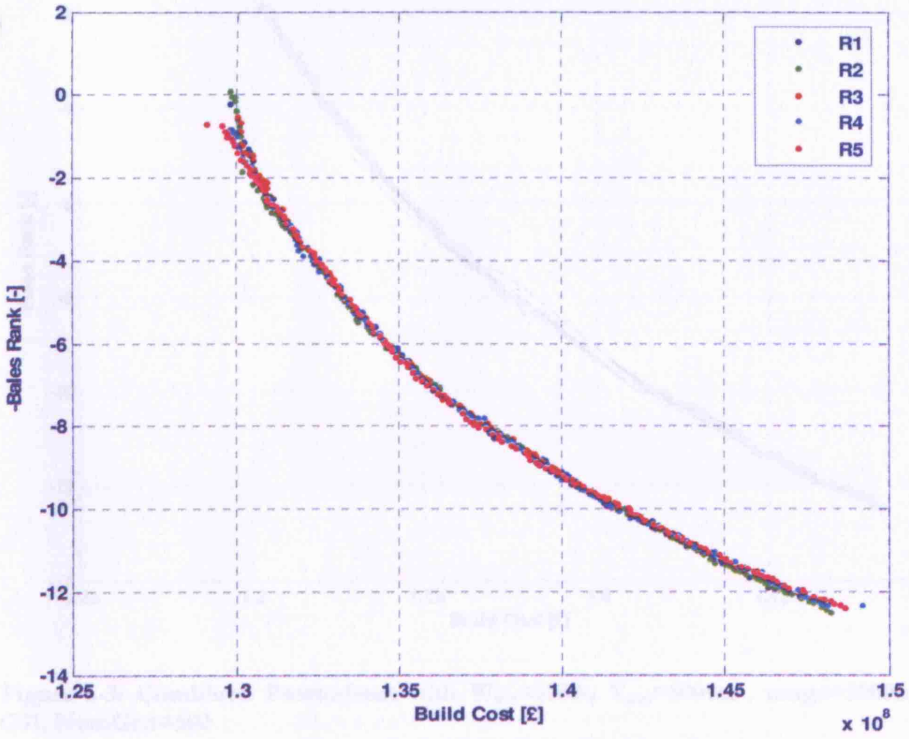

Figure 5-2: Pareto-fronts from five runs of the GA Tool; W_{pay}=1000t, V_{pay}=3000m³, range=5000nm, constraint set C01, NumGen=500

If the designer is interested in either end of the Pareto-front, where the convergence has not been very good, the design variables can be narrowed down to concentrate on this region and the Pareto-front regenerated to ensure better convergence. For example, suppose the designer is interested in designs with cost approximately £130M, which is near the left end of the Pareto-front. In this case, the designs in this region have C_P values that fall within [0.50, 0.52]. The designer may then use these as the lower and upper bounds of C_P, instead of the large range of [0.50, 0.70] as listed in Table 5-1. This can be done for the remaining design variables (D, ss and C_B) and the GA Tool can be executed again, which would usually give better convergence.

The results of the five runs can be combined to form a single Pareto-front, as shown in Figure 5-3. In this case, there are 237 designs on the Pareto-front. All of them are feasible designs: i.e., they do not violate any constraints.

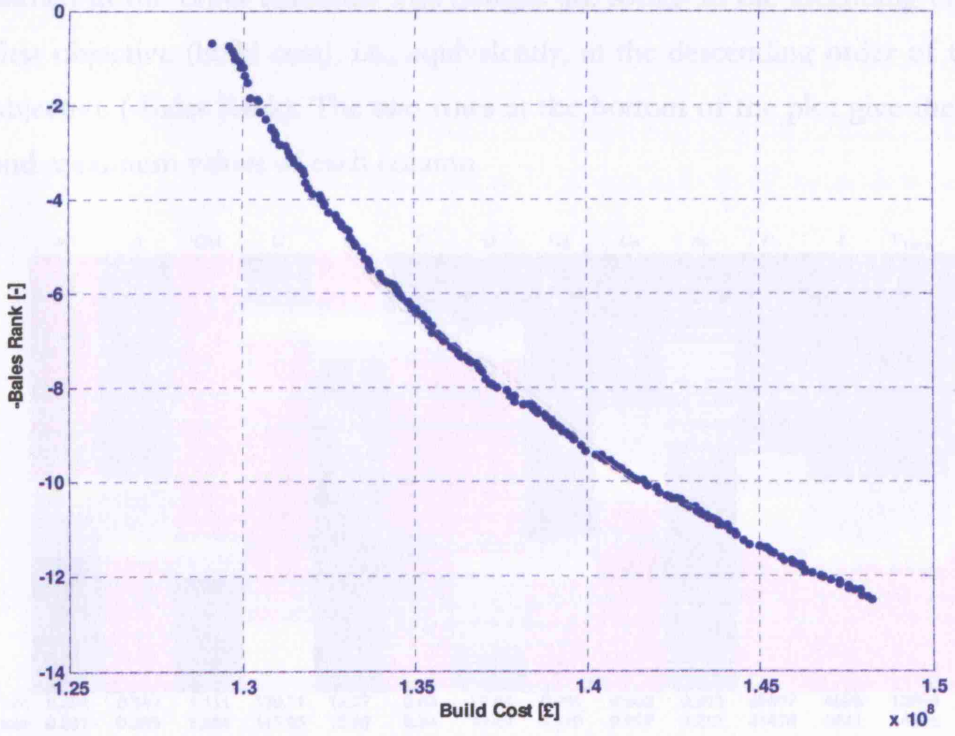

Figure 5-3: Combined Pareto-front with W_{pay}=1000t, V_{pay}=3000m³, range=5000nm, constraint set C01, NumGen=500

5.1.3. Analysis of the Pareto-front

The next step in the proposed design approach is the analysis of the Pareto-front. First the whole Pareto-front is examined to obtain the general trends of design parameters and performance characteristics considered as objectives while generating the Pareto-front. Next, a few representative designs are short-listed. The design and performance spaces around these short-listed designs are then examined in detail. These analyses are discussed in the following subsections.

Examination of the trends of design parameters and performance characteristics

A colour diagram of the Pareto-front is shown in Figure 5-4. The blue colour represents low values of parameters, and the red colour represents high values. The two objectives are shown in the last two columns, while the design parameters are shown in the other columns. The designs are sorted in the ascending order of the first objective (build cost), i.e., equivalently, in the descending order of the second objective (-Bales Rank). The two rows at the bottom of the plot give the minimum and maximum values of each column.

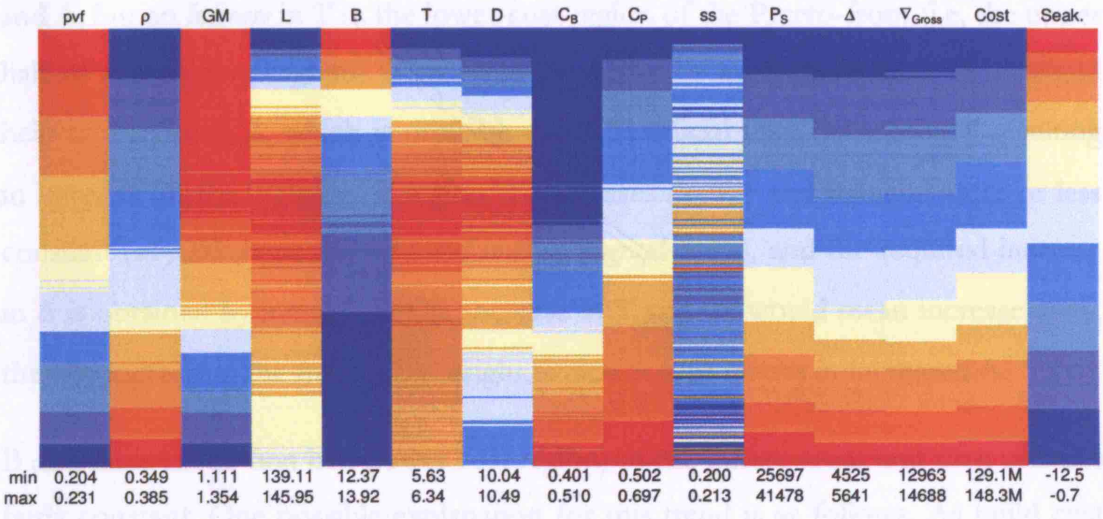

Figure 5-4: Colour diagram of the Pareto-front shown in Figure 5-3, consisting of 237 designs, showing the variation in design parameters and performance characteristics considered

The variation of colours indicates the trends of the parameters. Most of the parameters show fairly regular trends, with the exception of ss, which seems to

show considerable variation, albeit within a narrow range [0.200, 0.213]. The trends from the colour diagram are summarised in Table 5-2.

Table 5-2: Trends of the design parameters in relation to the performance parameters, for the colour diagram shown in Figure 5-4

Cost	Seak.	pvf	ρ	GM	L	B	T	D	C_B	C_P	ss	P_s	Δ	∇_{Gross}
⇧	⇩		⇧							⇧		⇧	⇧	⇧
		⇩		⇩		⇩								
					↑,↓		↑,↓	↑,↓	↔,↑		↔			

The table shows that improvement in seakeeping is obtained by increase in ρ, C_B, C_P, P_s, Δ and ∇_{Gross}, with corresponding reduction in pvf, GM and B. Interestingly, L, T and D seem to increase in the first half of the Pareto-front and slowly reduce thereafter. The explanation for this, along with the other general trends, is given below.

Bigger ships in general have better seakeeping. This is confirmed by the results which show that seakeeping is improved by increase in Δ and ∇_{Gross}. According to the Bales Rank formula (see Appendix H.6.5), seakeeping can be improved by increase in C_P, L and Δ, and decrease in T. The results do show an increase in C_P, L and Δ, but an *increase* in T in the lower-cost-region of the Pareto-front (i.e, the upper half of the colour diagram). This seems to occur because an increase in T would help in increasing Δ, which is probably more beneficial than decreasing T resulting in lower Δ. In the higher-cost-region, T decreases slightly and remains more or less constant (*why this happens is explained in the paragraph below*), and the required increase in Δ is obtained by increase in C_B. Increase in T and C_B would mean increase in P_s, thereby increasing the machinery weight, which in turn results in increased Δ.

B decreases in the first half (lower cost region) of the Pareto-front and then remains fairly constant. One possible explanation for this trend is as follows. As build cost increases both T and D increase, but their difference (freeboard) decreases. This, coupled with ss staying fairly constant, results in lower windage area, despite the increase in L. The reduction in windage area and the consequent reduction in wind

heeling moment reduce the required GM and consequently reduce B. The reduction in B coupled with increase in L and T results in increasing L/B and decreasing B/T. Once B/T reaches its lower bound, B cannot decrease and T cannot increase simultaneously. Thus, they stay fairly constant; in fact, both B and T decrease slightly such that B/T remains constant. The validity of reasoning can be verified by examining the constraints plot, shown in Figure 5-5, which confirms the trends of L/B and B/T with build cost.

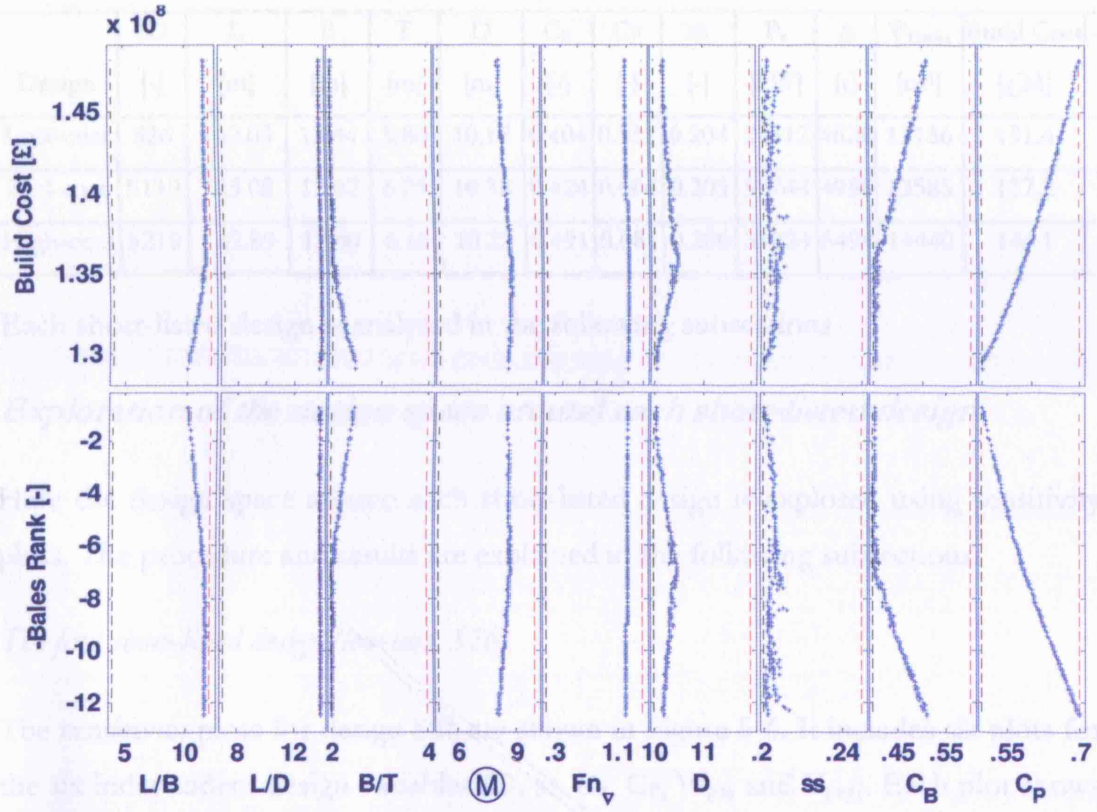

Figure 5-5: Constraints plot for the Pareto-front shown in Figure 5-3

The constraints plot confirms the increase in L/B and decrease in B/T in the lower-cost-region of the Pareto-front. Once B/T reaches its lower bound, C_B starts increasing, so that Δ can be increased to improve seakeeping. L/D remains on its upper bound throughout the Pareto-front, which probably prevents L from increasing further. The increase in C_B and C_P result in more volume in the underwater hull, and thus D decreases to maintain the required ∇_{Gross}. When D decreases, L also has to decrease to avoid L/D violating its upper bound. All these substantiate the trends observed in the colour diagram.

Short-listing of a few designs for detailed analyses

Having examined the Pareto-front consisting of a number of designs, the next task is to short-list a few designs for detailed analysis. For demonstration, it was decided to choose one design from the lower cost region, a second design from the higher cost region, and another design from the mid-region for detailed analysis. The characteristics of the short-listed designs are given in Table 5-3.

Table 5-3: Three designs short-listed from the Pareto-front

Design	ID [-]	L [m]	B [m]	T [m]	D [m]	C_B [-]	C_P [-]	ss [-]	P_s [kW]	Δ [t]	∇_{Gross} [m³]	Build Cost [£M]	-Bales [-]
Low-cost	S26	142.03	13.44	5.86	10.15	0.404	0.531	0.204	27312	4628	13136	131.4	-3.1
Mid-cost	S119	145.08	12.62	6.21	10.38	0.424	0.604	0.203	32744	4938	13585	137.2	-7.9
High-cost	S219	142.89	12.40	6.16	10.22	0.491	0.681	0.206	39824	5494	14440	146.1	-11.7

Each short-listed design is analysed in the following subsections.

Exploration of the design space around each short-listed design

Here the design space around each short-listed design is explored using sensitivity plots. The procedure and results are explained in the following subsections.

The first short-listed design (low-cost, S26)

The sensitivity plots for design S26 are shown in Figure 5-6. It includes six plots for the six independent design variables (D, ss, C_B, C_P, W_{pay} and V_{pay}). Each plot shows five design variants. The middle design in each plot is the same as S26. The other designs are with slight variation in the relevant independent design variable, with the other independent design variables staying the same as S26.

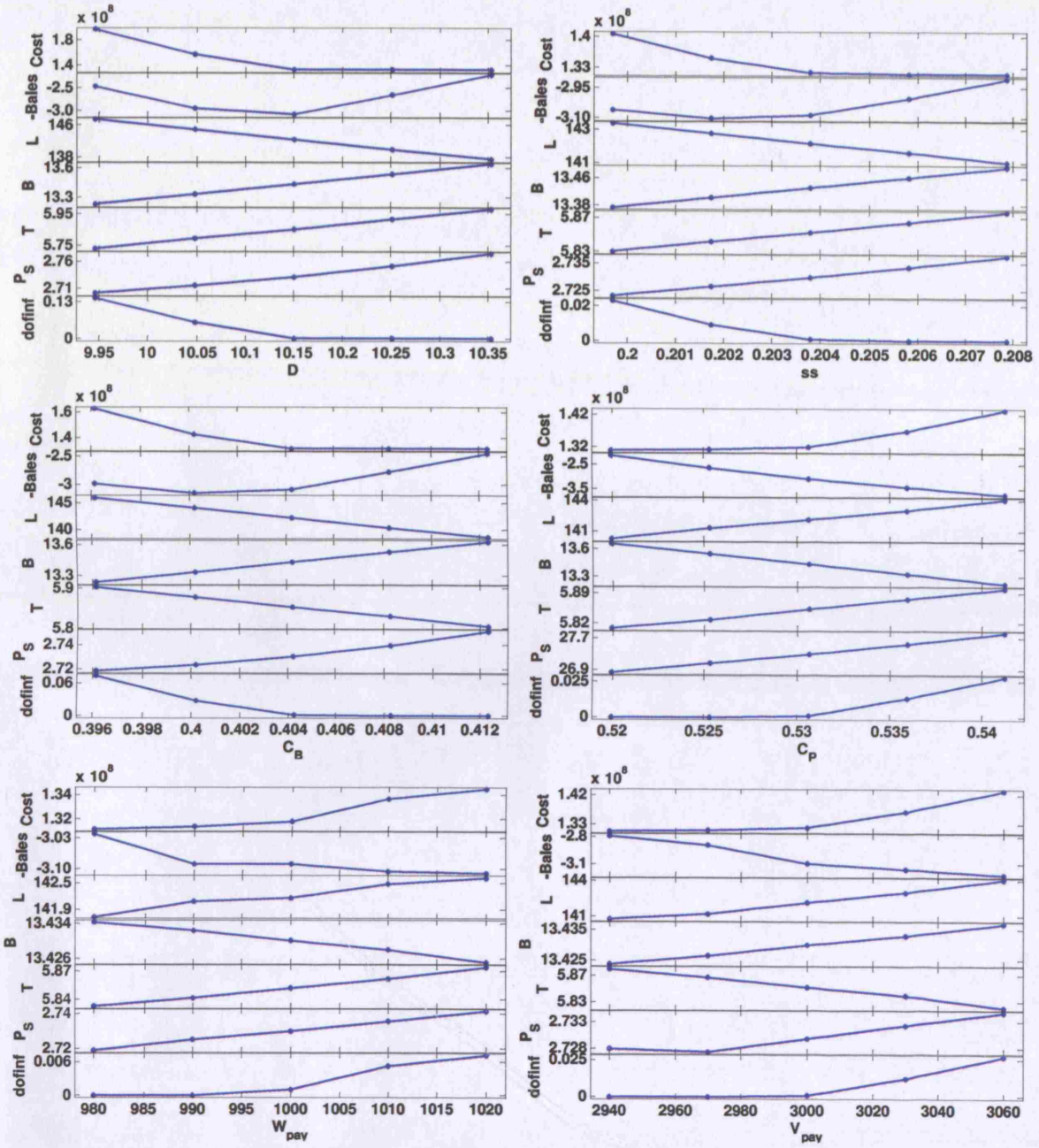

Figure 5-6: Sensitivity plots for the first short-listed design (low-cost, S26)

The sensitivity plots show that decreasing D, ss or C_B will result in infeasible ships (as indicated by the last graph in each subplot: dofinf > 0 for infeasible ships). Similarly, any increase in C_P, payload weight or payload volume will also result in infeasible ships. The cause of the infeasibility in each case is shown in Table 5-4. In all the cases, the upper bound of L/D is exceeded, in addition to D, ss and C_B crossing their lower bounds.

Table 5-4: Parameters that cause infeasibility – low-cost design (S26)

Parameter causing infeasibility	*comments*	*constraints violated*
D increase	-	
D decrease	infeasible	Upper bound of L/D; lower bound of D
ss increase	-	
ss decrease	infeasible	Upper bound of L/D; lower bound of ss
C_B increase	-	
C_B decrease	infeasible	Upper bound of L/D; lower bound of C_B
C_P increase	infeasible	Upper bound of L/D
C_P decrease	-	
W_{pay} increase	infeasible	Upper bound of L/D
W_{pay} decrease	-	
V_{pay} increase	infeasible	Upper bound of L/D
V_{pay} decrease	-	

Considering the feasible designs in the sensitivity plots, the trends can conveniently be tabulated as shown in Table 5-5. The table shows how the increase of each independent design variable affects the objectives and dependent design parameters. For example, in this case, increase in D will cause increase of -Bales Rank, as well as B, T and P_s, and decrease of L, while cost is not significantly affected. All these trends are reversed for decrease in D.

Table 5-5: Trends for the first short-listed design (S26) - summary

Independent design variable (Increase)	Objective (Increase)	Objective (Decrease)	Objective (Neutral)	Dependent parameters (Increase)	Dependent parameters (Decrease)	Dependent parameters (Neutral)
D	-Bales	-	Cost	B, T, P_s	L	-
ss	-Bales	-	Cost	B, T, P_s	L	-
C_B	-Bales	-	Cost	B, P_s	L, T	-
C_P	Cost	-Bales	-	L, T, P_s	B	-
W_{pay}	Cost	-Bales	-	L, T, P_s	B	-
V_{pay}	Cost	-Bales	-	L, B, P_s	T	-

The second short-listed design (mid-cost, S119)

The sensitivity plots for design S119 are shown in Figure 5-7.

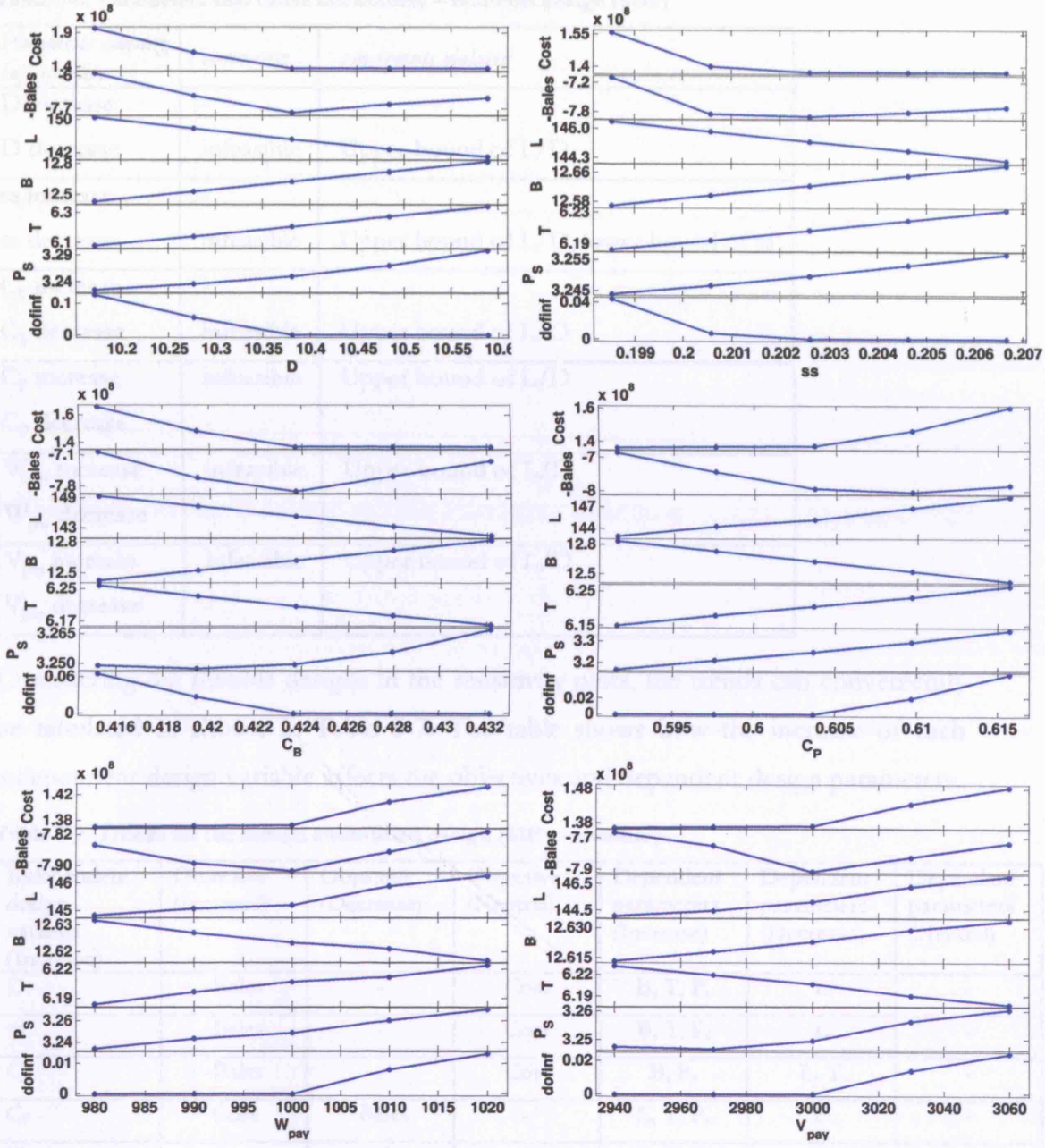

Figure 5-7: Sensitivity plots for the second short-listed design (mid-cost, S119)

The sensitivity plots show that decreasing D, ss or C_B will result in infeasible ships (as indicated by the last graph in each subplot: dofinf > 0 for infeasible ships). Similarly, any increase in C_P, payload weight or payload volume will also result in

infeasible ships. The cause of the infeasibility in each case is shown in Table 5-6. In all the cases, the upper bound of L/D gets violated, in addition to ss crossing its lower bound in one case.

Table 5-6: Parameters that cause infeasibility – mid-cost design (S119)

Parameter causing infeasibility	*comments*	*constraints violated*
D increase	-	
D decrease	infeasible	Upper bound of L/D
ss increase	-	
ss decrease	infeasible	Upper bound of L/D; lower bound of ss
C_B increase	-	
C_B decrease	infeasible	Upper bound of L/D
C_P increase	infeasible	Upper bound of L/D
C_P decrease	-	
W_{pay} increase	infeasible	Upper bound of L/D
W_{pay} decrease	-	
V_{pay} increase	infeasible	Upper bound of L/D
V_{pay} decrease	-	

Considering the feasible designs in the sensitivity plots, the trends can conveniently be tabulated as shown in Table 5-7. The table shows how the increase of each independent design variable affects the objectives and dependent design parameters.

Table 5-7: Trends for the second short-listed design (S119) - summary

Independent design variable (Increase)	Objective (Increase)	Objective (Decrease)	Objective (Neutral)	Dependent parameters (Increase)	Dependent parameters (Decrease)	Dependent parameters (Neutral)
D	-Bales	-	Cost	B, T, P_s	L	-
ss	-Bales	-	Cost	B, T, P_s	L	-
C_B	-Bales	-	Cost	B, P_s	L, T	-
C_P	Cost	-Bales	-	L, T, P_s	B	-
W_{pay}	Cost	-Bales	-	L, T, P_s	B	-
V_{pay}	Cost	-Bales	-	L, B, P_s	T	-

The third short-listed design (high-cost, S219)

The sensitivity plots for design S219 are shown in Figure 5-8.

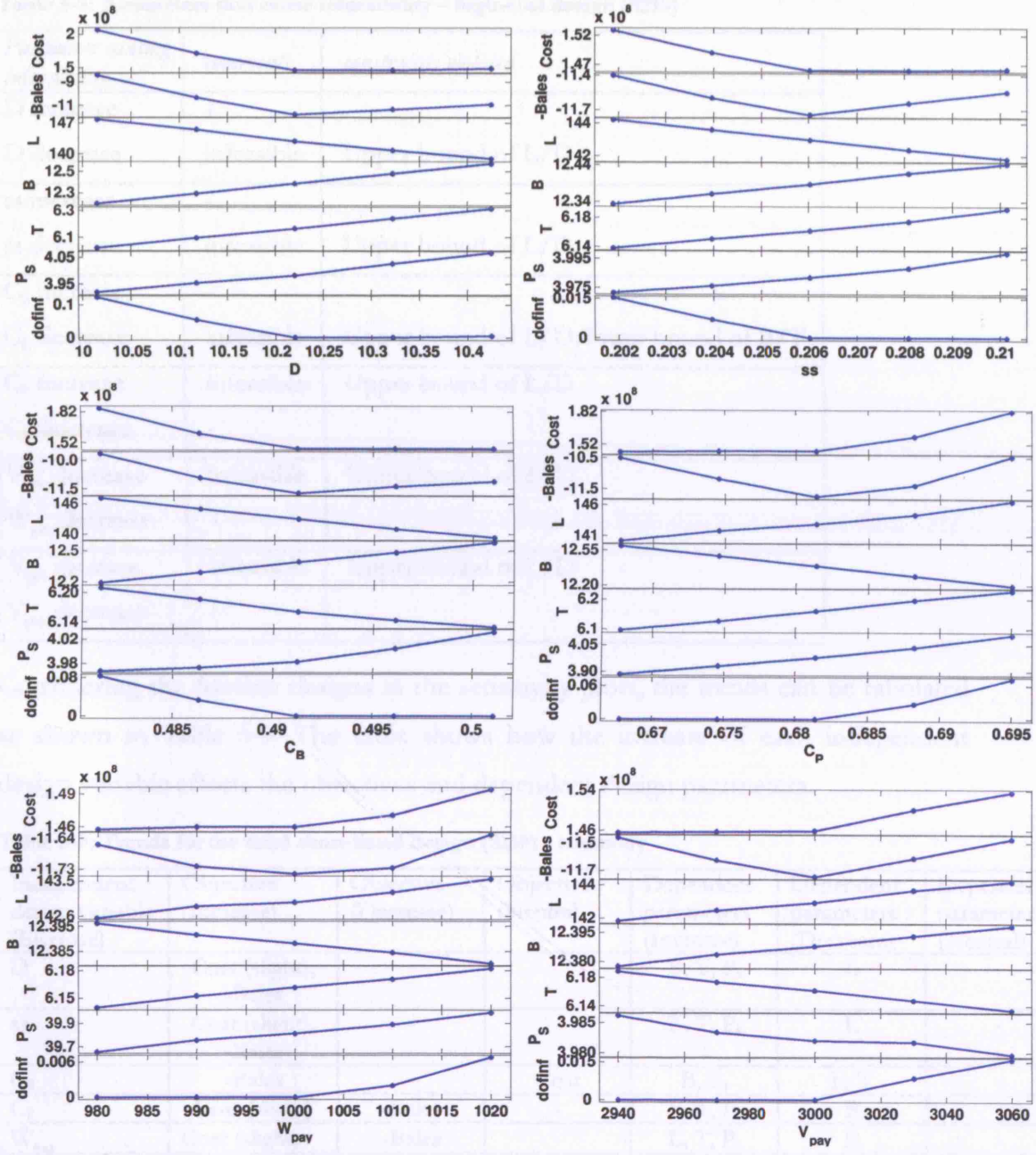

Figure 5-8: Sensitivity plots for the third short-listed design (high-cost, S219)

The sensitivity plots show that decreasing D, ss or C_B will result in infeasible ships (as indicated by the last graph in each subplot: dofinf > 0 for infeasible ships). Similarly, any increase in C_P, payload weight or payload volume will also result in

infeasible ships. The cause of the infeasibility in each case is shown in Table 5-8. In all the cases, the upper bound of L/D is exceeded, in addition to B/T crossing its lower bound in one case.

Table 5-8: Parameters that cause infeasibility – high-cost design (S219)

Parameter causing infeasibility	*comments*	*constraints violated*
D increase	-	
D decrease	infeasible	Upper bound of L/D
ss increase	-	
ss decrease	infeasible	Upper bound of L/D
C_B increase	-	
C_B decrease	infeasible	Upper bound of L/D; lower bound of B/T
C_P increase	infeasible	Upper bound of L/D
C_P decrease	-	
W_{pay} increase	infeasible	Upper bound of L/D
W_{pay} decrease	-	
V_{pay} increase	infeasible	Upper bound of L/D
V_{pay} decrease	-	

Considering the feasible designs in the sensitivity plots, the trends can be tabulated as shown in Table 5-9. The table shows how the increase of each independent design variable affects the objectives and dependent design parameters.

Table 5-9: Trends for the third short-listed design (S158) - summary

Independent design variable (Increase)	Objective (Increase)	Objective (Decrease)	Objective (Neutral)	Dependent parameters (Increase)	Dependent parameters (Decrease)	Dependent parameters (Neutral)
D	Cost (slight), -Bales	-	-	B, T, P_s	L	-
ss	Cost (slight), -Bales	-	-	B, T, P_s	L	-
C_B	-Bales	-	Cost	B, P_s	L, T	-
C_P	Cost (slight)	-Bales	-	L, T, P_s	B	-
W_{pay}	Cost (slight)	-Bales	-	L, T, P_s	B	-
V_{pay}	Cost (slight)	-Bales	-	L, B	T, P_s	-

Sensitivity of the three short-listed designs – qualitative comparison

The trends of the design parameters and objectives for the three short-listed designs are shown together in Table 5-10 for comparison. Increasing and decreasing trends

are indicated by the symbols '↑' and '↓' respectively, whereas indeterminate or insignificant variations are indicated by '↔'.

Table 5-10: Trends of design parameters and performance characteristics for the short-listed designs

	S26	S119	S219
Effect of increase in D			
Cost	↔	↔	↑ (slight)
-Bales Rank	↑	↑	↑
L	↓	↓	↓
B	↑	↑	↑
T	↑	↑	↑
P_s	↑	↑	↑
Effect of increase in ss			
Cost	↔	↔	↑ (slight)
-Bales Rank	↑	↑	↑
L	↓	↓	↓
B	↑	↑	↑
T	↑	↑	↑
P_s	↑	↑	↑
Effect of increase in C_B			
Cost	↔	↔	↔
-Bales Rank	↑	↑	↑
L	↓	↓	↓
B	↑	↑	↑
T	↓	↓	↓
P_s	↑	↑	↑
Effect of increase in C_P			
Cost	↑	↑	↑ (slight)
-Bales Rank	↓	↓	↓
L	↑	↑	↑
B	↓	↓	↓
T	↑	↑	↑
P_s	↑	↑	↑
Effect of increase in W_{pay}			
Cost	↑	↑	↑ (slight)
-Bales Rank	↓	↓	↓
L	↑	↑	↑
B	↓	↓	↓
T	↑	↑	↑
P_s	↑	↑	↑
Effect of increase in V_{pay}			
Cost	↑	↑	↑
-Bales Rank	↓	↓	↓
L	↑	↑	↑
B	↑	↑	↑
T	↓	↓	↓
P_s	↑ (slight)	↑ (slight)	↓ (slight)

The table shows that the design space exploration results in similar trends for the three designs. In other words, design space exploration leads to similar results irrespective of the region from which the design is chosen. This inference, however,

may not always be true: there may be cases when designs from different regions of the Pareto-front will show different trends during the design space exploration. This usually happens when there are discontinuities in the Pareto-front, for example as discussed in Section 6.2.3. In such cases, designs from different regions of the design space may show different trends.

In the present case, the effect on the objectives of changing a design variable falls into the following categories.

1. Cost remains constant, seakeeping improves/worsens (for changes in design variables D, ss, C_B)

2. One objective improves and the other worsens (for changes in design variables C_P, W_{pay} and V_{pay})

The first category is interesting since we can be sure to get an improved Pareto-front (improved seakeeping at constant cost) by suitably varying one of the corresponding design variables. But, from the plots, it can be seen that variation of the parameter required to get better seakeeping would result in the violation of one or more constraints. This confirms that the Pareto-front has reached convergence: if a design lay away from the Pareto-front, we should be able to find at least one of the design variables such that its slight variation would improve both the objectives (or improve one objective without worsening the other objective), without violating any design constraints.

Table 5-4, Table 5-6 and Table 5-8 show that small changes in some design variables result in constraint violation and infeasibility for variants of all the three designs. The upper bound of L/D and the lower bound of ss are important for all the three designs. In addition, the lower bounds of D and C_B are important for the lower cost design (S26), and the lower bound of B/T is important for the higher cost design (S219). These conclusions support the constraints plot as well (Figure 5-5).

Exploration of the performance space around each short-listed design

The last section explored the *design space* around each short-listed design. This involved changing each independent design variable by a small amount and examining its effect on design parameters as well as performance characteristics. In this section, the *performance space* around each short-listed design will be explored. This involves selecting a few surrounding designs in the performance space and examining their design parameters and performance characteristics. The designs are presented as star plots. A star plot template indicating the design parameter each 'spoke' represents is shown in Figure 5-9.

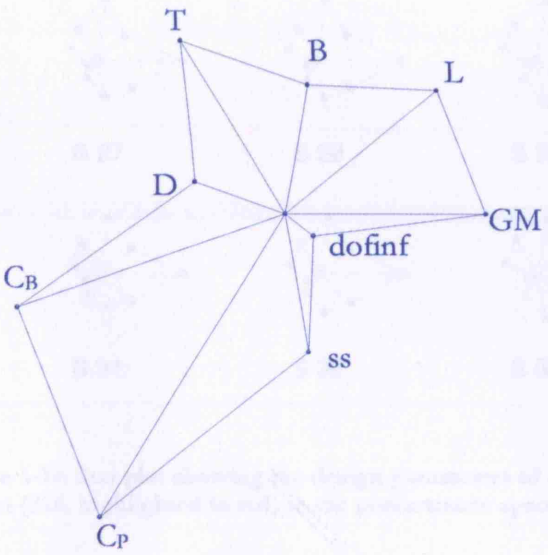

Figure 5-9: Star plot template showing the design parameter that each spoke represents

To explore the performance space, a few designs around each short-listed design are visualised at a time. This is shown in Figure 5-10, Figure 5-11 and Figure 5-12 for the three short-listed designs S26, S119 and S219. In each case, the nearby designs look the same, indicating that there are no drastic variations in design parameters in the vicinity of the three short-listed designs. The only exception is the slightly random variations in ss, especially for S219. This was found earlier while examining the colour diagram (Figure 5-4). It was found that the range of variation of ss in the whole Pareto-front is rather small (between 0.200 to 0.213, a variation of about 6%) and hence the random variations of ss as it appears here may be ignored. In spite of the small change in magnitude, the length of the spoke corresponding to ss seems to

vary a lot, which might seem surprising. This happens because all ranges of values, irrespective of their magnitude, are mapped to a normalised range of [0.1, 1], so that the lowest value is always plotted with a spoke length of 0.1 and the highest value with a spoke length of 1.

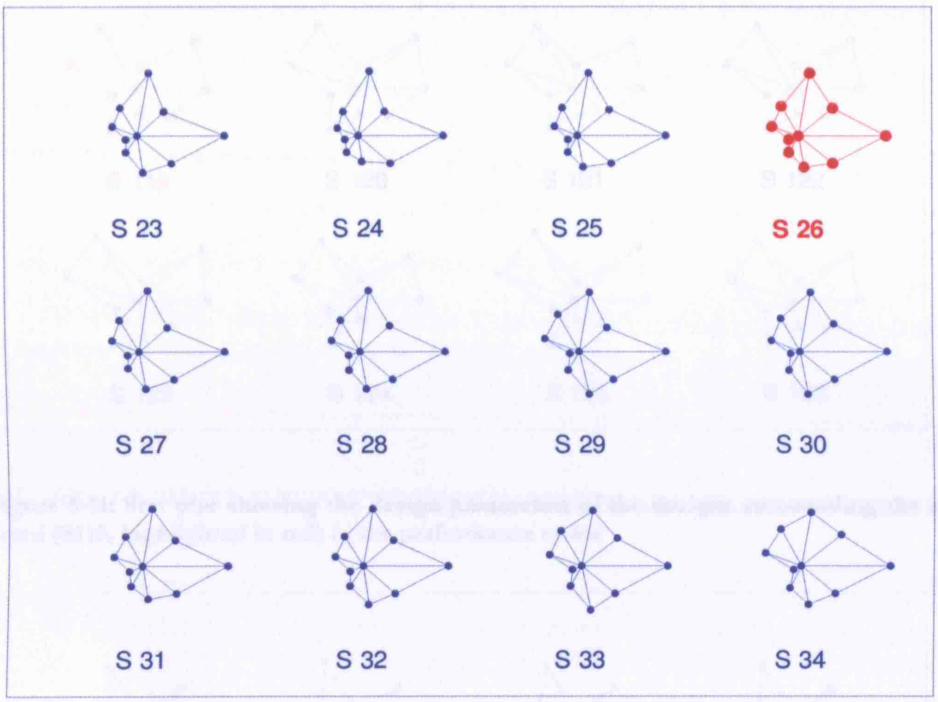

Figure 5-10: Star plot showing the design parameters of the designs surrounding the first short-listed design (S26, highlighted in red) in the performance space

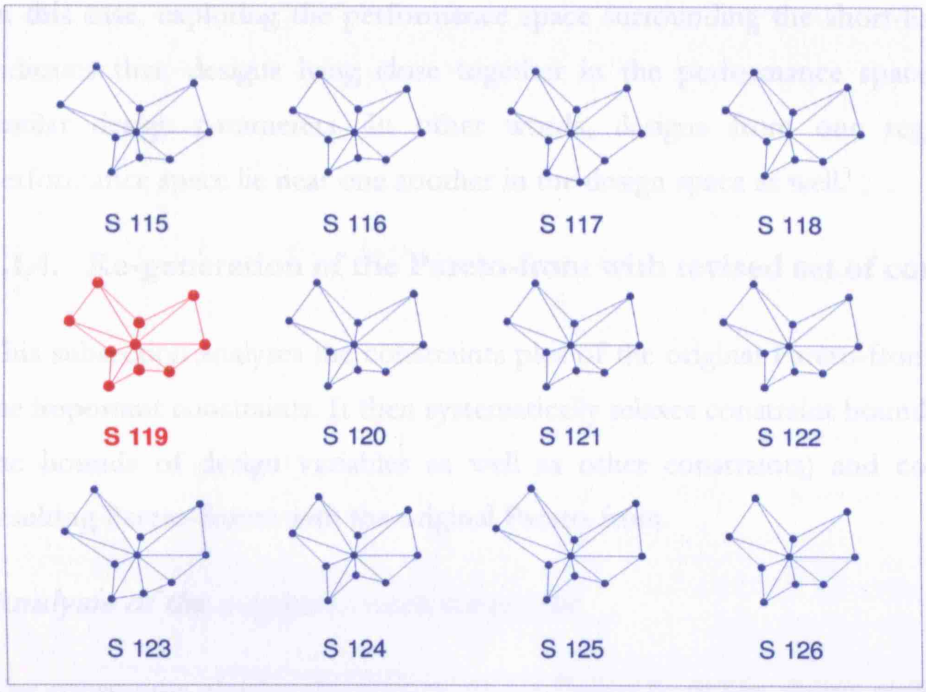

Figure 5-11: Star plot showing the design parameters of the designs surrounding the second short-listed (S119, highlighted in red) in the performance space

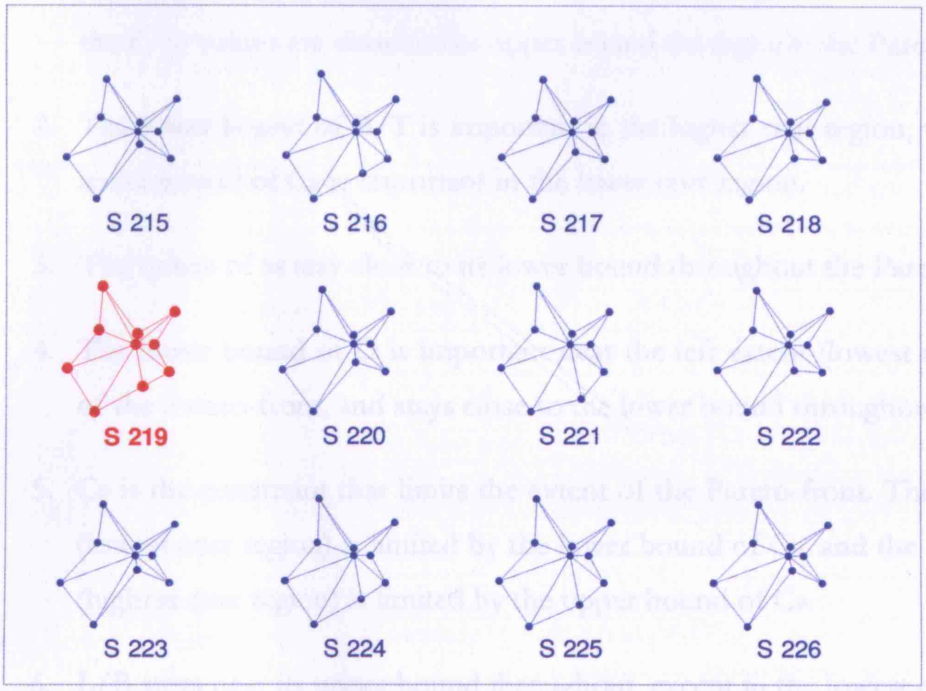

Figure 5-12: Star plot showing the design parameters of the designs surrounding the third short-listed design (S219, highlighted in red) in the performance space

In this case, exploring the performance space surrounding the short-listed designs indicates that, designs lying close together in the performance space have very similar design parameters. In other words, designs from one region of the performance space lie near one another in the design space as well.

5.1.4. Re-generation of the Pareto-front with revised set of constraints

This subsection analyses the constraints plot of the original Pareto-front to identify the important constraints. It then systematically relaxes constraint bounds (including the bounds of design variables as well as other constraints) and compares the resulting Pareto-fronts with the original Pareto-front.

Analysis of the original constraints plot

The constraints plot for the designs on the Pareto-front was shown earlier in Figure 5-5. The inferences from the constraints plot are:

1. The upper bound of L/D seems to be the most important constraint, since the L/D values are close to the upper bound throughout the Pareto-front.

2. The lower bound of B/T is important in the higher cost region, whereas the lower bound of C_B is important in the lower cost region.

3. The values of ss stay close to its lower bound throughout the Pareto-front.

4. The lower bound of D is important near the left extent (lowest cost region) of the Pareto-front, and stays close to the lower bound throughout.

5. C_P is the constraint that limits the extent of the Pareto-front. The left extent (lowest cost region) is limited by the lower bound of C_P, and the right extent (highest cost region) is limited by the upper bound of C_P.

6. L/B stays near its upper bound throughout, except in the lowest cost region.

7. The remaining constraints, Ⓜ and Fn_V, stay well within their bounds, and do not vary significantly.

From these, one can predict the expected effect on the Pareto-front of relaxing each constraint. This is summarised in Table 5-11.

Table 5-11: Expected effects of relaxing constraints on the quality of Pareto-front, based on the constraints plot (Figure 5-5)

Design variable / constraint	Lower / Upper bound)	Level of Importance	Expected effect of relaxing lower /upper bound on improving Pareto-front
D	lower bound	Imp.	Relaxing the lower bound should help to improve the Pareto-front near the left end of the Pareto-front (lowest cost region)
D	upper bound	Not imp.	-
ss	lower bound	Slightly imp.	Relaxing the lower bound may improve the Pareto-front throughout
ss	upper bound	Not imp.	-
C_B	lower bound	Imp.	Relaxing the lower bound should help improve the Pareto-front in the lower cost region
C_B	upper bound	Not imp.	-
C_P	lower bound	Imp.	Relaxing the lower bound should help extend the Pareto-front further to the left (lower cost region)
C_P	upper bound	Imp.	Relaxing the upper bound should help extend the Pareto-front further to the right (higher cost region)
B/T	lower bound	Very imp.	Relaxing the lower bound should help to improve the Pareto-front throughout, except near the left end (lowest cost region)
B/T	upper bound	Not imp.	-
L/B	lower bound	Not imp.	-
L/B	upper bound	Slightly imp.	Relaxing the upper bound may help to improve the Pareto-front, but only in conjunction with relaxing other important constraints, particularly the upper bound of L/D
L/D	lower bound	Not imp.	-
L/D	upper bound	Very imp.	Relaxing the upper bound should certainly improve the Pareto-front throughout
Ⓜ	lower bound	Not imp.	-
Ⓜ	upper bound	Not imp.	-
Fnv	lower bound	Not imp.	-
Fnv	upper bound	Not imp.	-

Constraint variations analysed

The bounds of design variables and constraints are systematically relaxed so that the resulting Pareto-front can be compared with the original Pareto-front. Among the independent design variables, W_{pay} and V_{pay} are part of the design inputs, and the effect of changing them is studied separately later in Section 5.1.5. The bounds of the remaining independent design variables (D, ss, C_B and C_P) are varied here. Among the constraints, relaxing of Fn_V has not been done. It is not a constraint normally imposed during the design process; it was included here only because the simplified resistance calculation used in the GA Tool would fail if Fn_V fell beyond the specified range.

The variations considered in the limiting values of the design variables and constraints are given in Table 5-12. C01 is the set of constraints used to generate the original Pareto-front. C02 relaxes the lower bound of D, while C03 relaxes its upper bound. C04 and C05 do the same for ss, and so on, until C16 and C17 for Ⓜ. The last set C18 relaxes both bounds for all the design variables and constraints simultaneously. For ease of identification, the relaxed value of a parameter is shown in shaded background.

Table 5-12: Constraint variations used for analysis

Constr. ID	Description		D	ss	C_B	C_P	B/T	L/B	L/D	Ⓜ
C01	Original	min	10	0.2	0.4	0.5	2	4	7	5
		max	12	0.25	0.6	0.7	4	12	14	10
C02	Lower D_{min}	min	**9.5**	0.2	0.4	0.5	2	4	7	5
		max	12	0.25	0.6	0.7	4	12	14	10
C03	Higher D_{max}	min	10	0.2	0.4	0.5	2	4	7	5
		max	**12.5**	0.25	0.6	0.7	4	12	14	10
C04	Lower ss_{min}	min	10	**0.15**	0.4	0.5	2	4	7	5
		max	12	0.25	0.6	0.7	4	12	14	10
C05	Higher ss_{max}	min	10	0.2	0.4	0.5	2	4	7	5
		max	12	**0.3**	0.6	0.7	4	12	14	10
C06	Lower C_{Bmin}	min	10	0.2	**0.3**	0.5	2	4	7	5
		max	12	0.25	0.6	0.7	4	12	14	10
C07	Higher C_{Bmax}	min	10	0.2	0.4	0.5	2	4	7	5
		max	12	0.25	**0.7**	0.7	4	12	14	10
C08	Lower C_{Pmin}	min	10	0.2	0.4	**0.4**	2	4	7	5
		max	12	0.25	0.6	0.7	4	12	14	10
C09	Higher C_{Pmax}	min	10	0.2	0.4	0.5	2	4	7	5
		max	12	0.25	0.6	**0.9**	4	12	14	10
C10	Lower B/T_{min}	min	10	0.2	0.4	0.5	**1**	4	7	5
		max	12	0.25	0.6	0.7	4	12	14	10
C11	Higher B/T_{max}	min	10	0.2	0.4	0.5	2	4	7	5
		max	12	0.25	0.6	0.7	**5**	12	14	10
C12	Lower L/B_{min}	min	10	0.2	0.4	0.5	2	**3**	7	5
		max	12	0.25	0.6	0.7	4	12	14	10
C13	Higher L/B_{max}	min	10	0.2	0.4	0.5	2	4	7	5
		max	12	0.25	0.6	0.7	4	**14**	14	10
C14	Lower L/D_{min}	min	10	0.2	0.4	0.5	2	4	**6**	5
		max	12	0.25	0.6	0.7	4	12	14	10
C15	Higher L/D_{max}	min	10	0.2	0.4	0.5	2	4	7	5
		max	12	0.25	0.6	0.7	4	12	**16**	10
C16	Lower $Ⓜ_{min}$	min	10	0.2	0.4	0.5	2	4	7	**4**
		max	12	0.25	0.6	0.7	4	12	14	10
C17	Higher $Ⓜ_{max}$	min	10	0.2	0.4	0.5	2	4	7	5
		max	12	0.25	0.6	0.7	4	12	14	**12**
C18	Relaxed all	min	**9.5**	**0.15**	**0.3**	**0.4**	**1**	**3**	**6**	**4**
		max	**12.5**	**0.3**	**0.7**	**0.9**	**5**	**14**	**16**	**12**

The Pareto-front obtained for all constraint combinations are combined into a single plot as shown in Figure 5-13.

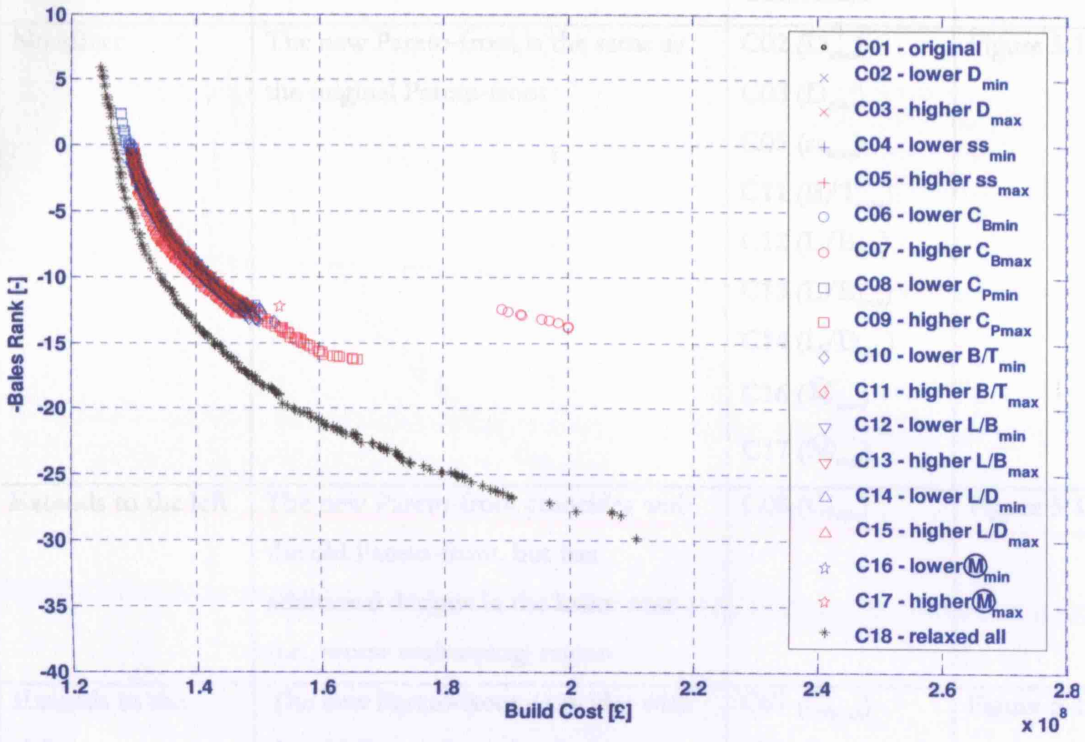

Figure 5-13: Pareto-fronts for constraint combinations C01 to C18

Relaxing all constraints (C18) produces a better Pareto-front than relaxing any single constraint, as expected. The Pareto-fronts for most constraints seem to overlap one another, making it rather difficult to compare them. To overcome this, they are divided into five groups. This division is based on an examination of all Pareto-fronts, which showed that the effect of relaxing a constraint falls into one of five categories, as listed in Table 5-13. The Pareto-fronts for these five categories are shown in Figure 5-14 to Figure 5-18. Note that the axes limits are not kept the same among these plots for clarity.

Table 5-13: Actual effects of relaxing constraints on the Pareto-front (based on the variations listed in Table 5-12)

Effect on the new Pareto-front	Explanation	Relaxed Constraints	Figure No.
No effect	The new Pareto-front is the same as the original Pareto-front	C02 (D_{min}) C03 (D_{max}) C05 (ss_{max}) C11 (B/T_{max}) C12 (L/B_{min}) C13 (L/B_{max}) C14 (L/D_{min}) C16 ($Ⓜ_{min}$) C17 ($Ⓜ_{max}$)	Figure 5-14
Extends to the left	The new Pareto-front coincides with the old Pareto-front, but has additional designs in the lower cost (i.e., worse seakeeping) region	C08 (C_{Pmin})	Figure 5-15
Extends to the right	The new Pareto-front coincides with the old Pareto-front, but has additional designs in the higher cost (i.e., better seakeeping) region	C07 (C_{Bmax}) C09 (C_{Pmax})	Figure 5-16
Partially improved	A part of the Pareto-front coincides with the original Pareto-front, while the rest is improved	C06 (C_{Bmin}) C10 (B/T_{min})	Figure 5-17
Wholly improved	The whole Pareto-front is improved	C04 (ss_{min}) C15 (L/D_{max}) C18 (all)	Figure 5-18 Figure 5-13

Figure 5-14 shows the constraints that have no effect on the Pareto-front. As seen from the plot, all the curves are very similar. The minor differences can be attributed to the inherent imprecise nature of the GA.

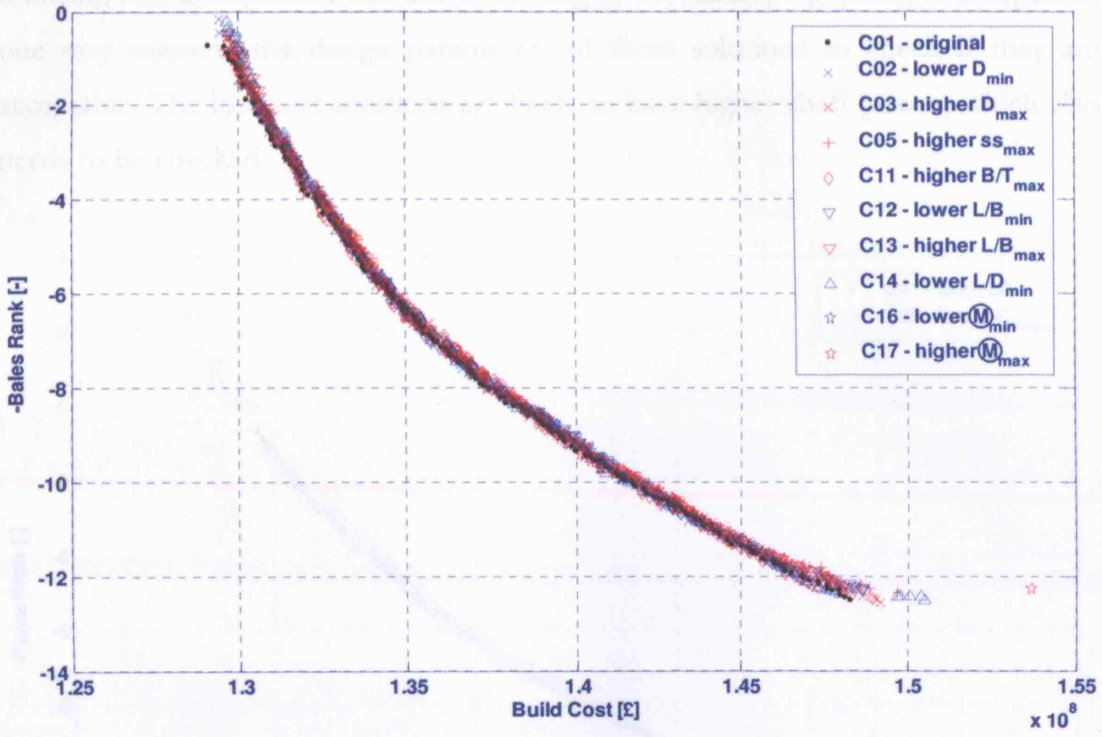

Figure 5-14: Constraints that do not affect the Pareto-front

The constraints that fall in the second category are shown in Figure 5-15. It shows that relaxing the lower bound of C_P (C08) extends the Pareto-front to the left: i.e., designs with lower cost are possible compared to the original Pareto-front. If reducing cost is important and the worsening of the seakeeping quality is acceptable, one may examine the design parameters of these solutions to check if they are acceptable. The low cost solutions are likely to have higher shaft power, which also needs to be checked.

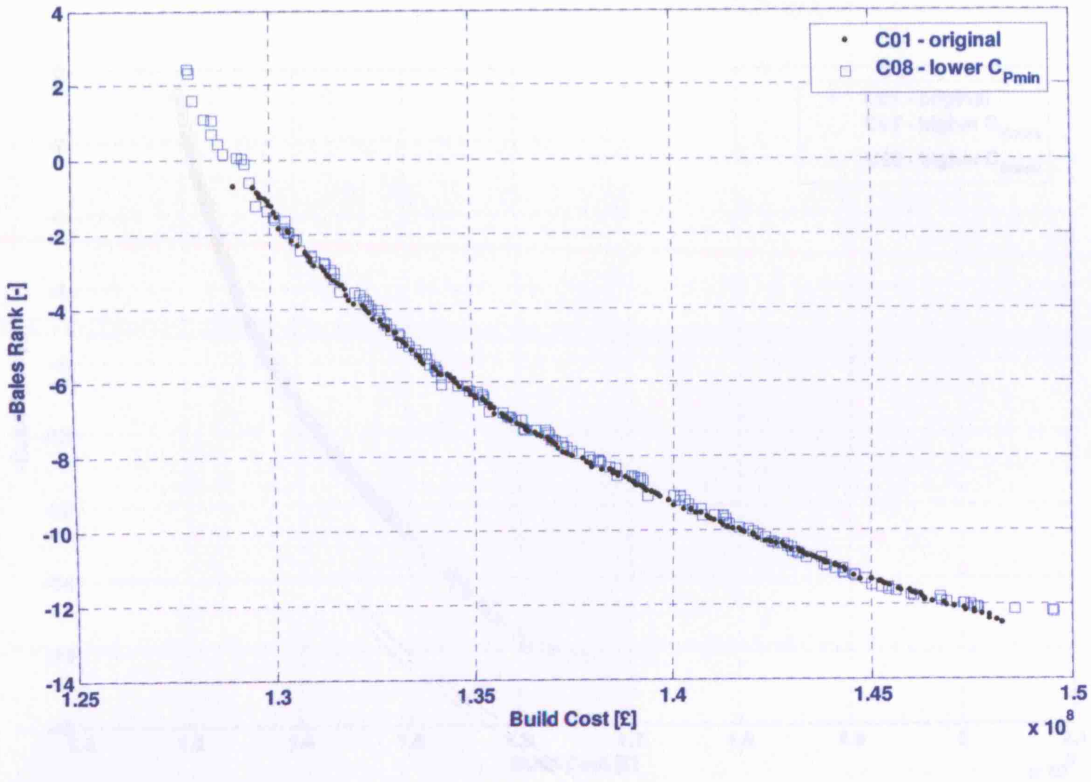

Figure 5-15: Constraint that extend the Pareto-front to the left – C08

Figure 5-16 shows the two constraints that extend the right end of the Pareto-front. These are the upper bounds of C_B and C_P. Their Pareto-fronts coincide with the original Pareto-front (C01) until its right hand end (i.e., higher cost and better seakeeping region), and then extend further. Relaxing the upper bound of C_P results in a continuous extension of the original Pareto-front; in contrast, relaxing the upper bound of C_B results in a discontinuity in the Pareto-front, so that substantial increase in cost is required to get even the slightest improvement in seakeeping. Why such a discontinuity occurs is discussed later in this section, on page 128.

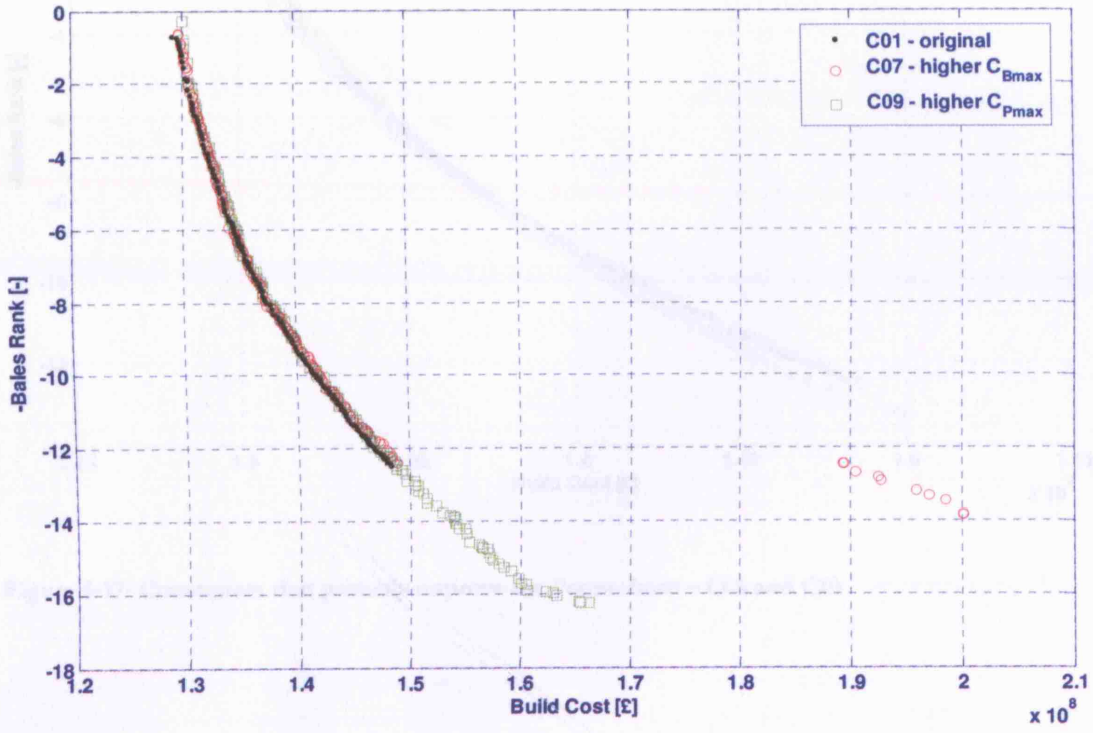

Figure 5-16: Constraints that extend the Pareto-front to the right – C07 and C09

Figure 5-17 shows that relaxing the lower bound of C_B provides a slight improvement to the Pareto-front in the region near the left hand end. Relaxing the lower bound of B/T improves the right half of the Pareto-front (beyond build cost > £137M and -Bales Rank < -8), while the left half remains unchanged.

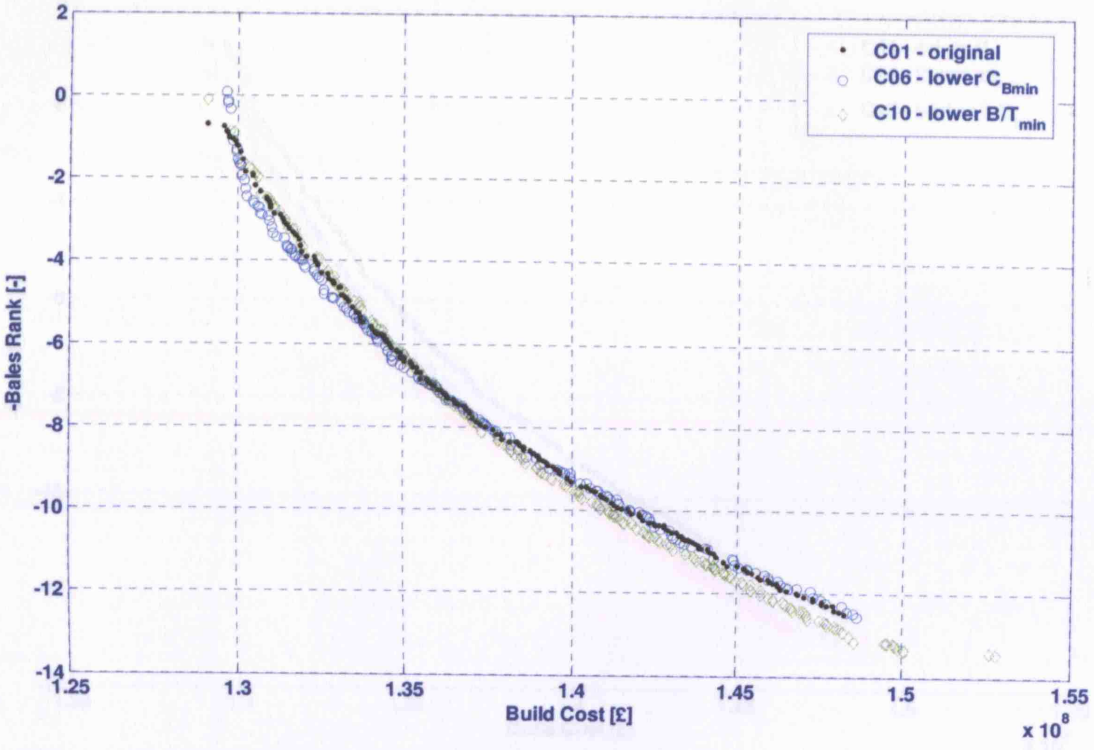

Figure 5-17: Constraints that partially improve the Pareto-front – C06 and C10

Figure 5-18 shows the two constraints that improve the whole Pareto-front. These are the lower bound of ss and the upper bound of L/D. In addition, relaxing all the constraints (C18) would give much better improvement throughout the whole Pareto-front, as was shown in Figure 5-13.

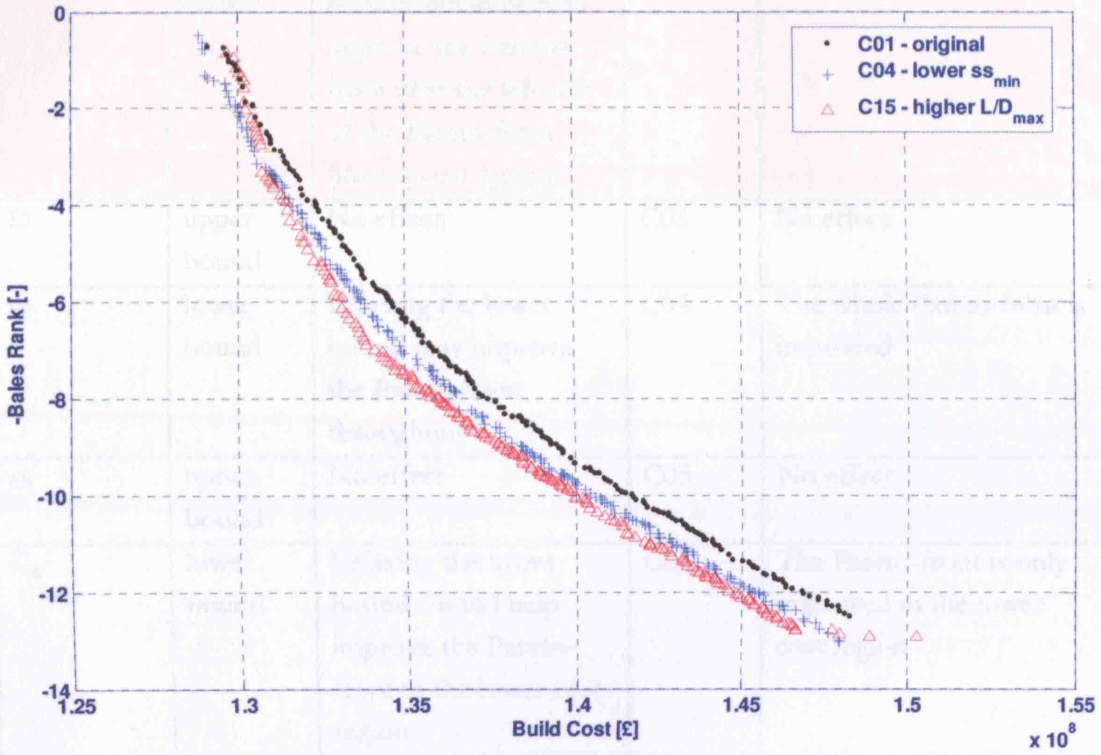

Figure 5-18: Constraints that wholly improve the Pareto-front – C04, C15 and C18 (C18 is not shown for clarity – see Figure 5-13)

Effect of constraint variations – expected vs actual effects

Based on the analysis of the constraints plot with the original set of constraints (C01), a table was created showing the expected effects of relaxing each constraint (Table 5-11). The constraints were then systematically relaxed (C02 to C18) and the Pareto-fronts re-generated. Comparison of each of these Pareto-fronts with the original Pareto-front (i.e., with constraint set C01) gave the actual effects of relaxing each constraint (Table 5-13). These two tables can now be examined to see how the actual effects compare with the expected effects. The results are shown in Table 5-14.

Table 5-14: Expected vs actual effects of relaxing constraints on the quality of the Pareto-front

Design variable / constraint	Lower / upper bound	Expected effect of relaxing lower /upper bound on improving Pareto-front	Constr ID	Actual effect of relaxing lower /upper bound on improving Pareto-front
D	lower bound	Relaxing the lower bound should help to improve the Pareto-front near the left end of the Pareto-front (lowest cost region)	C02	No effect
D	upper bound	No effect	C03	No effect
ss	lower bound	Relaxing the lower bound may improve the Pareto-front throughout	C04	The whole Pareto-front is improved
ss	upper bound	No effect	C05	No effect
C_B	lower bound	Relaxing the lower bound should help improve the Pareto-front in the lower cost region	C06	The Pareto-front is only improved in the lower cost region
C_B	upper bound	No effect	C07	The new Pareto-front coincides with the old Pareto-front, but has additional designs in the higher cost (i.e., better seakeeping) region
C_P	lower bound	Relaxing the lower bound should help extend the Pareto-front further to the left (lower cost region)	C08	The new Pareto-front coincides with the old Pareto-front, but has additional designs in the lower cost (i.e., worse seakeeping) region
C_P	upper bound	Relaxing the upper bound should help extend the Pareto-front further to the right (higher cost region)	C09	The Pareto-front is extended to the right

B/T	lower bound	Relaxing the lower bound should help to improve the Pareto-front throughout, except near the left end (lowest cost region)	C10	The Pareto-front is improved in the higher cost region
B/T	upper bound	No effect	C11	No effect
L/B	lower bound	No effect	C12	No effect
L/B	upper bound	Relaxing the upper bound may help to improve the Pareto-front, but only in conjunction with relaxing other important constraints such as the upper bound of L/D	C13	No effect
L/D	lower bound	No effect	C14	No effect
L/D	upper bound	Relaxing the upper bound should certainly improve the Pareto-front throughout	C15	The whole Pareto-front is improved
Ⓜ	lower bound	No effect	C16	No effect
Ⓜ	upper bound	No effect	C17	No effect

The obtained effects are in line with the expected results, except in two cases (C02 and C07), which are highlighted in the table. The reason behind this difference is explained below.

In the case of C02 (the lower bound of D), it is found that decreasing values of D would not be possible without increasing the value of L/D. However, the L/D values are already at its upper bound, and hence they cannot be improved any further. Hence the relaxing of C02 does not result in improvement of the Pareto-front.

In the case of C07 (the upper bound of C_B), the resulting Pareto-front remains the same within the extent of the original Pareto-front, but some additional designs are obtained with slight improvement in seakeeping but at much higher costs. These designs have lower values of L and higher values of B, T, D, C_B, P_s, Δ and ∇_{Gross} compared to the designs on the original Pareto-front. Thus they belong to a different region of the design space. The performance characteristics of this region of the design space could not be anticipated by consideration of the original constraints plot alone. This is discussed further in Section 7.2.

5.1.5. Re-generation of the Pareto-front with revised set of inputs

If some of the design inputs are flexible, it would be interesting to change them and see how it affects the Pareto-front. For example, the effect of different space margins added to the payload volume is discussed here. For demonstration, it was assumed that the minimum payload volume required was 2000m³. Additional Pareto-fronts were then generated with space margins of 1000, 2000, 3000, 5000 and 8000m³. The extreme values are admittedly unrealistic; however, they have been deliberately included to examine and demonstrate the behaviour of the Pareto-fronts. *(It may be clarified that the GA Tool at present does not have a provision to explicitly specify space margins. Instead, the effect of space margin is simulated by increasing the payload volume appropriately. For example, the effect of 1000m³ space margin on a payload volume of 2000m³ is achieved by running the GA Tool with a fictitious payload volume of 1000 + 2000 = 3000m³).*

The resulting Pareto-fronts are shown in Figure 5-19. It can be seen that increase in space margin, in general, shifts the Pareto-front to the right and downwards, i.e., increases cost and improves seakeeping. This means if the customer is willing to spend more, better seakeeping can be obtained, as one would normally expect.

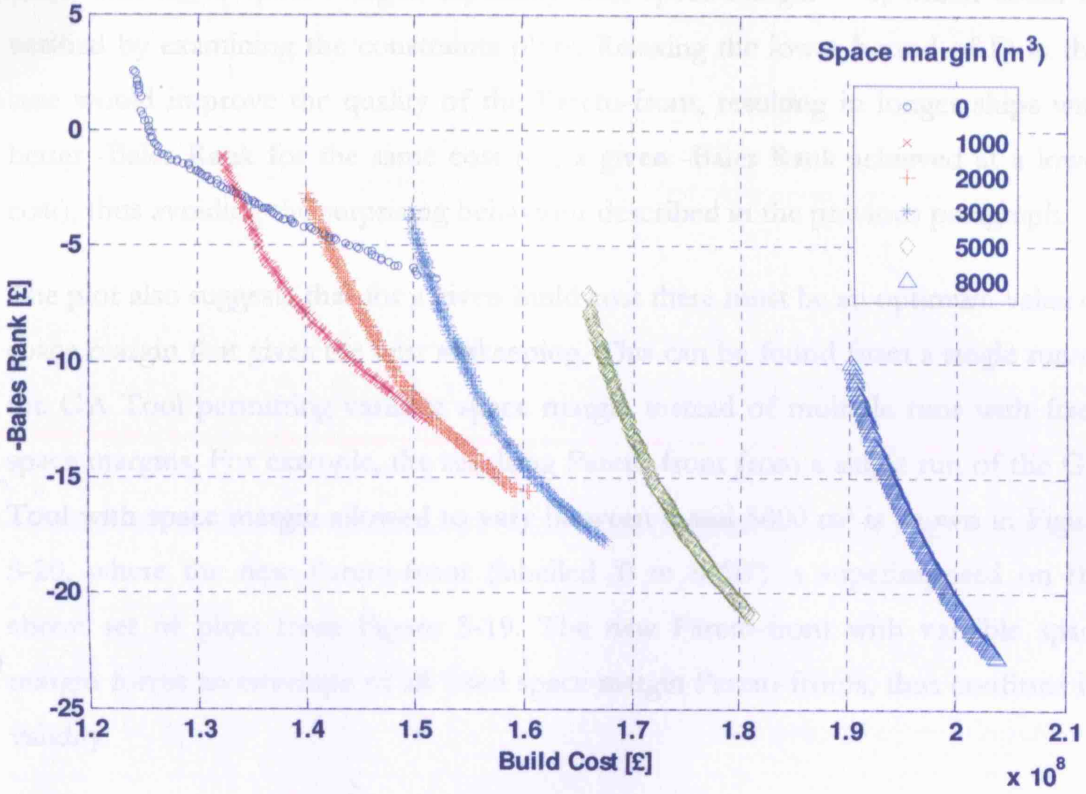

Figure 5-19: Pareto-fronts with different values for space margins

The plot shows some interesting results for the lower space margins. For example, at a build cost of £140M and no space margin, the -Bales Rank is about -4. Increasing the space margin to 1000m³ would give much better seakeeping for the same build cost (-Bales Rank = -8). This may seem quite surprising, because it shows that the seakeeping quality can be improved by just increasing the space margin, with no penalty in cost. However, increasing the space margin further to 2000 m³ would worsen the seakeeping (-Bales Rank = -3) at the same build cost.

This peculiar behaviour can be explained as follows. The set of constraints and design variable bounds were kept the same for all these cases, the only change being in the value of space margin. This may be reasonable for design variables such as C_B

and C_P, but not for D, since ships with low space margin, and consequently lower requirement of gross enclosed volume, are likely to have relatively lower values of D. In this example, the bounds of D were kept constant at [10, 12] irrespective of the space margin. The lower bound of D thus became the limiting constraint for the cases with lower space margin, especially with space margin = 0, which could be verified by examining the constraints plots. Relaxing the lower bound of D in this case would improve the quality of the Pareto-front, resulting in longer ships with better -Bales Rank for the same cost (or, a given -Bales Rank achieved at a lower cost), thus avoiding the surprising behaviour described in the previous paragraph.

The plot also suggests that for a given build cost there must be an optimum value of space margin that gives the best seakeeping. This can be found from a single run of the GA Tool permitting variable space margin instead of multiple runs with fixed space margins. For example, the resulting Pareto-front from a single run of the GA Tool with space margin allowed to vary between 0 and 8000 m^3 is shown in Figure 5-20, where the new Pareto-front (labelled '0 to 8000') is superimposed on the above set of plots from Figure 5-19. The new Pareto-front with variable space margin forms an envelope of all fixed space margin Pareto-fronts, thus confirms its validity.

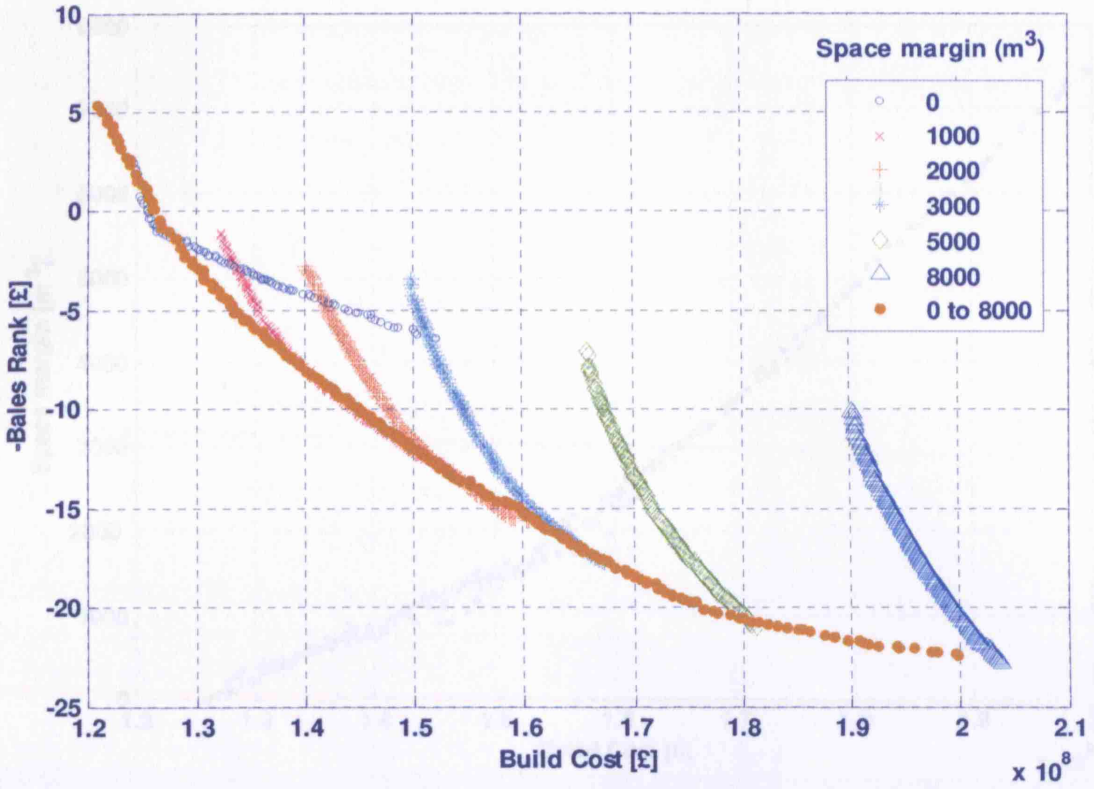

Figure 5-20: Pareto-front with variable space margin forming an envelope to the Pareto-fronts with fixed space margins

Consider the Pareto-front corresponding to variable space margin, i.e., the curve labelled '0 to 8000' in Figure 5-20. The values of space margin for the designs on this Pareto-front are shown in Figure 5-21. For a given build cost, the GA Tool determines the value of space margin that will produce the best -Bales Rank for that build cost. As the optimum value of space margin increases, the build cost increases and the seakeeping improves. This is because increase in space margin produces bigger ships (in terms of gross enclosed volume and displacement). Bigger ships usually have better seakeeping (as can be seen from the Bales Rank formula given in Appendix H.6.5), but will, in general, be more expensive to build.

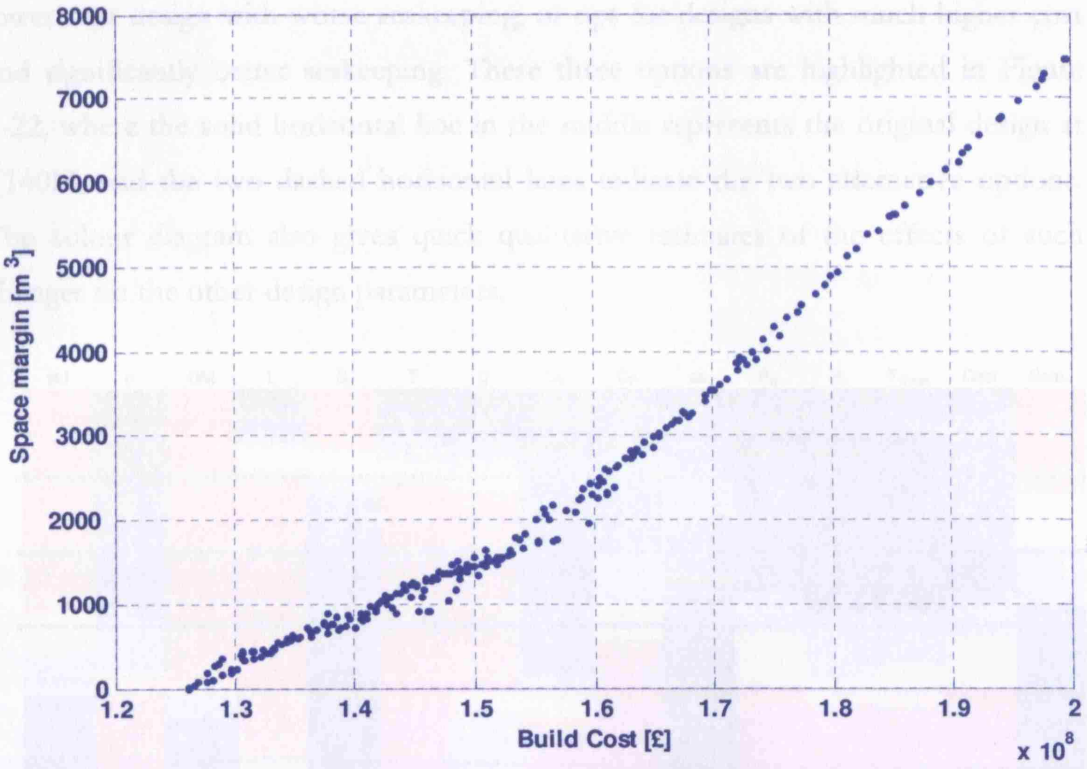

Figure 5-21: The values of space margin for the Pareto-front with variable space margin, shown in Figure 5-20

5.1.6. Customer-designer dialogue

The results of the analysis of the Pareto-front, the design space exploration and the performance space exploration can be used by the designer to aid in the dialogue with the customer about the design requirements.

For example, the original Pareto-front (Figure 5-3) can be used to inform the customer of the likely seakeeping qualities to be expected depending on the customer's budget. The colour diagram representation of the Pareto-front (Figure 5-4) could give more information about the trends in design parameters and performance characteristics. For example, suppose the customer is interested in designs that cost about £140M. These are the designs from around the middle of the Pareto-front, where L, T and D are in red, indicating high values for them. Examination of their characteristics shows that their draughts are around 6.3m. If the customer feels that this is too high (due to port limitations, for instance), the designer can use the colour diagram to suggest alternative options: either choose a

lower cost design with worse seakeeping, or opt for designs with much higher cost and significantly better seakeeping. These three options are highlighted in Figure 5-22, where the solid horizontal line in the middle represents the original design at £140M, and the two dashed horizontal lines indicate the two alternative options. The colour diagram also gives quick qualitative estimates of the effects of such changes on the other design parameters.

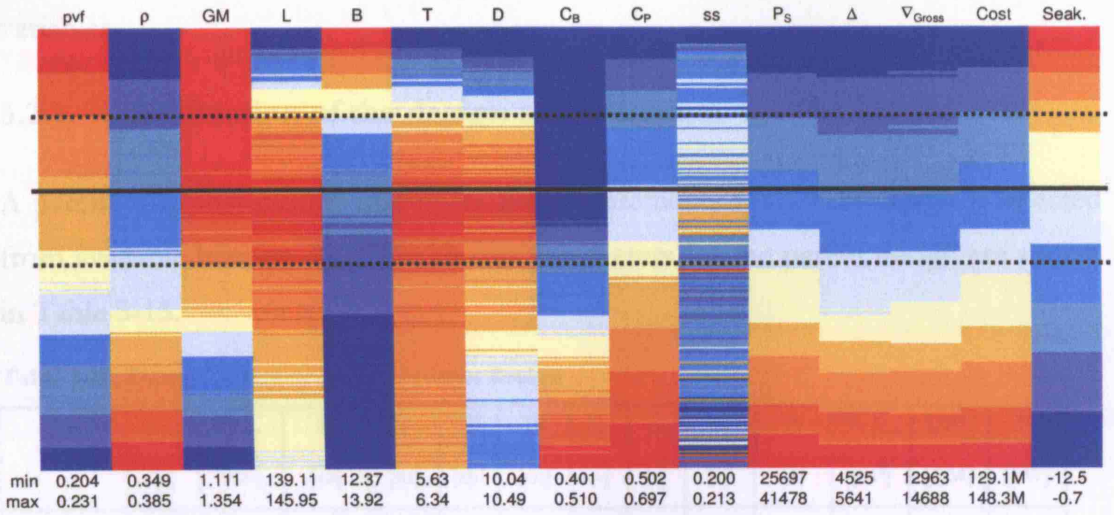

Figure 5-22: The colour diagram shown in Figure 5-4, highlighting the design of interest (indicated by the solid horizontal line) and two alternative options (the two dashed horizontal lines)

The design space exploration and the constraints plot show that the most important constraint for this design is the upper bound of L/D. If the customer is ready to adopt a special structural design that permits higher L/D, the designer can inform him what likely improvements in seakeeping are possible because of this. C_P is another important constraint – relaxing its lower bound will help to extend the Pareto-front to the lower cost region, whereas relaxing its upper bound will help to extend the Pareto-front to the higher cost region. In addition, lowering B/T and C_B will also be helpful. In this case, the designer may require performance analysis tools that have been shown to be valid within the range of C_P, C_B and B/T values considered.

5.2. Application of the proposed design approach for modifying a parent design

This section demonstrates the application of the proposed design approach for modifying an existing design. The scenario considered is when a parent design exists with similar, but not exactly the same, requirements as for a new design. The process is similar to Section 5.1, except for the narrower ranges of the design variables.

5.2.1. Specification of the design requirements

A parent ship that closely resembles the requirements for a new design is selected from available historic data. The design parameters for the parent design are shown in Table 5-15.

Table 5-15: Design parameters of the parent design

	W_{pay} [t]	V_{pay} [m³]	L [m]	B [m]	T [m]	D [m]	C_B [-]	C_P [-]	ss [-]	Δ [t]	∇_{Gross} [m³]	UPC [£M]	P_s [kW]
Parent	749.9	6259.2	145.10	15.71	5.52	11.00	0.50	0.63	0.250	6444	21786	287.0	37760

The customer requirements for the new design are assumed to be as follows:

- The new design should be for a higher payload weight of 800 t. The minimum payload volume requirement is 5000 m³; however, additional space margin can be used if it gives better seakeeping performance.
- The speed and endurance should be the same as the parent design (maximum speed = 30 kn; endurance speed = 18 kn at 5000 nm).
- The payload cost is the same, and the UPC should be limited to £300M. The shaft power should be limited to 40 MW.
- It is desired that the depth 'D' be kept the same as the parent design to keep the same configuration of decks. The draught 'T' should be kept the same as far as possible. The ss can be varied a little around the value of the parent design. There are no limitations on L, B, C_B or C_P.

- The best possible seakeeping (based on the Bales Rank criterion) should be obtained. The UPC should be minimised as far as possible.

It was decided to keep the same complement of 220 as for the parent design. Assuming a maximum space margin of 5000 m^3, the upper bound for payload volume is kept at a rather high value of 10000 m^3. Taking into account the customer requirements, the constraints shown in Table 5-16 are used. These are the same as the ones used in the last section (Table 5-1), except that D has been kept constant and ss varies only slightly. This is expected to demonstrate the trade-offs possible with rather large variations permitted for the underwater hull form, combined with only slight variation in the above-water hull form.

Table 5-16: Design constraints considered

	D	ss	C_B	C_P	B/T	L/B	L/D	Ⓜ
min	11	0.24	0.40	0.50	2	4	7	5
max	11	0.26	0.60	0.70	4	12	14	10

5.2.2. Generation of the Pareto-front

The design requirements were converted to the input data required by the GA Tool. The standard set of GA parameters was used (see Appendix H). Three objectives were used. The first two objectives were the minimisation of UPC and -Bales Rank, as done in Section 5.1.2. An additional consideration was that the draughts of the new designs should not depart from the draught of the parent design as far as possible. Thus, a third objective was included as the minimisation of the change in draught compared to the target draught, i.e., dT = absolute value of "draught – target draught". Hence this became a three-objective optimisation problem.

The generated Pareto-front (consisting of 1590 designs after removing a few infeasible designs that were present) is shown as a 3D plot in Figure 5-23. Each data point represents one discrete design in the performance space. The 3D plot is hard to visualise and interpret; hence the same Pareto-front is shown in Figure 5-24 as a 2D plot with the two axes representing two of the objectives, while the third objective is qualitatively indicated by the colour of the data point. In this case, the

two axes represent UPC and -Bales Rank, while the colour of each data point indicates the value of dT. Designs with low values of dT appear in blue, while those with high values of dT appear in red. Figure 5-25 shows the same Pareto-front in three 2D projections: XY, YZ and XZ. (For further information about different visualisation schemes of the Pareto-front, see Appendix J).

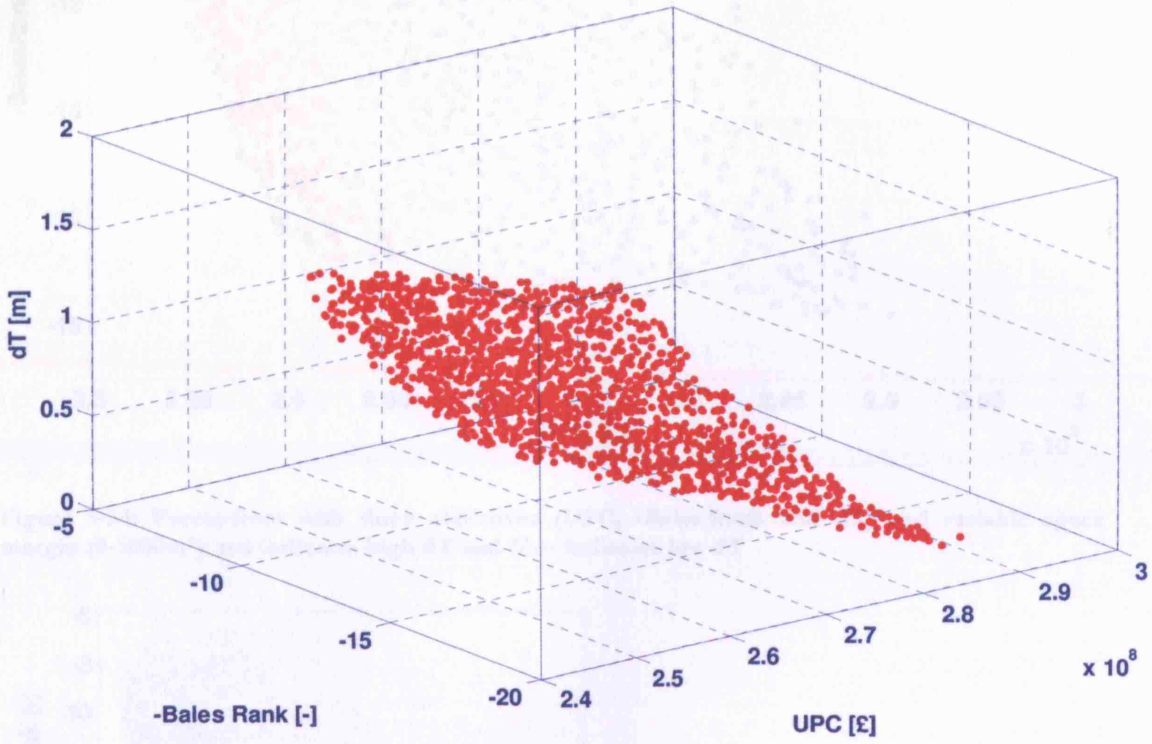

Figure 5-23: Pareto-front with three objectives (UPC, -Bales Rank and dT) and variable space margin (0-5000m³), as a 3D-plot

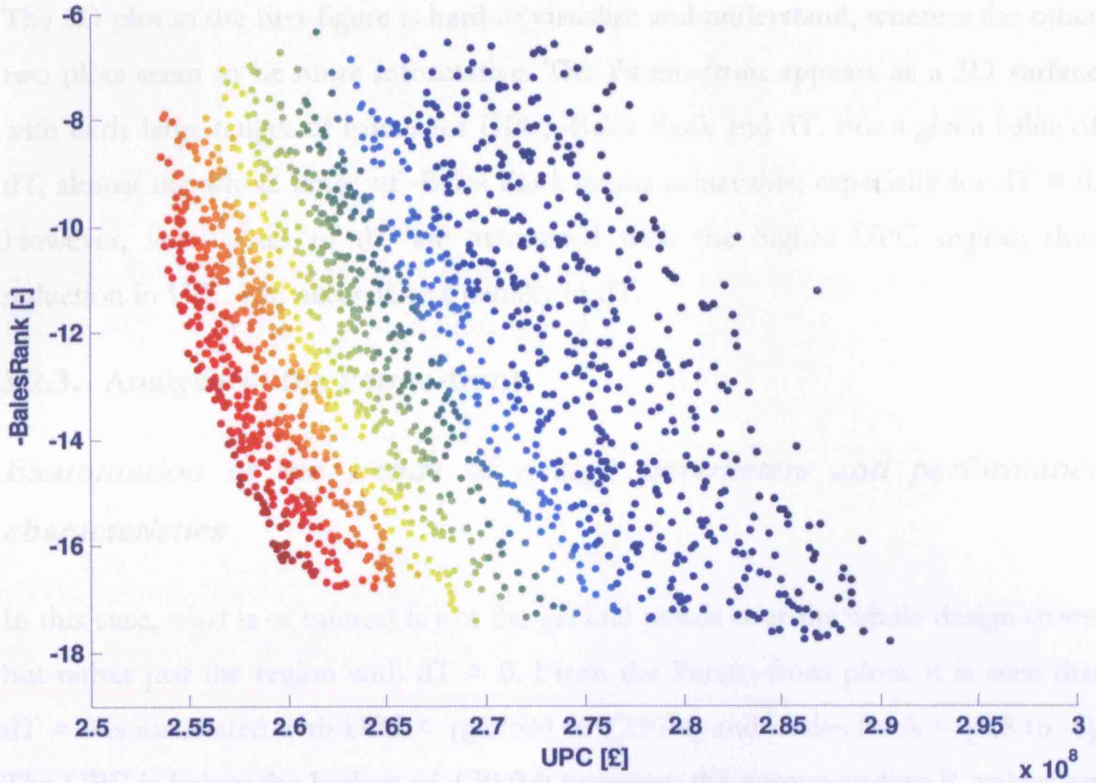

Figure 5-24: Pareto-front with three objectives (UPC, -Bales Rank and dT) and variable space margin (0-5000m³); red indicates high dT and blue indicates low dT

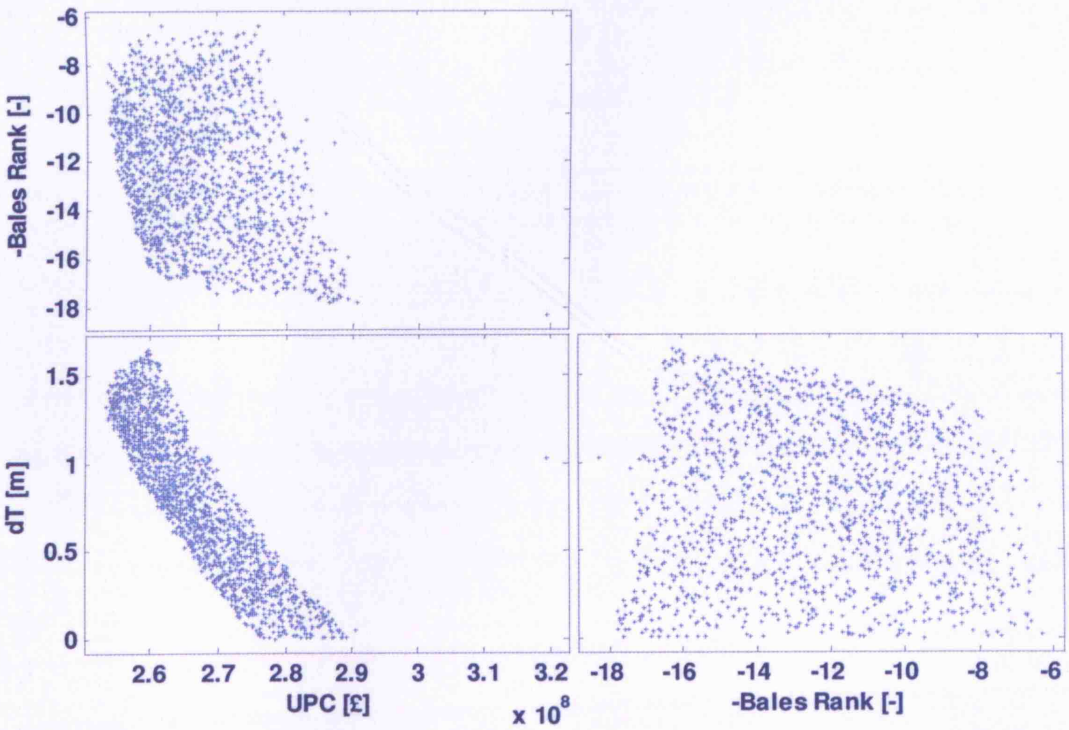

Figure 5-25: Pareto-front with three objectives (UPC, -Bales Rank and dT) and variable space margin (0-5000m³), shown as a matrix of 2D plots

The 3D plot in the first figure is hard to visualise and understand, whereas the other two plots seem to be more informative. The Pareto-front appears as a 3D surface with fairly large ranges of values for UPC, -Bales Rank and dT. For a given value of dT, almost the whole range of -Bales Rank seems achievable, especially for dT ≈ 0. However, low values of dT are associated with the higher UPC region; thus reduction in UPC will necessitate a penalty in dT.

5.2.3. Analysis of the Pareto-front

Examination of the trends of design parameters and performance characteristics

In this case, what is of interest is not the general trends over the whole design space, but rather just the region with dT ≈ 0. From the Pareto-front plots, it is seen that dT ≈ 0 is associated with UPC ≈ [£275M to £290M] and -Bales Rank ≈ [-18 to -6]. The UPC is below the budget of £300M; however, the corresponding P_s values are to be examined to ensure that they are below the target value of 40 MW. This is done in the next subsection, while short-listing suitable designs.

Short-listing of a few designs for detailed analysis

Having formed the Pareto-front consisting of a number of designs, the next task is to short-list a few designs for detailed analysis. The generated Pareto-front was filtered to focus on the region around UPC of £300M and dT close to 0. Designs with very bad -Bales Rank (i.e., poor seakeeping) were removed from this set. The final filtered set of designs is shown in Figure 5-26.

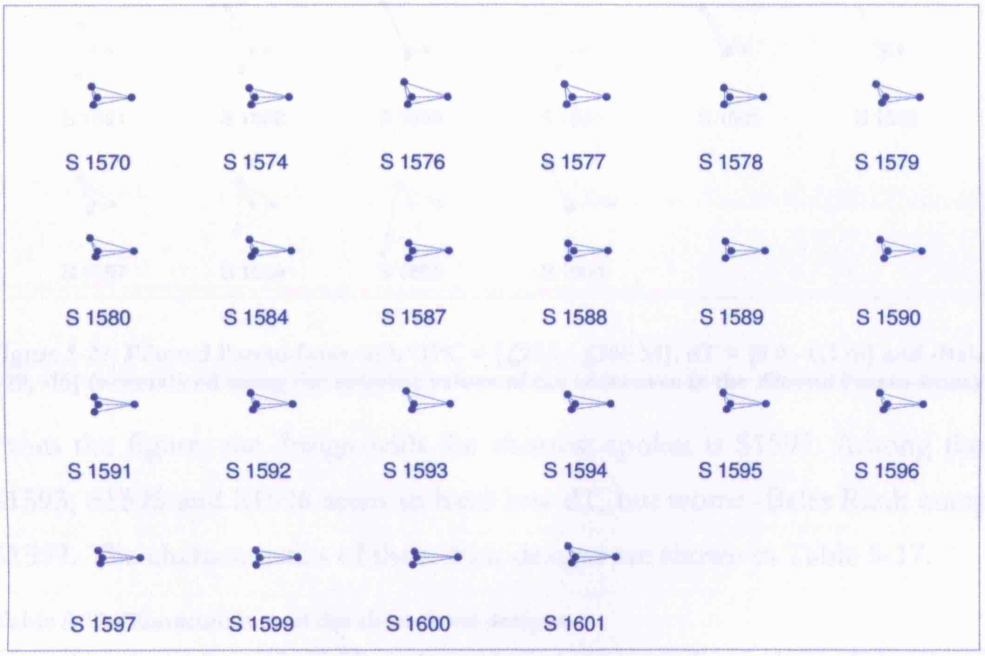

Figure 5-26: Filtered Pareto-front with UPC = [£285 - £305 M], dT = [0.0 - 0.1 m] and -Bales Rank = [-19, -16] (normalised using the extreme values of the objectives in the *whole* Pareto-front)

The designs all look very similar because they have been normalised using the extreme values of all Pareto-designs. Thus, the lowest value among *all* Pareto-designs is plotted with a spoke length of 0.1 and the highest value with a spoke length of 1. If, instead, the normalisation is carried out using the extreme values of the *filtered* set of designs, they can be more easily compared visually, as shown in Figure 5-27. One of the designs is labelled to show which objective each spoke represents.

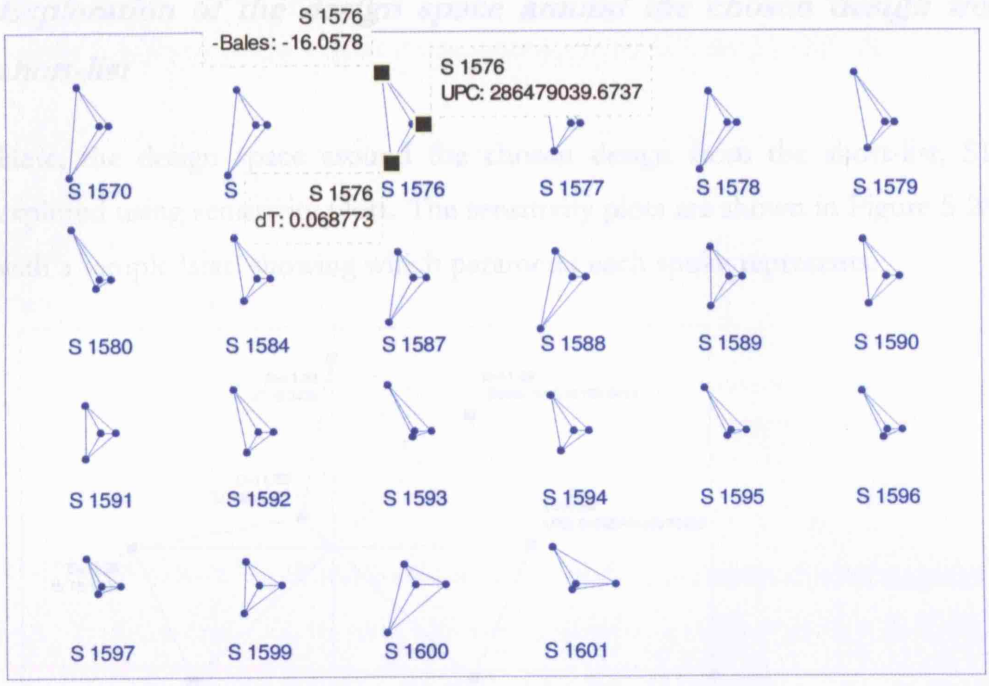

Figure 5-27: Filtered Pareto-front with UPC = [£285 - £305 M], dT = [0.0 - 0.1 m] and -Bales Rank = [-19, -16] (normalised using the extreme values of the objectives in the *filtered* Pareto-front)

From the figure, the design with the shortest spokes is S1597. Among the others, S1593, S1595 and S1596 seem to have low dT, but worse -Bales Rank compared to S1597. The characteristics of these four designs are shown in Table 5-17.

Table 5-17: Characteristics of the short-listed designs

	W_{pay} [t]	V_{pay} [m³]	L [m]	B [m]	T [m]	D [m]	C_B [-]	C_P [-]	ss [-]	P_s [kW]	Δ [t]	∇_{Gross} [m³]	UPC [£M]	-Bales [-]	dT [m]
S1593	800	6672	150.9	14.95	5.519	11.00	0.485	0.680	0.256	39059	6188	22083	288.2	-16.4	0.0006
S1595	800	6745	151.3	14.95	5.522	11.00	0.484	0.682	0.258	39130	6196	22215	288.6	-16.7	0.0019
S1596	800	6758	151.9	14.91	5.517	11.00	0.484	0.684	0.257	39175	6196	22247	288.6	-16.9	0.0029
S1597	800	6908	153.5	14.85	5.514	11.00	0.483	0.692	0.259	39293	6220	22522	289.1	-17.6	0.0056

All four short-listed designs have similar design parameters. The shaft power requirements for all of them are slightly less than the maximum allowable value of 40MW. If instead, they were higher than 40 MW, it would be necessary to re-run the GA Tool with the target P_s as another objective, and choose designs with $P_s < 40$ MW. This would presumably result in designs with worse -Bales Rank. Since the short-listed designs are all very similar, the one with the best -Bales Rank (S1597) is chosen for further analysis.

Exploration of the design space around the chosen design from the short-list

Here, the design space around the chosen design from the short-list, S1597, is explored using sensitivity plots. The sensitivity plots are shown in Figure 5-28, along with a sample 'star' showing which parameter each spoke represents.

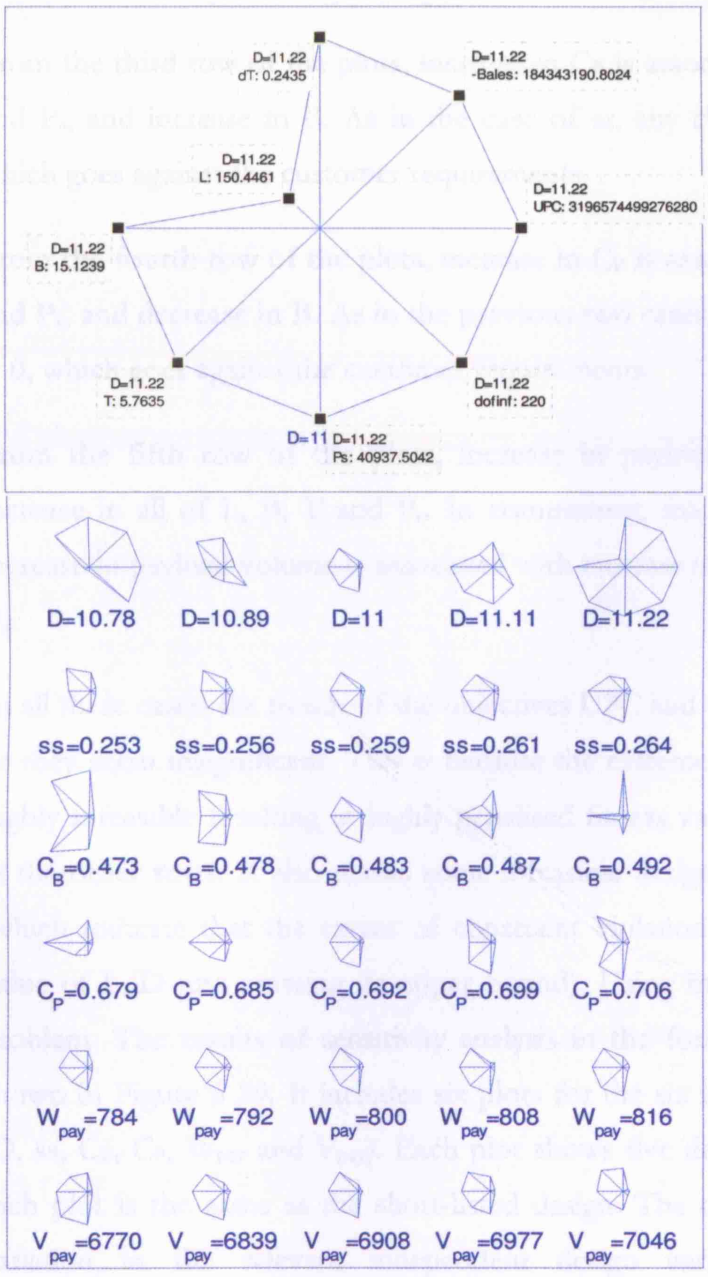

Figure 5-28: Sensitivity plots showing incremental design variants about the short-listed design S1597, presented as star plots (see Table 5-17 for design parameters and performance characteristics)

The first row of star plots shows that any change in D causes infeasibility. This is because, as given by the customer requirements, D is fixed at 11.0 m.

From the second row of the plots, increase in ss is associated with reduction in L and increase in B, T and P_s. As given by the customer requirements, change in T should be minimised; however, it is not possible to achieve this when ss is changed and other design variables remain the same.

From the third row of the plots, increase in C_B is associated with reduction in L, T and P_s, and increase in B. As in the case of ss, any change in T implies $dT > 0$, which goes against the customer requirements.

From the fourth row of the plots, increase in C_P is associated with increase in L, T and P_s, and decrease in B. As in the previous two cases, any change in T implies $dT > 0$, which goes against the customer requirements.

From the fifth row of the plots, increase in payload weight is associated with increase in all of L, B, T and P_s. In comparison, from the last row of the plots, increase in payload volume is associated with increase in L but reduction in B,T and P_s.

In all these cases, the trends of the objectives UPC and -Bales Rank are not obvious, or they seem insignificant. This is because the extreme designs in the first row are highly infeasible resulting in highly penalised fitness values, which mask the trends in the other rows. It also masks some infeasible designs with low values of dofinf (which indicate that the extent of constraint violation is little – for example, the value of L/D just crossing its upper bound). Using multiple 2D plots avoids this problem. The results of sensitivity analysis in the form of multiple 2D plots are shown in Figure 5-29. It includes six plots for the six independent design variables (D, ss, C_B, C_P, W_{pay} and V_{pay}). Each plot shows five designs. The middle design in each plot is the same as the short-listed design. The other designs are with slight variation in the relevant independent design variable, with the remaining independent design variables staying the same as the short-listed design.

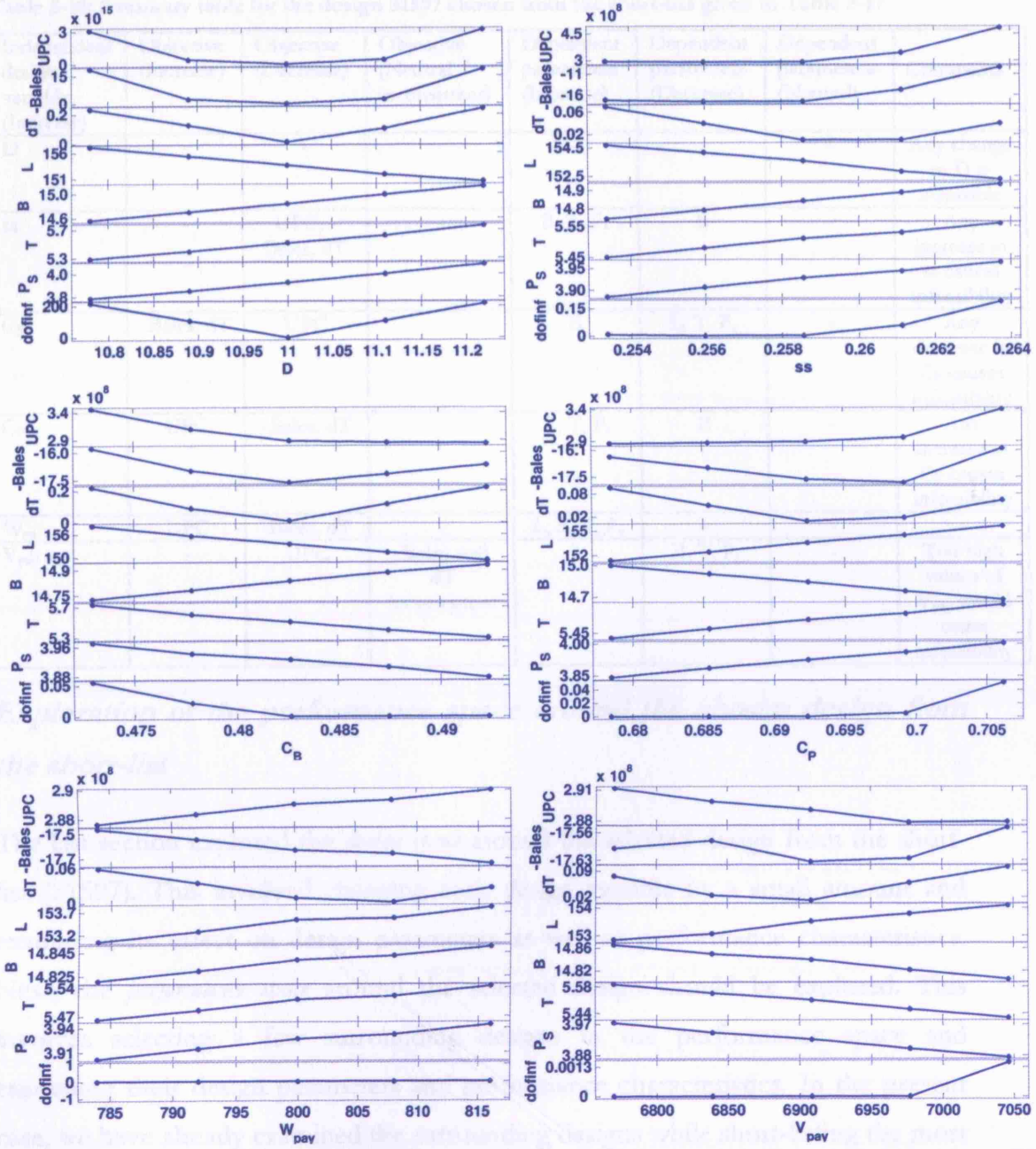

Figure 5-29: Sensitivity plots showing incremental design variants about the short-listed design S1597, presented as multiple 2D column plots (see Table 5-17 for design parameters and performance characteristics)

The trends from the sensitivity analysis plots can be tabulated as shown in Table 5-5. The table shows how the increase of each design parameter affects the objectives and dependent design parameters.

Table 5-18: Summary table for the design S1597 chosen from the short-list given in Table 5-17

Independent design variable (Increase)	Objective (Increase)	Objective (Decrease)	Objective (Neutral / inconsistent)	Dependent parameters (Increase)	Dependent parameters (Decrease)	Dependent parameters (Neutral)	Comments
D	-	-	-	-	-	-	Any change in D is infeasible
ss	-	UPC, -Bales, dT	-	B, T, P_s	L	-	Any increase in ss causes infeasibility
C_B	-Bales, dT	UPC	-	B	L, T, P_s	-	Any decrease in C_B causes infeasibility
C_P	UPC	-Bales, dT	-	L, T, P_s	B	-	Any increase in C_P causes infeasibility
W_{pay}	UPC	-Bales, dT	-	L, B, T, P_s	-	-	-
V_{pay}	-	UPC	-Bales and dT inconsistent	L	B, T, P_s	-	Too high values of V_{pay} would cause infeasibility

Exploration of the performance space around the chosen design from the short-list

The last section explored the *design space* around the selected design from the short-list (S1597). This involved changing each design variable by a small amount and examining its effect on design parameters as well as performance characteristics. Next, the *performance space* around the selected design should be explored. This involves selecting a few surrounding designs in the performance space and examining their design parameters and performance characteristics. In the present case, we have already examined the surrounding designs while short-listing the most suitable design (see Figure 5-27 and Table 5-17). Since the design requirements are rather narrow resulting in a single short-listed design, there is no scope for further performance space exploration.

5.2.4. Re-generation of the Pareto-front with revised set of constraints

The constraints plot of the original Pareto-front can be analysed to identify the important constraints. The constraint bounds can then be systematically relaxed and the resulting Pareto-fronts compared with the original Pareto-front.

Analysis of the original constraints plot

The constraints plot for the designs in the region of interest (corresponding to Figure 5-27) is shown in Figure 5-30.

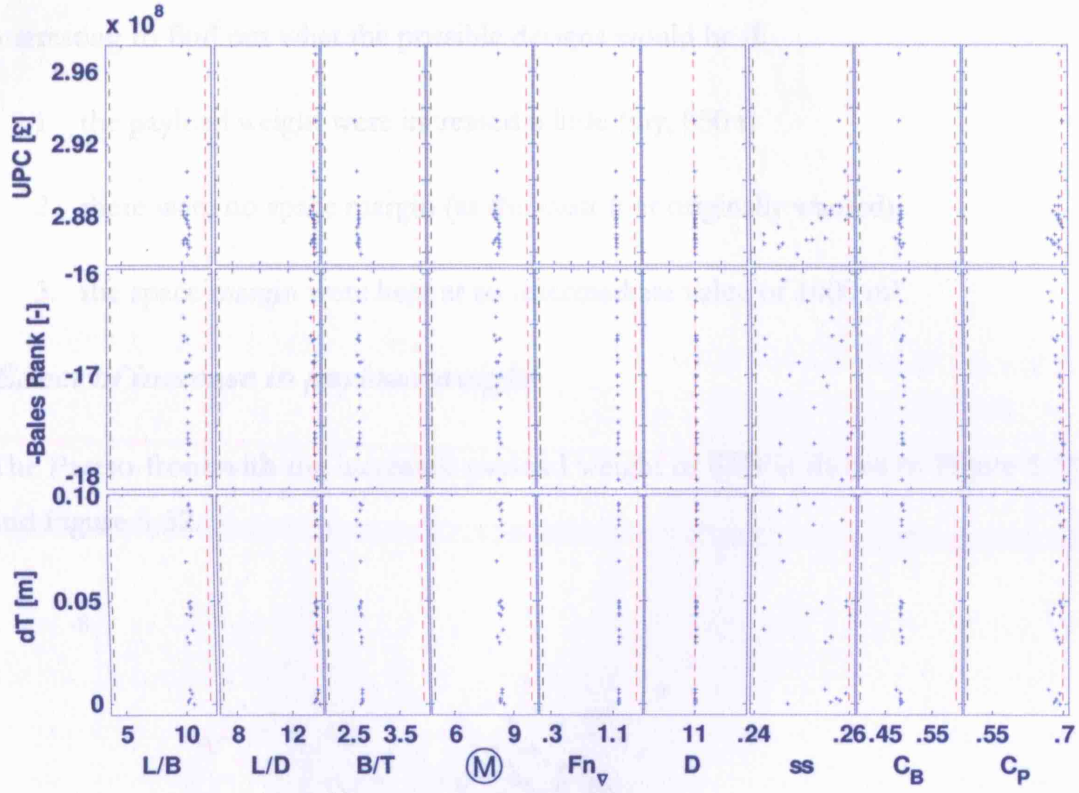

Figure 5-30: Constraints plot for the region of interest (i.e., UPC = [£285 - £305 M], dT = [0.0 - 0.1 m] and -Bales Rank = [-19, -16])

The constraints plots show that L/D and C_P are the most important constraints (apart from D, which is kept constant at 11.0 m), because their values are close to the upper bound throughout the Pareto-front. This suggests that if D is allowed to go higher, it would be beneficial. The upper bound of C_P could also be relaxed to get better performance characteristics. The values of ss show some scatter; however, the four short-listed designs, as seen from Table 5-17, all have similar values for ss.

5.2.5. Re-generation of the Pareto-front with revised set of inputs

The customer requirement translated into a payload weight of 800 t and minimum payload volume of 5000 m³. The final short-listed design had V_{pay}=6908 m³ (see Table 5-17), indicating a space margin of 6908 – 5000 = 1908 m³. It was considered interesting to find out what the possible designs would be if:

1. the payload weight were increased a little (say, 850 t)
2. there were no space margin (as the customer originally wanted)
3. the space margin were kept at an intermediate value of 1000 m³

Effect of increase in payload weight

The Pareto-front with the increased payload weight of 850t is shown in Figure 5-31 and Figure 5-32.

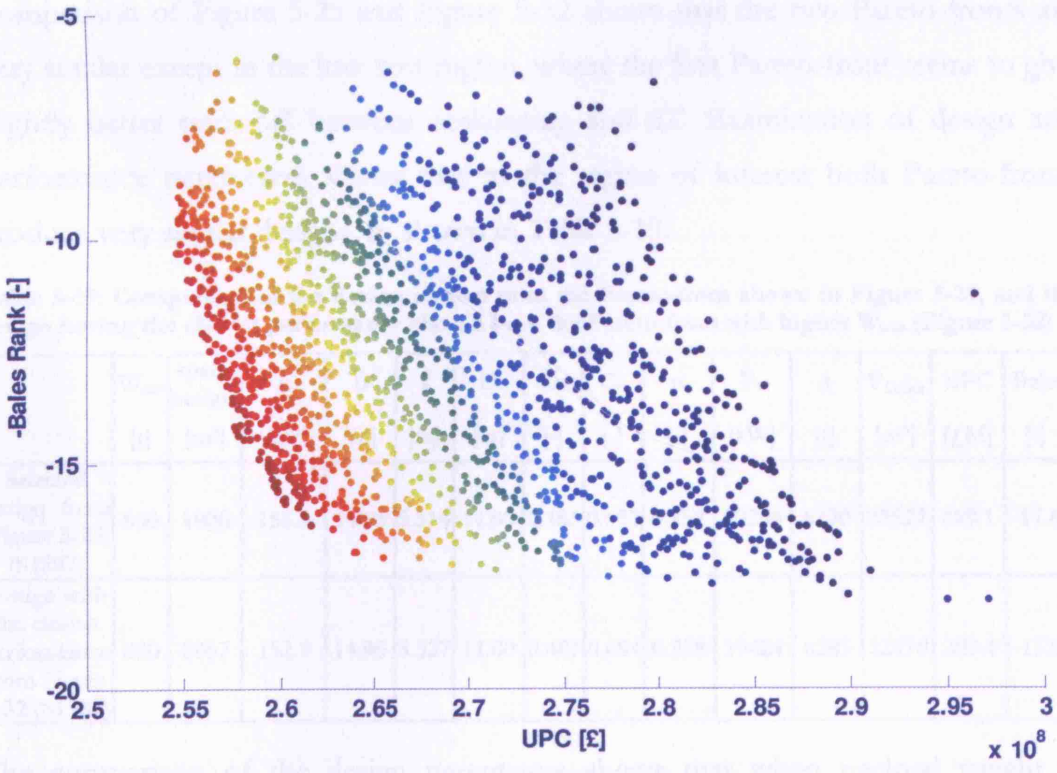

Figure 5-31: Pareto-front with three objectives (UPC, -Bales Rank and dT), with increased payload weight; red indicates high dT and blue indicates low dT

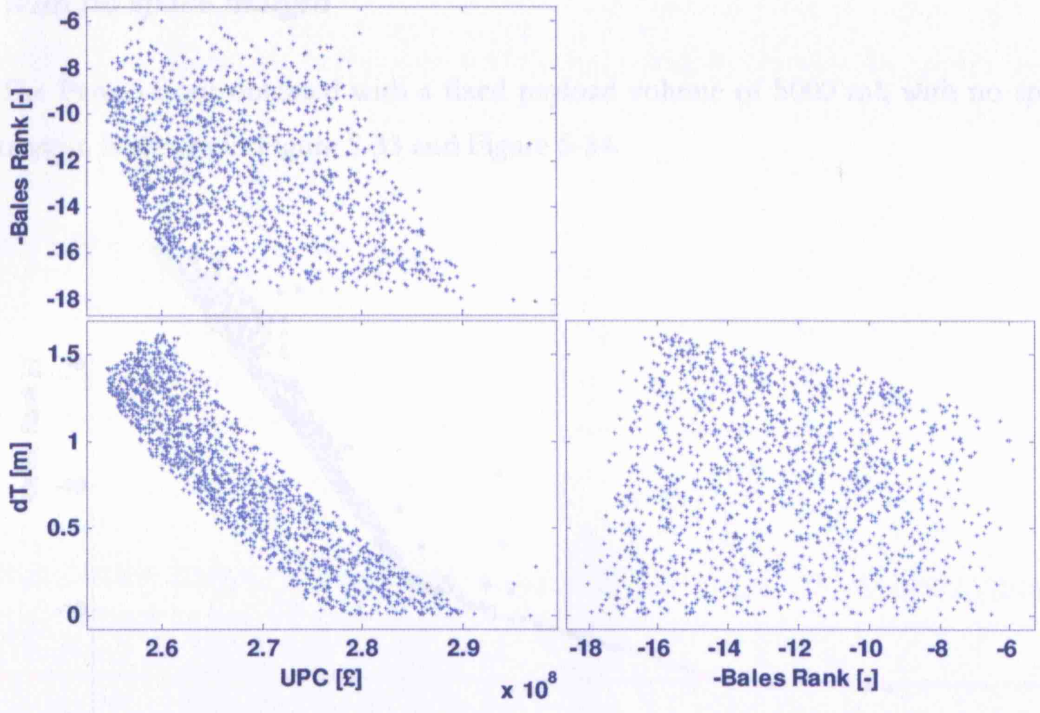

Figure 5-32: Pareto-front with three objectives (UPC, -Bales Rank and dT), with increased payload weight, shown as a matrix of 2D plots

Comparison of Figure 5-25 and Figure 5-32 shows that the two Pareto-fronts are very similar except in the low cost region, where the first Pareto-front seems to give slightly better trade-off between seakeeping and dT. Examination of design and performance parameters shows that in the region of interest both Pareto-fronts produce very similar designs, as shown in Table 5-19.

Table 5-19: Comparison of the design chosen from the Pareto-front shown in Figure 5-25, and the design having the closest performance chosen from the Pareto-front with higher W_{pay} (Figure 5-32)

	W_{pay} [t]	space margin [m³]	L [m]	B [m]	T [m]	D [m]	C_B [-]	C_P [-]	ss [-]	P_s [kW]	Δ [t]	∇_{Gross} [m³]	UPC [£M]	-Bales [-]	dT [m]
Selected design from Figure 5-25 (S1597)	800	1908	153.5	14.85	5.514	11.00	0.483	0.692	0.259	39293	6220	22522	289.1	-17.6	0.0056
Design with the closest performance from Figure 5-32 (S1587)	850	1867	152.3	14.96	5.527	11.00	0.487	0.684	0.258	39424	6285	22470	289.4	-17.0	0.0070

The comparison of the design parameters shows that when payload weight is increased, the optimum space margin reduces; so does the gross enclosed volume, but the displacement increases.

With no space margin

The Pareto-front obtained with a fixed payload volume of 5000 m³, with no space margin, is shown in Figure 5-33 and Figure 5-34.

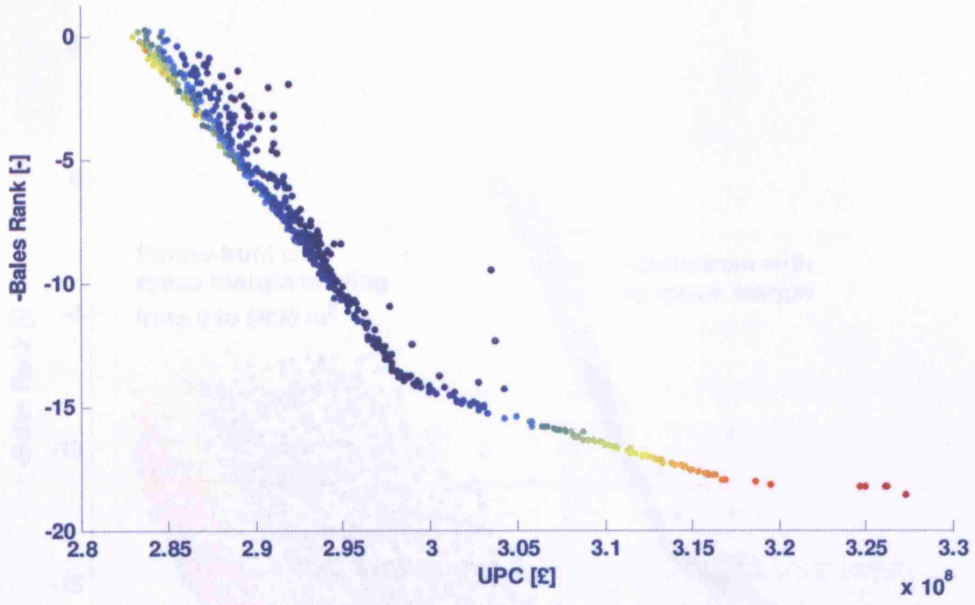

Figure 5-33: Pareto-front with three objectives (UPC, -Bales Rank and dT) and no space margin; red indicates high dT and blue indicates low dT

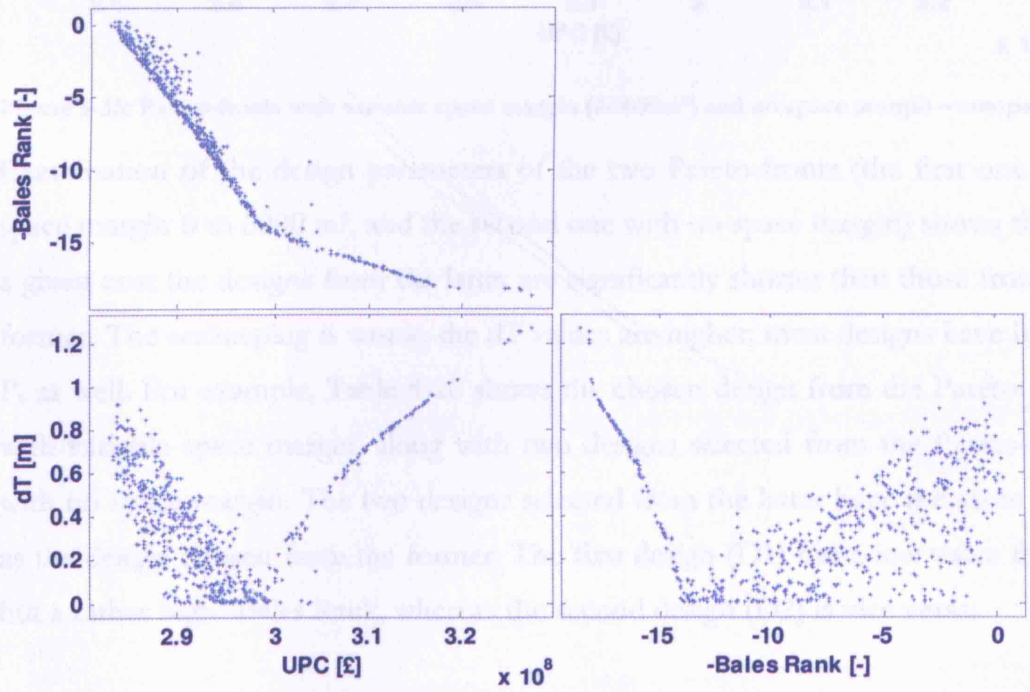

Figure 5-34: Pareto-front with three objectives (UPC, -Bales Rank and dT) and no space margin, shown as a matrix of 2D plots

Comparison of the above plots with the corresponding plots in Figure 5-24 and Figure 5-25 shows that keeping no space margin severely restricts the quality of the Pareto-front. To make the comparison easier, the two Pareto-fronts are shown in the same axes in Figure 5-35.

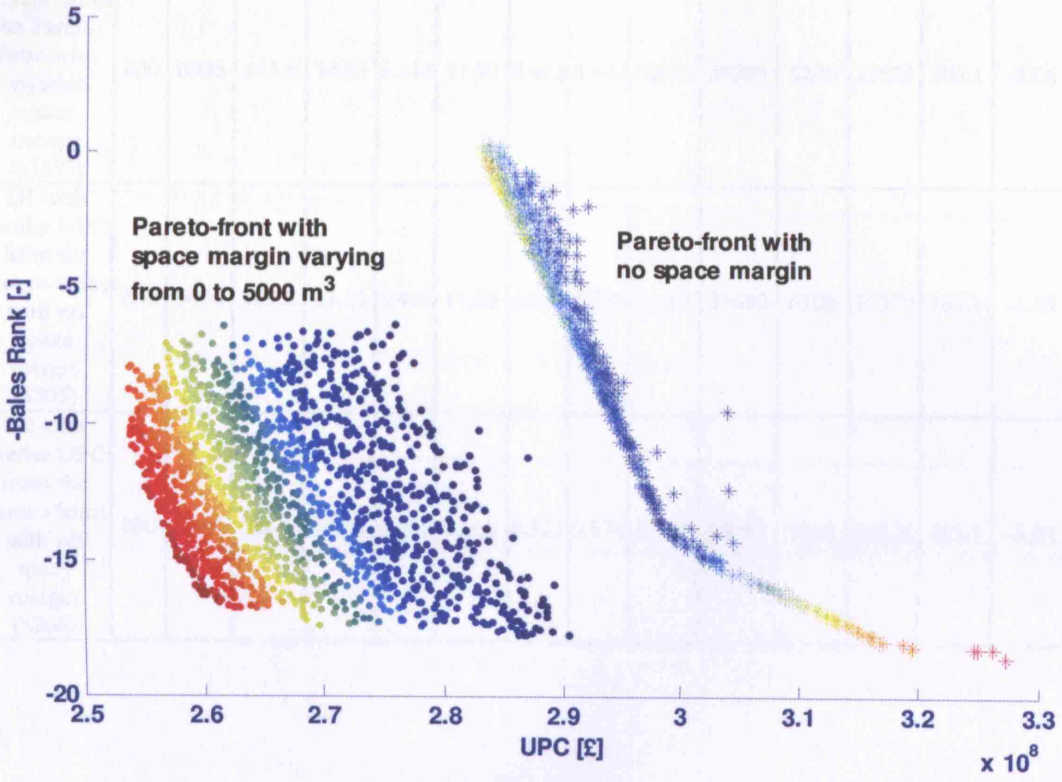

Figure 5-35: Pareto-fronts with variable space margin (0-5000m³) and no space margin – comparison

Examination of the design parameters of the two Pareto-fronts (the first one with space margin 0 to 5000 m³, and the second one with no space margin) shows that at a given cost the designs from the latter are significantly shorter than those from the former. The seakeeping is worse, the dT values are higher; most designs have higher P_s as well. For example, Table 5-20 shows the chosen design from the Pareto-front with variable space margin, along with two designs selected from the Pareto-front with no space margin. The two designs selected from the latter have the same UPC as the design chosen from the former. The first design (D1) has a low value for dT but a rather high -Bales Rank, whereas the second design (D2) is vice versa.

Table 5-20: Comparison of the design chosen from the Pareto-front with variable space margin (Figure 5-25), and the designs having the closest UPC from the Pareto-front with no space margin (Figure 5-34)

	W_{pay} [t]	V_{pay} [m^3]	L [m]	B [m]	T [m]	D [m]	C_B [-]	C_P [-]	ss [-]	P_s [kW]	Δ [t]	∇_{Gross} [m^3]	UPC [£M]	-Bales [-]	dT [m]
Selected design from the Pareto-front with variable space margin (S1597)	800	6908	153.5	14.85	5.514	11.00	0.483	0.692	0.259	39293	6220	22522	289.1	-17.6	0.0056
D1 with similar UPC from the Pareto-front with no space margin (S205)	800	5000	129.9	17.51	5.495	11.00	0.477	0.503	0.242	39690	6108	19379	289.1	-1.35	0.025
D2 with similar UPC from the Pareto-front with no space margin (S206)	800	5000	126.6	16.86	4.969	11.00	0.521	0.574	0.241	44099	5662	20123	289.1	-5.02	0.551

With space margin fixed at 1000m³

The Pareto-front obtained with a fixed space margin of 1000 m³, instead of variable space margin, is shown in Figure 5-36 and Figure 5-37.

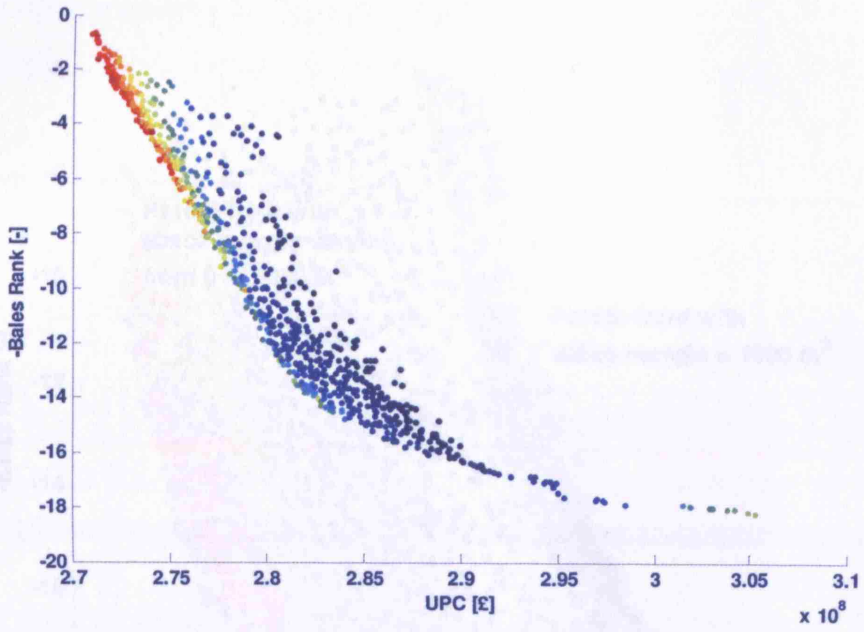

Figure 5-36: Pareto-front with three objectives (UPC, -Bales Rank and dT) and fixed space margin (1000 m³); red indicates high dT and blue indicates low dT

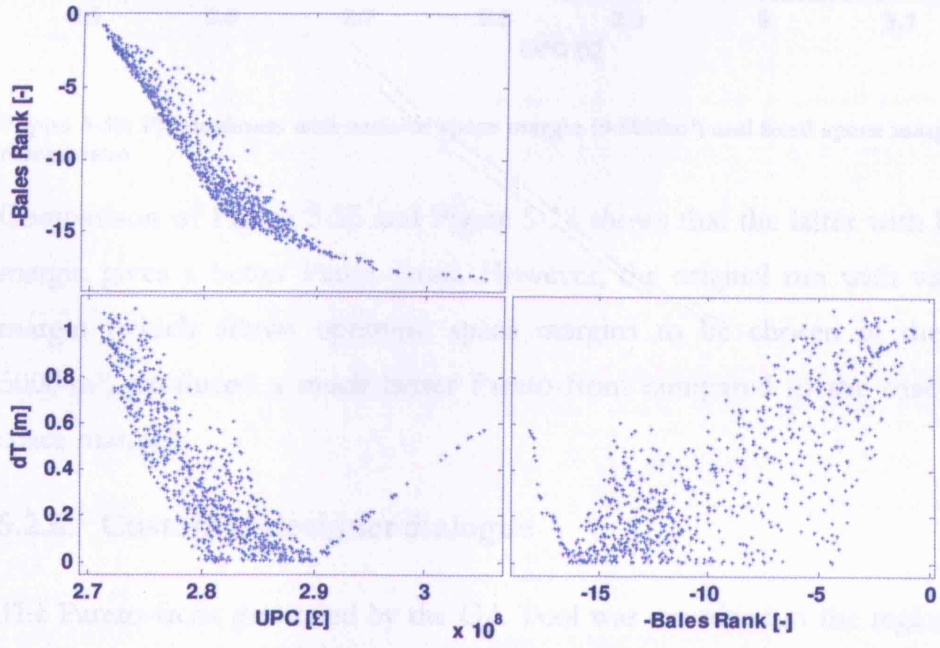

Figure 5-37: Pareto-front with three objectives (UPC, -Bales Rank and dT) and fixed space margin (1000 m³), shown as a matrix of 2D plots

Comparison of the above plots with the corresponding plots in Figure 5-24 and Figure 5-25 shows that fixing the space margin at 1000 m³ again restricts the quality of the Pareto-front, though the severity of restriction is less compared to the case of no space margin. To make the comparison easier, the two Pareto-fronts are shown in the same axes in Figure 5-38.

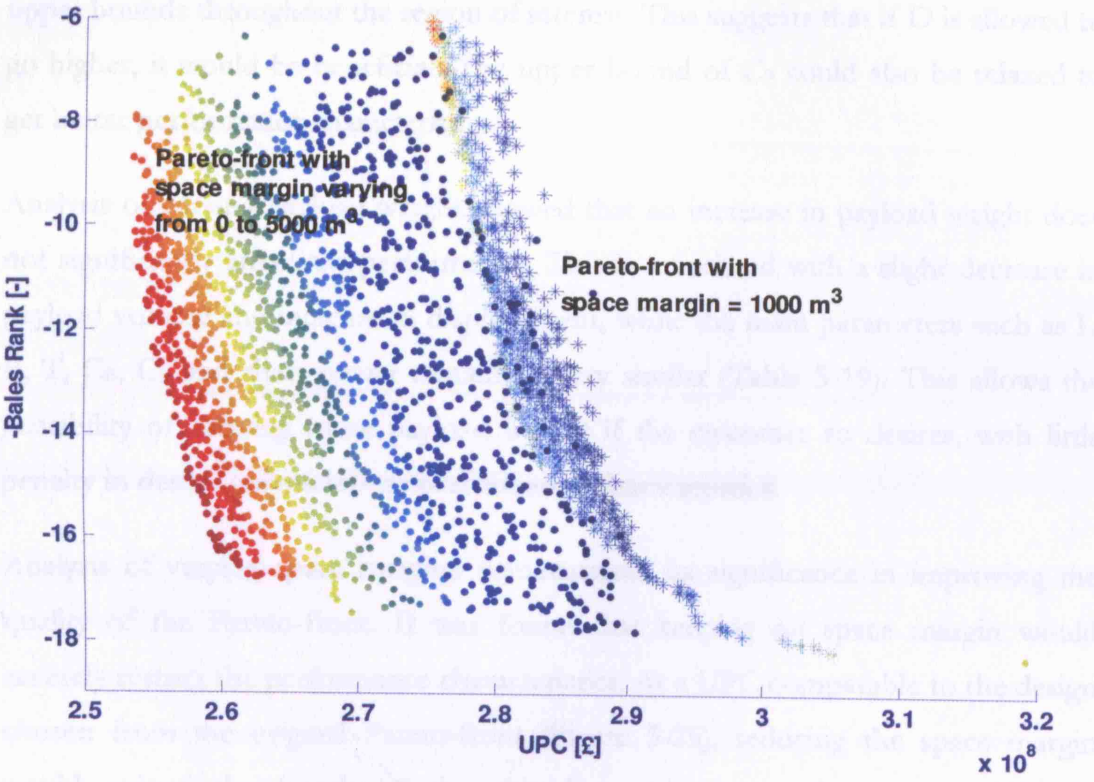

Figure 5-38: Pareto-fronts with variable space margin (0-5000m³) and fixed space margin (1000 m³) – comparison

Comparison of Figure 5-35 and Figure 5-38 shows that the latter with higher space margin gives a better Pareto-front. However, the original run with variable space margin (which allows optimum space margins to be chosen in the range 0 – 5000 m³) produced a much better Pareto-front compared to the cases with fixed space margins.

5.2.6. Customer-designer dialogue

The Pareto-front generated by the GA Tool was examined in the region of interest (i.e., around the specified UPC such that the change in draught is minimal). With the additional constraint on maximum shaft power, a few designs were short-listed in

Table 5-17. All the short-listed designs had very similar design and performance parameters; the one with the best -Bales Rank was selected as the final design from this short-list.

Analysis of constraints indicated that L/D and C_P are the most important constraints (apart from D, which is kept constant at 11.0 m). Both stay close to their upper bounds throughout the region of interest. This suggests that if D is allowed to go higher, it would be beneficial. The upper bound of C_P could also be relaxed to get better performance characteristics.

Analysis of varying payload weight showed that an increase in payload weight does not significantly affect the performance. This is associated with a slight decrease in payload volume and increase in displacement, while the main parameters such as L, B, T, C_B, C_P and shaft power remaining very similar (Table 5-19). This allows the possibility of carrying more payload weight if the customer so desires, with little penalty in design parameters or performance characteristics.

Analysis of varying space margins demonstrated its significance in improving the quality of the Pareto-front. It was found that keeping no space margin would severely restrict the performance characteristics. At a UPC comparable to the design chosen from the original Pareto-front (Figure 5-25), reducing the space margin would reduce the length of the ship but with the performance penalty in -Bales Rank and/or dT. For example, with no space margin, the ship length would be around 130m (instead of around 150m for the short-listed ship S1597 – see Table 5-20). Thus, if the customer wants a shorter ship, he can choose one with appropriately lower space margin.

The results of the analysis as summarised above would provide the basis for a discussion with the customer and lead to a suitable design being chosen for subsequent feasibility studies.

5.3. Application of the proposed design approach for handling design changes

The previous section demonstrated the application of the proposed design approach for concept design. This section describes how its can be used for handling design changes that may occur during the post-concept stage, or during early feasibility studies.

Design changes may be required during feasibility studies due to changes in customer requirements or changes in the estimated performance after more accurate performance analyses. Modifying the design at this stage could be very difficult and expensive; hence, it would be preferable to minimise the changes on key design parameters. The proposed design approach could assist in achieving this while ensuring that the required objectives continue to be met as far as possible.

5.3.1. Example scenario - original Pareto-front (3 objectives)

The Pareto-front used for the original concept design consisted of three objectives: minimisation of Build Cost, -Bales Rank and Length. Minimisation of length was included as an objective because of port limitations imposed as a customer constraint. The Pareto-front obtained, consisting of 520 designs, is shown in Figure 5-39 and Figure 5-40 in the 3-dimensional format and as three projections XY, XZ and YZ. The 3D format seems difficult to interpret in comparison with the three 2D projections. Other suitable graphical representations described in Appendix H could also be useful, when there may be more than three objectives.

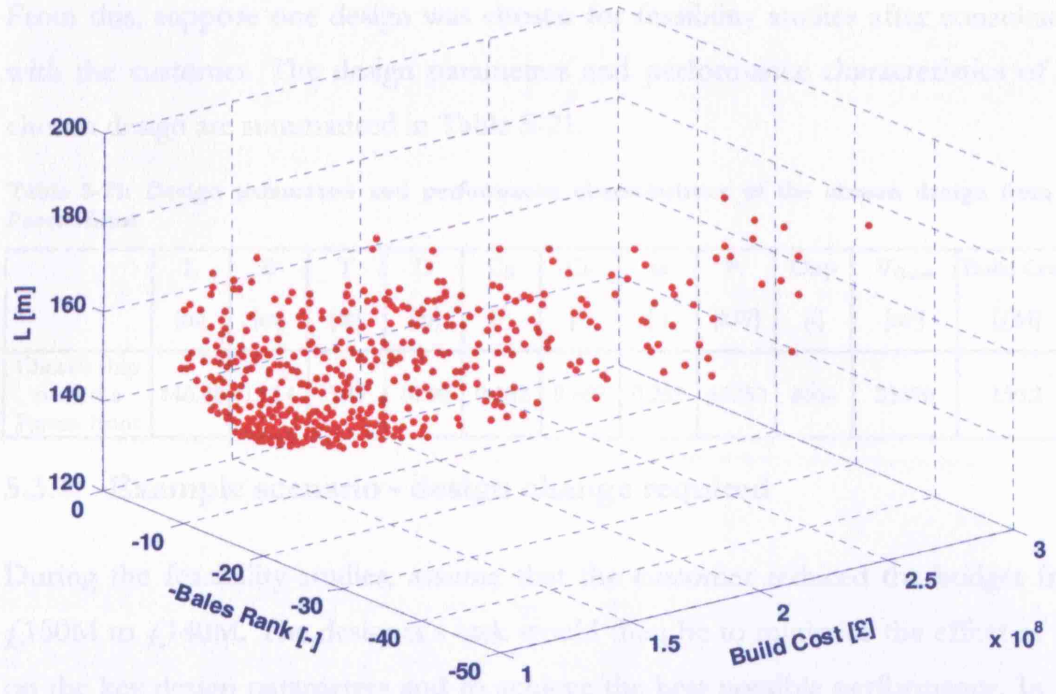

Figure 5-39: Pareto-front with three objectives (Build Cost, -Bales Rank and L), as a 3D plot

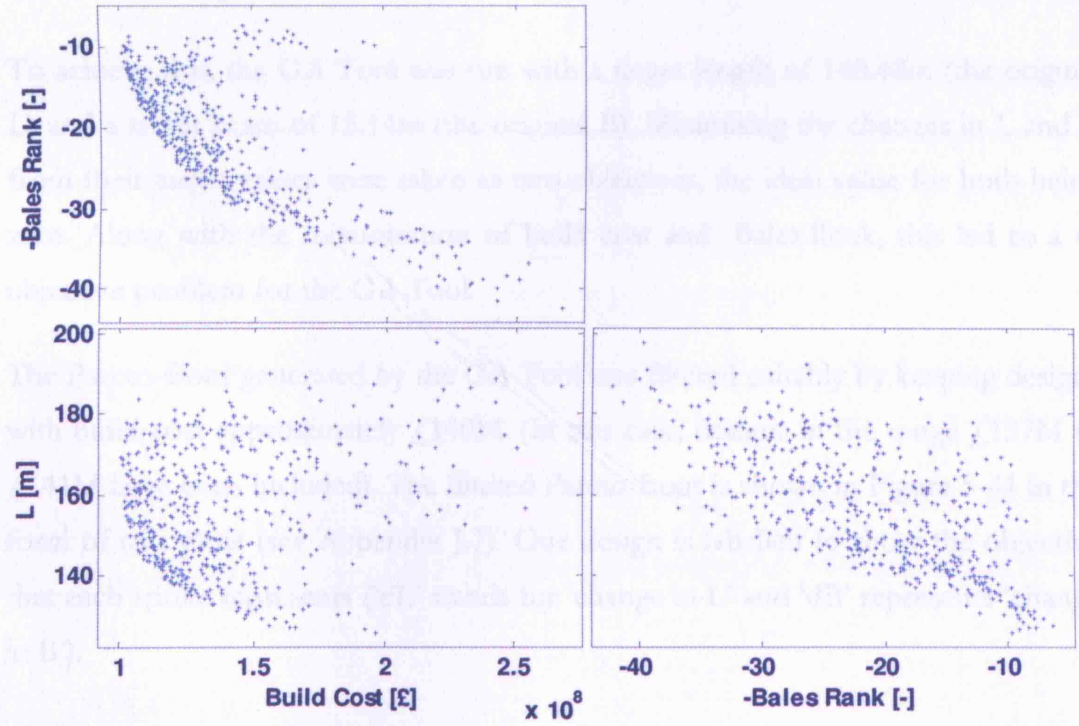

Figure 5-40: Pareto-front with three objectives (Build Cost, -Bales Rank and L), as a matrix of 2D plots

From this, suppose one design was chosen for feasibility studies after consultation with the customer. The design parameters and performance characteristics of the chosen design are summarised in Table 5-21.

Table 5-21: Design parameters and performance characteristics of the chosen design from the Pareto-front

	L [m]	B [m]	T [m]	D [m]	C_B [-]	C_P [-]	ss [-]	P_s [kW]	Disp [t]	∇_{Gross} [m³]	Build Cost [£M]	-Bales [-]
Chosen ship from the Pareto-front	140.48	15.14	5.43	10.92	0.682	0.807	0.269	66252	8066	25696	150.2	-21.4

5.3.2. Example scenario - design change required

During the feasibility studies, assume that the customer reduced the budget from £150M to £140M. The designer's task would then be to minimise the effect of this on the key design parameters and to achieve the best possible performance. In this case, the designer is likely to wish to minimise any changes to L and B to preserve the main deck layout.

To achieve this, the GA Tool was run with a target length of 140.48m (the original L) and a target beam of 15.14m (the original B). Minimising the changes in L and B from their target values were taken as two objectives, the ideal value for both being zero. Along with the minimisation of build cost and -Bales Rank, this led to a 4-objective problem for the GA Tool.

The Pareto-front generated by the GA Tool was filtered suitably by keeping designs with build cost approximately £140M. (In this case, designs in the range £137M to £141M have been included). The filtered Pareto-front is shown in Figure 5-41 in the form of star plots (see Appendix J.7). One design is labelled to show the objective that each spoke represents ('dL' stands for 'change in L' and 'dB' represents 'change in B').

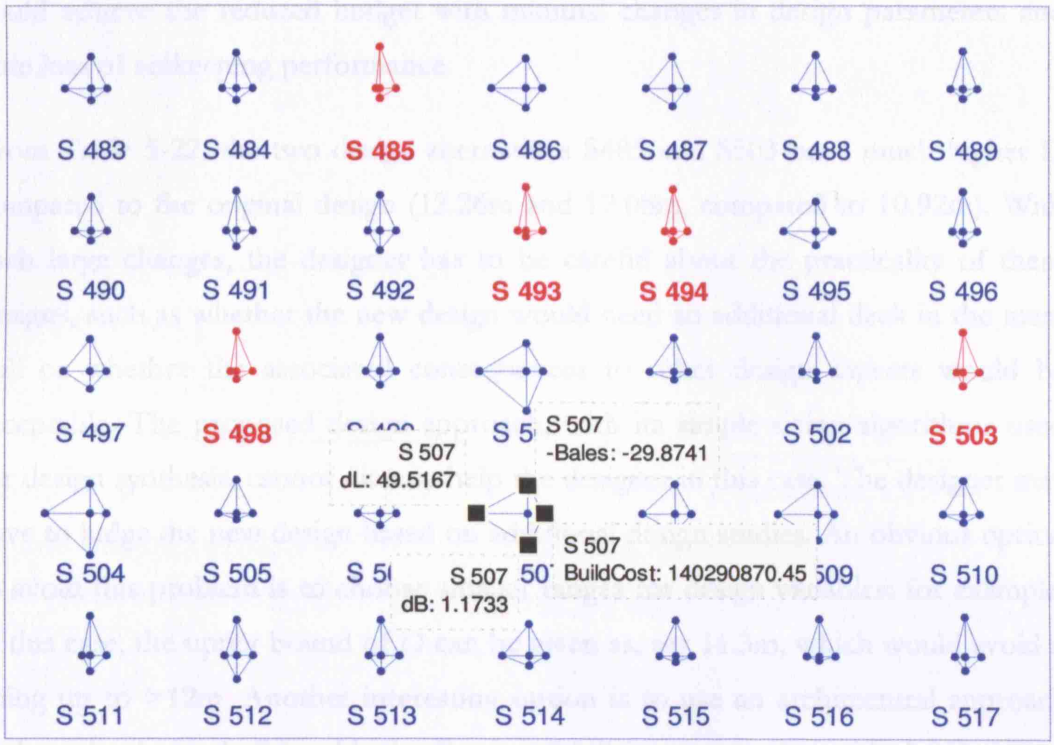

Figure 5-41: Star plots showing the post-concept design options with cost approximately £140M, 4 objectives. Suitable alternatives are highlighted in red.

The designer would look for a design having the shortest spokes for dL and dB, ideally both being zero. From the star plots, a few good alternatives can immediately be noted: S485, S493, S494, S498 and S503. Examining the values of all the spokes, the two most suitable options were chosen, S485 and S503. Their details are shown in Table 5-22, along with the original design for comparison.

Table 5-22: Post-concept design alternatives: reduced build cost of £140M, with minimum changes in L and B

	L [m]	B [m]	T [m]	D [m]	C_B [-]	C_P [-]	ss [-]	P_s [kW]	Δ [t]	∇_{Gross} [m³]	Build Cost [£M]	-Bales [-]	dL [m]	dB [m]
original design (Table 5-21)	140.48	15.14	5.43	10.92	0.682	0.807	0.269	66252	8066	25696	150.2	-21.4	0.00	0.00
S485	140.48	15.28	5.16	12.26	0.666	0.775	0.177	58319	7565	25746	137.6	-19.3	0.00	0.14
S503	140.81	15.48	5.49	12.08	0.635	0.762	0.217	57527	7796	26214	139.8	-19.6	0.32	0.34

The first option (S485) requires no change in L at all, and very little change in B. It has slightly less build cost as well, though at a marginally worse -Bales Rank. Thus, this option may be preferred over the second option. With this design, the designer

could achieve the reduced budget with minimal changes in design parameters and little loss of seakeeping performance.

From Table 5-22, the two design alternatives S485 and S503 have much higher D compared to the original design (12.26m and 12.08m, compared to 10.92m). With such large changes, the designer has to be careful about the practicality of these designs, such as whether the new design would need an additional deck in the main hull or whether the associated consequences to other design aspects would be acceptable. The proposed design approach, with its simple sizing algorithms used for design synthesis, cannot directly help the designer in this case. The designer may have to judge the new design based on additional design studies. An obvious option to avoid this problem is to choose smaller ranges for design variables: for example, in this case, the upper bound of D can be given as, say 11.3m, which would avoid it going up to >12m. Another interesting option is to use an architectural approach such as the design building blocks (Section 2.6.4) in combination with the proposed design approach. In this case, the designs suggested by the proposed design approach can be evaluated using the design building block approach to ensure that they satisfy the criterion that they are feasible and practical.

5.3.3. Example scenario – further restrictions in design parameters

Now consider another scenario where the original design remains the same and the customer wants to bring down the cost from £150M to £140M; however, since the design has progressed much further compared to the previous example, the designer would like to minimise changes to all main hull dimensions: L, B, D and T. The chosen alternative in the previous scenario was S485, as given in Table 5-22. For this, dD = 12.26-10.92 = 1.34m and dT = 5.43-5.16 = 0.27m. The designer would like to find out if it is possible to reduce these by re-running the GA Tool with dD and dT as additional objectives.

To achieve this, the GA Tool was run with the following target values (i.e., the original values of L, B, D and T):

- target L = 140.48m

- target B = 15.14m
- target D = 10.92m
- target T = 5.43m.

Changes in L, B, D and T from their target values become four objectives, the ideal value for all being zero. Along with the minimisation of build cost and -Bales Rank, they make this a 6-objective design problem. The resulting Pareto-front is filtered by keeping only those designs having build cost approximately £140M. The filtered Pareto-front is presented in Figure 5-42 in the form of star plots. One design is shown separately to identify the objective that each spoke represents.

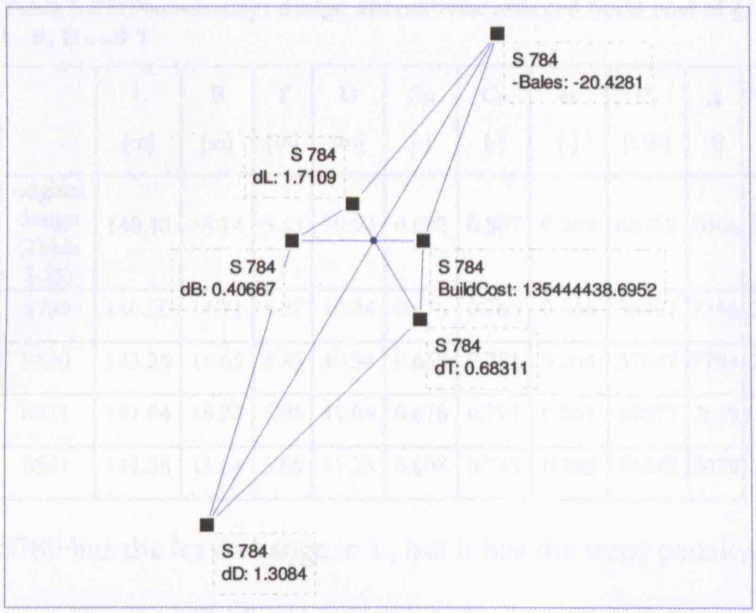

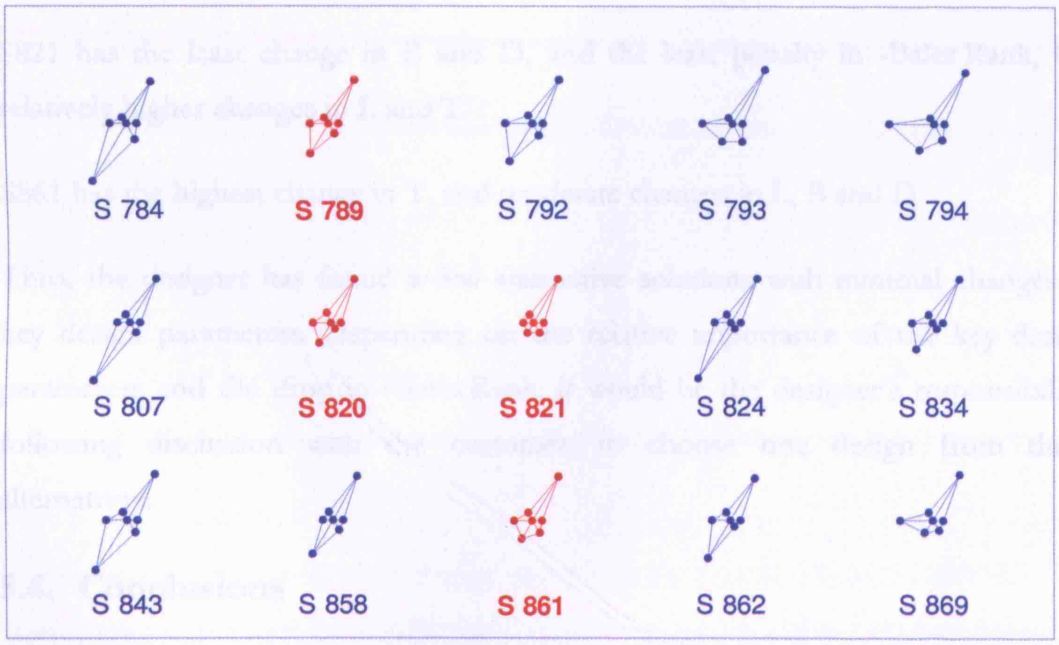

Figure 5-42: Star plots showing the post-concept design options with cost approximately £140M, 6 objectives. Suitable alternatives are highlighted in red.

As earlier, the designs of interest in Figure 5-42 are the ones with the smallest spokes for dL, dB, dD and dT. The designs S789, S820, S821 and S861 seem reasonably good. Their characteristics are given in Table 5-23.

Table 5-23: Post-concept design alternatives: reduced build cost of £140M, with minimum change in L, B, D and T

	L [m]	B [m]	T [m]	D [m]	C_B [-]	C_P [-]	ss [-]	P_s [kW]	Δ [t]	∇_{Gross} [m³]	Build Cost [£M]	-Bales [-]	dL [m]	dB [m]	dD [m]	dT [m]
original design (Table 5-21)	140.48	15.14	5.43	10.92	0.682	0.807	0.269	66252	8066	25696	150.2	-21.4	0.00	0.00	0.00	0.00
S789	140.50	14.71	5.27	10.34	0.676	0.765	0.266	56957	7546	22974	135.8	-18.0	0.01	0.43	0.58	0.16
S820	143.28	14.65	5.45	10.58	0.665	0.781	0.264	57647	7794	23750	138.6	-19.9	2.79	0.49	0.34	0.02
S821	141.94	15.28	5.06	11.04	0.678	0.793	0.263	59577	7629	26251	138.7	-20.5	1.46	0.14	0.12	0.36
S861	141.38	15.64	5.86	11.23	0.608	0.743	0.288	56642	8079	25903	142.5	-19.4	0.90	0.50	0.31	0.44

S789 has the least change in L, but it has the most penalty in -Bales Rank.

S820 has the least change in T, but the change in L is significant at 2.79m.

S821 has the least change in B and D, and the least penalty in -Bales Rank, but relatively higher changes in L and T.

S861 has the highest change in T, and moderate changes in L, B and D.

Thus, the designer has found a few alternative solutions with minimal changes in key design parameters. Depending on the relative importance of the key design parameters and the drop in -Bales Rank, it would be the designer's responsibility, following discussion with the customer, to choose one design from these alternatives.

5.4. Conclusions

This chapter demonstrated the use of the proposed design approach for three potential applications.

The first application was ab-initio concept design. Two objectives (minimising build cost and -Bales Rank) were considered, along with a fictitious set of design requirements. Analysis of the design space and the performance space for this example showed that there are no major changes in design parameters in the neighbourhood of the designs of interest. Design inputs and constraints that

severely limit the Pareto-front were identified and analysed. It was found that the original Pareto-front could be significantly improved by relaxing certain constraints, or using a higher space margin. Suitable design solutions were identified that could be the basis for a discussion with the customer and subsequent selection.

This application demonstrates the ability of the proposed design approach to provide useful design insights. Some of these may be obvious to the designer based on his experience and knowledge, but this may not always be the case. For example, the colour diagram in Figure 5-4 shows that ships with better seakeeping quality have larger displacement 'Δ', as one would expect from the Bales Rank formulation (Appendix H.6.5). However, the same colour diagram also shows that for seakeeping to improve, the draught 'T' first increases and then decreases. This is probably difficult to anticipate because a decrease in T should be better for seakeeping, as per the Bales Rank formulation. Further scrutiny of the colour diagram shows that, in this case, the increase in T allows an increase in Δ, the combined effect of which seems to be beneficial for seakeeping. However, continuing this trend at some point results in the violation of a constraint (the lower bound of B/T). The proposed design approach, through the use of genetic algorithms, still manages to find solutions with improved seakeeping by the manipulation of design variables, such as C_B and C_P, combined with the reduction in T. Such insights would not have been possible using traditional design approaches.

The second application of the proposed design approach was to modify a parent design to achieve the desired design requirements. It was demonstrated that the same design approach as for ab-initio concept design could be applied here, the difference being the narrower ranges for some of the design variables.

The third application was to minimise the effect of changes in design requirements on key design parameters. The required changes were treated as additional objectives to be achieved and the proposed design approach was applied with these additional objectives. The examples used a reduced budget as the changed requirement. A similar procedure can be used for other design changes such as top speed and payload; however, its applicability will become more limited as the

required design departure increases. Such changes would be difficult to achieve using traditional design approaches because there is no systematic procedure to solve such problems; the designer is unlikely to be in a position to decide in advance which of the many design parameters can be changed to achieve the desired goal.

The next chapter examines how the results of the proposed design approach compare with the results of a traditional design approach applied to three example naval combatant designs.

6. The proposed design approach compared with the traditional design approach – examples

This chapter compares the results of the proposed design approach with those obtained using a traditional design approach. The design methodology followed for the MSc Ship Design Exercise at UCL is chosen as the traditional design approach. Three student designs are selected for demonstration: a large frigate (approximately 6400 t displacement), a small frigate (approximately 4700 t displacement) and a corvette (approximately 1800 t displacement). The design approach followed in the Ship Design Exercise is outlined, and the methodology followed for comparison with the proposed design approach is described. Both the UCL Ship Design Exercise and the implementation of the proposed design approach follow the same design synthesis procedure (see Section 2.6.1) as well as weight, space and cost algorithms, ensuring the validity of the comparison. Conclusions are drawn from the comparison between the two approaches. A diagram relating different sections within this chapter is shown in Figure 6-1.

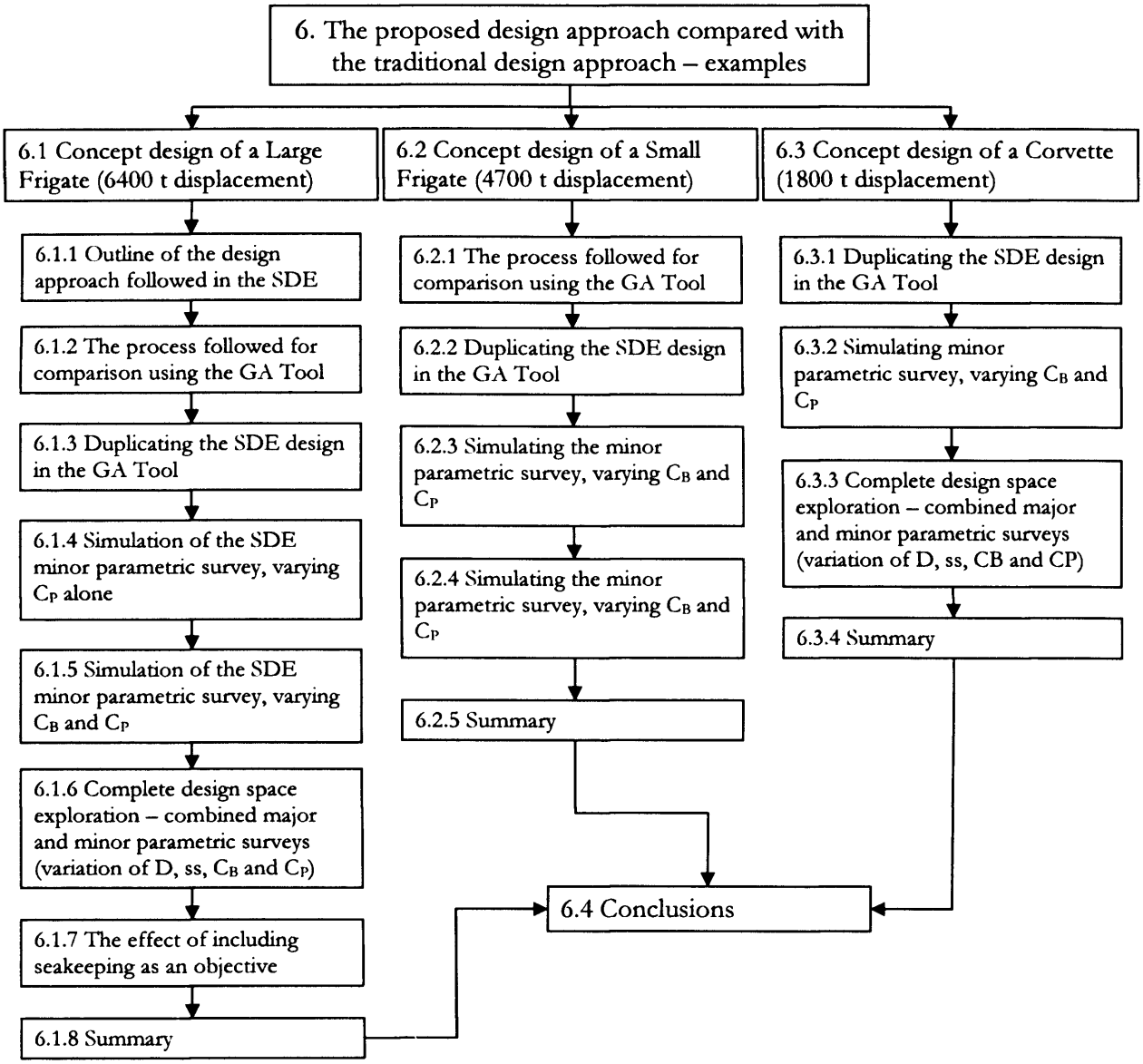

Figure 6-1: Outline of Chapter 6

6.1. Concept design of a Large Frigate (6400 t displacement)

This section applies the proposed design approach to a large frigate already designed by a traditional design approach. A frigate designed in 2004 as part of the UCL MSc in Naval Architecture Ship Design Exercise (SDE) [126] is chosen. The design approach followed in the SDE is described, followed by the process used for comparison with the proposed design approach. The results are discussed.

6.1.1. Outline of the design approach followed in the SDE

The following are the steps involved in the SDE design process, as seen from the naval architect's report [126]. See Section 2.6.1 for a description of the UCL ship design process.

1. The required payload weight and volume are decided from a cost-capability analysis.

2. Suitable values for D, ss, C_B and C_P are assumed based on historical data. Appropriate constraints are also assumed. Initial sizing gives gross size and main dimensions. The design is "numerically balanced"; i.e. the total weights and volumes of ship components match the displacement and gross enclosed volume of the ship.

3. A major parametric survey is carried out by varying D and ss within appropriate ranges $[D_{min},D_{max}]$ and $[ss_{min},ss_{max}]$. The most suitable design that satisfies all constraints is chosen. The corresponding D and ss are used for the next stage. *(In this case, a design near the middle of the feasible design window has been chosen, so that the design is not likely to violate any design constraints even after the minor parametric survey, which is the next step of the design process).*

4. A minor parametric survey is carried out varying C_B and C_P alone within appropriate ranges $[C_{Bmin},C_{Bmax}]$ and $[C_{Pmin},C_{Pmax}]$. The most suitable design that satisfies all constraints is chosen. The design obtained at the end of minor parametric survey is "re-balanced", i.e., it is ensured that the required

weight and volume are equal to the actual weight and volume of the ship. *(In the case of the present design, though the SDE report specifies a [C_{Bmin},C_{Bmax}] the actual minor parametric survey has been done with constant C_B. The ship with the least P_s is chosen as the final design, though its UPC was found to be slightly higher than the customer's original budget).*

The final SDE design is hereafter referred to as the "SDE Parent".

The SDE design approach is shown diagrammatically in Figure 6-2. The small circles represent the variations of a parameter. The large circles represent the optimum values chosen, and the small dots represent the values discarded. Hence the major parametric survey determines the most suitable values for D and ss, with C_B and C_P fixed to median values. Then, with the chosen values of D and ss, C_B and C_P are varied during the minor parametric survey and the most suitable values of C_B and C_P are selected.

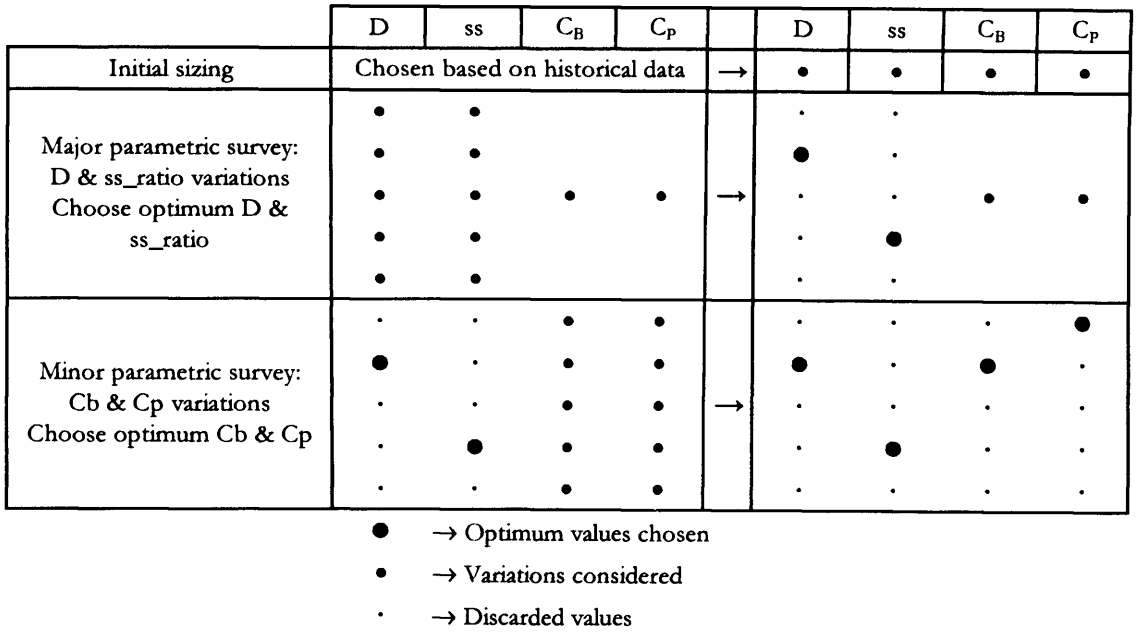

Figure 6-2: SDE design approach

6.1.2. The process followed for comparison using the GA Tool

The process followed to enable comparison of the output from the SDE with that from the GA Tool is as follows:

1. Duplicate the final SDE design ("SDE Parent") in the GA Tool such that its design parameters and performance characteristics match the SDE Parent as far as possible. This duplicated design is hereafter referred to as the "GA Parent".

2. Run the GA Tool by varying C_P alone, as was done in the minor parametric survey during the SDE. UPC and P_s are taken as the two objectives, since they are the ones of interest in the SDE. The GA Parent should be among the Pareto-designs, since the design space explored in both cases is the same.

3. Vary C_B and C_P, as usually done during the SDE minor parametric survey. Run the GA Tool with UPC and P_s as the two objectives. Compare the designs on the Pareto-front with the GA Parent. The aim is to estimate how much improvement could have been obtained if the SDE process had varied C_B and C_P simultaneously, instead of varying C_P alone.

4. Vary D, ss, C_B and C_P to explore the complete design space considered during the SDE design process (i.e., major and minor parametric surveys taken together). Run the GA Tool with UPC and P_s as the two objectives. Compare the designs on the Pareto-front with the GA Parent. The aim is to estimate how much improvement could have been obtained by using the proposed design approach instead of the traditional SDE design process.

These steps are described in the following subsections.

6.1.3. Duplicating the SDE design in the GA Tool

The first step was to create the GA Parent by modelling the SDE Parent in the GA Tool. To create the GA Parent, the design inputs used for the SDE Parent were duplicated as fixed inputs into the GA Tool. In spite of following the same design procedure and algorithms, the GA Parent was found to have slightly different design parameters compared to the SDE Parent. This occurred because not all the assumptions involved in using the design algorithms during SDE were available. To better match the GA Parent with the SDE Parent, the weight estimate, volume

estimate, GM estimate and cost estimate within the GA Tool had to be adjusted by a small factor. This required a few trial runs with different values for each coefficient.

The comparison between the SDE Parent and the GA Parent is shown in Table 6-1. Note that the SDE Parent is the same design used earlier in Section 5.2 for demonstrating the application of the proposed design approach for modifying a parent design.

Table 6-1: Design parameters for the Large Frigate - SDE Parent vs GA Parent

	W_{pay} [t]	V_{pay} [m^3]	speed [kn]	L [m]	B [m]	T [m]	D [m]	C_B [-]	C_P [-]	ss [-]	Δ [t]	∇_{Gross} [m^3]	UPC [£M]	P_s [kW]
SDE Parent	749.9	6259.2	30	145.10	15.71	5.52	11.00	0.50	0.63	0.250	6444	21786	287.0	37760
GA Parent	750	6259	30	145.20	15.71	5.51	11.00	0.50	0.63	0.250	6439	21797	287.0	38672

From the table, it is seen that the design parameters for the two ships are very similar.

The range of design variables considered during the whole SDE process is summarised below:

D = [11.0, 12.0]

ss = [0.178, 0.300]

C_B = [0.44, 0.52]

C_P = [0.53, 0.63]

The constraints considered during the SDE design process are:

L > 134m ("minimum length for upper deck layout")

B > 15m ("minimum beam for flight deck and hangar")

L/D <= 14.0

5 <= Ⓜ <= 9

The same ranges of design variables and constraints are used in the GA Tool.

In addition, the SDE report states that the C_P chosen should be reasonably high for 'ease of construction'. This has to be kept in mind when selecting suitable designs from the Pareto-front.

6.1.4. Simulating the SDE minor parametric survey, varying C_P alone

The minor parametric survey in SDE was done varying C_P alone (see Section 6.1.1). The selection of the most suitable design was based on shaft power P_s. This design was found to have a UPC slightly higher than the customer's budget (£287M instead of £280M). The same variation in C_P was used for the GA Tool. Two objectives were used – minimisation of shaft power and minimisation of UPC. The resulting Pareto-front is shown in Figure 6-3. The GA Parent is also shown for comparison.

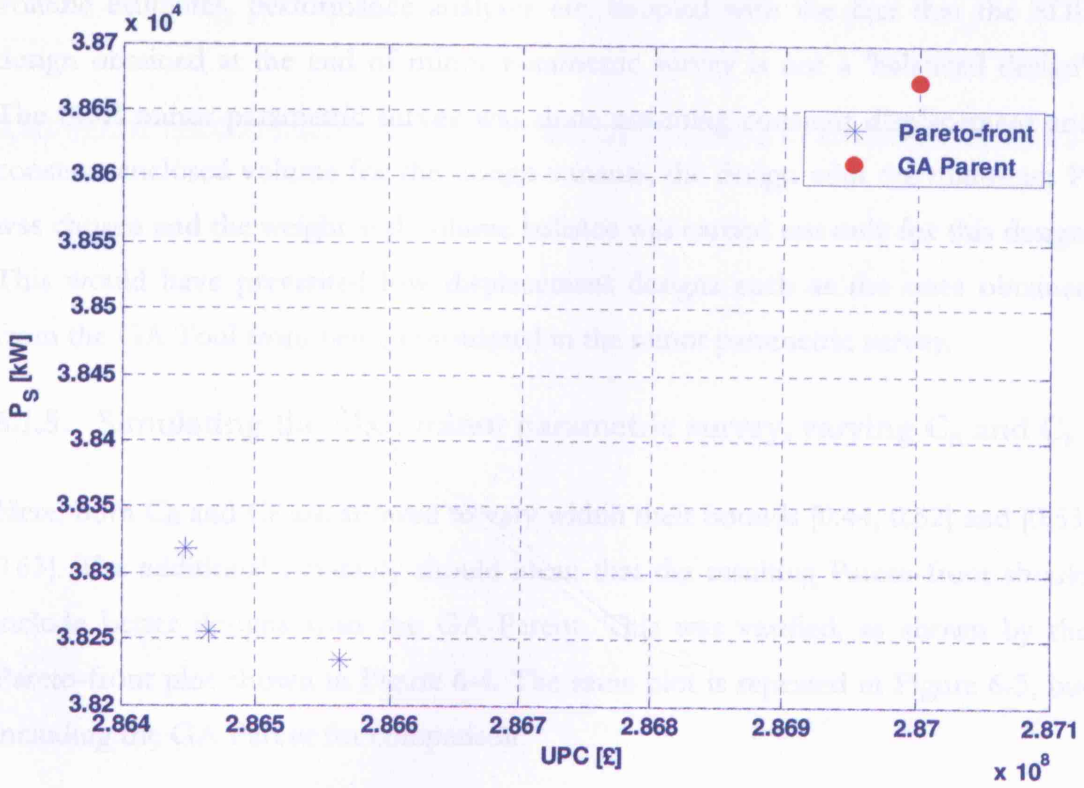

Figure 6-3: Pareto-front for the Large Frigate, with C_P variations only and two objectives (UPC and P_S)

The ranges of the shaft power and UPC in the results are both rather small, indicating that the two are compatible objectives. The values of shaft power are very similar to the value of the GA Parent, [38230-38320kW] against [38672kW];

similarly, the values of UPC are also very similar to that of the GA Parent, [£286.4M - £286.6M] against [£287.0M]. The design parameters for these designs are also found to be very similar to those of the GA Parent, as given in Table 6-2.

Table 6-2: The design parameters of the three Large Frigate designs on the Pareto-front (PF-1, PF-2 and PF-3), in comparison with those of the GA Parent

	L [m]	B [m]	T [m]	D [m]	C_B [-]	C_P [-]	SS [-]	Δ [t]	∇_{Gross} [m³]	UPC [£M]	P_s [kW]
GA Parent	145.20	15.71	5.51	11.00	0.500	0.630	0.250	6439	21797	287.0	38672
PF-1	143.83	15.82	5.48	11.00	0.500	0.621	0.250	6395	21688	286.4	38350
PF-2	144.02	15.84	5.47	11.00	0.500	0.621	0.250	6394	21687	286.5	38255
PF-3	144.05	15.85	5.47	11.00	0.500	0.620	0.250	6404	21702	286.6	38252

The minor differences can be attributed to the differences in weight estimates, volume estimates, performance analyses etc, coupled with the fact that the SDE design obtained at the end of minor parametric survey is not a 'balanced design'. The SDE minor parametric survey was done assuming constant displacement and constant enclosed volume for the design variants; the design with the minimum P_s was chosen and the weight and volume balance was carried out only for this design. This would have prevented low displacement designs such as the ones obtained from the GA Tool from being considered in the minor parametric survey.

6.1.5. Simulating the SDE minor parametric survey, varying C_B and C_P

Here, both C_B and C_P are allowed to vary within their bounds [0.44, 0.52] and [0.53, 0.63]. The additional flexibility should mean that the resulting Pareto-front should include better designs than the GA Parent. This was verified, as shown by the Pareto-front plot shown in Figure 6-4. The same plot is repeated in Figure 6-5, but including the GA Parent for comparison.

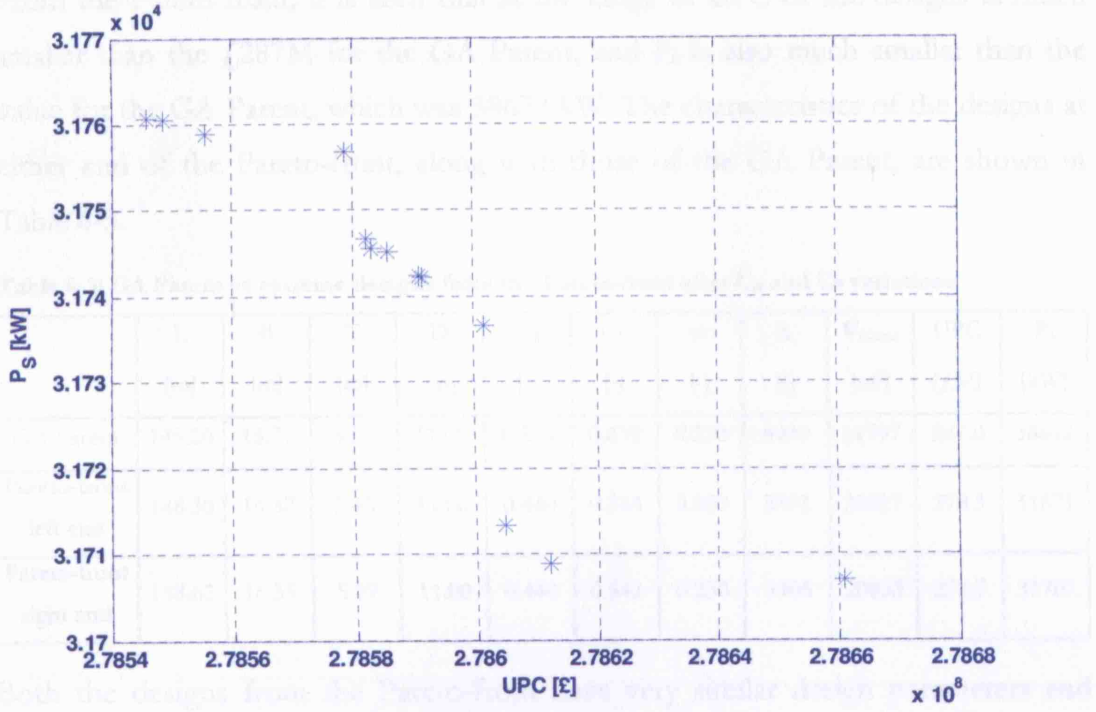

Figure 6-4: Pareto-front for the Large Frigate, with C_B and C_P variations and two objectives (UPC and P_S)

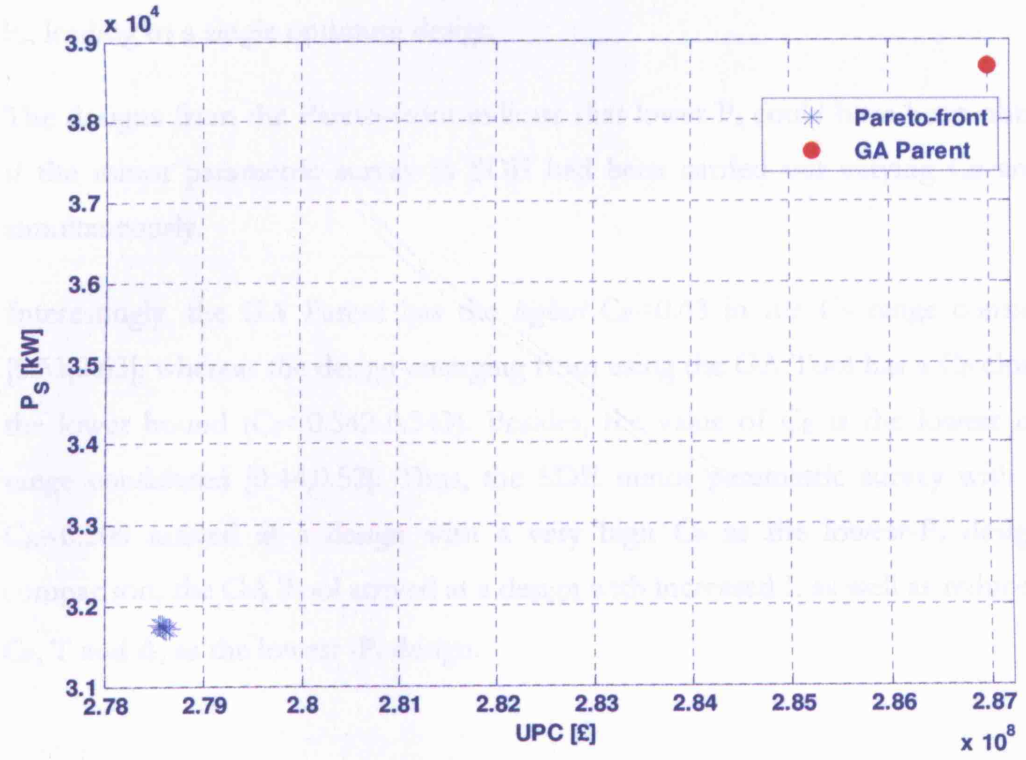

Figure 6-5: Pareto-front for the Large Frigate, with C_B and C_P variations, and two objectives (UPC and P_S); GA Parent is included for comparison

From the Pareto-front, it is seen that at the range of UPC of the designs is much smaller than the £287M for the GA Parent, and P_s is also much smaller than the value for the GA Parent, which was 38672 kW. The characteristics of the designs at either end of the Pareto-front, along with those of the GA Parent, are shown in Table 6-3.

Table 6-3: GA Parent vs extreme designs from the Pareto-front after C_B and C_P variations

	L [m]	B [m]	T [m]	D [m]	C_B [-]	C_P [-]	ss [-]	Δ [t]	∇_{Gross} [m³]	UPC [£M]	P_s [kW]
GA Parent	145.20	15.71	5.51	11.00	0.500	0.630	0.250	6439	21797	287.0	38672
Pareto-front left end	148.30	16.32	5.40	11.00	0.440	0.543	0.250	5891	20927	278.5	31671
Pareto-front right end	148.63	16.35	5.39	11.00	0.440	0.542	0.250	5905	20953	278.7	31707

Both the designs from the Pareto-front have very similar design parameters and performance characteristics. This happens because UPC and P_s are compatible objectives; hence minimisation of UPC is more or less equivalent to minimisation of P_s, leading to a single optimum design.

The designs from the Pareto-front indicate that lower P_s could have been obtained if the minor parametric survey in SDE had been carried out varying C_B and C_P simultaneously.

Interestingly, the GA Parent has the *highest* C_P=0.63 in the C_P range considered [0.53,0.63], whereas the design emerging from using the GA Tool has a C_P closer to the lower bound (C_P=0.542-0.543). Besides, the value of C_B is the lowest in the range considered [0.44,0.52]. Thus, the SDE minor parametric survey with fixed C_B=0.500 arrived at a design with a very high C_P as the lowest-P_s design; in comparison, the GA Tool arrived at a design with increased L as well as reduced C_B, C_P, T and Δ, as the lowest -P_s design.

6.1.6. Complete design space exploration – combined major and minor parametric surveys (variation of D, ss, C_B and C_P)

The GA Tool was run with the same set of design variable bounds and constraints as used in the SDE major and minor parametric surveys. This is repeated below:

D = [11.0, 12.0]

ss = [0.178, 0.300]

C_B = [0.44,0.52]

C_P = [0.53,0.63]

L > 134m ("minimum length for upper deck layout")

B > 15m ("minimum beam for flight deck and hangar")

L/D <= 14.0

5 <= Ⓜ <= 9

Two objectives were used: minimise UPC and minimise P_s. The resulting Pareto-front is shown in Figure 6-6, along with the GA Parent for comparison.

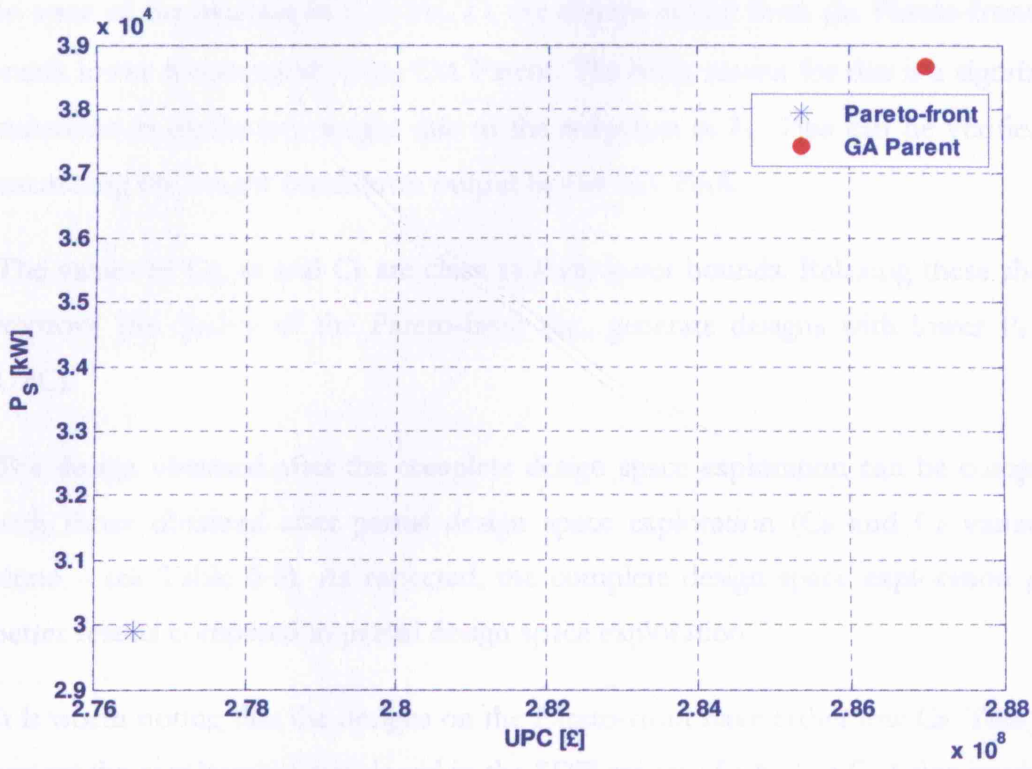

Figure 6-6: Pareto-front for the Large Frigate, with complete design space exploration and two objectives (UPC and P_S); GA Parent is included for comparison

The Pareto-front consists of just a single design with UPC = £276.5M and P_s = 29906 kW. This confirms that UPC and P_s are compatible objectives. The design that emerges from the Pareto-front analysis has lower UPC and P_s than the GA Parent. Its design parameters, along with those of the GA Parent, are given in Table 6-4.

Table 6-4: Design parameters for the single Large Frigate design on the Pareto-front

	L [m]	B [m]	T [m]	D [m]	C_B [-]	C_P [-]	ss [-]	Δ [t]	∇_{Gross} [m³]	UPC [£M]	P_s [kW]
GA Parent	145.20	15.71	5.51	11.00	0.500	0.630	0.250	6439	21797	287.0	38672
Pareto-front design	158.02	15.94	5.06	11.33	0.443	0.530	0.181	5787	20755	276.5	29906

It can be seen that the ship from the Pareto-front has:

- higher L
- slightly higher B and D
- lower T, C_B, C_P, ss, P_s, Δ and ∇_{Gross}

In spite of the increase in L, B and D, the chosen design from the Pareto-front has much lower Δ compared to the GA Parent. The likely reason for this is a significant reduction in machinery weight due to the reduction in P_s. This can be verified by examining the weight breakdown output by the GA Tool.

The values of C_B, ss and C_P are close to their lower bounds. Relaxing these should improve the quality of the Pareto-front (i.e., generate designs with lower P_s and UPC).

The design obtained after the complete design space exploration can be compared with those obtained after partial design space exploration (C_B and C_P variations alone – see Table 6-3). As expected, the complete design space exploration gives better results compared to partial design space exploration.

It is worth noting that the designs on the Pareto-front have rather low C_P. This goes against the requirement mentioned in the SDE report of a higher C_P being preferred for ease of construction. Besides, low C_P values are likely to result in poor

seakeeping qualities, based on Bales Rank. Thus, it is interesting to compare the seakeeping qualities of the designs of the Pareto-front with those of the original design, though seakeeping was not considered at all during the SDE:

Table 6-5: Comparison of the seakeeping quality of the Large Frigate design from the SDE and the design from the Pareto-front after complete design space exploration

	-Bales Rank [-]
GA Parent	-12.8
Pareto-design	-8.2

Thus, the seakeeping quality of the design on the Pareto-front is not as good as that of the GA Parent. This is as expected, because minimum P_s designs are compatible with minimum cost designs and will thus have reduced seakeeping performance (based on Bales Rank).

Due to this, a separate run was done with fixed C_P (at 0.63, i.e., the value of the GA Parent), and the GA Tool was run by varying D, ss and C_B. The resulting Pareto-front produced a single design (since UPC and P_s are compatible objectives). The design parameters and performance of this design is given in Table 6-6.

Table 6-6: Design parameters of the single Large Frigate design on the Pareto-front with fixed C_P (varying D, ss and C_B)

	L [m]	B [m]	T [m]	D [m]	C_B [-]	C_P [-]	ss [-]	Δ [t]	∇_{Gross} [m³]	UPC [£M]	P_s [kW]
GA Parent	145.20	15.71	5.51	11.00	0.500	0.630	0.250	6439	21797	287.0	38672
Pareto-design	156.98	15.00	5.10	11.21	0.510	0.630	0.180	6273	21566	284.6	36197

Thus, even if the C_P is fixed at a high value, it is still possible to have a design with better UPC and P_s compared to the GA Parent, though it is not as good as the one obtained with a lower C_P in Table 6-4. Besides, this ship was found to have a -Bales Rank of -14.5, which is better than the GA Parent that had -12.8.

6.1.7. The effect of including seakeeping as an objective

The SDE design focussed on achieving a feasible design within the target UPC. Only in the final stage, while varying C_P after fixing all other design parameters, was

there an attempt to examine an objective (i.e., achieve minimum P_s). The GA runs in the last section demonstrated that ships with low P_s generally have reduced seakeeping qualities, though fixing a high C_P value would ensure better seakeeping qualities (based on Bales Rank). Instead of fixing the C_P at the outset, it is possible to consider multiple objectives in the GA Tool while exploring the whole design space. Thus, a seakeeping measure (-Bales Rank) was included as an additional objective, along with UPC and P_s. The design variables D, ss, C_B and C_P are varied, as done before. The results are discussed here and the designs on the Pareto-front are compared with the GA Parent.

The Pareto-front obtained, consisting of 346 designs, is shown in Figure 6-7, Figure 6-8 and Figure 6-9, in three different formats. Note that the Pareto-front appears to be a curve on the 3D plane rather than a surface. This is because of the compatibility between UPC and P_s, effectively reducing the Pareto-front to a 2-dimensional problem. For comparison, Figure 6-9 shows the GA Parent also.

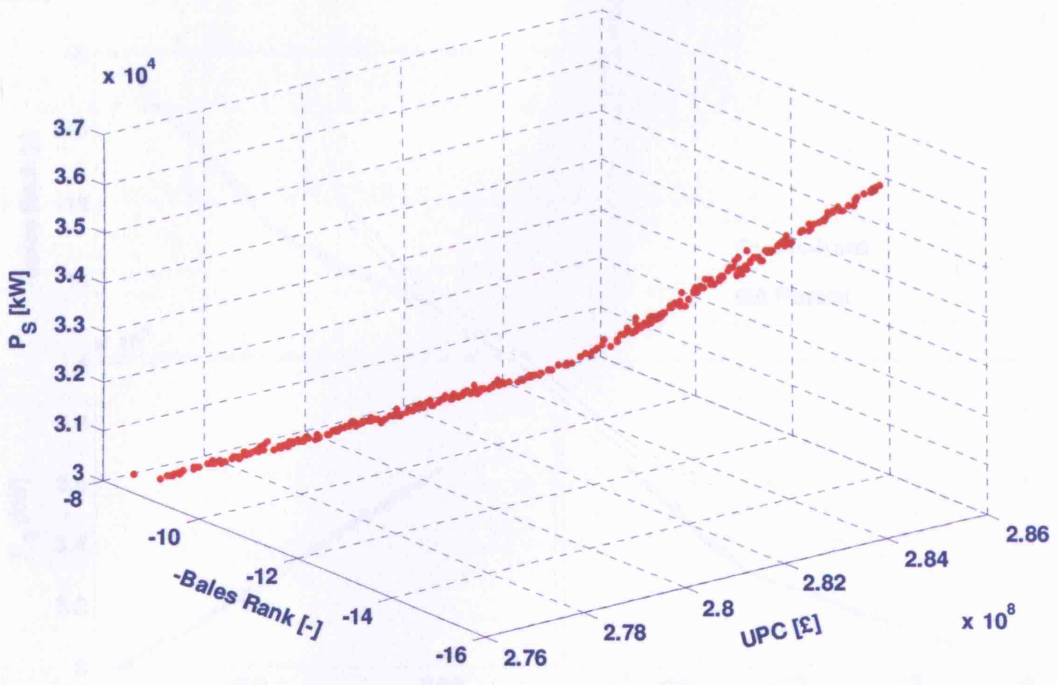

Figure 6-7: Pareto-front for the Large Frigate, with complete design space exploration and three objectives (UPC, -Bales Rank and P_s); 3D plot

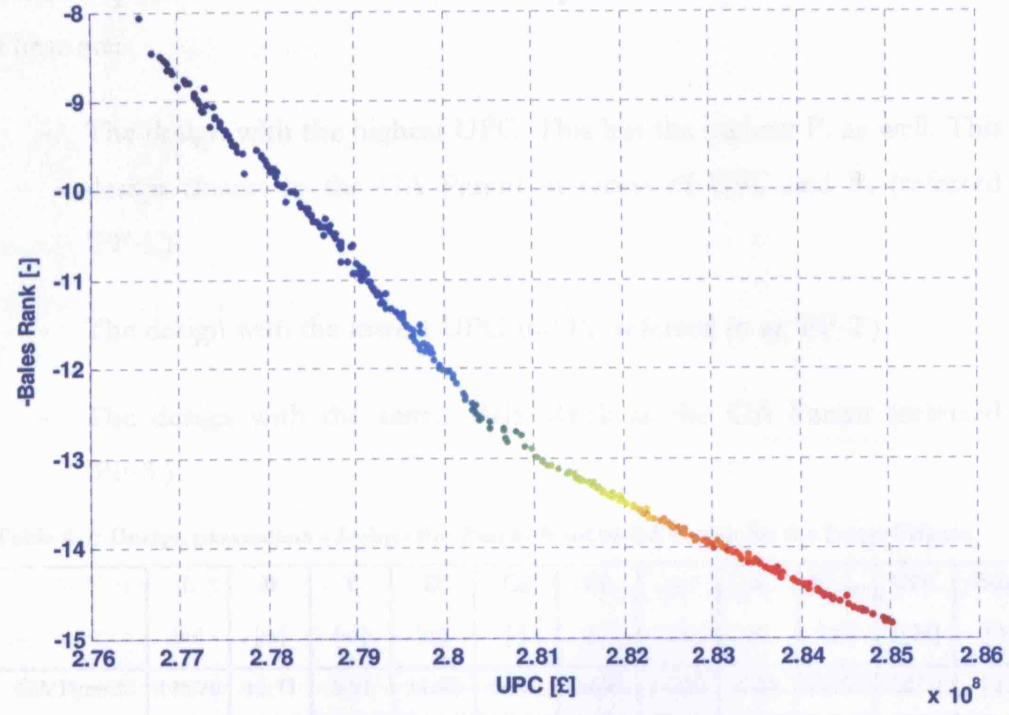

Figure 6-8: Pareto-front for the Large Frigate, with complete design space exploration and three objectives (UPC, -Bales Rank and P_s); red indicates high values of P_s and blue indicates low values of P_s

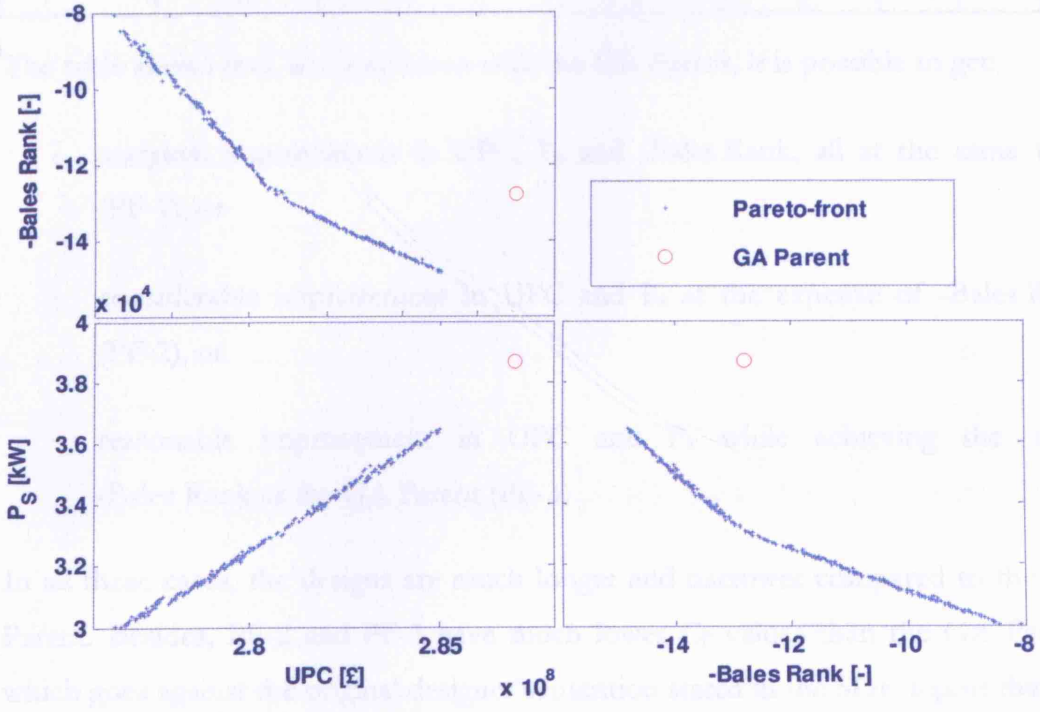

Figure 6-9: Pareto-front for the Large Frigate, with complete design space exploration and three objectives (UPC, -Bales Rank and P_s); matrix of 2D plots; GA Parent is included for comparison

Three ships from the Pareto-front are compared with the GA Parent in Table 6-7. These are:

- The design with the highest UPC. This has the highest P_s as well. This is the design closest to the GA Parent in terms of UPC and P_s (referred to as 'PF-1')
- The design with the lowest UPC and P_s (referred to as 'PF-2')
- The design with the same -Bales Rank as the GA Parent (referred to as 'PF-3')

Table 6-7: Design parameters - 3-objective Pareto-front vs GA Parent for the Large Frigate

	L [m]	B [m]	T [m]	D [m]	C_B [-]	C_P [-]	ss [-]	Δ [t]	∇_{Gross} [m³]	UPC [£M]	-Bales [-]	P_s [kW]
GA Parent	145.20	15.71	5.51	11.00	0.500	0.630	0.250	6439	21797	287.0	-12.8	38672
PF-1	157.53	15.00	5.89	11.28	0.442	0.627	0.242	6306	21619	285.0	-14.8	36426
PF-2	157.16	15.98	5.03	11.32	0.447	0.531	0.180	5785	20745	276.6	-8.07	30002
PF-3	161.69	15.11	5.48	11.60	0.441	0.588	0.180	6048	21217	280.9	-12.7	33045

The table shows that, in comparison with the GA Parent, it is possible to get:

- marginal improvement in UPC, P_s and -Bales Rank, all at the same time (PF-1), or
- considerable improvement in UPC and P_s at the expense of -Bales Rank (PF-2), or
- reasonable improvement in UPC and P_s while achieving the same -Bales Rank as the GA Parent (PF-3)

In all these cases, the designs are much longer and narrower compared to the GA Parent. Besides, PF-2 and PF-3 have much lower C_P values than the GA Parent, which goes against the original designer's intention stated in the SDE report that the C_P should be as high as possible to facilitate ease of construction. However, the C_P

of PF-1 is very close to that of the GA Parent. With its lower UPC and P_s, it could possibly be a good alternative to the GA Parent.

A colour diagram showing the trends of the design parameters and performance characteristics is given in Figure 6-10. The colour diagram shows that L and D are maximum near the middle of the Pareto-front and minimum near the ends. This seems to be a consequence of the constraint 'B>15m'. As UPC increases and seakeeping improves, B decreases until it reaches 15m, while L and D keep increasing. After this point, B cannot reduce further. In this region, further improvement in seakeeping is achieved through the increase in T and C_P, and consequent increase in P_s, Δ and ∇_{Gross}. When this happens, L and D decrease, and the resultant reduction in main hull volume is compensated by increasing the superstructure volume through increase in ss. The decrease in D and increase in ss have opposing effects on KG, and consequently GM: in this case, the result seems to be a reduction in GM, which in turn causes a reduction in B/T. The reduction in B/T is achieved by keeping B constant and increasing T. The variation in C_B appears rather irregular in the colour diagram; however, the examination of design parameters shows that the actual range of variation is [0.44,0.45] which is quite small.

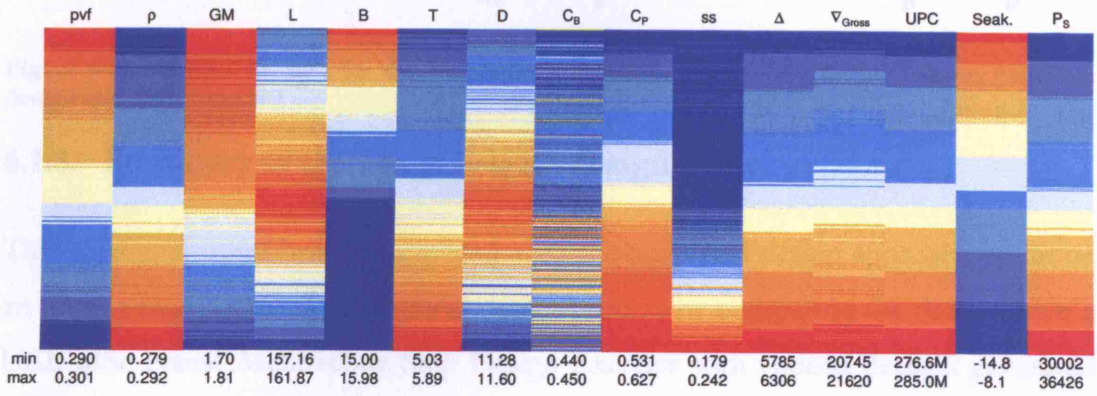

Figure 6-10: Colour diagram of the Pareto-front shown in Figure 6-9, consisting of 346 designs (Large Frigate, complete design space exploration)

The constraints plot corresponding to this Pareto-front is shown in Figure 6-11. It shows that the upper bound of L/D and the lower bound of C_B are the limiting constraints for the whole Pareto-front. The upper bound of Ⓜ and the lower bound

of ss remain important for a large part, while the lower and upper bounds of C_P limit the extent of the Pareto-front. Relaxing these constraints should improve the quality of the Pareto-front.

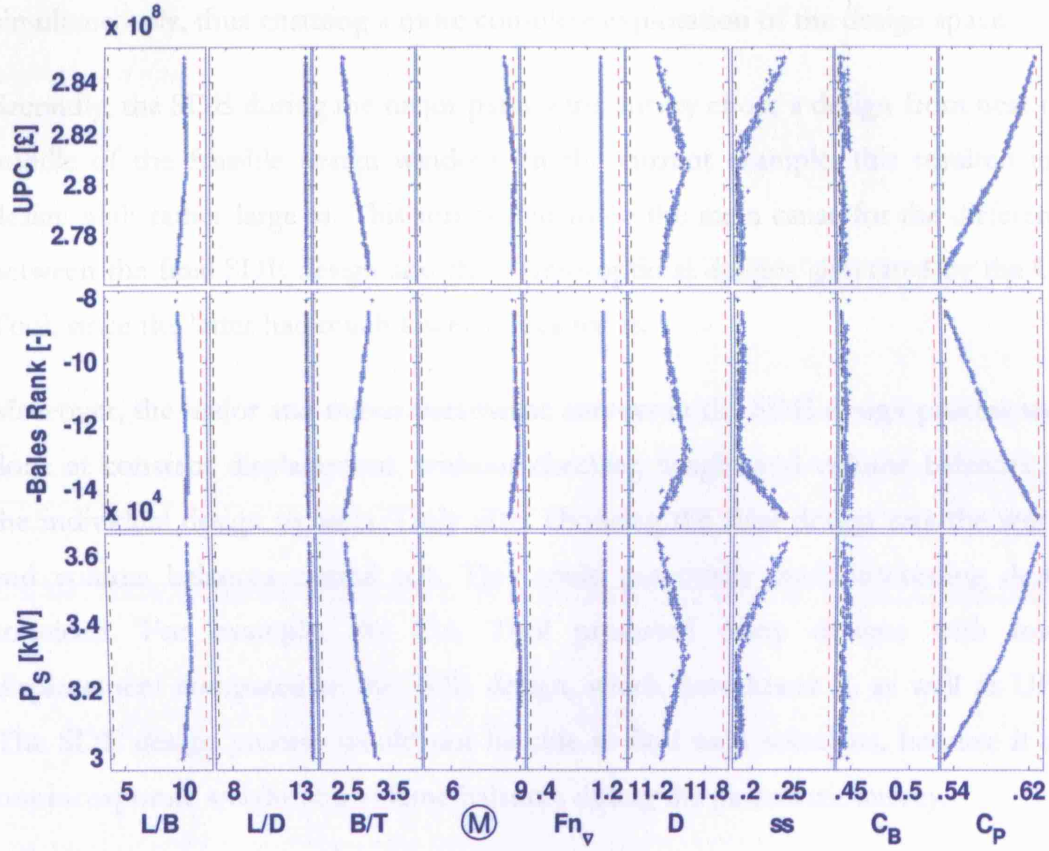

Figure 6-11: Constraints plot for the Pareto-front shown in Figure 6-9 (Large Frigate, complete design space exploration)

6.1.8. Summary of the Large Frigate design study

This section showed how the application of the proposed design approach could be an improvement over the traditional design process by comparing the design from a UCL MSc Naval Architecture Ship Design Exercise with various designs generated using the GA Tool. It was found that the designs from the GA Tool offer better performance characteristics compared to the design from the Ship Design Exercise.

Firstly, the SDE process used a limited two-stage exploration of the design space. In the first stage (the major parametric survey), C_B and C_P were kept constant based on historical data, and D and ss were varied. The aim was to select the most suitable

values for D and ss. These selected values of D and ss were kept constant in the second stage (the minor parametric survey) and C_B and C_P were varied. (*In the example chosen, C_B also was fixed during the minor parametric survey; only the variations in C_P were considered*). In comparison, the GA Tool varied all these four design parameters simultaneously, thus ensuring a more complete exploration of the design space.

Secondly, the SDE during the major parametric survey chose a design from near the middle of the feasible design window. In the current example, this resulted in a design with rather large ss. This turned out to be the main cause for the difference between the final SDE design and the Pareto-optimal designs generated by the GA Tool, since the latter had much lower values for ss.

Moreover, the major and minor parametric surveys in the SDE design process were done at constant displacement, without checking weight and volume balances for the individual design variants. Only after choosing the final design was the weight and volume balances carried out. This could potentially mask interesting design solutions. For example, the GA Tool produced many designs with lower displacement compared to the SDE design, which have lower P_s as well as UPC. The SDE design process would not be able to find such solutions, because it did not incorporate weight and volume balances during the parametric survey.

Finally, the SDE process used a very limited view of the objectives to be achieved. Only during the minor parametric survey was there an attempt to include an objective, which was to minimise P_s. In contrast, the GA Tool involved the evaluation of multiple objectives for all design variants. The current demonstration presented three objectives: UPC, P_s and -Bales Rank.

In summary, the results from the GA Tool offer better exploration of the design space and better investigation of the required objectives compared to the SDE design process. The performance characteristics of the designs obtained from the GA Tool were found superior to the final SDE design, even after taking into account the design intent that the C_P has to be as high as possible in view of ease of construction.

6.2. Concept design of a Small Frigate (4700 t displacement)

Similar to Section 6.1, this section compares the results of the proposed design approach when applied to an existing design. A general purpose frigate designed in 2006 as part of the UCL MSc Ship Design Exercise (SDE) is chosen for demonstration [127]. The process used in the GA Tool for comparison with the SDE is discussed in the following subsections. The design approach followed during the SDE is the same as described earlier in Section 6.1 and is not repeated here.

6.2.1. The process followed for comparison using the GA Tool

The comparison between the SDE and the proposed design approach is done in a manner similar to the Large Frigate Section 6.1. The difference is that in the case of the Large Frigate, the minor parametric survey was done varying C_P alone, whereas in the present case, it is done by varying both C_B and C_P. The steps involved in the comparison process are repeated below:

1. Duplicate the final SDE design ("SDE Parent") in the GA Tool such that its design parameters and performance characteristics match the SDE Parent as far as possible. This duplicated design is hereafter referred to as the "GA Parent".

2. Vary C_B and C_P, as done during the SDE minor parametric survey. Run the GA Tool with UPC, -Bales Rank and P_s as objectives. Compare the designs on the Pareto-front with the GA Parent.

3. Vary D, ss, C_B and C_P to explore the complete design space considered during the SDE design process (i.e., major and minor parametric surveys taken together). Run the GA Tool with UPC, -Bales Rank and P_s as objectives. Compare the designs on the Pareto-front with the GA Parent. The aim is to estimate how much improvement could have been obtained by using the proposed design approach instead of the traditional SDE design process.

These steps are described in the following subsections.

6.2.2. Duplicating the SDE design in the GA Tool

The first step was to create the GA Parent by modelling the SDE Parent in the GA Tool. To do this, the design inputs used for the SDE Parent were duplicated as fixed inputs into the GA Tool. In order to better match the GA Parent with the SDE Parent, where the precise design choices are no longer available the weight estimate, volume estimate, GM estimate and cost estimate within the GA Tool had to be adjusted by a small factor. This required a few trial runs with different values for each coefficient.

The comparison between the SDE Parent and the GA Parent is shown in Table 6-8. The Bales Rank for the SDE Parent is left blank because it was not calculated during the SDE.

Table 6-8: Design parameters for the Small Frigate - SDE Parent vs GA Parent

	W_{pay} [t]	V_{pay} [m^3]	speed [kn]	L [m]	B [m]	T [m]	D [m]	C_B [-]	C_P [-]	ss [-]	P_s [kW]	Δ [t]	∇_{Gross} [m^3]	UPC [£M]	-Bales [-]
SDE Parent	316.34	3189.2	30	127.96	15.73	5.08	11.20	0.45	0.57	0.20	33740	4707	16933.5	271.44	-
GA Parent	316.34	3189.2	30	126.21	15.63	5.17	11.20	0.45	0.57	0.20	35181	4706	16940	271.44	-4.4

From the table, it is seen that the design parameters for the GA Parent are very similar to the SDE Parent.

The range of design variables considered during the whole SDE process is summarised below [127]:

D = [8.3, 13.3] (corresponding to minimum hull depths for three internal decks and five internal decks)

ss = [0.18, 0.32]

C_B = [0.43, 0.53]

C_P = [0.49, 0.66]

The constraints considered during the SDE design process were [127]:

L > 115m ("based on preliminary upper deck layout");

10 <= L/D <= 14 ("hull slenderness ratio for structural integrity reasons");

5 <= Ⓜ <= 9 ("based on seakeeping and powering requirements");

B > 14m ("requirements of accommodating two Merlin helos in hangar");

D > 4.52m ("based on the largest gas turbine height to be accommodated").

Other considerations:

Draught – The minimum limit was based on propeller diameter to be used and the maximum limit was based on providing sufficient space at the quarter deck for the VDS launching and recovery;

Midship Coefficient C_M/Prismatic coefficient C_P – To be selected based on fitting of main machinery;

Hull slenderness ratio Ⓜ – To be chosen based on seakeeping and powering requirements. Larger values (Ⓜ > 8) give good seakeeping characteristics and less resistance at higher speeds.

The same ranges of design variables and constraints were used in the GA Tool.

6.2.3. Simulating the minor parametric survey, varying C_B and C_P

Here, both C_B and C_P were allowed to vary within their bounds [0.43, 0.53] and [0.49, 0.66]. This, in effect, duplicated the minor parametric survey done during the SDE. Since the same region of the design space was being explored by both the SDE and the GA Tool, the design obtained from the SDE was expected to be among the Pareto-designs produced by the GA Tool. In addition, the GA Tool was expected to generate other trade-off design options as well.

The Pareto-front generated by the GA Tool is shown in different formats in Figure 6-12, Figure 6-13 and Figure 6-14. In this case, there are 442 designs on the Pareto-front.

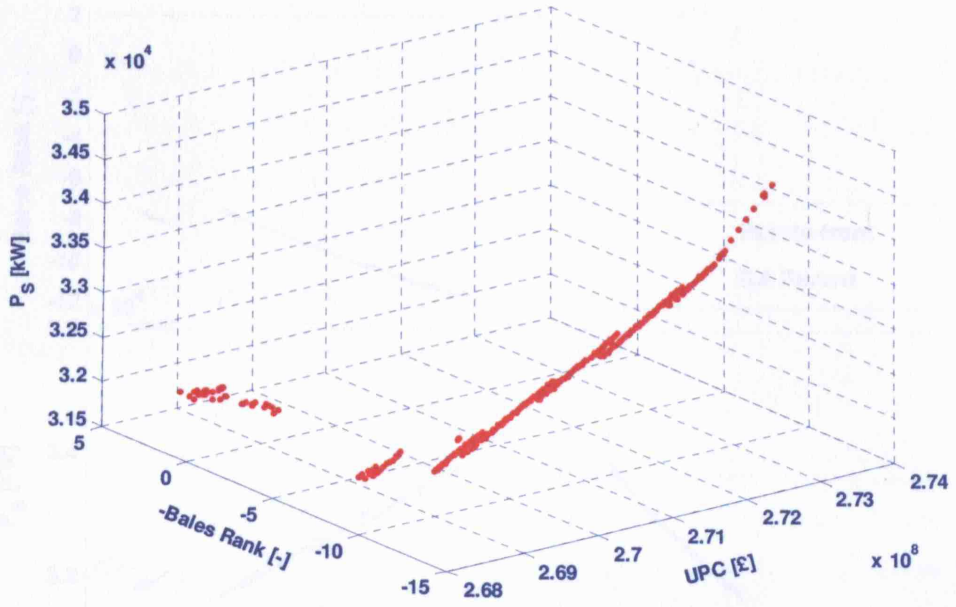

Figure 6-12: Pareto-front for the Small Frigate, with C_B and C_P variations, and three objectives (UPC, -Bales Rank and P_S); 3D plot

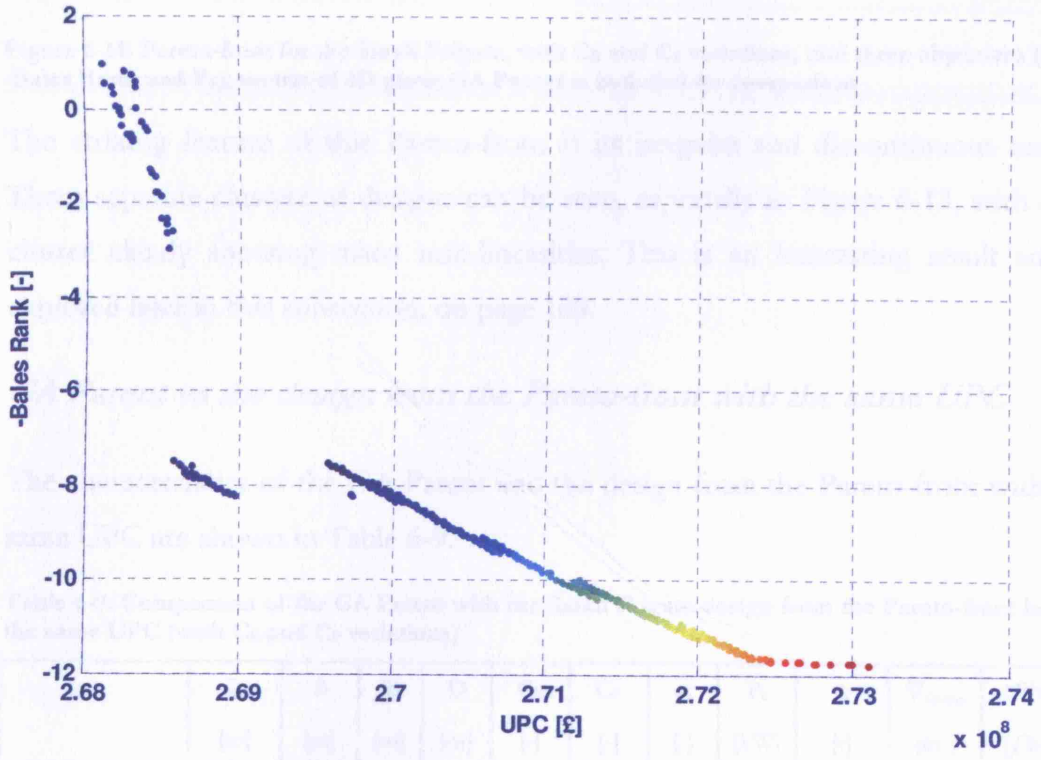

Figure 6-13: Pareto-front for the Small Frigate, with C_B and C_P variations, and three objectives (UPC, -Bales Rank and P_S); red indicates high P_s and blue indicates low P_s

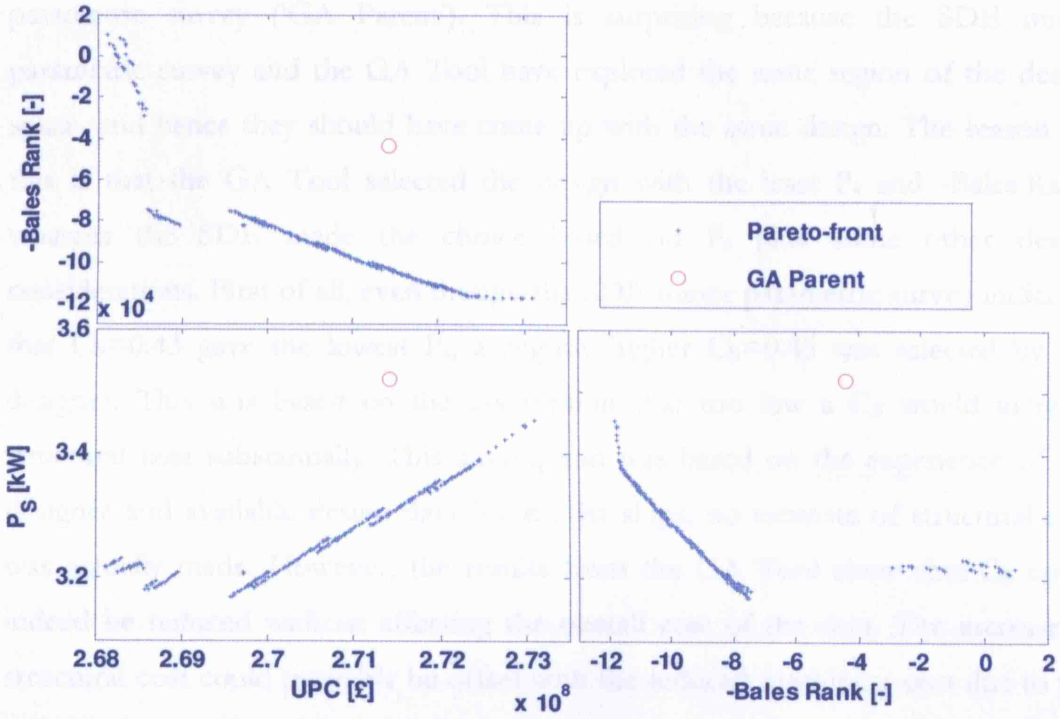

Figure 6-14: Pareto-front for the Small Frigate, with C_B and C_P variations, and three objectives (UPC, -Bales Rank and P_S); matrix of 2D plots; GA Parent is included for comparison

The striking feature of this Pareto-front is its irregular and discontinuous nature. Three separate clusters of designs can be seen, especially in Figure 6-13, with each cluster clearly showing many non-linearities. This is an interesting result and is explored later in this subsection, on page 189.

GA Parent vs the design from the Pareto-front with the same UPC

The characteristics of the GA Parent and the design from the Pareto-front with the same UPC are shown in Table 6-9.

Table 6-9: Comparison of the GA Parent with the Small Frigate design from the Pareto-front having the same UPC (with C_B and C_P variations)

	L [m]	B [m]	T [m]	D [m]	C_B [-]	C_P [-]	ss [-]	P_s [kW]	Δ [t]	∇_{Gross} [m³]	UPC [£M]	-Bales [-]
GA Parent	126.21	15.63	5.17	11.20	0.450	0.570	0.20	35181	4706	16940	271.44	-4.4
Equal cost design from the Pareto-front	138.60	14.26	5.54	11.20	0.430	0.634	0.20	33043	4827	17154	271.44	-10.4

Table 6-9 shows that the design produced by the Pareto-front analysis has better -Bales Rank as well as P_s compared to the design produced by the SDE minor

parametric survey ('GA Parent'). This is surprising because the SDE minor parametric survey and the GA Tool have explored the same region of the design space, and hence they should have come up with the same design. The reason for this is that the GA Tool selected the design with the least P_s and -Bales Rank, whereas the SDE made the choice based on P_s plus some other design considerations. First of all, even though the SDE minor parametric survey indicated that C_B=0.43 gave the lowest P_s, a slightly higher C_B=0.45 was selected by the designer. This was based on the assumption that too low a C_B would increase structural cost substantially. This assumption was based on the experience of the designer and available design data for similar ships; no estimate of structural cost was actually made. However, the results from the GA Tool show that C_B could indeed be reduced without affecting the overall cost of the ship. The increase in structural cost could probably be offset with the reduced machinery cost due to the reduced P_s.

The SDE minor parametric survey fixed the C_B at 0.45 and then the choice of C_P was examined. This was done considering the midship space requirement for machinery fit. It was decided to choose a low value of C_P but not too low, and a compromise value of 0.57 was deemed sufficient for fitting the machinery. Again, it is seen that the choice of C_P was governed primarily by previous similar ship designs.

Because of these reasons, the design suggested by the GA Tool after exploring the variations in C_B and C_P is rather different from the design chosen after the minor parametric survey by the SDE designer.

Discontinuities in the Pareto-front obtained varying C_B and C_P

As noted earlier, the Pareto-front resulting from the variations in C_B and C_P show different clusters with varying performance characteristics. The three main clusters (as seen in Figure 6-13) can be categorised as follows:

Cluster-1: the low-UPC region (UPC < £268.5M, -Bales Rank > -4)

Cluster-2: the mid-UPC region (UPC £268.5M to £269.0M, -Bales Rank -9 to -7)

Cluster-3: the high-UPC region (UPC > £269.5M)

The transition from Cluster-1 to Cluster-2 involves a large drop in Bales Rank, combined with slight differences in UPC and P_S. In comparison, the transition between Cluster-2 and Cluster-3 is much smaller in terms of all the three objectives.

The reasons for the discontinuities resulting in these design clusters are investigated here. This is done in three steps. Firstly, the colour diagram is examined looking for any irregularities or sudden changes in trends. Secondly, the constraints plots are examined to see how the transition regions appear in them. Thirdly, the star plots around the transition regions are examined, along with the actual numerical values of the design and performance parameters.

Analysis of the colour diagram

First, the colour diagram can be examined for any irregularities (Figure 6-15). Near the top of the plot, a clear discontinuity can be spotted, where seakeeping changes from red to light blue colour. (A dotted line is shown on the plot for easy identification). Some of the other columns also show sudden changes here: most notably L, B, T and C_P. Examination of the values of the parameters in this region indicates that this is the transition from Cluster-1 to Cluster-2. Thus, the sudden drop in seakeeping during this transition is associated with sudden increase in L, T and C_P, as well as sudden reduction in B.

The rest of the colour diagram does not show any sudden variations. Thus, the transition between Cluster-2 and Cluster-3 is not clearly visible in the colour diagram, indicating that the changes in design parameters and performance characteristics for this transition are probably rather small.

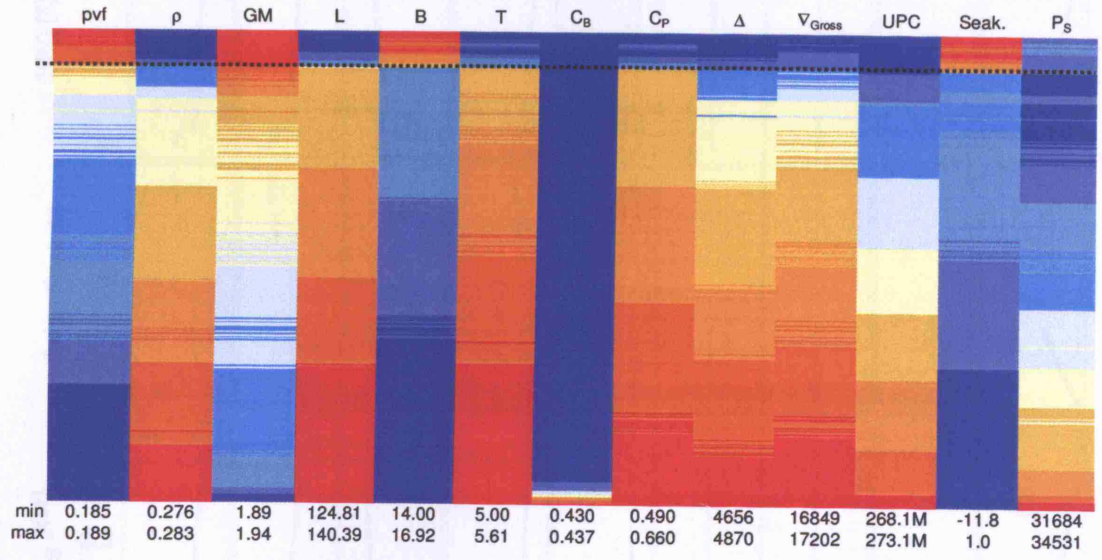

Figure 6-15: Colour diagram of the Pareto-front shown in Figure 6-14, consisting of 442 designs (Small Frigate; C_B and C_P variations)

Analysis of the constraints plot

The constraints plot corresponding to the Pareto-front is shown in Figure 6-16. It confirms that there is a sudden change in most constraints between Cluster-1 (low UPC) and Cluster-2 (mid UPC), whereas there is very little change between Cluster-2 (mid UPC) and Cluster-3 (high UPC). For example, consider the subplot corresponding to UPC and L/B (the top left corner). It shows that L/B suddenly increases from Cluster-1 to Cluster-2, whereas the change is very little between Cluster-2 and Cluster-3. Similar trends can be found in the case of L/D, B/T, Ⓜ and C_P. This confirms the conclusion from the colour diagram that the transition between Cluster-2 and Cluster-3 does not involve major changes in design parameters.

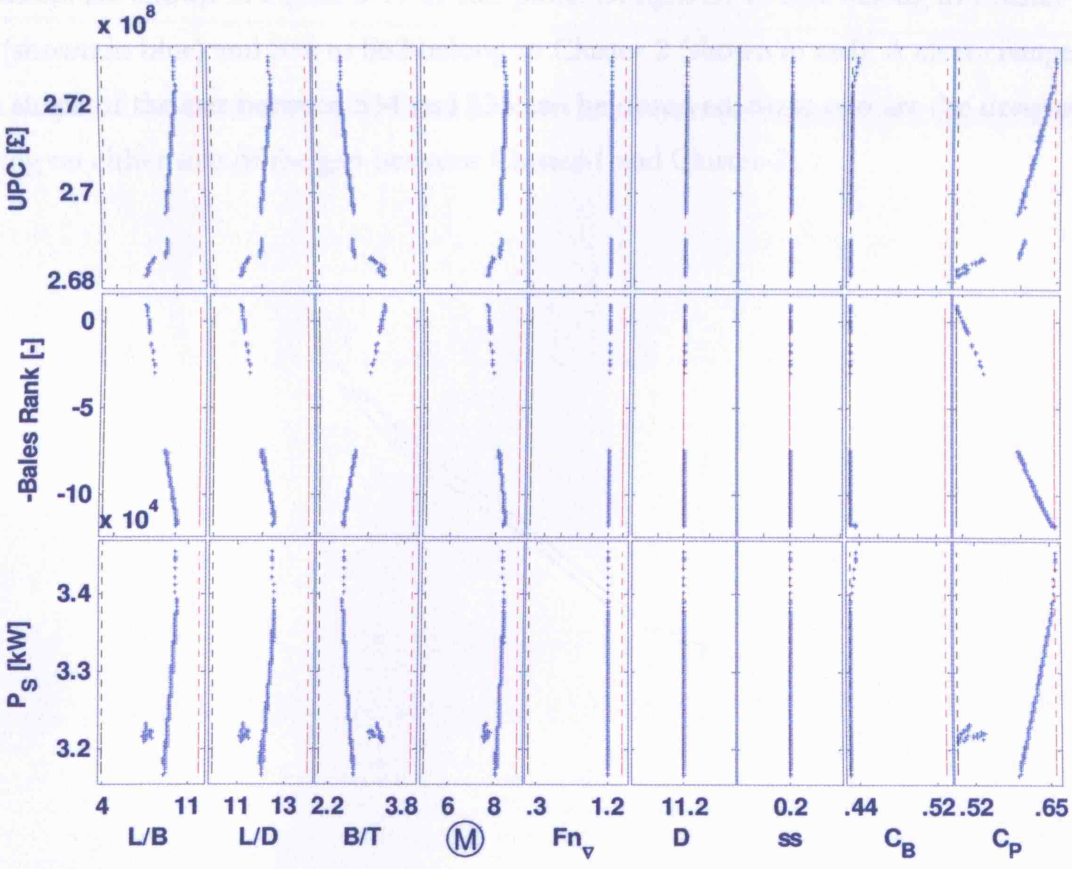

Figure 6-16: Constraints plot of the Pareto-front shown in Figure 6-14 (Small Frigate; C_B and C_P variations)

The constraints plot shows that none of the constraints are close to violation in the transition regions (apart from C_B, which remains close to its lower bound almost throughout the Pareto-front). Besides, numerical examination of the design parameters in this region indicates that the additional constraints considered for this design (minimum values for L, B and D) are also well away from their bounds. Hence, the analysis of the constraints provides no clue for the reasons for the discontinuities in this Pareto-front.

Analysis of star plots around the transition regions

Finally, the star plots can be used to examine the design parameters. First, the region around the first transition (Cluster-1 to Cluster-2, as identified from the colour diagram) was investigated. The design parameters of all the designs in these two clusters are shown in Figure 6-17 as star plots. Designs S1 to S34 belong to Cluster-1 (shown in blue) and S35 to S62 belong to Cluster-2 (shown in red). A clear change in shape of the star between S34 and S35 can be observed; these two are the designs lying on either side of the gap between Cluster-1 and Cluster-2.

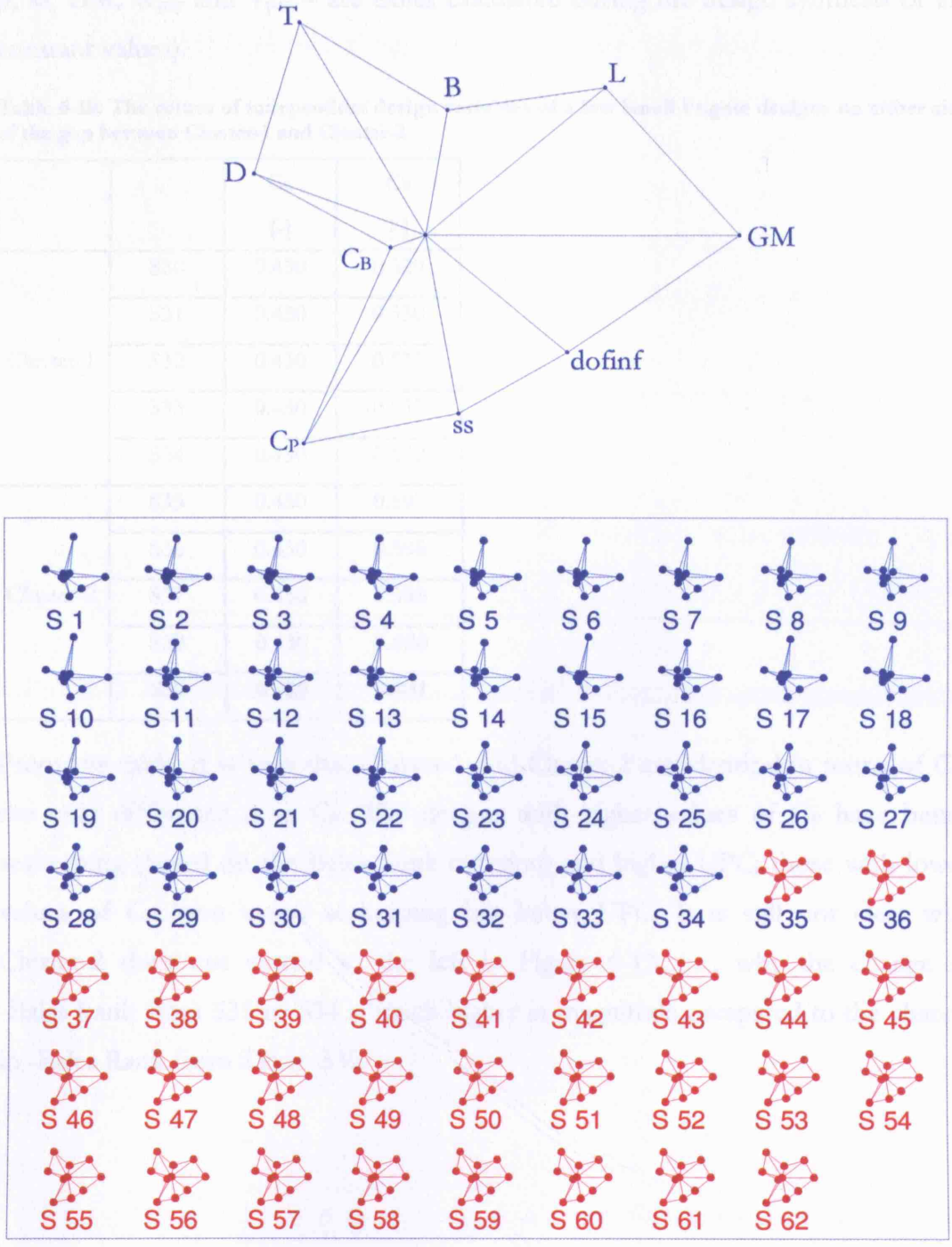

Figure 6-17: Star plots showing the design parameters of all designs on the Pareto-front for the Small Frigate with UPC < £269M, showing the 'jump' in design parameters between designs S34 and S35. A star template is shown separately to identify each spoke. Design parameters are normalised with respect to the extreme values of all designs on the Pareto-front.

Since we are considering variations in C_B and C_P alone, they are the only independent design variables in this case. Their values for a few designs on either side of the gap are shown in Table 6-10. (The remaining design variables – D, pvf,

ρ, ss, GM, W_{pay} and V_{pay} – are either calculated during the design synthesis or are constant values).

Table 6-10: The values of independent design variables of a few Small Frigate designs on either side of the gap between Cluster-1 and Cluster-2

		C_B [-]	C_P [-]
Cluster-1	S30	0.430	0.529
	S31	0.430	0.530
	S32	0.430	0.533
	S33	0.430	0.537
	S34	0.430	0.532
Cluster-2	S35	0.430	0.597
	S36	0.430	0.598
	S37	0.430	0.598
	S38	0.430	0.600
	S39	0.430	0.601

From the table, it is seen that Cluster-1 and Cluster-2 are identical in terms of C_B; the only difference is in C_P. The designs with higher values of C_P have better seakeeping (based on the Bales Rank criterion) and higher UPC; those with lower values of C_P have worse seakeeping but better UPC. It is still not clear why Cluster-2 does not extend to the left in Figure 6-13; i.e., why the change in -Bales Rank from S35 to S34 is much higher in magnitude compared to the change in -Bales Rank from S36 to S35.

Next, the design space around S35 is examined using the sensitivity plots with respect to C_P. This is shown in Figure 6-18. The plot shows that any change in C_P results in higher P_s, and consequently higher UPC. In other words, C_P=0.597 is the optimum value for resistance and powering. Hence, further decrease of C_P below 0.597 would worsen all three objectives of UPC, seakeeping and P_s. When this happens, the GA tool locates a design from another region of the design space that can give lower UPC, but slightly worse P_s and much worse -Bales Rank. This is the design S34.

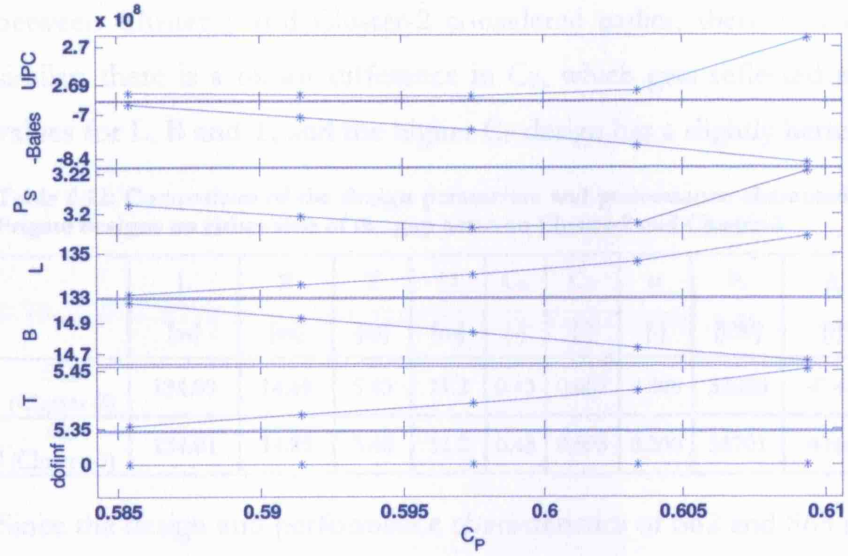

Figure 6-18: Sensitivity plots for C_P for the Small Frigate design S35

Comparison of the characteristics of the two designs S34 and S35 on either side of the gap between Cluster-1 (low UPC) and Cluster-2 (mid UPC) are given in Table 6-11. As noted earlier, the only independent design variable that differs between these two designs is C_P. Lower C_P is associated with lower waterplane inertia, and thus B increases to maintain the required GM. The increase in B is offset by the decrease in both L and T so that the change in displacement is not significant. In summary, the lower C_P design S34, after design synthesis, results in lower L and T, and higher B in comparison with the higher C_P design S35, though the displacement and enclosed volume are not very different. The large difference in -Bales Rank between the two designs seems to be due to the fact that the Bales Rank formula is heavily dependent on the value of C_P.

Table 6-11: Comparison of the design parameters and performance characteristics of the two Small Frigate designs on either side of the gap between Cluster-1 and Cluster-2

	L [m]	B [m]	T [m]	D [m]	C_B [-]	C_P [-]	ss [-]	P_s [kW]	Δ [t]	∇_{Gross} [m^3]	UPC [£M]	-Bales [-]
S34 (Cluster-1)	128.81	16.00	5.16	11.20	0.430	0.532	0.200	32176	4689	16934	268.56	-2.6
S35 (Cluster-2)	134.15	14.82	5.40	11.20	0.430	0.597	0.200	31842	4729	16974	268.57	-7.5

Now, consider the gap between Cluster-2 (mid UPC) and Cluster-3 (high UPC) in the Pareto-front (Figure 6-13). The characteristics of the designs on either side of this gap, S62 and S63, are given in Table 6-12. Unlike the case of the discontinuity between Cluster-1 and Cluster-2 considered earlier, these two designs seem very similar: there is a minor difference in C_P, which gets reflected in slightly different values for L, B and T, and the higher C_P design has a slightly better -Bales Rank.

Table 6-12: Comparison of the design parameters and performance characteristics of the two Small Frigate designs on either side of the gap between Cluster-2 and Cluster-3

	L [m]	B [m]	T [m]	D [m]	C_B [-]	C_P [-]	ss [-]	P_s [kW]	Δ [t]	∇_{Gross} [m^3]	UPC [£M]	-Bales [-]
S62 (Cluster-2)	134.89	14.69	5.43	11.2	0.43	0.607	0.200	32080	4741	16998	269.0	-8.22
S63 (Cluster-3)	134.81	14.85	5.40	11.2	0.43	0.595	0.200	31701	4766	17052	269.6	-7.52

Since the design and performance characteristics of S62 and S63 are so similar, they are not widely separated in the design or performance spaces. However, there seems to be a clear transition between them. The reason for this transition seems to stem from a very different source. It seems to have been caused by the warship weight and space algorithms, which include a number of discrete and non-linear relationships. The number of some of the ship components is based on the gross enclosed volume of the ship. Enclosed volume of 17000m^3 is an important figure for some of the components: for example, the number of pumps and air compressors are taken as 3 each if the enclosed volume of the ship is up to 17000m^3, and 4 if it is more than 17000m^3. In this case, S62 has an enclosed volume of 16998m^3 and S63 has 17052m^3, thus falling on either side of the limit of 17000m^3. Hence, S62 has two pumps and air compressors while S63 has three. This causes the sudden changes between S62 and S63.

6.2.4. Complete design space exploration – combined major and minor parametric surveys (variation of D, ss, C_B and C_P)

The GA Tool was run with the same set of design variable bounds and constraints as used in the SDE major and minor parametric surveys. Three objectives were used: minimise UPC, minimise -Bales Rank and minimise P_s. The resulting Pareto-front, comprising 261 designs, is shown in Figure 6-19, Figure 6-20 and Figure 6-21.

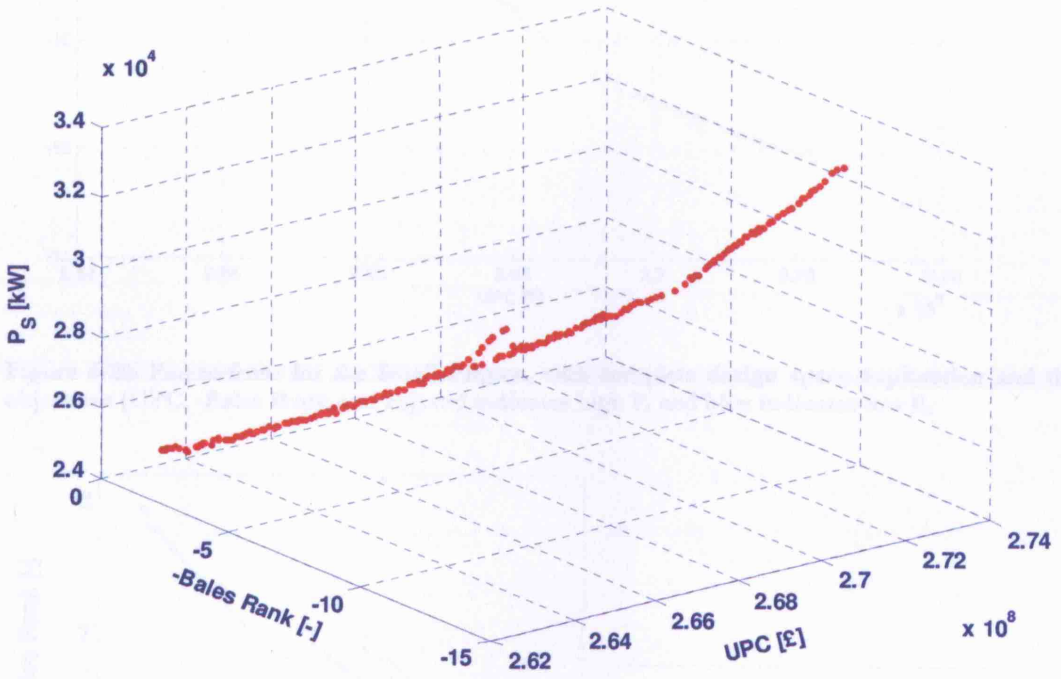

Figure 6-19: Pareto-front for the Small Frigate, with complete design space exploration and three objectives (UPC, -Bales Rank and P_S); 3D-plot

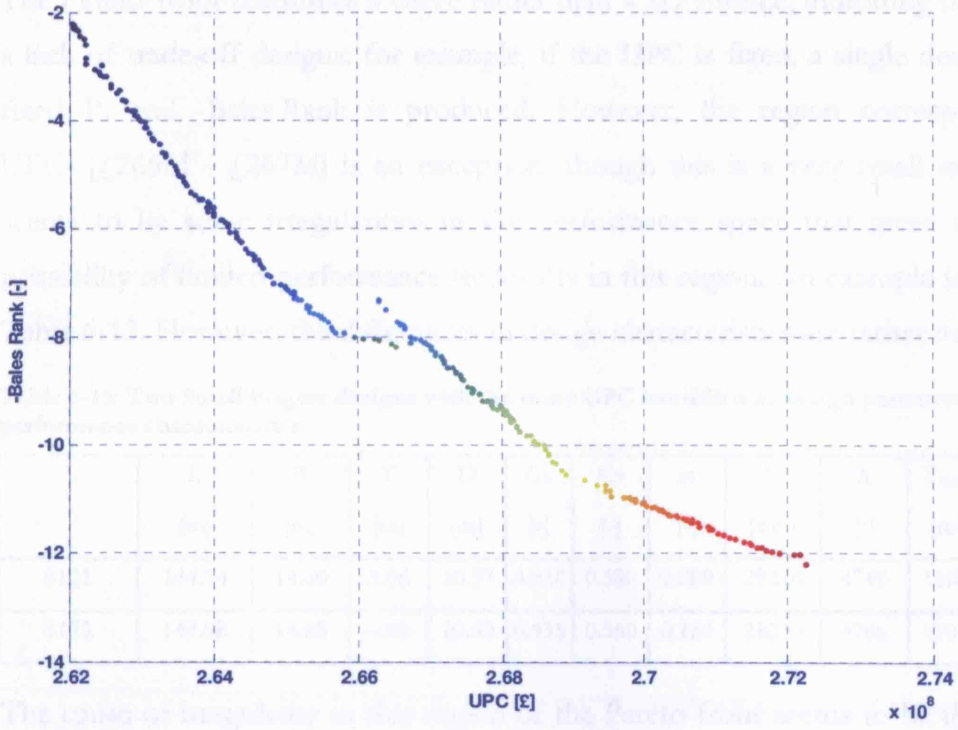

Figure 6-20: Pareto-front for the Small Frigate, with complete design space exploration and three objectives (UPC, -Bales Rank and P_S); red indicates high P_s and blue indicates low P_s

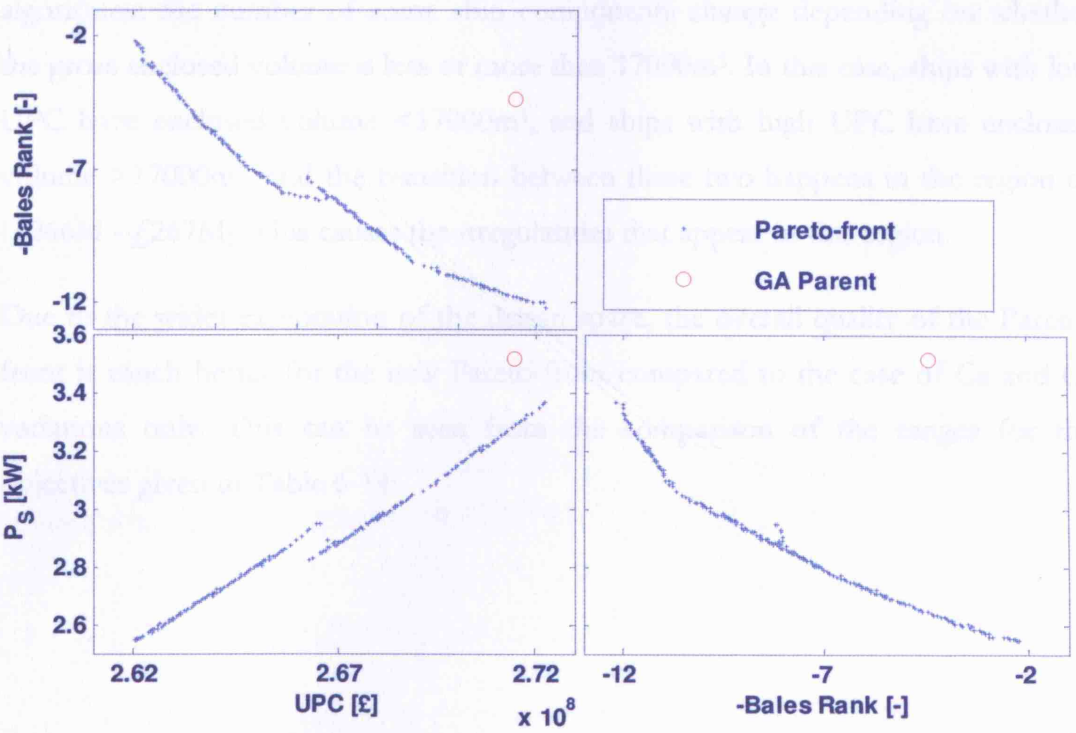

Figure 6-21: Pareto-front for the Small Frigate, with complete design space exploration and three objectives (UPC, -Bales Rank and P_S); matrix of 2D plots; GA Parent is shown for comparison

The Pareto-front resembles a curve rather than a 2D surface, indicating that there is a lack of trade-off designs: for example, if the UPC is fixed, a single design with a fixed P_s and -Bales Rank is produced. However, the region corresponding to UPC=[£266M - £267M] is an exception: though this is a very small range, there seems to be some irregularities in the performance space that gives rise to the possibility of limited performance trade-offs in this region. An example is shown in Table 6-13. However, the differences in design characteristics are rather not large.

Table 6-13: Two Small Frigate designs with the same UPC but different design parameters and other performance characteristics

	L [m]	B [m]	T [m]	D [m]	C_B [-]	C_P [-]	ss [-]	P_s [kW]	Δ [t]	∇_{Gross} [m³]	UPC [£M]	-Bales [-]
S121	144.14	14.60	5.06	10.57	0.434	0.580	0.209	29246	4740	16999	266.3	-8.07
S122	147.98	14.68	4.92	10.59	0.435	0.560	0.189	28240	4766	17047	266.3	-7.34

The cause of irregularity in this region of the Pareto-front seems to be the same as was found in the case of C_B and C_P variations only. As mentioned earlier, enclosed volume of 17000m³ is an important figure for the warship weight and space algorithms: the number of some ship components change depending on whether the gross enclosed volume is less or more than 17000m³. In this case, ships with low UPC have enclosed volume <17000m³, and ships with high UPC have enclosed volume >17000m³, and the transition between these two happens in the region of [£266M - £267M]. This causes the irregularities that appear in this region.

Due to the wider exploration of the design space, the overall quality of the Pareto-front is much better for the new Pareto-front compared to the case of C_B and C_P variations only. This can be seen from the comparison of the ranges for the objectives given in Table 6-14:

Table 6-14: Minimum and maximum values of objectives – comparison between the two Pareto-fronts for the Small Frigate design study

Objective	Pareto-front with C_B and C_P variations only		Pareto-front varying D, ss, C_B and C_P	
	Minimum	Maximum	Minimum	Maximum
UPC [£M]	268.13	273.11	262.05	272.25
-Bales Rank [-]	-11.8	0.99	-12.2	-2.21
P_s [kW]	31684	34531	25456	33671

Table 6-15 compares the design parameters and performance characteristics of the GA Parent with three alternative designs chosen from the Pareto-front. The three alternatives are:

- The Pareto-design with the closest UPC as the GA Parent (£271.44M)
- The Pareto-design with the closest -Bales Rank as the GA Parent (-4.4)
- The Pareto-design with the closest P_s as the GA Parent (35181 kW)

Table 6-15: Comparison of the GA Parent with alternative designs from the Pareto-front for the Small Frigate design study (with complete design space exploration)

	L [m]	B [m]	T [m]	D [m]	C_B [-]	C_P [-]	ss [-]	Δ [t]	∇_{Gross} [m³]	UPC [£M]	-Bales [-]	P_s [kW]
GA Parent	126.21	15.63	5.17	11.20	0.450	0.570	0.200	4706	16940	271.44	-4.4	35181
Closest UPC #251	143.84	14.01	5.35	10.31	0.439	0.644	0.251	4854	17186	271.41	-11.8	32792
Closest Bales #37	146.34	15.31	4.71	10.48	0.435	0.519	0.188	4700	16941	263.16	-4.36	26378
Closest P_s #261	141.97	14.00	5.38	10.14	0.444	0.657	0.269	4864	17189	272.25	-12.2	33671

Comparison between Table 6-15 and Table 6-9 indicates that the simultaneous exploration of the whole design space results in much better designs compared to the limited design space exploration done during the SDE parametric survey.

The Pareto-front plots, Figure 6-19, Figure 6-20 and Figure 6-21, showed the performance space. A colour diagram representation of the Pareto-front is shown in Figure 6-22, to examine the design space and performance space simultaneously. The trends of the design parameters and performance characteristics seem fairly regular, except a small region near the middle, which corresponds to the transition region [£266M-£267M] noted earlier.

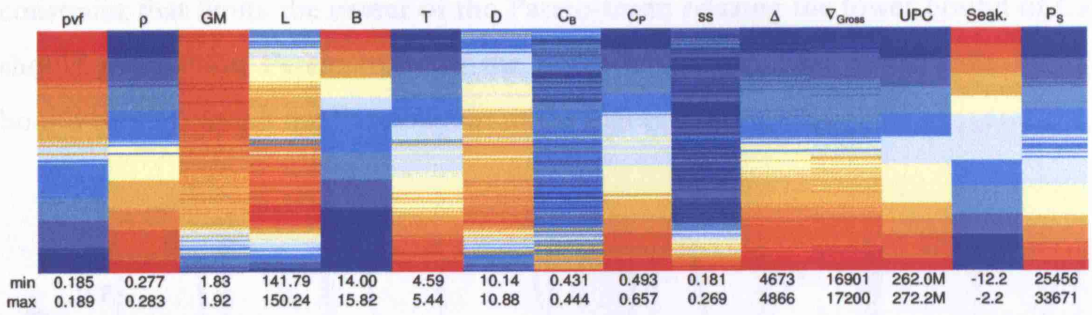

Figure 6-22: Colour diagram of the Pareto-front shown in Figure 6-21, consisting of 261 designs (Small Frigate, complete design space exploration)

The constraints plot for the Pareto-front is given in Figure 6-23. From the plot, L/D is close to its upper bound throughout the Pareto-front. Ⓜ, ss and C_B are also close to their bounds over a large range of the Pareto-front. Relaxing one or more of these constraints should help to improve the quality of the Pareto-front (i.e., for a given UPC, the Pareto-front after relaxing these constraints should include designs with better -Bales Rank and/or P_s compared to the current Pareto-front). C_P is the constraint that limits the extent of the Pareto-front: relaxing the lower bound of C_P should extend the Pareto-front to the lower cost region and relaxing its upper bound should extend the Pareto-front to the higher cost region.

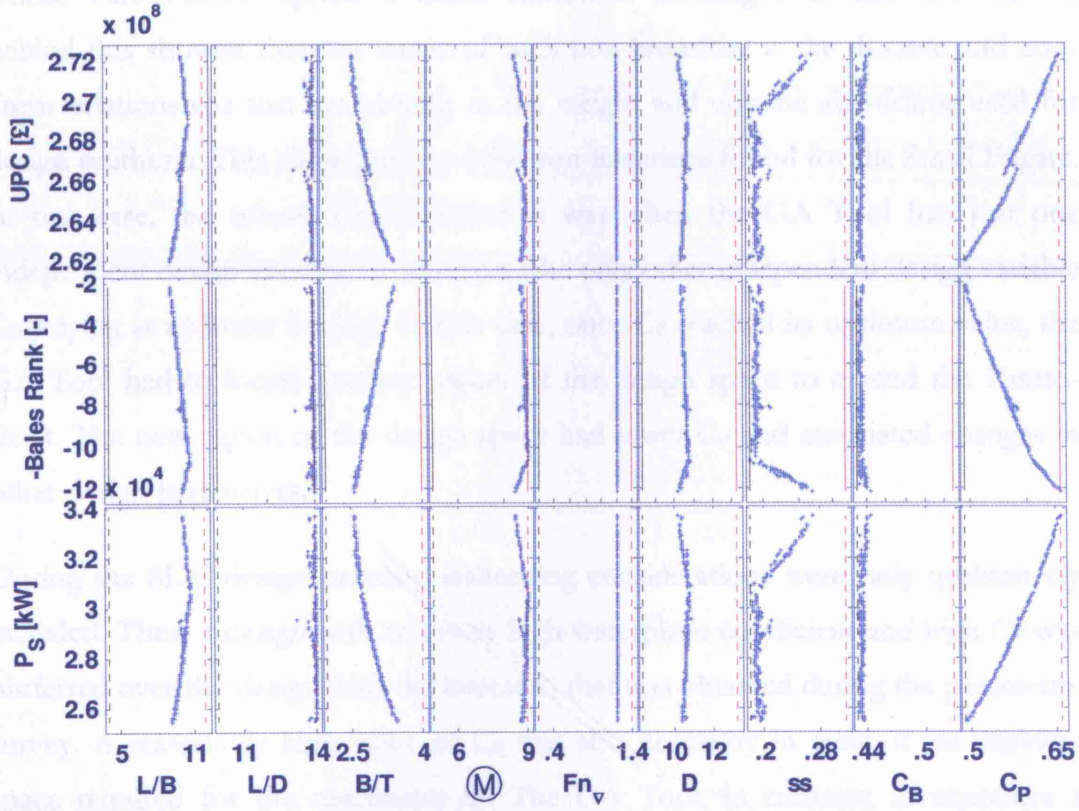

Figure 6-23: Constraints plot for the Pareto-front shown in Figure 6-21 (Small Frigate; complete design space exploration)

6.2.5. Summary of the Small Frigate design study

By comparing a Small Frigate designed during a UCL Ship Design Exercise with corresponding designs generated using the GA Tool, this section showed how the application of the proposed design approach could assist in the concept design process.

The Pareto-fronts obtained in the case of the Small Frigate gave some interesting design insights. These Pareto-fronts showed many non-linearities and discontinuities. This is in contrast with the case of the Large Frigate (Section 6.1), whose Pareto-fronts appeared much smoother. Investigations into the reasons behind this showed that one cause of such non-linearities is the discrete and non-linear relationships that are present in the weight and volume algorithms used for design synthesis. This caused most of the non-linearities found for the Small Frigate. In one case, the reason was different: it was when the GA Tool had just one independent design variable C_P to adjust (the only other independent design variable C_B staying at its lower bound). In this case, once C_P reached its optimum value, the GA Tool had to locate another region of the design space to extend the Pareto-front. The new region of the design space had lower C_P and associated changes in other design parameters.

During the SDE design process, seakeeping considerations were only qualitatively included. Thus, a design with relatively high waterplane coefficient and high C_P was preferred over the design with the lowest P_s that was obtained during the parametric survey. A reasonably high value of C_P was also necessary in view of the midship space required for the machinery fit. The GA Tool, in contrast, incorporates a measure of merit for seakeeping, albeit rather crude.

6.3. Concept design of a Corvette (1800 t displacement)

Similar to Section 6.1 and Section 6.2, this section compares the results of the proposed design approach when applied to an existing design. A monohull corvette designed as part of the UCL MSc Naval Architecture Ship Design Exercise (SDE) in 1994 has been chosen [128]. The design approach followed in the SDE and the process used in the GA Tool for comparison are similar to Section 6.1 and Section 6.2, and hence are not repeated here.

6.3.1. Duplicating the SDE design in the GA Tool

The first step was to create the GA Parent by modelling the SDE Parent in the GA Tool. This was done following a similar procedure as in Section 6.1 and Section 6.2. The comparison between the SDE Parent and the GA Parent is shown in Table 6-16. The Bales Rank of the SDE Parent is kept blank because it was not calculated during the SDE.

Table 6-16: Design parameters for the Corvette - SDE Parent vs GA Parent

	W_{pay} [t]	V_{pay} [m^3]	speed [kn]	L [m]	B [m]	T [m]	D [m]	C_B [-]	C_P [-]	ss [-]	P_s [kW]	Δ [t]	∇_{Gross} [m^3]	UPC [£M]	-Bales [-]
SDE Parent	104.833	1036.7	28.6	86.71	11.50	4.31	8.30	0.410	0.600	0.16	20800	1811	6024	70	-
GA Parent	104.833	1036.7	28.6	87.64	11.60	4.24	8.30	0.410	0.600	0.16	20463	1810	5935	70	+3.26

From the table, it is seen that the design parameters for the GA Parent are very similar to the SDE Parent.

The range of design variables considered during the whole SDE process, as given in [128] is summarised below:

$D = [7.5, 8.3]$

$ss = [0.16, 0.28]$

$C_B = [0.40, 0.50]$

$C_P = [0.55, 0.65]$

The constraints considered during the SDE design process are:

L > 81m (based on preliminary upper deck layout);

B > 11.5m (based on required width for the flight deck);

T > 3.0m.

The same ranges of design variables and constraints are used in the GA Tool.

Seakeeping characteristics are very important, because the area of operations is the North Atlantic and the sea conditions are usually severe.

6.3.2. Simulating minor parametric survey, varying C_B and C_P

The minor parametric survey in the SDE was done keeping D and ss constant (8.3 and 0.16 respectively), with variations in C_B = [0.40, 0.50] and C_P = [0.55, 0.65]. Since the same region of the design space is being explored by both the SDE and the GA Tool, the design obtained from the SDE should be among the Pareto-designs produced by the GA Tool. In addition, the GA Tool should generate other trade-off design options as well. The Pareto-front generated by the GA Tool, comprising 3098 designs, is shown in different formats in Figure 6-24, Figure 6-25 and Figure 6-26. GA Parent is included in Figure 6-26 for comparison.

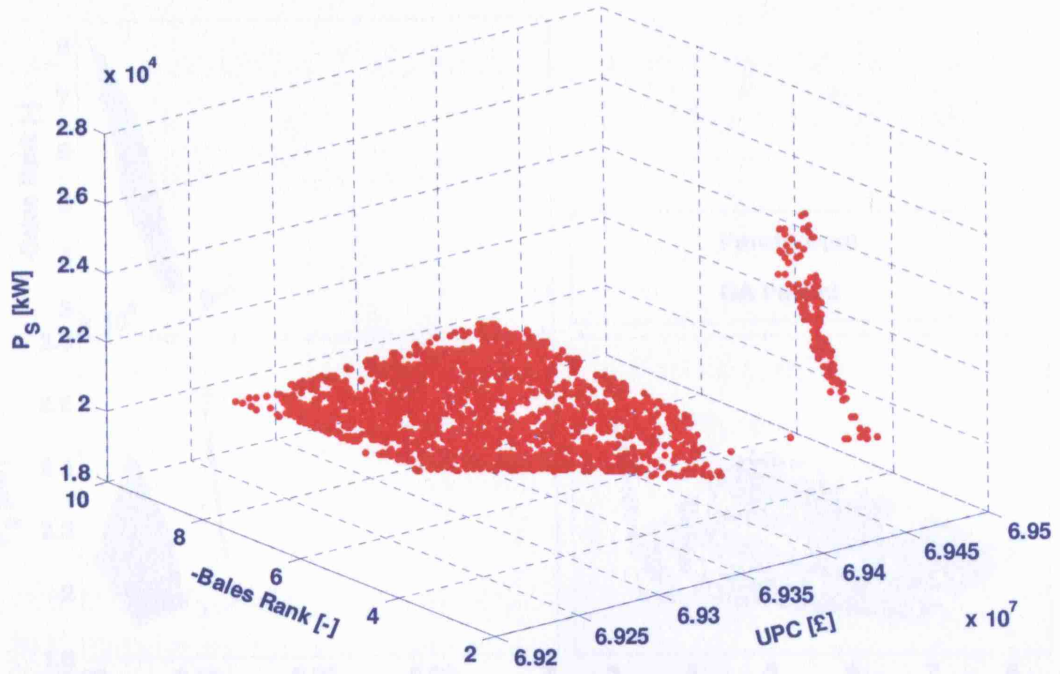

Figure 6-24: Pareto-front for the Corvette, with C_B and C_P variations, and three objectives (UPC, -Bales Rank and P_S); 3D plot

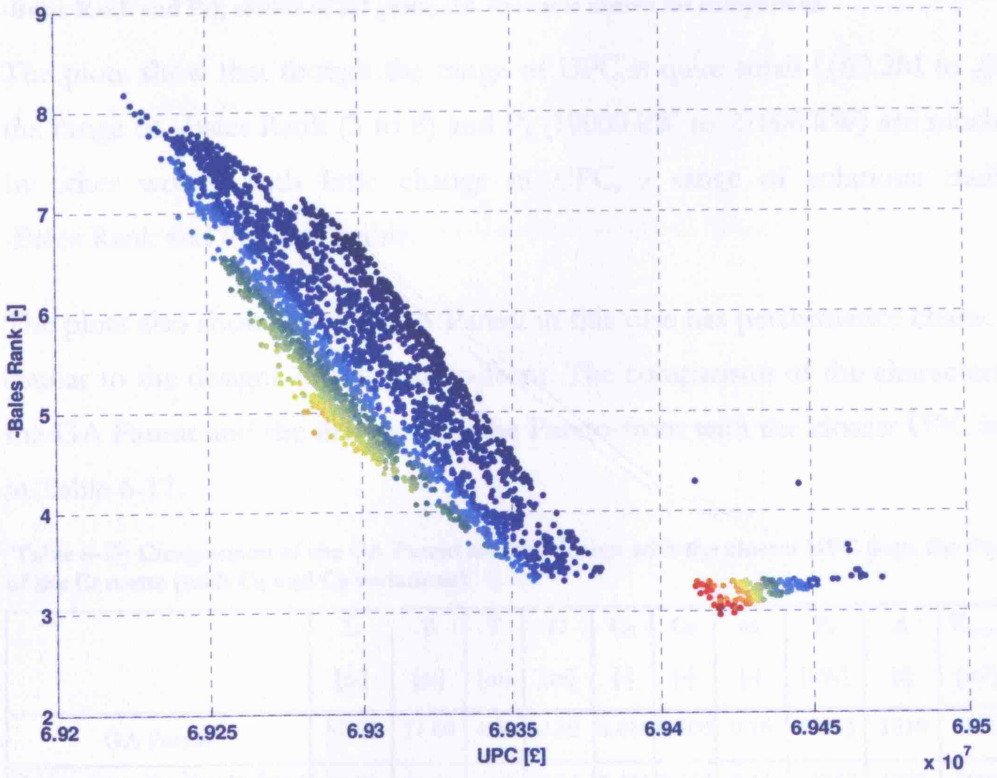

Figure 6-25: Pareto-front for the Corvette, with C_B and C_P variations, and three objectives (UPC, -Bales Rank and P_S); red indicates high P_s and blue indicates low P_s

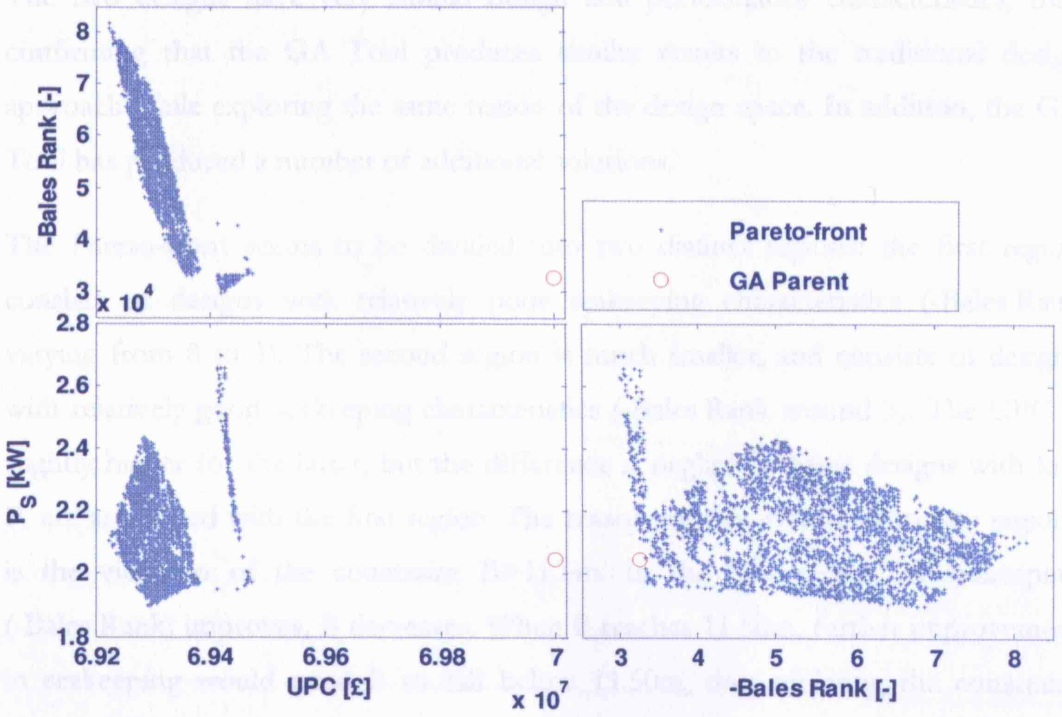

Figure 6-26: Pareto-front for the Corvette, with C_B and C_P variations, and three objectives (UPC, -Bales Rank and P_S); matrix of 2D plots; GA Parent is shown for comparison

The plots show that though the range of UPC is quite small (£69.2M to £69.5M), the range of -Bales Rank (3 to 8) and P_s (19000 kW to 27000 kW) are much larger. In other words, with little change in UPC, a range of solutions trading off -Bales Rank and P_s are possible.

The plots also show that the GA Parent in this case has performance characteristics similar to the designs on the Pareto-front. The comparison of the characteristics of the GA Parent and the design from the Pareto-front with the closest UPC is shown in Table 6-17.

Table 6-17: Comparison of the GA Parent and the design with the closest UPC from the Pareto-front of the Corvette (with C_B and C_P variations)

	L [m]	B [m]	T [m]	D [m]	C_B [-]	C_P [-]	ss [-]	P_s [kW]	Δ [t]	∇_{Gross} [m³]	UPC [£M]	-Bales [-]
GA Parent	87.64	11.60	4.24	8.30	0.410	0.600	0.16	20463	1810	5935	70.0	+3.26
Design from the Pareto-front with closest UPC (S3098)	87.63	11.50	4.29	8.30	0.401	0.598	0.16	19747	1777	5808	69.5	+3.34

The two designs have very similar design and performance characteristics, thus confirming that the GA Tool produces similar results to the traditional design approach while exploring the same region of the design space. In addition, the GA Tool has produced a number of additional solutions.

The Pareto-front seems to be divided into two distinct regions: the first region consists of designs with relatively poor seakeeping characteristics (-Bales Rank varying from 8 to 3). The second region is much smaller, and consists of designs with relatively good seakeeping characteristics (-Bales Rank around 3). The UPC is slightly higher for the latter, but the difference is negligible. Most designs with low P_s are associated with the first region. The reason for this division into two regions is the violation of the constraint B>11.5m. In the first region, as seakeeping (-Bales Rank) improves, B decreases. When B reaches 11.50m, further improvement in seakeeping would need B to fall below 11.50m, thus violating the constraint B>11.5. When this happens, the genetic algorithms locate another region of the design space with higher B and lower L. This helps to extend the Pareto-front to the better seakeeping (higher UPC) region. This can be verified from Table 6-18, which shows the characteristics of two designs on either side of the gap between the two regions.

Table 6-18: Comparison of characteristics of the two designs on either side of the gap in the Pareto-front of the Corvette

	L [m]	B [m]	T [m]	D [m]	C_B [-]	C_P [-]	ss [-]	P_s [kW]	Δ [t]	∇_{Gross} [m³]	UPC [£M]	-Bales [-]
The best seakeeping design from the poorer seakeeping region (S2923)	***87.46***	***11.50***	4.29	8.3	0.400	***0.597***	0.16	19677	1771	5787	69.38	3.44
The worst seakeeping design from the better seakeeping region (S2924)	***86.92***	***11.68***	4.26	8.3	0.400	***0.584***	0.16	19504	1773	5804	69.41	4.30

A colour diagram representation of the Pareto-front is shown in Figure 6-27. The trends from the colour diagram do not seem very clear. This is because at any given UPC, there are many solutions trading off -Bales Rank and P_S. If the designer is interested in a particular region of the Pareto-front, that region alone can be selected and the colour diagram re-generated to see the trends more clearly (for example, all designs with P_S approximately 20000 kW). Despite this difficulty in understanding the overall trends, the colour diagram clearly shows the separation of the designs into two distinct regions. The separation is clearly noticeable near the bottom end of the colour diagram. The magnitude of variation in some parameters is negligible (for example, pvf changes from 0.178 to 0.179), whereas some others show significant differences (for example, L decreases from 87.6 to 81.0). Thus, the colour diagram demonstrates its potential to highlight discontinuities in the Pareto-front and give a quick qualitative comparison of the trends of design parameters as well as performance characteristics.

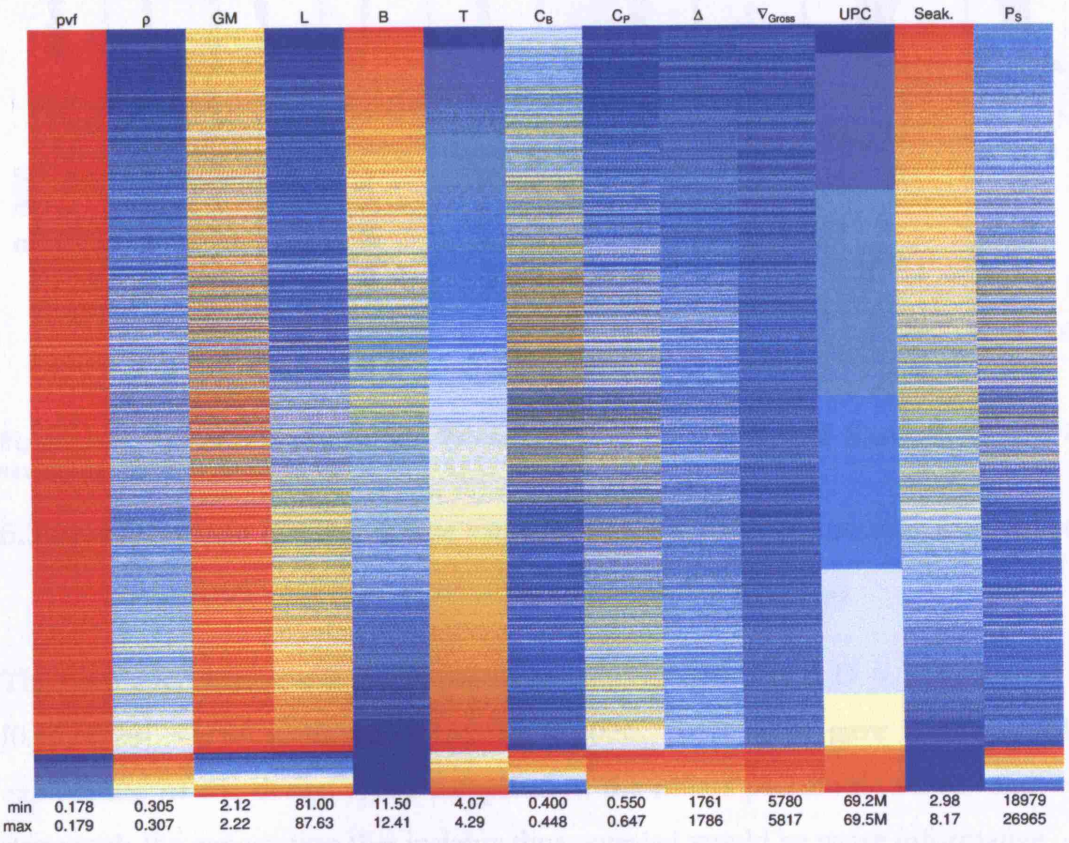

Figure 6-27: Colour diagram of the Pareto-front shown in Figure 6-26, consisting of 3098 designs (Corvette; C_B and C_P variations)

The constraints plot for the Pareto-front is shown in Figure 6-28. All designs stay close to the upper bound of Fn_V throughout the Pareto-front. Among the others, the lower bound of C_B and both the bounds of C_P seem important. The numerical examination of the results show that among the additional constraints specified (mentioned in Section 6.3.1; not shown in the constraints plot), both L>81 and B>11.5 seem very important: the former limits the Pareto-front primarily in the lower UPC region and the latter in the higher UPC region.

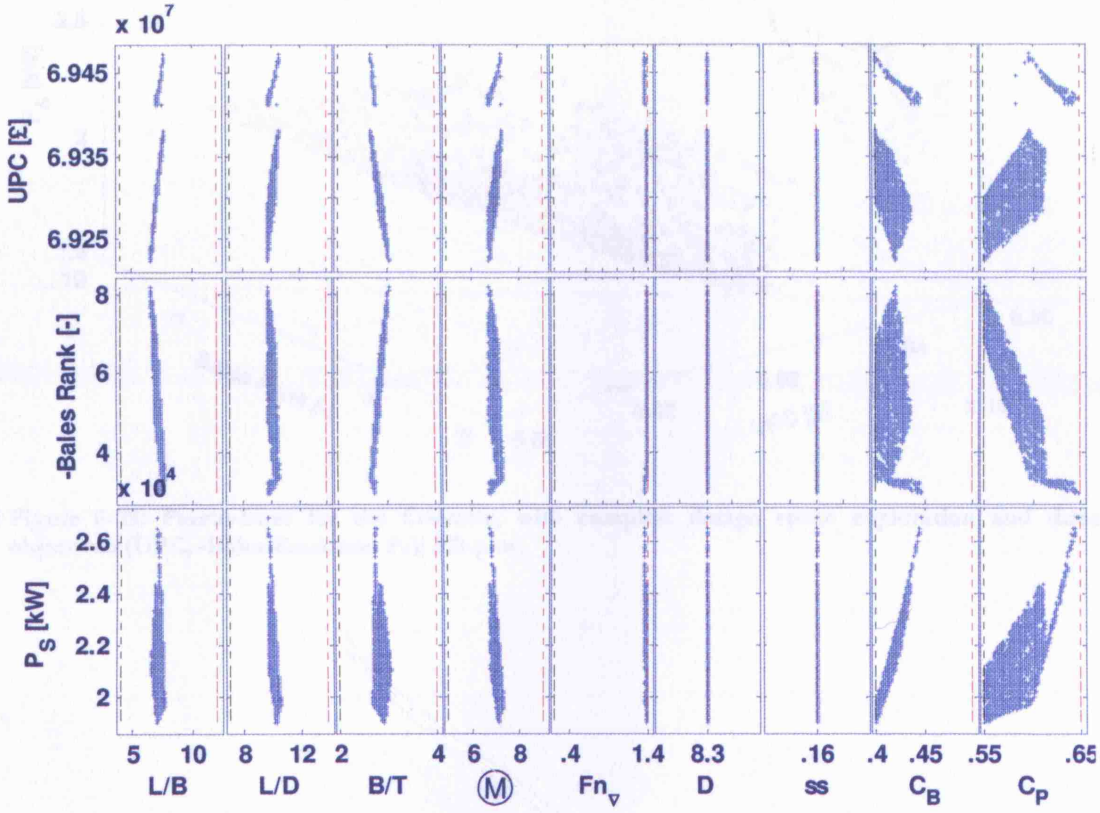

Figure 6-28: Constraints plot for the Pareto-front shown in Figure 6-26 (Corvette; C_B and C_P variations)

6.3.3. Complete design space exploration – combined major and minor parametric surveys (variation of D, ss, C_B and C_P)

The combined major and minor parametric survey considered D = [7.5, 8.3], ss = [0.16, 0.28], C_B = [0.40, 0.50] and C_P = [0.55, 0.65]. This gave a much wider exploration of the design space compared to the minor parametric survey and was done with the expectation that insights thus revealed would be more informative.

The Pareto-front generated by the GA Tool, consisting of 917 designs, is shown in different formats in Figure 6-29, Figure 6-30 and Figure 6-31. The GA Parent is shown in Figure 6-31 for comparison.

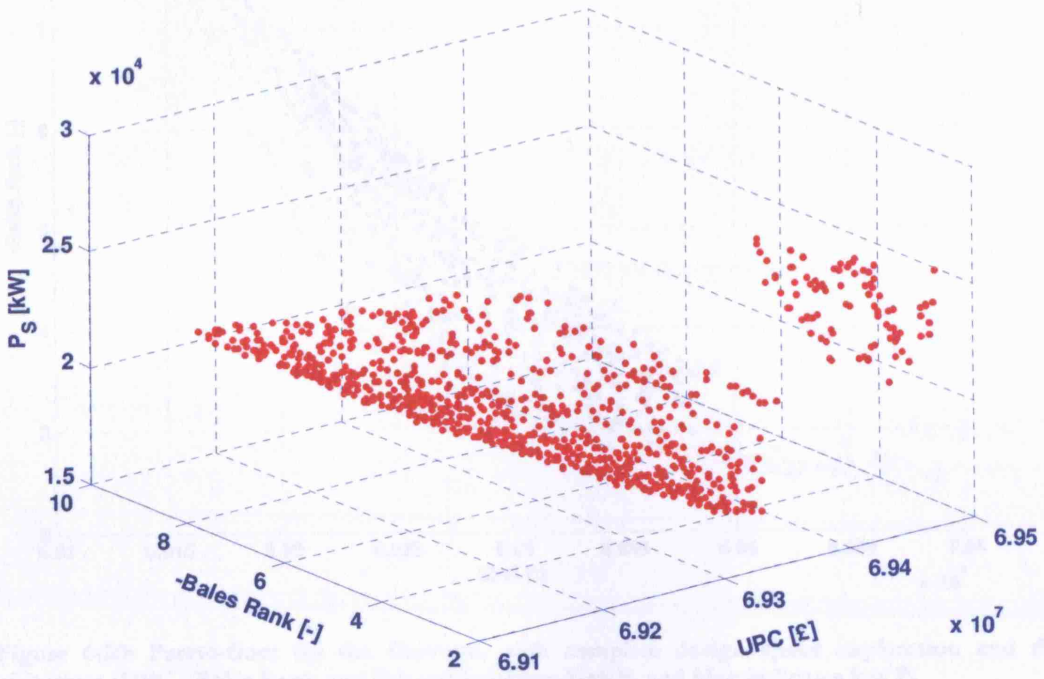

Figure 6-29: Pareto-front for the Corvette, with complete design space exploration and three objectives (UPC, -Bales Rank and P_S); 3D-plot

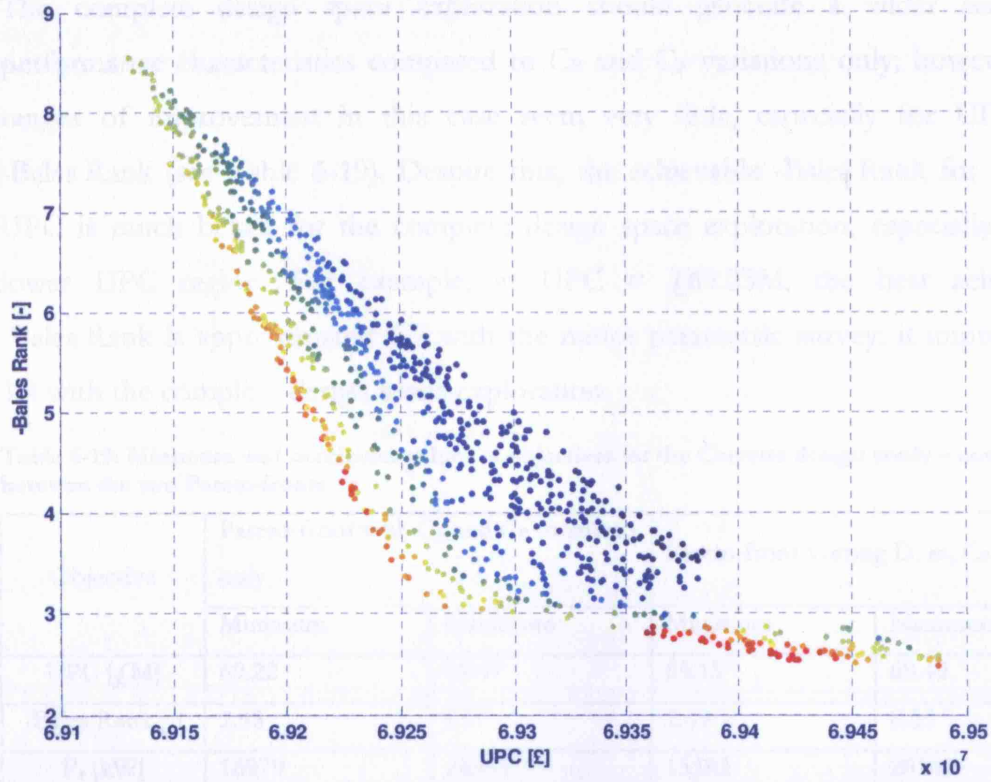

Figure 6-30: Pareto-front for the Corvette, with complete design space exploration and three objectives (UPC, -Bales Rank and P_S); red indicates high P_s and blue indicates low P_s

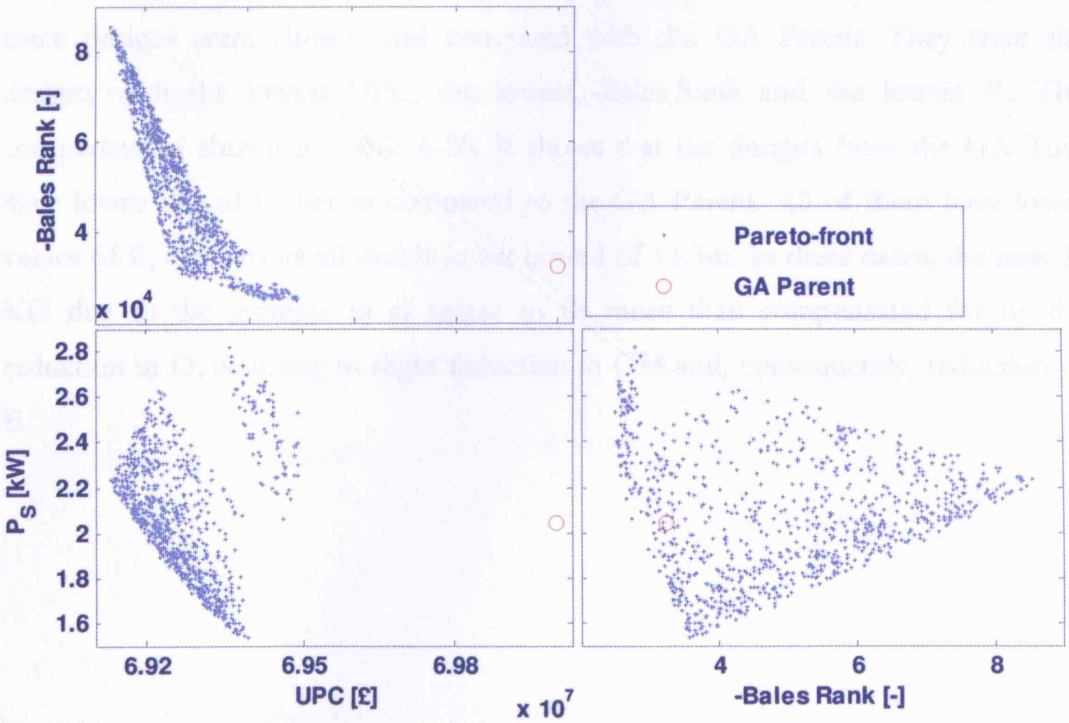

Figure 6-31: Pareto-front for the Corvette, with complete design space exploration and three objectives (UPC, -Bales Rank and P_S); matrix of 2D plots; GA Parent is shown for comparison

The complete design space exploration should generate a wider range of performance characteristics compared to C_B and C_P variations only; however, the ranges of improvement in this case seem very little, especially for UPC and -Bales Rank (see Table 6-19). Despite this, the achievable -Bales Rank for a given UPC is much better for the complete design space exploration, especially in the lower UPC region. For example, at UPC = £69.25M, the best achievable -Bales Rank is approximately 6.7 with the minor parametric survey; it improves to 3.4 with the complete design space exploration.

Table 6-19: Minimum and maximum values of objectives for the Corvette design study – comparison between the two Pareto-fronts

Objective	Pareto-front with C_B and C_P variations only		Pareto-front varying D, ss, C_B and C_P	
	Minimum	Maximum	Minimum	Maximum
UPC [£M]	69.22	69.47	69.13	69.49
-Bales Rank [-]	2.98	8.17	2.49	8.55
P_s [kW]	18979	26965	15382	28142

Numerical filtering of the Pareto-front showed that out of 917 Pareto-designs, 16 were better in all the three objectives compared to the GA Parent. Among these, three designs were chosen and compared with the GA Parent. They were the designs with the lowest UPC, the lowest -Bales Rank and the lowest P_s. The comparison is shown in Table 6-20. It shows that the designs from the GA Tool have lower D and higher ss compared to the GA Parent. All of them have lower values of B, close to its allowable lower bound of 11.5m. In these cases, the raise in KG due to the increase in ss seems to be more than compensated for by the reduction in D, resulting in slight reduction in GM and, consequently, reduction of B.

Table 6-20: Comparison of the GA Parent and the closest design from the Pareto-front of the Corvette (with complete design space exploration)

	L [m]	B [m]	T [m]	D [m]	C_B [-]	C_P [-]	ss [-]	P_s [kW]	Δ [t]	∇_{Gross} [m^3]	UPC [£M]	-Bales [-]
GA Parent	87.64	11.60	4.24	***8.30***	0.410	0.600	***0.16***	20463	1810	5935	70.0	+3.26
The design with the lowest UPC among those with better performance characteristics than the GA Parent (S645)	88.34	11.50	3.77	***7.55***	0.451	0.596	***0.186***	20085	1768	5788	69.30	+3.23
The design with the best -Bales Rank among those with better performance characteristics than the GA Parent (S813)	88.71	11.50	4.15	***7.56***	0.407	0.596	***0.234***	19281	1768	5783	69.37	+2.99
The design with the lowest P_s among those with better performance characteristics than the GA Parent (S824)	90.35	11.53	4.13	***7.66***	0.401	0.582	***0.216***	18054	1769	5786	69.38	+3.25

The table shows that the performance characteristics of the designs chosen from the Pareto-front are very similar to those of the GA Parent. For example the UPC, -Bales Rank and P_s of the design S645 are as follows (the corresponding values for the GA Parent are given in parentheses): £69.3M (£70.0M), +3.23 (+3.26) and 20085kW (20463 kW). Interestingly, the design parameters are seen to be rather different: S645 has considerably lower T and D, as well as higher L, C_B and ss compared to the GA Parent. Thus, designs from distinct regions of the design space seem to produce similar performance characteristics.

A colour diagram for the Pareto-front is shown in Figure 6-32, along with the corresponding constraints plot in Figure 6-33. Similar to the case of the C_B and C_P variations, the trends from the colour diagram do not seem very clear; however, the separation into two regions does stand out (near the bottom end of the plot). From the constraints plot, the lower and upper bounds of C_B and C_P limit the extent of the Pareto-front; Fn_∇ also seems important since its values stay close to the upper bound throughout the Pareto-front. Among the additional constraints (specified in Section 6.3.1; not shown in the constraints plot), both L>81 and B>11.5 are found to be the limiting constraints for the Pareto-front, in the low-UPC and high-UPC region respectively.

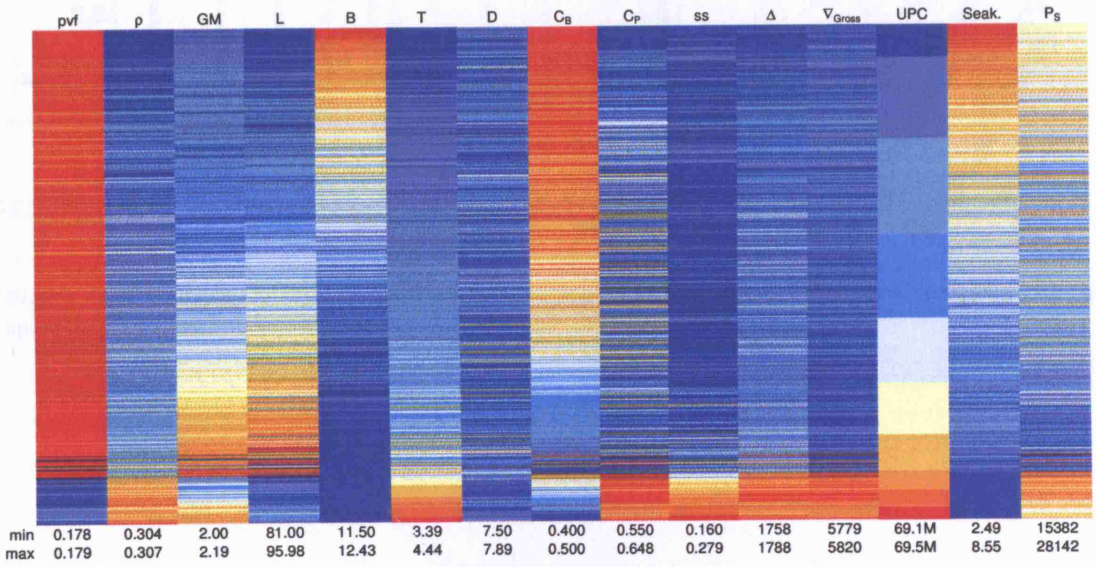

Figure 6-32: Colour diagram of the Pareto-front shown in Figure 6-31, consisting of 917 designs (Corvette; complete design space exploration)

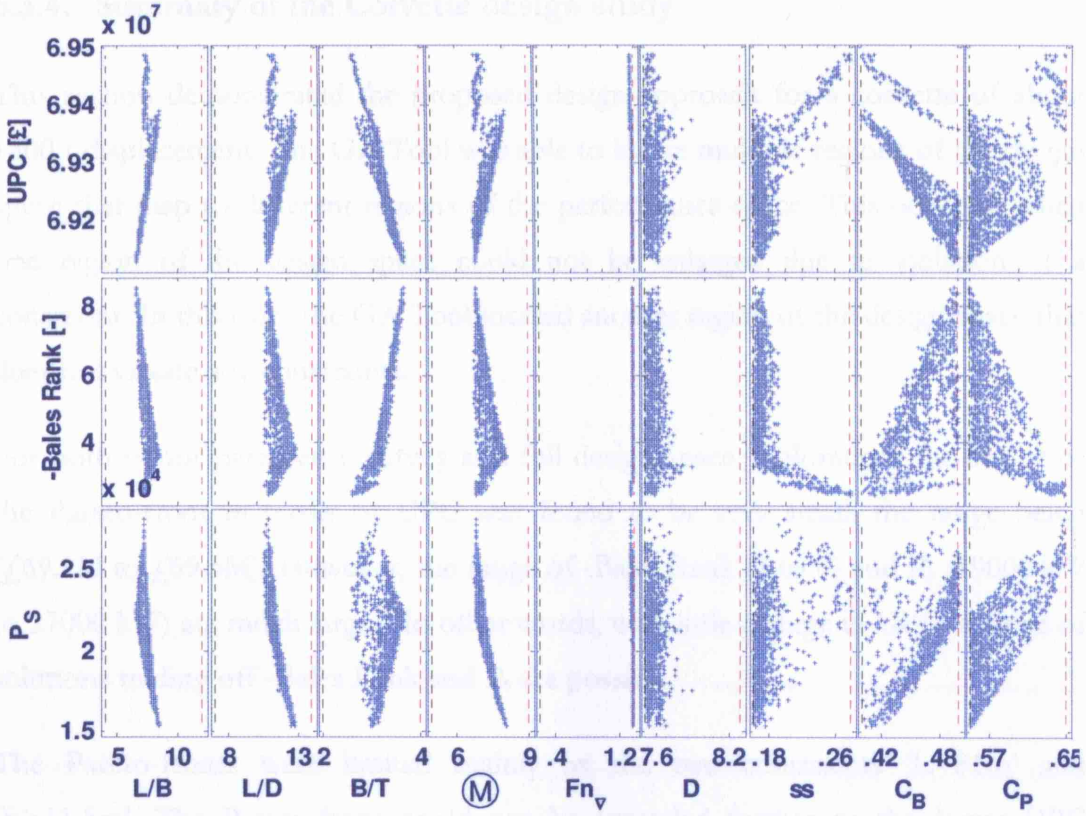

Figure 6-33: Constraints plot for the Pareto-front shown in Figure 6-31 (Corvette; complete design space exploration)

6.3.4. Summary of the Corvette design study

This section demonstrated the proposed design approach for a corvette of about 1800 t displacement. The GA Tool was able to locate multiple regions of the design space that map to different regions of the performance space. This occurred when one region of the design space could not be enlarged due to violation of a constraint. In this case, the GA Tool located another region of the design space that does not violate any constraints.

For both minor parametric survey and full design space exploration, the extent of the Pareto-front in terms of UPC was found to be very small, the range being (£69.1M to £69.5M). However, the range of -Bales Rank (3 to 8) and P_s (19000 kW to 27000 kW) are much larger. In other words, with little change in UPC, a range of solutions trading off -Bales Rank and P_s are possible.

The Pareto-fronts were limited mainly by the two constraints 'L>81m' and 'B>11.5m'. The Pareto-front could not be extended further to the lower UPC region because it would violate the constraint 'L>81m'. Similarly, it could not be extended to the higher UPC region without violating the constraint 'B>15m'.

Unlike the cases of the Large Frigate and the Small Frigate, the performance characteristics of the Corvette SDE design are found to be very close to those of the Pareto-designs. This seems to be partly because of the limitations to the Pareto-front imposed by the two constraints 'L>81m' and 'B>11.5m'. Despite the similarity in performance characteristics, Table 6-20 shows that the design parameters of the Pareto-designs are markedly different from the GA Parent. This demonstrates that designs from distinct regions of the design space may sometimes have similar performance characteristics.

6.4. Conclusions

This chapter applied the proposed design approach to three existing naval combatant designs, originally designed by MSc Naval Architecture students at UCL during the Ship Design Exercise (SDE). The first one was a large frigate of about 6400 t displacement [126], the second one was a small frigate of 4700 t displacement [127] and the third one was a corvette of 1800 t displacement [128]. The proposed design approach was able to produce better designs than the parent designs in terms of the performance characteristics considered: minimise UPC, maximise seakeeping capability (Bales Rank) and minimise P_s.

In the case of the large frigate and the small frigate, the Pareto-front was found to resemble a curve rather than a surface. This indicates that for a given UPC there is a single design on the Pareto-front with a fixed -Bales Rank and P_s. This is found to be in contrast to the corvette whose Pareto-front does resemble a 3D-surface; hence, for a given UPC, there can be many solutions trading off -Bales Rank and P_s. The lack of trade-off solutions for the large frigate and the small frigate is evident from their colour diagrams as well (Figure 6-10 and Figure 6-22): there is a smooth variation of colours indicating that as UPC increases -Bales Rank decreases and P_s increases. The variation of colours in the colour diagram for the corvette (Figure 6-31), on the other hand, is not smooth, indicating the trade-offs between the performance characteristics.

The examples also demonstrated that the Pareto-fronts can sometimes be non-linear and discontinuous. This may happen due to many reasons. One of them is the violation of constraints, which would force genetic algorithms to move from one region of the design space to another. The discrete and non-linear relationships present in the algorithms used for design synthesis may also cause non-linearities. In addition, a design parameter sometimes reaches its optimum value, so that any change in it can only worsen the objectives; this also would force genetic algorithms to move to another region of the design space, thereby creating discontinuities in the Pareto-front.

7. Discussion

This chapter reviews the proposed design approach as described and demonstrated in the earlier chapters, keeping in mind the original aim of the thesis. First, the aim of the thesis is reviewed in light of the demonstration of the proposed design approach. The insights derived from the applications of the proposed design approach are summarised, followed by its advantages and limitations in comparison with traditional design approaches. The future of the proposed design approach is also briefly discussed.

7.1. Review of the aim of the thesis

In Chapter 1, the aim of this thesis was defined as "to develop a new transparent and interactive design approach based on multi-objective optimisation, identify its advantages and limitations, demonstrate it with specific examples, and compare the results with the traditional ship design methods". This aim has been achieved through the description of proposed design approach in Chapter 4, the demonstrations of its applications in Chapter 5, and the comparison of its results with the traditional design approach in Chapter 6.

Chapter 4 discusses the implementation of the new open and interactive design approach. The ability of the proposed design approach to explore a wider area of the design space compared to traditional design approaches is emphasised. The genetic algorithms help to create the Pareto-front, which consists of the set of optimal solutions incorporating the extreme values of all the objectives considered. This helps the designer to concentrate on the optimal region of the design space, as opposed to traditional design approaches where the designer does not know how far the current design might be from the Pareto-front. It also ensures that any combinations of objectives can quickly be assessed for feasibility. The chapter also shows how the analysis of the Pareto-front can assist in deriving design insights about the whole Pareto-front as well as about the individual designs.

Chapter 5 demonstrates three potential applications of the proposed design approach using fictitious sets of design requirements. The demonstrations confirm the potential of the proposed design approach to examine a wide region of the design space and locate the Pareto-front. It also shows the utility of the Pareto-front by analysing it to generate trends of design parameters and performance characteristics, to identify the most important constraints and design inputs, and to assess their influence on the characteristics of the Pareto-front.

Chapter 6 applies the proposed design approach to three existing naval combatant concept designs. The results of the proposed design approach are compared with the original designs produced using a traditional design approach (the UCL MSc Naval Architecture ship design process) and the advantages of the proposed design approach are demonstrated for the three case studies.

The applications of the proposed design approach in Chapter 5 and Chapter 6 demonstrate its transparent and interactive nature. It does not suggest prescriptive solutions; instead, it allows the designer to interrogate the Pareto-front and examine suitable designs in more detail. This transparent and interactive nature of the proposed design approach helps to avoid the "black-box" nature of multi-objective optimisation, thereby helping to make it attractive to practising designers and improving its applicability for preliminary ship design. This achieves the aim of the thesis, in that the proposed design approach has been demonstrated to be transparent and interactive, and its advantages and limitations are demonstrated with examples of potential applications and comparison with traditional ship design methods.

7.2. Insights gained from the applications of the proposed design approach

This section discusses the design insights gained from various applications of the proposed design approach. The strengths of the proposed design approach are examined in comparison with traditional design approaches as well as current applications of multi-objective optimisation in ship design. Finally, the insights obtained from different ways of analysing the Pareto-front are discussed.

Comparison of the proposed design approach and traditional design approaches

The proposed design approach helps in providing useful insights about the current design that are unlikely to be revealed using traditional design approaches. The analysis of the Pareto-front can provide a better understanding of the design requirements and constraints. This understanding can then aid the designer in an informed dialogue with the customer about the requirements and potential solutions, which in turn facilitates the selection of suitable designs for subsequent feasibility studies and detailed design.

The proposed design approach is seen to have three applications: ab-initio concept design, modification of a parent design and modifications required post-concept or early feasibility stages of the design process. Traditional design approaches work well only for the second of these applications – to modify a parent design. This is because traditional design approaches are based on the basis ship method; thus, modification of a parent design with minor changes in various design parameters implies a narrow search of a well-understood region of the design space, which can be handled well by traditional design approaches. However, these may not be so successful for the other two applications. For example, even though traditional design approaches are used for ab-initio concept design, they are not good at handling the wide design space exploration demanded by the flexibility of design parameters. This problem is usually overcome by making appropriate assumptions based on historical data, which narrows down the design space to be explored.

However, it also narrows down the design options and some assumptions could eliminate potentially good design alternatives. In comparison, the proposed design approach, with its ability to provide a wide search of the design space, is ideally suited for ab-initio concept design. For example, in the case of the Large Frigate (Section 6.1), the original design based on the UCL in Naval Architecture ship design process fixed a high value for superstructure ratio in the initial stages of the design process, based on the designer's experience and available design data. However, the proposed design approach showed that a much lower value of superstructure ratio would have been a better choice to reduce UPC and shaft power.

Similarly, the third application – modifying a design following changes in design requirements at later stages of the design process – is something that traditional design approaches have difficulty accommodating. The examples considered involve a reduction in the customer's budget after significant progress has been made in the design process. The customer is ready to accept a lower level of performance (for example, lower seakeeping quality) because of the reduced budget, but the designer has to decide how best to achieve the required reduction in cost. It is not apparent which parameters are to be changed to achieve this. Moreover, the designer may wish to minimise changes in major design parameters, such as L, B, T, and D, to avoid repeating major analyses, re-doing the deck layout etc. It is virtually impossible to do this using traditional design approaches because there is no systematic procedure to achieve these goals. The designer will have to depend on his experience and judgement to try out different variations to see if they give the desired results. On the other hand, the proposed design approach can achieve this directly by executing the GA Tool with additional objectives, such as the required target values for L, B, T and D. This is a significant advantage of the proposed design approach over traditional design approaches.

The design examples used in this thesis are from the UCL Ship Design Exercise based on the UCL MSc in Naval Architecture ship design process [35]. The UCL design process is based on the basis ship method, but permits limited design space exploration. The 'Initial Sizing' stage produces a numerically balanced design based

on basis ship data. In the second and third stages, i.e., the major and minor parametric surveys, the design is assumed to have the same displacement and enclosed volume as that balanced design, though some of its design parameters have been changed. The weight and volume balance is carried out only at the very end of the minor parametric survey, after finalising the design parameters. This approach may sometimes mean potentially good designs are not being considered, in contrast to the proposed design approach. For example, Section 6.1 showed that some of the good design alternatives had lower displacement and enclosed volume compared to the design obtained from the Ship Design Exercise. The Ship Design Exercise missed them because of the assumption of constant displacement and constant enclosed volume.

Another flaw in traditional design approaches relates to the choice of a suitable design taken from the feasible region in the design space. The demonstrations of the proposed design approach show that the designs on the Pareto-front often lie close to the boundaries of one or more constraints. So, for a feasible region of the design space bounded by various design constraints, the optimal solutions usually lie close to the boundaries of this region. (In this context, the term "optimal solutions" means a set of designs that have been optimised based on a given set of criteria. However, this set of criteria may not encompass all the important design aspects.) In traditional design approaches, the designer would not usually select a design too close to the boundaries of the feasible region. This usual practice is to ensure that any changes to design parameters as the design gets refined will not push the design over some constraint boundaries that may cause poor performance characteristics. For example, in the major parametric survey stage of the UCL ship design process, the feasible design window is determined and then, taking due account of some design and performance aspects, a design near the middle of the design window is chosen. This is done anticipating that no constraints will be violated even after modifications to design parameters in the next stage of the design process (the minor parametric survey). The results of the proposed design approach show that this practice is unlikely to produce an optimal solution. Besides, the proposed design approach, through design space and performance space exploration, helps to ensure

the selection of a robust design; hence minor changes in any design parameter are unlikely to result in major changes in the performance characteristics of such a design.

Comparison of the proposed design approach and the current applications of multi-objective optimisation in ship design

Most of the current applications of multi-objective optimisation (MOO) in ship design are limited to two objectives, primarily because of the limitations in interpretation and visual representation of results. In comparison, the proposed design approach is truly multi-objective, so that a large number of objectives can be analysed simultaneously (up to six objectives have been demonstrated in this thesis). The difficulties in interpreting the results are overcome by adopting novel ways of analysing and visualising the Pareto-front. These include the colour diagram representation of the Pareto-front to show general trends of design parameters and performance characteristics, and the use of star plots to visually compare various designs in the design space as well as the performance space. However, even with these representations, the more the number of objectives, the more difficult it becomes to interpret the results. For example, when there are just two objectives to consider, the overall trends of the design parameters are easy to understand in a colour diagram: one objective increases while the other decreases, and one can examine the corresponding trends in design parameters. However, when there are three or more objectives, the trends may not be obvious. For example, for the corvette design considered in Section 6.3, the 3-objective Pareto-front for the full exploration of the design space results in a 3D surface. Thus, for a given value of one objective, there are a number of solutions trading off the other two objectives. This made the interpretation of the trends of the design parameters from the colour diagram rather difficult (Figure 6-32). In contrast, the 3-objective Pareto-front obtained for the full design space exploration for the large frigate (Section 6.1) appeared as a curve rather than a surface and the trends could easily be interpreted from the colour diagram (Figure 6-10). One way to overcome this difficulty is to filter the Pareto-front appropriately. For example, in the case of the corvette design (Section 6.3), one may fix the P_s to about 20000 kW and then examine the UPC and

-Bales Rank of all such designs along with their design parameters in a colour diagram to reveal the trends. Another way is to examine star plots or local slopes plots for a few designs in the neighbourhood of a design of interest, which would show the trends of design parameters and performance characteristics.

One of the advantages of genetic algorithms, as stated in the literature, is that they are capable of generating the Pareto-front even in the presence of non-linear and discrete relationships among design variables. The existence of multiple clusters, discontinuities and non-linearities seen in some of the Pareto-fronts generated by the GA Tool (e.g. Section 6.2.3) confirm this ability of genetic algorithms when applied to preliminary ship design. Conventional optimisation methods using gradient-based or pattern search techniques usually find it difficult to handle non-linear and discrete relationships [113,129].

The structure of the Pareto-front

The Pareto-front could be a rather smooth surface (e.g.: modifying a parent design, Figure 5-23) or a surface showing significant discontinuities (e.g.: the small frigate, Figure 6-12), or a mix of these. There seem to be three main causes for non-linearities or discontinuities, as explained below.

The first reason is the violation of one or more design constraints. When genetic algorithms find that the Pareto-front in a region of the design space cannot be extended further because of the violation of constraints, they try to locate another region that does not violate any constraints. The new region gives rise to a new cluster of designs. The extent of each cluster is determined by the limiting constraints for that cluster. The separation between clusters is usually very prominent. The discontinuous Pareto-front for 'C07 – higher C_{Bmax}' in Figure 5-16 is an example of this.

The second type of discontinuity occurs when an independent design variable reaches its optimum value, so that no change in that variable can further improve any of the objectives. This is likely to happen when most of the design parameters remain fixed, leaving the genetic algorithms with few independent design variables

to adjust. In this case, genetic algorithms try to locate another region of the design space to improve at least one objective. An example of this is Figure 6-13 which shows three clusters of designs with two large gaps separating them. The gap between Cluster-1 (the low-UPC region) and Cluster-2 (the mid-UPC region) in this case is caused by the design variable C_P reaching its optimum value, thus forcing genetic algorithms to locate another region of the design space to extend the Pareto-front.

The third type of discontinuity occurs due to the complexity of the algorithms used for design synthesis or performance analysis. They usually appear as minor non-linearities instead of large gaps. For example, the Pareto-fronts in Section 6.2 were created using the detailed weight and volume groupings for warships, as given in [28]; these Pareto-fronts do not appear very smooth. With reference to Figure 6-13, there are three clusters of designs separated by two large gaps. Besides, in Cluster-3 (the high-UPC region), four minor 'jumps' can be seen clearly – at UPC = £269.9, £270.6, £271.3 and £272.0M. These jumps, as well as the gap between Cluster-2 and Cluster-3, are caused by the warship weight and space algorithms, which include a number of discrete and non-linear relationships. For instance, the number of some of the ship components is based on the gross enclosed volume of the ship. Enclosed volume of 17000m^3 is an important figure for some of the components: for example, the number of pumps and air compressors are taken as 3 each if the enclosed volume of the ship is up to 17000m^3, and 4 if it is more than 17000m^3. In the case of the small frigate, the minimum enclosed volume of all ships on the Pareto-front is about 16850m^3 and the maximum about 17200m^3, thus falling on either side of the limit of 17000m^3. Hence, some of the designs have two pumps and air compressors while others have three. Such non-linear relationships cause non-linearities in the Pareto-front. In contrast, the Pareto-fronts included in Section 5.2 were created using simpler weight and space algorithms based on merchant ship weight and volume groups: structure, machinery and outfit (as given in [28]); they appear much smoother. In reality, a ship design would consist of a number of discrete equipment and distributed systems; hence, if they are taken into

account during the design process, the Pareto-front is unlikely to be smooth or regular.

The presence of non-linear relationships in design synthesis or performance analysis may not always result in the creation of non-linear Pareto-fronts. For example, the large frigate (Figure 6-9) does not show any obvious discontinuities, in contrast with the small frigate (Figure 6-13). The minimum enclosed volume for the designs on the Pareto-front for the large frigate is about 20900m^3, higher than the limit of 17000m^3. Hence, all of them have three pumps and compressors according to the algorithms employed, and there are no resulting non-linearities unlike the example of the small frigate. There are of course many such non-linear relationships in the weight and volume algorithms; hence, depending on the design and performance characteristics of the ships on the Pareto-front, the non-linearities may or may not appear. In fact, closer inspection does reveal several minor non-linearities in the Pareto-front for the large frigate as well (Figure 6-9).

Trends of design parameters and performance characteristics

The example demonstrations suggest that the information obtained from the analysis of the Pareto-front, such as the trends of design parameters and performance characteristics, always have physical explanations. Some of them can be expected from the knowledge and experience of the designer (for example, ships with larger displacements tend to have better seakeeping). However, some of the others are difficult to anticipate in advance (for example, how the trends of design parameters might change when one design constraint reaches its lower or upper bound). Analysis of such unexpected findings helps to improve the designer's understanding of the concept design process in general and the current design in particular.

The examples considered in Chapter 6 demonstrate that the trends from the Pareto-front and the constraints plot are not universal: they depend on the design inputs and constraints. However, some of the trends seem to be generic. For example, the improvement in seakeeping corresponds to increase in displacement and C_P. This directly follows the formulation of the Bales Rank used to assess the seakeeping

performance. However, improvement in seakeeping seems to be also associated with a decrease in B/T. It may not be obvious why this happens, since the Bales Rank formulation does not directly relate to B/T. One explanation is that T increases so that displacement can increase, which will improve seakeeping. The increase in T reduces freeboard; consequently, windage area and wind heeling moment decrease, resulting in reduced requirement of GM, which in turn reduces B. The reduction in B and the increase in T result in reduction of B/T. Thus, careful inspection of such trends and investigation into the underlying reasons can help to improve the designer's understanding of the design.

Analysis of design constraints

The investigation of constraints is an important aspect in the analysis of the Pareto-front. The constraints plot can demonstrate the relative importance of various constraints; they can also help to predict the qualitative effect on the Pareto-front of varying each constraint. This could help in the customer-designer dialogue, for example, to clarify which constraints are best to be relaxed to get the required improvement in performance in the region of interest.

Interestingly, the observation that a constraint seems irrelevant or unimportant in a constraints plot, implying that relaxing it will not make any difference to the Pareto-front, may not in fact be correct. A case in point is Figure 5-16, where the relaxation of the upper bound of C_B resulted in extending the Pareto-front further, which was not anticipated from the analysis of the original constraints plot. This happens because relaxing a constraint opens up another region of the design space for exploration. The examination of the original constraints plot cannot predict if the new region of the design space will improve the Pareto-front or not, since the characteristics of the new region is unknown at that point. Hence, it is important that the effect of relaxing each constraint is examined, even though some of them may appear irrelevant or unimportant.

Similarly, relaxing more than one constraint simultaneously would improve the Pareto-front much more than relaxing them individually. Figure 5-13 suggests this,

where the simultaneous relaxation of all constraints resulted in a much better Pareto-front compared to relaxing them individually.

Analysis of design inputs

The investigation of the variation of design inputs is another important stage of the analysis of the Pareto-front. Many examples show that increasing the space margin, and thus increasing the size of the ship, could significantly improve the quality of the Pareto-front if seakeeping performance is to be maximised. However, indefinite increase of space margin would not help: there seems to be an optimum space margin that gives the best performance trade-off for a given set of design requirements. Depending on the design requirements, it may be possible to accept a design with appropriate space margin, with due consideration given to the changes in design parameters.

7.3. Limitations of the proposed design approach

The limitations of the proposed design approach are seen to be two-fold: firstly, the limitations due to the nature of the design approach itself, and secondly resulting from the implementation of the design approach through genetic algorithms. The former involves issues such as the inability to tackle non-numerate design considerations, whereas the latter involves issues such as the difficulty in ensuring convergence to the true Pareto-front.

The first limitation relates to the objectives that can be considered within the proposed design approach. Since the approach is based on multi-objective optimisation, the overall performance of the designs on the Pareto-front depends on the objectives specified. Only those characteristics that can be expressed and evaluated numerically can be specified as objectives; thus, subjective aspects such as aesthetics, layout, producibility etc are difficult to be incorporated. There have been attempts to combine genetic algorithms and graph theory to optimise layout by using suitable performance measures such as the adjacency of compartments and the cost of transporting materials between different compartments, as found in [21,55,130-133]. However, many other aspects still require the designer's judgement.

The proposed design approach, through its open and interactive nature, provides the designer with the freedom to examine suitable designs in terms of such subjective considerations before making a final selection. Approaches that allow the integration of architectural issues with a numerical synthesis in the early stages of the ship design process, such as the Design Building Block approach [25], may be helpful in this context.

The proposed design approach generates a number of design options forming the Pareto-front. It also provides different ways to visualise and analyse the Pareto-front so that the designer can examine the trends and characteristics of various designs. However, it does not suggest a prescriptive solution as the best design. Numerical techniques such as MCDM can help in this decision making process. However, the proposed design approach has not directly incorporated them because it is seen as a guide to the designer during the design process and during his dialogue with the customer, rather than a tool to generate a prescriptive "optimum" design solution.

Genetic algorithms cannot guarantee convergence to the true Pareto-front, though for practical purposes the results should be near-optimal, based on the selected objective functions [134-136]. The designer has to check if the Pareto-front has reached convergence. The proposed design approach deals with this problem in three ways. Firstly, multiple runs with the same input data are used to generate multiple Pareto-fronts. Visual comparison of the Pareto-fronts will show if all of them have converged to the same Pareto-front, or if there are any large variations. Secondly, the GA Tool has the capability to extend an existing Pareto-front for more generations. For example, if a Pareto-front is created after 100 generations, it is possible to extend it for another 100 generations. The two Pareto-fronts can be compared to check if there are any large variations. However, neither of these methods offers a fail-safe mechanism to ensure true convergence. The third way is to use the design space exploration to check convergence. For example, consider a representative design on a Pareto-front with two objectives. If a small change in an independent design variable improves both the objectives without violating any constraints, it means that the concerned design is not Pareto-optimal and that the

Pareto-front has not yet reached convergence around that design. More generations may be necessary to improve convergence.

While generating the Pareto-front, the penalty approach is used to distinguish between feasible and infeasible designs. In this approach, if a design violates any constraint bounds or design variable bounds, its fitness values are penalised suitably. Higher violations attract higher penalties. However, there is no precise way of determining the optimum penalty. If the penalty is very low, many infeasible designs may appear in the Pareto-front. Very high penalties will avoid this problem and ensure that the Pareto-front will contain only feasible designs; however, this has another difficulty: when the optimal design parameters correspond to a constraint boundary, too high a penalty for crossing that boundary will 'confuse' the GA. This is because designs on one side of the boundary will have very good fitness, while designs on the other side, though having similar design parameters, will have rather bad fitness (as a result of the large penalty). This will effectively drive the designs away from the constraint boundary, i.e., away from the optimal region. In summary, it is difficult to determine the optimum values of penalties to be used for constraint violation. However, experience with the GA Tool shows that a vast range of penalties can be used without greatly affecting the quality of the Pareto-front. More information on this is given in Appendix H.7.

Another limitation concerns the computational time. To generate the Pareto-front, the GA Tool needs to synthesise and analyse a number of designs across a large number of generations. For a typical run with a population size of 100 and number of generations 1000, the number of designs will be 100*1000 = 100000. In addition, more designs need to be synthesised during the application of the genetic operators. The total computational time required is significant: typically about one hour for the above example on a PC with 3.40 GHz dual processors and 3.24 GB of RAM. Most of this time is taken up in evaluating the performance characteristics of the designs; the genetic algorithms themselves take very little of the total computational time. Thus, fast performance analysis modules are necessary to reduce computational time. At present, simple regression formulae have been used to achieve this. However, this means the applicability of the GA Tool is limited by the suitability of

the performance analysis methods used. Moreover, regression effectively gives an average of many solutions, whereas optimisation searches for the best possible solutions. Performance methods based on fundamental principles may be more accurate; however, they may be associated with increase in computational time. Appropriate alternative performance analysis methods, such as those based on artificial neural networks, may help to improve the accuracy of performance prediction and reduce the computational time. Such approaches have been found in the recent literature: for example, Koh et al [137] combine CFD and ANN to predict wave resistance. One may also keep in mind that since the concept design stage is concerned with the relative merits of various design solutions, speed of computation is probably more important than absolute accuracy in performance analysis.

Exploring the performance space involves determining the local slopes along each objective. Since the tool does not generate a continuous performance space, but only an approximation of it represented by discrete designs, the local slopes obtained may not be very accurate. Hence, due care should be taken while interpreting the results of the local slopes, especially when the number of objectives is high. It may be possible to fit an n-dimensional response surface to the performance space (where 'n' is the number of objectives), as suggested in [103]. This would avoid the problem with the discrete designs. However, this has not been implemented in the current version of the proposed design approach.

The final limitation is that the design tool at present is restricted to displacement monohulls. It is possible to replace the monohull design synthesis module with another type of ship, with associated modifications to the design variables used by the genetic algorithms. However, the applicability of the algorithms used for design synthesis and performance analysis has to be ensured for the type of ship to be designed. This may become difficult for innovative ships and radically new configurations, which ought to be addressed specifically in concept design. For such ship types, simple algorithms based on existing ships and design practice are unlikely to be available, and hence the applicability of the proposed design approach may be subject to unacceptably higher uncertainties.

7.4. Future of the proposed design approach

This thesis through example applications and comparison with a traditional design approach (the UCL design process) has demonstrated the advantages of the proposed design approach: the wider search of the design space and the design insights developed through the analysis of the Pareto-front. It is hoped that the open and interactive nature of this approach, coupled with the advantages mentioned above, should make it attractive to practising designers for the concept stage of the ship design process. The main findings from this research were summarised in a paper presented at the International Conference on Computer Applications in Shipbuilding (ICCAS 2007) (Appendix L) and the response from practising designers was encouraging. To realise the potential of the proposed design approach, the Matlab-based design tool using genetic algorithms will have to be improved upon to convert it from an academic design research tool to a design tool able to be readily used in the ship design industry. The changes required to achieve this are discussed in the next chapter.

The design tool as implemented, however, is ready to use as a replacement for the current UCL MSc Naval Architecture ship design process. It has implemented the monohull design synthesis procedure given in the UCL MSc Naval Architecture Ship Design Procedure [35] as well as the weight and space algorithms given in the Ship Design Data Book [28]. Besides, the tool is modular in nature, so that any module can be replaced with other suitable modules. For example, the Holtrop resistance calculation [29] may easily be replaced with another suitable method.

8. Recommendations for further work

Experience with the proposed design approach through its applications and analysis of results has shown that the capability of the approach can be improved by incorporating some additional functionalities to the GA Tool, as discussed below.

1. A Matlab-based design tool has been used to demonstrate the proposed design approach. At present, the design tool includes a single ship type – displacement monohulls. The approach will become much more beneficial if it includes multiple ship types. For example, it could include monohulls, catamarans and trimarans simultaneously. Then, the generated Pareto-front would show which of these three ship types is best suitable for the current set of design requirements. In fact, it may show that monohulls are better in one region of the Pareto-front, while catamarans or trimarans are better in another region. It could also show that the same level of performance may be achieved by different types of ships with different design parameters. Such a design tool will enhance the value of the proposed design approach for early stage ship design to assess and compare the perceived advantages of various ship types.

   Some modifications to the design tool are necessary to achieve this. Firstly, appropriate design synthesis modules will have to be developed for the additional ship types. This may present some difficulty for unconventional hull forms due to the scarcity of historic design data to guide the synthesis algorithms. Secondly, additional performance analysis modules appropriate for each ship type will have to be developed. Thirdly, the genetic algorithms need to be modified to deal with multiple ship types. This would require an additional design variable to represent the ship type. More design variables may be required depending on the types of ships present: for example, for catamarans the distance between the side hulls will have to be included. Finally, the genetic operators may have to be modified to handle the new design variables. For example, the ship type would be a discrete design variable unlike continuous variables such as C_B or C_P that can take any value

within the specified range. This would mean that the genetic operators have to be capable of handling such discrete variables appropriately.

2. The Pareto-front consists of a number of designs that appear as discrete points in the design space and the performance space. This sometimes makes it difficult to interpret the trends of the design parameters and performance characteristics. This is especially important while exploring the performance space around a short-listed design with more than two objectives. A response surface fitting, for example as suggested in [103], may help to better portray the trends of the performance characteristics and design parameters.

3. In practice, the designer may not be interested in the whole Pareto-front; instead, certain regions of the Pareto-front may be preferred instead of a wider coverage [138]. However, the design tool at present does not distinguish between different regions of the Pareto-front. It should be possible to direct the search by genetic algorithms to the region of interest. For example, the designer may allow the tool to run for a few generations, examine the results, and specify his preferences among a few solutions. The tool can then continue to run, but focussing on the region based on the designer's preferences [139]. Such a method will add value to the design tool by making it more interactive.

4. Hirata [140] has used a "micro-GA" to reduce computational time. In brief, micro-GA is an elitist GA with frequent re-initialisation of the population. It uses the same genetic operators as conventional GAs, the only difference being that the micro-GA uses very small population sizes compared to conventional GAs. This often results in convergence to local optima. To ensure global optimum, the GA is re-started from the achieved local optimum by retaining the best individual and randomly re-initialising the others. The low population size of the micro-GA is claimed to reduce the computational time required, despite the fact that multiple runs may be necessary to ensure global optimum. The applicability of the micro-GA for the new design tool could be investigated.

5. The proposed design approach, as implemented by the candidate using a Matlab-based design tool using genetic algorithms, may be used to replace the current UCL ship design process followed in the MSc Ship Design Exercise for designing monohull warships. Experience of the use of the design tool as part of the Ship Design Exercise could provide further inputs into the capabilities of the tool and further functionalities required. By incorporating such additional capabilities, it could be developed into a practical design tool useful for the industry for the concept stage of the ship design process. To achieve this, the design approach will have to be improved upon to convert it from an academic design research tool to a design tool applicable to the ship design industry. This may require developing a user-friendly design interface, adding more flexibility in the analysis of the Pareto-front by developing and implementing more visualisation methods, and incorporating relatively fast performance analysis tools capable of providing good relative comparison of performance.

9. Conclusions

This thesis has described the development of a new design approach applicable for the concept design stage of the ship design process. The proposed design approach is demonstrated through various examples and comparisons with existing designs produced using traditional design approaches. These examples demonstrate the advantages of the proposed design approach, in terms of its ability to explore a wide region of the design space and identify the Pareto-front consisting of design solutions optimised to specific objectives, and to visualise and analyse the Pareto-front to derive design insights. It is considered that the open and interactive nature of the proposed design approach, in contrast with the "black-box" nature of the typical optimisation-based approaches that produce prescriptive solutions will make it attractive to practising designers.

The proposed design approach has currently been implemented by means of a design tool in Matlab based on genetic algorithms (see Appendix H). This design tool incorporates a synthesis module based on the UCL MSc in Naval Architecture Ship Design Procedure [35]. The tool uses algorithms based on the UCL Ship Design Data Book [28] to estimate the weight and space requirements of the ship components. This makes it an ideal replacement for the current Ship Design Procedure followed at UCL. Experience with the proposed design approach may reveal the need for more functionality in the design tool, in addition to the work already identified in this thesis. It is hoped that the proposed design approach will thus evolve into an industrial standard in future, and will help to create better ships in shorter time than possible today.

References

1. Andrews, D. J. 1994, "Preliminary Warship Design", *Transactions of the Royal Institution of Naval Architects*, Vol. 136, pp. 37-55.

2. Andrews, D. J. 2003, "Marine Design - Requirement Elucidation rather than Requirement Engineering", in *Proc. IMDC '03, 8th International Marine Design Conference, 5-8 May 2003*, Papanikolaou, A., ed., Athens, Greece, pp. 2-18.

3. Andrews, D. J. 1998, "A Comprehensive Methodology for the Design of Ships (and Other Complex Systems)", *Proceedings of the Royal Society A: Mathematical, Physical and Engineering Sciences*, Vol. 454, No. 1968, pp. 187-211.

4. Devine, M. D. 1986, "ASSET - A Computer Aided Engineering Tool for the Early Stage Design of Advanced Marine Vehicles", in *8th Advanced Marine Systems Conference, Sept 22-24, 1986*, San Diego, USA.

5. Neti, S. N. 2005, *Ship Design Optimization Using ASSET*, Master's Thesis, Ocean Engineering, Virginia Polytechnic, Blacksburg, Virginia, USA.

6. Lavis, D. R. & Goubault, P. 2003, "Physics-based Ship Design Synthesis", in *Proc. IMDC '03, 8th International Marine Design Conference, 5-8 May 2003, Vol.I*, Papanikolaou, A., ed., Athens, Greece, pp. 21-35.

7. Lavis, D. R. & Forstell, B. G. 2006, "The Cost-Benefit of Emerging Technologies using Physics-based Ship-Design Synthesis", http://www.ccdott.org/fast99_conference/BandLavis_Presentation/band.pdf accessed on 29-3-2006.

8. Pareto, V. 1906, *Manuale di Economia Politica*, Societa Editrice Libraria, Milan, Italy.

9. Day, A. H. & Doctors, L. J. 1997, "Design of Fast Ships for Minimal Resistance and Motions", in *Proc. IMDC '97, 6th International Marine Design Conference, 23-25 Jun 1997, Vol.I*, Sen, P. & Birmingham, R. W., eds., Newcastle upon Tyne, UK, pp. 569-583.

10. Brown, A. & Thomas, M. 1998, "Reengineering the Naval Ship Concept Design Process", in *Proc. From Research to Reality in Ship Systems Engineering Symposium, Sep 1998*, Essex, UK, pp. 277-289.

11. Brown, A. & Salcedo, J. 2003, "Multiple-Objective Optimization in Naval Ship Design", *Naval Engineers Journal*, Vol. 115, No. 4, pp. 49-61.

12. Boulougouris, E. K. & Papanikolaou, A. 2003, "Optimisation of Naval Ships with Genetic Algorithms for Enhanced Survivability", in *Proc. IMDC '03, 8th International Marine Design Conference, 5-8 May 2003, Vol.II*, Papanikolaou, A., ed., Athens, Greece, pp. 727-740.

13. Maisonneuve, J. J., Harries, S., Marzi, J., Raven, H. C., Viviani, U., & Piippo, H. 2003, "Towards Optimal Design of Ship Hull Shapes", in *Proc. IMDC '03, 8th International Marine Design Conference, 5-8 May 2003*, Papanikolaou, A., ed., Athens, Greece, pp. 31-42.

14. Olcer, A. I., Tuzcu, C., & Turan, O. 2003, "Internal Hull Subdivision Optimisation of Ro-Ro Vessels in Multiple Criteria Decision Making Environment", in *Proc. IMDC '03, 8th International Marine Design Conference, 5-8 May 2003, Vol.I*, Papanikolaou, A., ed., Athens, Greece, pp. 338-350.

15. Peri, D. & Campana, E. F. 2003, "Multidisciplinary Design Optimization of a Naval Combatant", *Journal of Ship Research*, Vol. 47, No. 1, pp. 1-12.

16. Zaraphonitis, G., Boulougouris, E., & Papanikolaou, A. 2003, "An Integrated Optimization Procedure for the Design of Ro-Ro Passenger Ships of Enhanced Safety and Efficiency", in *Proc. IMDC '03, 8th International Marine Design Conference, 5-8 May 2003, Vol.I*, Papanikolaou, A., ed., Athens, Greece, pp. 312-323.

17. Brown, A. & Mierzwicki, T. 2004, "Risk Metric for Multi-Objective Design of Naval Ships", *Naval Engineers Journal*, Vol. 116, No. 2, pp. 55-71.

18. Parsons, M. G. & Scott, R. L. 2004, "Formulation of Multicriterion Design Optimization Problems for Solution with Scalar Numerical Optimization Methods", *Journal of Ship Research*, Vol. 48, No. 1, pp. 61-76.

19. Boulougouris, E. K. & Papanikolaou, A. D. 2006, "Hullform Optimization of a High Speed Wave Piercing Monohull", in *Proc. IMDC 2006, 9th International Marine Design Conference, 16-19 May 2006, Vol.2*, Ann Arbor, USA, pp. 559-581.

20. Zalek, S. F., Parsons, M. G., & Papalambros, P. Y. 2006, "Multicriterion Design Optimization of Monohull Vessels for Propulsion and Seakeeping", in *Proc. IMDC 2006, 9th International Marine Design Conference, 16-19 May 2006, Vol.2*, Ann Arbor, USA, pp. 533-557.

21. Slapnicar, V. & Grubisic, I. 2003, "Multi-criteria Optimization Model of Deck Layout Design", in *Proc. IMDC '03, 8th International Marine Design Conference, 5-8 May 2003, Vol.I*, Papanikolaou, A., ed., Athens, Greece, pp. 98-109.

22. Sen, P. 1992, "Marine Design: the Multiple Criteria Approach", *Transactions of the Royal Institution of Naval Architects*, Vol. 134, pp. 261-276.

23. Erikstad, S. O. 2003, *Introduction to Marine Systems Design Models and Methods (TMR4115 - Design Methods, Lecture Note #1)*, Norwegian University of Science and Technology (NTNU), Trondheim.

24. Keane, A. J., Price, W. G., & Schachter, R. D. 1991, "Optimization Techniques in Ship Concept Design", *Transactions of the Royal Institution of Naval Architects*, Vol. 133, pp. 123-139.

25. Andrews, D. J. 2003, "A Creative Approach to Ship Architecture", *International Journal of Maritime Engineering*, Vol. 145, No. 3, pp. 229-252.

26. Brown, D. K. 1987, "The Architecture of Frigates", in *Proc. Warship '87: International Symposium on Anti-submarine Warfare, 11-13 May 1987, Vol.II*, RINA, London.

27. Carreyette 1978, "Preliminary Ship Cost Estimation", *Transactions of the Royal Institution of Naval Architects.*

28. UCL 1996, *MSc Ship Design Data Book*, NAME Office, Department of Mechanical Engineering, London, UK.

29. Holtrop, J. 1984, "A Statistical Re-analysis of Resistance and Propulsion Data", *International Shipbuilding Progress*, Vol. 31, No. 363, pp. 272-276.

30. Bales, N. K. 1980, "Optimizing the Seakeeping Performance of Destroyer-Type Hulls", in *13th ONR Symposium on Naval Hydrodynamics*, Tokyo, Japan.

31. Walden, D. A. 1983, "Extension of the Bales Seakeeping Rank Factor Concept", in *Proc. 20th American Towing Tank Conference (ATTC), 2-4 Aug 1983*, Hoboken, New Jersey, USA.

32. The Mathworks Inc. 2005, "Matlab", http://www.mathworks.com/products/matlab accessed on 9-4-0005.

33. Gale, P. A. 2003, "The Ship Design Process", in *Ship Design and Construction, Vol.I*, Lamb, T., ed., The Society of Naval Architects & Marine Engineers, Jersey City, USA, ISBN 0939773406, p. 5_1-5_40.

34. Cushing, C. R. 2003, "The Ship Acquisition Process", in *Ship Design and Construction, Vol.I*, Lamb, T., ed., The Society of Naval Architects & Marine Engineers, Jersey City, USA, ISBN 0939773406, p. 4_1-4_26.

35. UCL 2004, *MSc Ship Design Procedure*, NAME Office, Department of Mechanical Engineering, London, UK.

36. Brown, D. K. 1996, *An Overview of Surface Warship Design Practice*, 2 edn, Andrews, D. J. & Fellows, D. C., eds., NAME Office, Department of Mechanical Engineering, UCL, London, UK.

37. Lamb, T. 1986, *Engineering for Ship Production*, The Society of Naval Architects and Marine Engineers, Ann Arbor, USA.

38. Harvey-Evans, J. 1959, "Basic Design Concepts", *Naval Engineers Journal*, Vol. 71, pp. 671-678.

39. Andrews, D. J. 1981, "Creative Ship Design", *Transactions of the Royal Institution of Naval Architects*, Vol. 123, pp. 447-471.

40. van Griethuysen, W. J. 2000, "Marine Design - can Systems Engineering cope?", in *Proc. IMDC 2000, 7th International Marine Design Conference, 21-24 May 2000*, Kyongju, Korea.

41. Rydill, L. J. 1969, "No, the Future of the Corps is not in Systems Architecture", *Journal of the Royal Corps of Naval Constructors.*

42. Hoset, K. & Erichsen, S. 1997, "General Design Theory and its Influence on the Design of Ships", in *Proc. IMDC '97, 6th International Marine Design Conference, 23-25 Jun 1997, Vol.I*, Sen, P. & Birmingham, R. W., eds., Newcastle upon Tyne, UK, pp. 103-121.

43. Parsons, M. G. 2003, "Parametric Design", in *Ship Design and Construction, Vol.I*, Lamb, T., ed., The Society of Naval Architects & Marine Engineers, Jersey City, USA, ISBN 0939773406, p. 11_1-11_48.

44. Pham, D. T. & Karaboga, D. 1998, *Intelligent Optimisation Techniques: Genetic Algorithms, Tabu Search, Simulated Annealing and Neural Networks*, Springer, London, UK, ISBN 1852330287.

45. Tribon Solutions 2004, "Tribon M3", www.aveva.com/uploads/tribonm3brochure.pdf accessed on 12-9-0007.

46. SENER IngenierÃa y Sistemas SA 2007, "FORAN", http://www.foran.es accessed on 12-9-2007.

47. Dassault Systemes & IBM 2007, "CATIA", http://www.3ds.com/products-solutions/brands/CATIA/; http://www-306.ibm.com/software/applications/plm/catiav5 accessed on 12-9-0207.

48. Napa Ltd 2007, "NAPA", http://www.napa.fi accessed on 12-9-2007.

49. Graphics Research Corporation Limited 2007, "Paramarine", http://www.grc-ltd.co.uk/products/paramarine/index.psp accessed on 12-9-2007.

50. Schiller, T. R., Daidola, J. C., Kloetzli, J. W., & Pfister, J. 2001, "Portfolio of Ship Designs: Early-Stage Design Tools", *Marine Technology*, Vol. 38, No. 2, pp. 71-91.

51. Andreasen, M. M. 2003, "Design Methodology - Design Synthesis", in *Proc. IMDC '03, 8th International Marine Design Conference, 5-8 May 2003, Vol.I*, Papanikolaou, A., ed., Athens, Greece, p. II-1-II-18.

52. Andrews, D. J., Atlar, M., Drake, K., Gee, N., Levander, K., Sen, P., & Snaith, G. J. 1997, "IMDC State of the Art Report on Design Methods", in *Proc. IMDC '97, 6th International Marine Design Conference, 23-25 Jun 1997, Vol.II*, Sen, P. & Birmingham, R. W., eds., Newcastle upon Tyne, UK.

53. Andrews, D. J., Keane, R. G. J., Lamb, T., Sen, P., & Vassalos, D. 2006, "IMDC State of the Art Report on Design Methodology", in *Proc. IMDC 2006, 9th International Marine Design Conference, 16-19 May 2006, Vol.1*, Ann Arbor, USA, pp. 79-103.

54. UCL 2004, *Hydrodynamic Aspects of Ship Design*, NAME Office, Department of Mechanical Engineering, London, UK.

55. Halvacioglu, S. & Insel, M. 2003, "An Expert System Approach to Container Ship Layout Design", *International Shipbuilding Progress*, Vol. 50, No. 1 & 2, pp. 19-34.

56. Alkan, A. D. & Gulez, K. 2004, "A Knowledge-Based Computational Design Tool for Determining Preliminary Stability Particulars of Naval Ships", *Naval Engineers Journal*, Vol. 116, No. 4, pp. 37-51.

57. van Hees, M. T. 1992, "Quaestor: a Knowledge-based System for Computations in Preliminary Ship Design", in *Proc. PRADS '92, 5th International Symposium on Practical Design of Ships and Mobile Units*, Caldwell, J. & Ward, G., eds., Newcastle upon Tyne, UK.

58. Sha, O. P., Ray, T., & Gokarn, R. P. 1994, "An Artificial Neural Network Model for Preliminary Ship Design", in *Proc. ICCAS '94, 8th International Conference on Computer Applications in Shipbuilding, 5-9 Sep 1994, Vol.2*, Bremen, Germany, pp. 10-15.

59. Ando, H., Yamato, H., Sato, M., Karasawa, T., Tamura, Y., Shirayama, S., & Masuda, H. 2003, "A Research on Knowledge-centred System for Ship Basic Design – Semantic Web Approach", in *Proc. IMDC '03, 8th International Marine Design Conference, 5-8 May 2003, Vol.I*, Papanikolaou, A., ed., Athens, Greece, pp. 168-179.

60. Delatte, B. & Butler, A. 2003, "An Object-Oriented Model for Conceptual Ship Design Supporting Case-Based Design", *Marine Technology*, Vol. 40, No. 3, pp. 158-167.

61. Welsh, M. & Hills, W. 1991, "An Expert System for Use in Concept Design", in *Proc. IMSDC'91, 4th International Marine (System) Design Conference, 27 May 1991, Vol.1*, Kobe, Japan.

62. Stearns, H., Payne, P., & Smith, G. 1991, "Designing a Knowledge Based Ship Design System", in *Proc. IMSDC'91, 4th International Marine (System) Design Conference, 27 May 1991, Vol.1*, Kobe, Japan.

63. van Oers, B. & van Hees, M. 2006, "Combining a Knowledge System with Computer-aided Design", in *Proc. COMPIT '06, 5th International Conference on Computer Applications and*

Information Technology in the Maritime Industries, 8-10 May 2006, Grimmelius, H. T., ed., Oegstgeest, The Netherlands.

64. Lee, K.-Y. & Lee, K.-H. 1996, "Knowledge-based Optimum Conceptual Ship Design", *Ship Technology Research*, Vol. 43, No. 3, pp. 106-114.

65. Lee, D. 1997, "Multiobjective Design of a Marine Vehicle with Aid of Design Knowledge", *International Journal for Numerical Methods in Engineering*, Vol. 40, No. 14, pp. 2665-2677.

66. Sanecka, K. & Wojdala, K. 2000, "Optimisation Models and Base of Knowledge in System for Preliminary Ship Design", in *Proc. Marine Technology 2000, International XIX Scientific Conference of Naval Architects and Marine Engineers; 4-6 May 2000, Vol.2*, Szczecin - Dziwnęwek, Poland, pp. 249-256.

67. Lee, D. 1999, "Hybrid System Approach to Optimum Design of a Ship", *Artificial Intelligence for Engineering Design, Analysis and Manufacturing*, Vol. 13, No. 1, pp. 1-11.

68. Vassalos, D. 1997, "A Thematic Network on "Design for Safety" – an Integrated Approach to Safe Ship Design", in *Proc. IMDC '97, 6th International Marine Design Conference, 23-25 Jun 1997*, Sen, P. & Birmingham, R. W., eds., Newcastle upon Tyne, UK, pp. 299-312.

69. Vassalos, D., Konovessis, D., & Vassalos, G. C. 2003, "A Risk-based Framework on Ship Design for Safety", in *Proc. IMDC '03, 8th International Marine Design Conference, 5-8 May 2003, Vol.I*, Papanikolaou, A., ed., Athens, Greece, pp. 224-238.

70. Vassalos, D. 2004, "Risk-based Design: from Philosophy to Implementation", in *Proc. 2nd International Maritime Safety Conference on Design for Safety, 27-30 Oct 2004*, Sakai, Japan.

71. Vassalos, D. 2005, "Passenger Ship Safety - Containing the Risk", in *Proc. International Symposium on Ship Operations, Management & Economics, 12-13 May 2005. Session C - Safety and Environment*, Athens, Greece.

72. Aksu, S., Vassalos, D., Tuzcu, C., Mikelis, N., & Swift, P. 2004, "A Risk-based Design Methodology for Marine Pollution Prevention and Control", in *Proc. International Conference on Design & Operation of Double Hull Tankers, 25-26 Feb 2004*, London, UK.

73. Andrews, D. J. 1986, "An Integrated Approach to Ship Synthesis", *Transactions of the Royal Institution of Naval Architects*, Vol. 128, pp. 73-102.

74. Andrews, D. J. & Dicks, C. 1997, "The Building Block Methodology Applied to Advanced Naval Ship Design", in *Proc. IMDC '97, 6th International Marine Design Conference, 23-25 Jun 1997*, Sen, P. & Birmingham, R. W., eds., Newcastle upon Tyne, UK, pp. 3-19.

75. Andrews, D. J., Burger, D., & Zhang, J. 2005, "Design for Production using the Design Building Block Approach", *International Journal of Maritime Engineering*, Vol. 147.

76. Andrews, D. J. & Pawling, R. 2003, "SURFCON - A 21st Century Design Tool", in *Proc. IMDC '03, 8th International Marine Design Conference, 5-8 May 2003*, Papanikolaou, A., ed., Athens, Greece, pp. 150-166.

77. Pawling, R. 2007, *The Application of the Design Building Block Approach to Innovative Ship Design*, Doctoral Thesis, Department of Mechanical Engineering, University College London

78. Lamb, T. 1969, "A Ship Design Procedure", *Marine Technology*, Vol. 6, No. 4, pp. 362-404.

79. Lamb, T. & Kotinis, M. 2003, "A Set-based Ship Design Synthesis System", in *Proc. IMDC '03, 8th International Marine Design Conference, 5-8 May 2003, Vol.II*, Papanikolaou, A., ed., Athens, Greece, pp. 575-587.

80. Parsons, M. G., Singer, D. J., & Sauter, J. A. 1999, "A Hybrid Agent Approach for Set-Based Conceptual Ship Design", in *Proc. ICCAS '99, 10th International Conference on Computer Applications in Shipbuilding. Jun 7-11 1999, Vol 2*, Cambridge, Massachusetts, USA, pp. 207-221.

81. Murphy, R. D., Sabat, D. J., & Taylor, R. J. 1965, "Least Cost Ship Characteristics by Computer Techniques", *Marine Technology*, Vol. 2, pp. 174-202.

82. Mandel, P. & Leopold, R. 1966, "Optimization Methods Applied to Ship Design", *Transactions of the Society of Naval Architects and Marine Engineers*, Vol. 74, pp. 477-521.

83. Moe, J. & Lund, S. 1968, "Cost and Weight Minimization of Structures with Special Emphasis on Longitudinal Strength Members of Tankers", *Transactions of the Royal Institution of Naval Architects*, Vol. 110, pp. 43-70.

84. Nowacki, H., Brusis, F., & Swift, P. M. 1970, "Tanker Preliminary Design - An Optimization Problem with Constraints", *Transactions of the Society of Naval Architects and Marine Engineers*, Vol. 78, pp. 357-390.

85. Robertson, A. J. S., Buxton, I. L., Sen, P., & Hills, W. 1992, *A Feasibility Study of Multiple Criteria Decision Making Applied to Multi-Role Naval Vessels*, Department of Marine Technology, University of Newcastle-upon-Tyne, MoD Research Agreement 2043/96/DSc(Sea).

86. Ray, T. & Sha, O. P. 1994, "Multicriteria Optimization Model for a Containership Design", *Marine Technology*, Vol. 31, No. 4, pp. 258-268.

87. Ray, T. 1997, "Ship Design Trends through Simulation using the Multiple Criteria Decision Making Framework", in *Proc. IMDC '97, 6th International Marine Design Conference, 23-25 Jun 1997, Vol.I*, Sen, P. & Birmingham, R. W., eds., Newcastle upon Tyne, UK, pp. 189-200.

88. Trincas, G., Zotti, I., Kahu, O., & Totolici, S. 1997, "Multi-Criterial Design of Fast Monohulls for the Adriatic Shortsea Shipping Network", in *Proc. FAST '97, 4th International Conference on Fast Sea Transportation, 21-23 Jul 1997, Vol.1*, Sydney, Australia, pp. 191-200.

89. Hutchison, K. W. & Sen, P. 1998, "Multiple Criteria Design Optimisation of Ro-Ro Passenger Ferries with Consideration of Recently Proposed Probabilistic Stability Standards", in *Proc. PRADS '98, 7th International Symposium on Practical Design of Ships and Mobile Units, 20-25 Sep 1998*, The Hague, The Netherlands, pp. 303-312.

90. Sen, P. & Yang, J.-B. 1998, *Multiple Criteria Decision Support in Engineering Design*, Springer, London, ISBN 9783540199328.

91. Yu, L. & Tan, J. 2003, "IAHP Method Applied in Optimizing Ship Types", in *Proc. IMDC '03, 8th International Marine Design Conference, 5-8 May 2003, Vol.I*, Papanikolaou, A., ed., Athens, Greece, pp. 88-97.

92. Barone, M. & Bertorello, C. 2004, "Design Optimization of Trimaran Hull by Multiattribute Concept", in *Proc. PRADS 2004, International Symposium on Practical Design of Ships and Mobile Units*, Lübeck-Travemünde, Germany, pp. 270-277.

93. Hootman, J. C. & Whitcomb, C. 2005, "A Military Effectiveness Analysis and Decision Making Framework for Naval Ship Design and Acquisition", *Naval Engineers Journal*, Vol. 117, No. 3, pp. 43-61.

94. Coello, C. A. C. 1999, "A Comprehensive Survey of Evolutionary-Based Multiobjective Optimization Techniques", *Knowledge and Information Systems*, Vol. 1, No. 3, pp. 269-308.

95. Coello, C. A. C. 1999, "An Updated Survey of Evolutionary Multiobjective Optimization Techniques: State of the Art and Future Trends", in *Proc. CEC99, Congress on Evolutionary Computation, 6-9 Jul 1999, Vol.1*, Washington DC, USA, pp. 3-13.

96. Lampinen, J. 2000, "Multiobjective Nonlinear Pareto-Optimization", http://www.it.lut.fi/kurssit/04-05/010778000/Pareto.pdf.

97. Srinivas, N. & Deb, K. 1994, "Multiobjective optimization using nondominated sorting genetic algorithms", *Evolutionary Computation*, Vol. 2, No. 3, pp. 221-248.

98. Shahak, S. 1998, *Naval Ship Concept Design: an Evolutionary Approach*, Master's Thesis, Department of Ocean Engineering, Massachusetts Institute of Technology, Cambridge, Massachusetts, USA.

99. Mierzwicki, T. S. 2003, *Risk Index for Multi-Objective Design Optimization of Naval Ships*, Master's Thesis, Ocean Engineering, Virginia Polytechnic, Blacksburg, Virginia, USA.

100. Zaraphonitis, G., Papanikolaou, A., & Mourkoyannis, D. 2003, "Hull-form Optimisation of High Speed Vessels with respect to Wash and Powering", in *Proc. IMDC '03, 8th International Marine Design Conference, 5-8 May 2003, Vol.II*, Papanikolaou, A., ed., Athens, Greece, pp. 43-54.

101. 2003, "FANTASTIC Project - Functional Design and Optimisation of Ship Hull Forms (EC GROWTH Project GRD1-1999-10666/G3RD-CT 2000-00096)", http://www.ec-nantes.fr/sirehna/fantastic/fantastic.htm accessed on 15-11-2005.

102. Brown, A., Wayne, N., Neti, S. N., Young, B., & Garner, M. 2004, *Optimization and Overall Measure of Effectiveness (OMOE) for the Preliminary Design of LHA(R)*, NSWC CISD Innovation Cell Project Report, Virginia Tech, Blacksburg, Virginia, USA.

103. Whitfield, R. I., Hills, B., & Coates, G. 2005, "The Application of Multi-Objective Robust Design Methods in Ship Design", in *Proc. ICCAS '99, 10th International Conference on Computer Applications in Shipbuilding. Jun 7-11 1999, Vol.2*, Cambridge, Massachusetts, USA.

104. Triantaphyllou, E. 2000, *Multi-criteria Decision Making Methods: a Comparative Study*, Kluwer Academic Publishers, Dordrecht, The Netherlands, ISBN 0792366077.

105. Hwang, C. L. & Yoon, K. P. 1981, *Multiple Attribute Decision Making: Methods and Applications*, Springer-Verlag, New York, USA, ISBN 0387105581.

106. Zanic, V., Grubisic, I., & Trincas, G. 1992, "Multi-Attribute Decision Making System Based on Random Generation of Non-dominated Solutions: An Application to Fishing Vessel Design", in *Proc. PRADS '92, 5th International Symposium on Practical Design of Ships and Mobile Units, Vol.2*, Caldwell, J. & Ward, G., eds., Newcastle upon Tyne, UK, pp. 1443-1460.

107. Grubisic, I. & Zanic, V. 1997, "Sensitivity of Multiattribute Design to Economy Environment: Shortsea Ro-Ro Vessels", in *Proc. IMDC '97, 6th International Marine Design*

Conference, 23-25 Jun 1997, Vol.I, Sen, P. & Birmingham, R. W., eds., Newcastle upon Tyne, UK, pp. 201-216.

108. Saaty, T. L. 1980, *The Analytic Hierarchy Process: Planning, Priority Setting and Resource Allocation*, McGraw-Hill, New York, USA, ISBN 0070543712.

109. Belton, V. 1986, "A Comparison of the Analytic Hierarchy Process and a Simple Multi-Attribute Value Function", *European Journal of Operational Research*, Vol. 26, No. 1, pp. 7-21.

110. Dalton, J. A., Sen, P., Norman, P. W., & Whittle, S. 2006, "Applying Optimisation Techniques to a System Design Tool", in *Proc. IMDC 2006, 9th International Marine Design Conference, 16-19 May 2006, Vol.2*, Ann Arbor, USA, pp. 61-84.

111. Todd, D. 1997, *Multiple Criteria Genetic Algorithms in Engineering Design and Operation*, Doctoral Thesis, Department of Marine Technology, University of Newcastle, UK

112. Streichert, F. 2005, "Introduction to Evolutionary Algorithms", http://www-ra.informatik.uni-tuebingen.de/mitarb/streiche/publications/Introduction_to_Evolutionary_Algorithms.pdf accessed on 16-12-2005.

113. Bäck, T. 1996, *Evolutionary Algorithms in Theory and Practice : Evolution Strategies, Evolutionary Programming, Genetic Algorithms*, Oxford University Press, New York, USA, ISBN 9780195099713.

114. Veldhuizen, v. D. A. & Lamont, G. B. 1998, *Multiobjective Evolutionary Algorithm Research: A History and Analysis*, Air Force Institute of Technology, Wright-Patterson AFB, Ohio, USA, TR-98-03.

115. Engelbrecht, A. P. 2005, *Fundamentals of Computational Swarm Intelligence*, John Wiley & Sons, Chichester, UK, ISBN 9780470091913.

116. Fieldsend, J. E. 2004, "Multi-objective Particle Swarm Optimisation Methods", http://www.dcs.ex.ac.uk/academics/jefields/pso_tech.pdf accessed on 12-11-2006.

117. Ray, T., Gokarn, R. P., & Sha, O. P. 1995, "A Global Optimization Model for Ship Design", *Computers in Industry*, Vol. 26, No. 2, pp. 175-192.

118. Maisonneuve, J. J. & Viviani, U. 2003, "Optimal Design of Ship Hull Forms: the FANTASTIC Project", in *Proc. NAV 2003, International Conference on Ship and Shipping Research, 24-27 June 2003*, Palermo, Italy.

119. Maisonneuve, J. J. 2003, "Advances in Optimal Design Technologies", http://www.ec-nantes.fr/sirehna/fantastic/PublicationsDocuments/Nav03_OptDes.pdf accessed on 22-11-2005.

120. Maisonneuve, J. J. 2004, "SIRENHA's Background in Optimal Design", http://www.ec-nantes.fr/sirehna/gallery/modeFrontier/SirehnaOptimisation.pdf accessed on 22-11-2005.

121. van Griethuysen, W. J. 1989, *On the Geometry of Monohull Warships*, PhD Thesis, Department of Mechanical Engineering, University College London, U.K.

122. van Griethuysen, W. J. 1994, "On the Choice of Monohull Warship Geometry - A Technique for Optimizing Hull Forms for Seakeeping, High Speed Resistance and Fuel Consumption Performance", *Transactions of the Royal Institution of Naval Architects*, Vol. 136, pp. 57-76.

123. Wolf, R., Dickmann, J., & Boas, R. 2004, "Ship Design Using Heuristic Optimization Methods", http://www.twocw.net/mit/NR/rdonlyres/Aeronautics-and-Astronautics/16-888Spring-2004/BADEDA1F-754C-463A-B77E-80C116A21D28/0/finrep_wofdickbos.pdf.

124. Thomas, M. W. 1998, *A Pareto Frontier for Full Stern Submarines via Genetic Algorithm*, PhD Thesis, Department of Ocean Engineering, Massachusetts Institute of Technology, Cambridge, Massachusetts, USA.

125. Vasudevan, S. 2007, *The GA Tool User Guide Ver 1.0*, Internal Report, NAME Office, Department of Mechanical Engineering, UCL, London, UK.

126. Babur, Z. 2004, *TRIBAL Class General Purpose Frigate (Monohull)*, MSc Naval Architecture Ship Design Report, Department of Mechanical Engineering, UCL.

127. Hussain, A. & McCarthy, D. J. 2006, *General Purpose Frigate*, MSc Naval Architecture Ship Design Report, Department of Mechanical Engineering, UCL.

128. Guerreiro, G. 1994, *Monohull Corvette*, MSc Naval Architecture Ship Design Report, Department of Mechanical Engineering, UCL.

129. Michalewicz, Z. 1994, *Genetic Algorithms + Data Structures = Evolution Programs*, Springer-Verlag, Berlin, Germany, ISBN 9783540580904.

130. Lee, K.-Y., Han, S.-N., & Roh, M.-I. 2002, "Optimal Compartment Layout Design for a Naval Ship using an Improved Genetic Algorithm", *Marine Technology*, Vol. 39, No. 3, pp. 159-169.

131. Lee, K.-Y., Roh, M.-I., & Jeong, H.-S. 2005, "An Improved Genetic Algorithm for Multi-floor Facility Layout Problems Having Inner Structure Walls and Passages", *Computers and Operations Research*, Vol. 32, pp. 879-899.

132. Daniels, A. S. & Parsons, M. G. 2006, "An Agent-based Approach to Space Allocation in General Arrangements", in *Proc. IMDC 2006, 9th International Marine Design Conference, 16-19 May 2006, Vol.2*, Ann Arbor, USA, pp. 673-695.

133. Nick, E., Parsons, M. G., & Nehrling, B. 2006, "Fuzzy Optimal Allocation of Spaces to Zone-decks in General Arrangements", in *Proc. IMDC 2006, 9th International Marine Design Conference, 16-19 May 2006, Vol.2*, Ann Arbor, USA, pp. 651-671.

134. Deb, K. 2001, *Multi-objective Optimization using Evolutionary Algorithms*, John Wiley & Sons, ISBN 047187339X.

135. Zitzler, E., Deb, K., & Thiele, L. 2000, "Comparison of Multiobjective Evolutionary Algorithms: Empirical Results", *Evolutionary Computation*, Vol. 8, No. 2, pp. 173-195.

136. Doctors, L. J., Day, A. H., & Node, S. 1995, "Hydrodynamically Optimal Hull Forms for River Ferries", in *Proc. International Symposium on High Speed Vessels for Transport and Defence, 23-24 Nov 1995*, RINA, London.

137. Koh, L., Atlar, M., Mesbahi, E., Janson, C.-E., Larsson, L., & Abt, C. 2005, "Novel Design and Hydrodynamic Optimisation of a High-Speed Hull Form", in *Proc. HPMV 2005, 5th International Conference on High Performance Marine Vessels, 9-10 Apr 2005*, Shanghai, China.

138. Todd, D. S. & Sen, P. 1999, "Directed Multiple Objective Search of Design Spaces using Genetic Algorithms and Neural Networks", in *Proc. Genetic and Evolutionary Computation Conference, Vol.2*, Banzhaf, W., ed., San Francisco, USA, pp. 1738-1743.

139. Sen, P. 2001, "Communicating Preferences in Multiple-Criteria Decision-Making: the Role of the Designer", *Journal of Engineering Design*, Vol. 12, No. 1, pp. 15-24.

140. Hirata, N. 2004, "Comparison of Genetic Algorithm and Gradient-based Method Applied to Ship Shape Optimisation", *Journal of the Kansai Society of Naval Architects*, No. 241, pp. 59-65.

141. Whitfield, R. I., Duffy, A. H. B., Wu, Z., & Meehan, J. 2001, "Intelligent Design Guidance", in *Proc. ICED '03, International Conference on Engineering Design, 19-21 Aug 2001*, Stockholm, Sweden.

142. Percival, S., Hendrix, D., & Noblesse, F. 2001, "Hydrodynamic optimization of ship hull forms", *Applied Ocean Research*, Vol. 23, No. 6, pp. 337-355.

143. Center for the Commercial Deployment of Transportation Technologies California State University (CCDoTT) 2003, "Optimization Tool Development Based on Neural Networks", ftp://www.foundation.csulb.edu/CCDoTT/Deliverables/2002/task%202.20/task%202.20_opttools%20FY%2002.pdf accessed on 6-6-2005.

144. Center for the Commercial Deployment of Transportation Technologies California State University (CCDoTT) 2003, "CAD-Based CFD Tool Development and Application", ftp://www.foundation.csulb.edu/CCDoTT/Deliverables/2002/task%202.20/task%202.20_cadbasedcfdtools%20FY%2002.pdf accessed on 6-6-2005.

145. Marzi, J. 2003, *Use of CFD Methods for Hullform Optimisation in a Model Basin*, MARNET - CFD Workshop, Haslar 20/21-03-2003.

146. Grigoropoulos, G. J. 2004, "Hull Form Optimization for Hydrodynamic Performance", *Marine Technology*, Vol. 41, No. 4, pp. 167-182.

147. Hooke, R. & Jeeves, T. A. 1961, "Direct Search Solution of Numerical and Statistical Problems", *Journal of the Association for Computing Machinery*, Vol. 8, pp. 212-229.

148. Powell, M. D. J. 1964, "An Efficient Method for Finding the Minimum of a Function of Several Variables without Calculating Derivatives", *The Computer Journal*, Vol. 7, pp. 155-162.

149. Fletcher, R. & Reeves, C. M. 1964, "Function Minimization by Conjugate Gradients", *The Computer Journal*, Vol. 7, No. 2, pp. 149-154.

150. Mitchell, M. 1996, *An Introduction to Genetic Algorithms*, MIT Press, Cambridge, Massachusetts, USA, ISBN 9780262631853.

151. Parmee, I. C. 2001, *Evolutionary and Adaptive Computing in Engineering Design*, Springer-Verlag London, ISBN 1852330295.

152. Morishita, M. & Akagi, S. 2005, "Hull Form Optimisation for Fast Ships Using Simulated Annealing (SA) Method", in *Proc. COMPIT'05, 4th International Conference on Computer and IT Applications in the Maritime Industries; 8-11 May 2005*, Hamburg, Germany, pp. 250-256.

153. Hung, Y.-F., Chen, C.-P., Shih, C.-C., & Hung, M.-H. 2003, "Using Tabu Search with Ranking Candidate List to Solve Production Planning Problems with Setups", *Computers & Industrial Engineering*, Vol. 45, pp. 615-634.

154. Rajesh, J., Gupta, K., Kusumarkar, H. S., Jayaraman, V. K., & Kulkarni, B. D. 2003, "A Tabu Search Based Approach for Solving a Class of Bilevel Programming Problems in Chemical Engineering", *Journal of Heuristics*, Vol. 9, pp. 307-319.

155. Trincas, G., Zanic, V., & Grubisic, I. 1994, "Comprehensive Concept Design of Fast Ro-Ro Ships by Multi-Attribute Decision Making", in *Proc. IMDC '94, 5th International Marine Design Conference*, Delft, The Netherlands, pp. 403-418.

156. Horn, J. & Nafpliotis, N. 1993, *Multi-Objective Optimization using the Niched Pareto Genetic Algorithm*, IlliGAL Report No. 93005, Illinois Genetic Algorithms Laboratory, University of Illinois at Urbana-Champaign, Illinois, USA.

157. Hearn, G. E., Wright, P. N. H., & Hills, W. 1995, "Seakeeping for Design: Development and Application of an Inverse Analysis Design Methodology to Multihull Forms", in *Proc. International Conference on Seakeeping and Weather, 28 Feb - 1 Mar 1995*, RINA, London.

158. Nobukawa, H. & Zhou, G. 1996, "Discrete Optimization of Ship Structures with Genetic Algorithms", *Journal of the Society of Naval Architects Japan*, Vol. 179, pp. 293-301.

159. Subramani, D. & Sen, P. 1996, "Ship Subsivision using Genetic Algorithm", in *Proc. 2nd International Conference on Adaptive Computing in Engineering Design and Control '96*, Parmee, I. C., ed., Plymouth, UK, pp. 152-158.

160. Day, A. H. & Doctors, L. J. 1997, "Resistance Optimization of Displacement Vessels on the Basis of Principal Parameters", *Journal of Ship Research*, Vol. 41, No. 4, pp. 249-259.

161. Day, A. H. & Doctors, L. J. 1997, "Design of Fast Ships for Minimal Motions", in *Proc. 7th International Offshore and Polar Engineering Conference. Part 4 (of 4), 25-30 May 1997*, Honolulu, USA, pp. 677-683.

162. Hearn, G. E. & Wright, P. N. H. 1997, "Seakeeping for Design: Optimisation of Motion Responses and Wave Making Resistance of Catamarans via the Application of a Genetic Algorithm", in *Proc. FAST '97, 4th International Conference on Fast Sea Transportation, 21-23 Jul 1997, Vol.1*, Sydney, Australia, pp. 231-240.

163. Zhou, G., Nobukawa, H., & Yang, F. 1997, "Discrete Optimization of Cargo Ship with Large Hatch Opening by Genetic Algorithms", in *Proc. ICCAS '97, 9th International Conference on Computer Applications in Shipbuilding, 13-17 Oct 1997, Vol.1*, Yokohama, Japan, pp. 231-246.

164. Camponogara, E. & Talukdar, S. N. 1997, "A Genetic Algorithm for Constrained and Multiobjective Optimization", in *Proc. 3NWGA, 3rd Nordic Workshop on Genetic Algorithms and Their Applications, University of Vaasa*, Alander, J. T., ed., Vaasa, Finland, pp. 49-62.

165. Rhee, K.-P., Lee, S. Y., & Sung, Y. J. 1998, "Estimation of Manoeuvring Coefficients from PMM Test by Genetic Algorithm", in *Proc. MAN '98, International Symposium and Workshop on Forces Acting on a Manoeuvring Vessel, 16-18 Sep 1998*, Val de Reuil, France, pp. 77-87.

166. Liu, C. & Yao, Z. 1998, "Genetic Evaluative Algorithm is Used in Ship Preliminary Design", in *Proc. 2nd Conference for New Ship & Marine Technology into the 21st Century, 25-27 Jun 1998*, Hong Kong, pp. 226-233.

167. Hearn, G. E. & Wright, P. N. H. 1998, "Optimal Hull Form Design for Seakeeping and Resistance: a Genetic Algorithm Based Inverse Method", in *Proc. OC'98, 3rd Osaka Colloquium on Advanced CFD Applications to Ship Flow and Hull Form Design, 25-26 May 1998*, Osaka, Japan, pp. 499-514.

168. Birmingham, R. W. & Smith, T. A. G. 1998, "Automatic Hull Form Generation: A Practical Tool for Design and Research", in *Proc. PRADS '98, 7th International Symposium on Practical Design of Ships and Mobile Units, 20-25 Sep 1998*, The Hague, The Netherlands, pp. 281-288.

169. Scott, J. A., Todd, D. S., & Sen, P. 1998, "An Evolutionary Approach to the Scheduling of Ship Design and Production Processes", in *Proc. PRADS '98, 7th International Symposium on Practical Design of Ships and Mobile Units, 20-25 Sep 1998*, The Hague, The Netherlands, pp. 351-358.

170. Salcedo, J. 1999, *Selecting Optimum Parameter Values for Pareto-Genetic Optimization of Complex Systems,* Master of Science Thesis, Virginia Polytechnic, Blacksburg, Virginia, USA.

171. Karim, M. & Ikehata, M. 2000, "A Genetic Algorithm (GA) Based Optimisation Technique for the Design of Marine Propeller", in *Proc. Propellers/Shafting 2000 Symposium, 20-21 Sep 2000*, Virginia Beach, USA.

172. Yasukawa, H. 2000, "Ship Form Improvement using Genetic Algorithm", *Ship Technology Research*, Vol. 47, No. 1, pp. 35-44.

173. Day, A. H. & Doctors, L. J. 2000, "The Survival of the Fittest - Evolution Tools for Hydrodynamic Design of Ship Hull Form", *Transactions of the Royal Institution of Naval Architects*, Vol. 142, pp. 182-197.

174. Dejhalla, R., Mrsa, Z., & Vukovic, S. 2001, "Application of Genetic Algorithm for Ship Hull Form Optimisation", *International Shipbuilding Progress*, Vol. 48, No. 2, pp. 117-133.

175. Dejhalla, R., Vukovic, S., & Mrsa, Z. 2001, "Numerical Optimisation of the Ship Hull from a Hydrodynamic Standpoint", *Brodogradnja*, Vol. 49, No. 3, pp. 289-294.

176. Lee, K.-Y. & Roh, M.-I. 2001, "An Efficient Genetic Algorithm Using Gradient Information for Ship Structural Design Optimization", *Ship Technology Research*, Vol. 48, pp. 161-170.

177. Szelangiewicz, T. & Cepowski, T. 2002, "An Approach to Optimisation of Ship Design Parameters with Accounting for Seakeeping Ability", *Polish Maritime Research*, Vol. 9, No. 4, pp. 8-16.

178. Dejhalla, R., Mrsa, Z., & Vukovic, S. 2002, "A Genetic Algorithm Approach to the Problem of Minimum Ship Wave Resistance", *Marine Technology*, Vol. 39, No. 3, pp. 187-195.

179. Koushan, K. 2003, "Automatic Hull Form Optimisation Towards Lower Resistance and Wash using Artificial Intelligence", in *Proc. FAST 2003, 7th International Conference on Fast Sea Transportation, 7-10 Oct 2003*, Ischia, Italy.

180. Chen, S., Ando, J., & Nakatake, K. 2003, "Multi-objective Optimisation of Ship Hull Form for Wavemaking Resistance", *Trans Soc Naval Architects West Japan*, No. 106, pp. 191-200.

181. Giassi, A., Bennis, F., & Maisonneuve, J.-J. 2003, "Multi-objective Optimisation of Ship Hull with Distributed Applications", in *Proc. ASME Design Engineering Technical Conferences and Computers and Information in Engineering Conference, 2-6 Sep 2003, Vol.2A*, Chicago, USA, pp. 291-300.

182. Lowe, T. W. & Steel, J. 2003, "Conceptual Hull Design Using a Genetic Algorithm", *Journal of Ship Research*, Vol. 47, No. 3, pp. 222-236.

183. Gammon, M. A. & Alkan, A. 2003, "Initial Vessel Design by Evolutionary Optimisation", in *Proc. IMDC '03, 8th International Marine Design Conference, 5-8 May 2003, Vol.I*, Papanikolaou, A., ed., Athens, Greece, pp. 76-87.

184. Boulougouris, E. K. & Papanikolaou, A. 2004, "Optimisation of the Survivability of Naval Ships by Genetic Algorithms", in *Proc. COMPIT '04, 3rd International EuroConference on Computer Applications and Information Technology in Maritime Industries, 9-12 May 2004*, Siguenza, Spain, pp. 175-189.

185. Boulougouris, E. K., Papanikolaou, A., & Zaraphonitis, G. 2004, "Optimisation of Arrangements of Ro-Ro Passenger Ships with Genetic Algorithms", *Ship Technology Research*, Vol. 51, No. 3, pp. 99-105.

186. Pinto, A. & Campana, E. F. 2005, "A Multi-Swarm Algorithm for Multi-Objective Ship Design Problems", in *Proc. COMPIT'05, 4th International Conference on Computer and IT Applications in the Maritime Industries; 8-11 May 2005*, Hamburg, Germany, pp. 62-76.

187. Mason, A. & Couser, P. 2005, "Optimisation of Vessel Resistance Using Genetic Algorithms and Artificial Neural Networks", in *Proc. COMPIT'05, 4th International Conference on Computer and IT Applications in the Maritime Industries; 8-11 May 2005*, Hamburg, Germany, pp. 440-451.

188. Lowe, T. W. 2005, "Design of Partial Differential Equation Hull Surfaces Using Genetic Algorithms", *Ship Technology Research*, Vol. 52, No. 3, pp. 12-133.

189. Keane, A. J. 1996, "A Brief Comparison of Some Evolutionary Optimization Methods", in *Modern Heuristic Search Methods*, Rayward-Smith, V. et al., eds., John Wiley & Sons, Chichester, UK, pp. 255-272.

190. Jang, C. D. & Shin, S. H. 1997, "A Study on the Optimum Structure Design for Oil Tankers Using Multi-Objective Optimization", in *Proc. IMDC '97, 6th International Marine Design Conference, 23-25 Jun 1997, Vol.I*, Sen, P. & Birmingham, R. W., eds., Newcastle upon Tyne, UK, pp. 217-230.

191. Campana, E. F., Fasano, G., & Pinto, A. 2005, "Particle Swarm Optimization: Dynamic System Analysis for Parameter Selection in Global Optimization Frameworks", http://www.dis.uniroma1.it/~fasano/Cam_Fas_Pin_23_2005.pdf accessed on 14-11-2006.

192. Mouser, C. R. & Dunn, S. A. 2005, "Comparing Genetic Algorithms and Particle Swarm Optimisation for an Inverse Problem Exercise", http://anziamj.austms.org.au/V46/CTAC2004/Mous/Mous.pdf accessed on 14-11-2006.

193. Jones, K. O. 2005, "Comparison of Genetic Algorithm and Particle Swarm Optimisation", in *Proc. CompSysTech'05, International Conference on Computer Systems and Technologies, 16-17 Jun 2005*, Varna, Bulgaria.

194. Poloni, C., Fearon, M., & NG, D. 1996, "Parallelisation of Genetic Algorithm for Aerodynamic Design Optimisation", in *Proc. 2nd International Conference on Adaptive Computing in Engineering Design and Control '96*, Parmee, I. C., ed., Plymouth, UK, pp. 59-64.

195. Day, A. H., Doctors, L. J., & Armstrong, N. A. 1997, "Concept Evaluation for Large Very-high-speed Vessels", in *Proc. FAST '97, 4th International Conference on Fast Sea Transportation, 21-23 Jul 1997, Vol.1*, Sydney, Australia, pp. 65-84.

196. Peri, D., Campana, E. F., & Dattola, R. 2005, "Multidisciplinary Design Optimisation of a Frigate", *Ship Technology Research*, Vol. 52, No. 4, pp. 151-158.

197. Mitchell, M. & Forrest, S. 1994, "Genetic Algorithms and Artificial Life", *Artificial Life*, Vol. 1, No. 3, pp. 267-289.

198. Yang, B. S., Yeun, Y.-S., & Ruy, Y.-S. 2002, "Managing Approximation Models in Multiobjective Optimization", *Structural and Multidisciplinary Optimization*, Vol. 24, No. 2, pp. 141-156.

199. Sommersel, T. 1997, "Application of Genetic Algorithms in Practical Ship Design", in *Proc. IMDC '97, 6th International Marine Design Conference, 23-25 Jun 1997, Vol.I*, Sen, P. & Birmingham, R. W., eds., Newcastle upon Tyne, UK, pp. 611-626.

200. Boulougouris, E., Papanikolaou, A. D., & Mermiris, G. 2005, *LOGBASED Methodology Toolkit*, 6th Framework Programme, European Commission, FP6-1708-WP2-T2.1.

201. Peri, D. & Campana, E. 2005, "High-Fidelity Models and Multiobjective Global Optimization Algorithms in Simulation-based Design", *Journal of Ship Research*, Vol. 49, No. 3, pp. 159-175.

202. Peri, D. & Campana, E. 2005, "Global Optimisation for Safety and Comfort", in *Proc. COMPIT'05, 4th International Conference on Computer and IT Applications in the Maritime Industries; 8-11 May 2005*, Hamburg, Germany, pp. 477-486.

203. Fonseca, C. M. & Fleming, P. J. 1993, "Genetic Algorithms for Multiobjective Optimization: Formulation, Discussion and Generalization", in *Proc. 5th International Conference on Genetic Algorithms*, Urbana-Champaign, Illinois, USA, pp. 416-423.

204. Fonseca, C. M. & Fleming, P. J. 1995, "Multiobjective Genetic Algorithms Made Easy: Selection, Sharing and Mating Restriction", in *Proc. GALESIA, First International Conference on Genetic Algorithms in Engineering Systems: Innovations and Applications, 12-14 Sep 1995*, Sheffield, UK, pp. 45-52.

205. Horn, J., Nafpliotis, N., & Goldberg, D. E. 1994, "A Niched Pareto Genetic Algorithm for Multiobjective Optimization", in *Proc. 1st IEEE Conference on Evolutionary Computation, IEEE World Congress on Computational Intelligence, 27-29 Jun 1994, Vol.1*, Orlando, USA, pp. 82-87.

206. Parmee, I. C. 1996, "The Maintenance of Search Diversity for Effective Design Space Decomposition using Cluser-Oriented Genetic Algorithms (COGA) and Multi-Agent Strategies (GAANT)", in *Proc. 2nd International Conference on Adaptive Computing in Engineering Design and Control '96*, Parmee, I. C., ed., Plymouth, UK, pp. 128-138.

207. Grefenstette, J. J. 1986, "Optimization of Control Parameters for Genetic Algorithm", *IEEE Transactions on Systems, Man and Cybernetics*, Vol. 16, No. 1, pp. 122-128.

208. ESTECO 2003, "ModeFrontier", http://www.esteco.it/Products/modeFrontier/ accessed on 15-12-2005.

209. Engineous Software 2005, "iSIGHT", http://www.engineous.com/index.htm accessed on 15-12-2005.

210. Brown, A. J., Moon, W., & Louis, M. 2002, "Structural Design for Crashworthiness in Ship Collisions", *Transactions of the Society of Naval Architects and Marine Engineers*, Vol. 110, pp. 499-512.

211. The Mathworks Inc. 2005, "Genetic Algorithm and Direct Search Toolbox (Matlab)", www.mathworks.com accessed on 15-12-2005.

212. ADOPTECH 2005, "DARWIN", http://www.adoptech.com/software/Darwin.htm accessed on 15-12-2005.

213. Joines, J. 1996, "Genetic Algorithm Optimization Toolbox (GAOT)", http://www.daimi.au.dk/~pmn/Matlab/dochome/toolbox/GAOT/gaotindex.html accessed on 10-10-2005.

214. Tan, K. C., Lee, T. H., Khoo, D., & Khor, E. F. 2001, "A Multi-objective Evolutionary Algorithm Toolbox for Computer-aided Multi-objective Optimization", *IEEE Transactions on Systems, Man and Cybernetics: Part B (Cybernetics)*, Vol. 31, No. 4, pp. 537-556.

215. Popov, A. 2005, "Genetic Algorithms for Optimization - GAmin - toolbox for MATLAB", http://www.tu-harburg.de/~soap0883/#programs accessed on 10-10-2005.

216. GEATBx 2005, "GEATbx: Genetic and Evolutionary Algorithm Toolbox for use with Matlab", http://www.geatbx.com/ accessed on 26-11-2005.

217. Deb, K., Pratap, A., Agarwal, S., & Meyarivan, T. 2002, "A Fast and Elitist Multiobjective Genetic Algorithm: NSGA-II", *IEEE Transactions on Evolutionary Computation*, Vol. 6, No. 2, pp. 182-197.

218. Uniechowski, S. R. 1951, "Stability Curves for New Designs", *Journal of American Society of Naval Engineers*, Vol. 63, p. 311.

219. Inselberg, A. 1985, "The Plane with Parallel Coordinates", *The Visual Computer*, Vol. 1, pp. 69-91.

220. Wegman, E. J. 1990, "Hyperdimensional data analysis using parallel coordinates", *Journal of the American Statistical Association*, Vol. 85, No. 411, pp. 664-675.

221. Fleming, P. J., Purshouse, R. C., & Lygoe, R. J. 2005, "Many-Objective Optimization: An Engineering Design Perspective", in *Proc. EMO2005, Evolutionary Multi-Criterion Optimization, LNCS 3410*, Springer, Heidelberg, pp. 14-32.

Appendix A. WMTC 2006 Paper: A value focused approach to ship design synthesis, analysis, and selection

Originally presented at WMTC 2006, London, March 2006

S Maroju, S Syamsundar, M DeLorme
Stevens Institute of Technology, USA
S Vasudevan
University College London, UK
R Datla, M Pennotti, M Bruno
Stevens Institute of Technology, USA

SYNOPSIS

A novel ship-design strategy, involving an extended design space search and optimization using advanced techniques such as neural nets and genetic optimization is presented here. Integral to the process is the separation of customer requirements from the knowledge about existing designs or 'expert opinion' that prematurely restricts the design space before it is sufficiently explored. This is achieved through the coding of customer preferences using value functions and is used to obtain ordinal rankings for a population of ship designs whose performance is predicted by a neural net module. Finally, the population is iteratively optimized using genetic algorithms to reveal an optimal design in terms of the stated preferences. A limited model was built in MATLAB in order to demonstrate the concept and point to the future possibilities with this ongoing research.

INTRODUCTION

The design of a naval craft is driven by the customer requirements in terms of payload, speed, range and the desired acquisition and operational costs. These initial requirements may often be qualitative and inconsistent. The design is then realized by iterative refinement and adjustments to these requirements. However, the inherent subjectivity of requirements is not actively exploited by the design process since, even with the use of modern design tools and practices, this process produces a design that may not represent an optimal trade-off from among the set of feasible designs because, simple weighted measures of overall effectiveness may not accurately reflect the preferences of the customer. In order to ensure optimum design from the perspective of desired performance, value functions may be elicited from the customer in order to quantitatively model the underlying preferences and identify the acceptable trade-offs. This provides for the initial separation of the customer's preferences from expert 'opinions' which

---

Author Biographies: Soma Maroju is a Research Assistant and PhD. Candidate at Stevens Institute of Technology. His research, in addition to performance prediction using ANN's involves the analysis and prediction of vessel behaviors using both physical and numerical modeling. He has a Masters Degree in Computer Science from The University of North Carolina, Charlotte. **Srikanth Syamsundar** is pursuing an interdisciplinary PhD in Systems Engineering and Naval Architecture at Stevens Institute of Technology. His research interest includes requirements synthesis and application of decision theory in engineering design. He has a Masters Degree in Ocean Engineering from Stevens Institute of Technology. **Michael F. DeLorme** is a Research Engineer at the Davidson Laboratory at Stevens Institute of Technology. He is a PhD. Candidate at Stevens Institute of Technology. His research involves physical modeling and empirical analysis of vessel performance and behavior with an emphasis in small craft design and development. **Sojan Vasudevan** is a Naval Architect currently doing PhD at University College London investigating the application of innovative optimisation techniques in the design of hull forms for improved hydrodynamic performance. **Raju Datla** is a research associate professor at Stevens Institute of Technology, manages the experimental marine hydrodynamics research at the institute's Davidson Laboratory and teaches courses in naval architecture and ocean engineering. **Michael C. Pennotti**, Ph.D. is Industry Professor of Systems Engineering and Director of the SDOE Program at Stevens Institute of Technology. Prior to joining Stevens in 2001, Dr. Pennotti was a systems engineering leader at Bell Laboratories and held a number of executive positions at AT&T, Lucent Technologies and Avaya. **Michael S. Bruno** is Director of the Center for Maritime Systems and Professor of Ocean Engineering at Stevens Institute of Technology, Hoboken, New Jersey. His research and teaching interests include ocean observation systems, coastal ocean dynamics, maritime security, and estuary and ocean water quality.

tend to prematurely define the solution. This is equivalent to relaxing requirements with imposition of penalties and rewards so that, the preference for an attribute level may vary non-linearly with changes in attribute level. This enables a better representation of the customer's preferences that will effectively reduce the need to iteratively adjust requirements. The approach is demonstrated by means of analysis tools that are based on artificial neural networks (ANN) and a design tool based on genetic algorithm (GA) techniques developed by the authors. ANNs are found to be more effective than traditional simple regression methods and design curves at performance prediction. GA techniques are used for optimization and are found to be very effective at achieving near optimal solutions. The unique combination of multi-attribute value functions for defining the design objectives, ANNs for performance analysis, and GAs for optimization is useful in improving the ship design process through a wider, systematic exploration of design space, thereby promoting design innovation.

CONCEPT OVERVIEW

Requirements seek to guide the engineer in developing a solution to the extent that they specify the input/output for the system, desired performance, constraints, technology etc, at various levels of granularity[1]. Such requirements related to the hull subsystem design may specify for instance, displacement, range for a given speed, seakeeping characteristics, top speed, cost, etc. However, the urge to 'get on' with the design process often means that requirements are specified all too narrowly and the benefit associated with unexplored design space is lost. Adding complexity to this problem is the difficulty in finding a solution that satisfies the entire set of requirements. The normal development process involves iterative adjustments to design parameters leading to the possibility that the final solution may not be optimal in terms of the stakeholders' preferences. This paper proposes a strategy to overcome this difficulty by suitably relaxing the requirement space by imposition of penalties and rewards through constituent value functions that are independent of the solution space. This enables a true separation of the requirements driving the design from the design space consisting of feasible designs. This process entails coding of stakeholder preferences using value functions to rank different designs based on their performance measures. The performance measures for a specific combination of design parameters are predicted by means of an analysis module based on artificial neural nets. The ranking measure for each design is then used by optimization routine based on genetic algorithms to create/refine a population of designs. This process is illustrated in Fig.1.

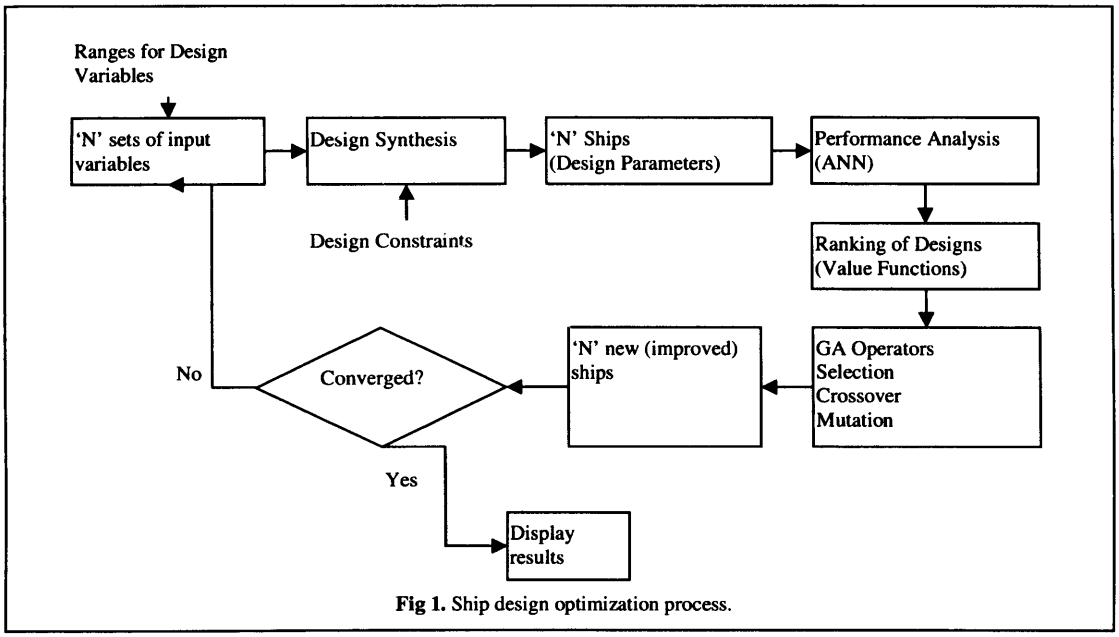

Fig 1. Ship design optimization process.

CODING OF REQUIREMENTS

There are many established methods for analytic decision making and the prominent among them include multi-attribute utility theory based methods[2-7], and Analytic hierarchy process (AHP)[8,9]. Though differences in solutions offered by different methods to the same problem might invoke skepticism, the number of real world applications of decision analysis demonstrates that analytic modeling support is

well worth the time and effort[1]. Lately there is evidence of approaches that combine both the methods where the value functions are used in conjunction with weights derived from AHP[10].
Specifically for our problem, we can use the additive utility model which has been applied to a wide variety of operations research problems. Though the use of additive utility models may not be completely justified, they are fairly easy to work with and are valid in cases where the preference for objectives are value independent of each other or only have weak dependence.
The additive model is given by Equation(1)

$$U(\bar{A}) = \sum_i w_i V_i(p_i) \tag{1}$$

where $V_i(p_i)$ is the value function over the ith level performance objective and w_i is the scaling factor associated with it. The value function is referred to as the utility function if it is influenced by uncertain events, which is not the case for the purpose of this paper. The scaling factors are normalized so that they sum to 1. For this paper, the exponential value function was used to model $V_i(p_i)$ given its effectiveness in modeling both linear and non-linear utility functions. Linear models are sufficient where the direction of preference takes precedence over how the preference varies over changing attribute levels. Linear models are equivalent to the overall measure of effectiveness (OMOE) when they are constructed as weighted sum of attributes. Non-linear models come into focus where sensitive design parameters such as top speed are involved, where small changes to a parameter can greatly affect overall perceived value of the design. In such cases, non-linear models may better represent stakeholder preferences over the range of the attribute level under consideration than simpler weighted sum measures. Furthermore, attribute range can be expanded with suitable imposition of penalties/rewards so as to ensure an expansive search of the design space. The exponential value function can emulate both linear and non-linear models by choosing an appropriate shape parameter ρ.The general form of the exponential value function[11] (for monotonically increasing values) is given by Equation (2)

$$V(x) = \frac{1 - e^{(-\mu(x - x^L)/\rho)}}{1 - e^{(-(x^H - x^L)/\rho)}} \tag{2}$$

For decreasing functions x^L is replaced by x^H in the numerator. Here, μ is the gradient parameter and is equal to 1 for an increasing function and -1 for a decreasing function, ρ is the shape parameter and x^L, x^H are the location parameters. ρ determines the convexity of the function so that function is concave for positive ρ and vice-versa. The function becomes linear as $\rho \to \pm\infty$. Given the versatility of the exponential value function, it can be used to model preferences for speed, seakeeping components, drag, displacement etc . The exact values for the shape and location parameters can be determined by fitting the exponential value function to responses obtained from the elicitation process. For further details the reader is referred to Keeney and Kirkwood[3, 11, 12]. Once the value functions are determined, they can then be used to generate a fitness score $U(A)$, for each design, provided that performance measures pertaining to each design is available. This is achieved by the analysis module based on neural nets and is described in the following section.

NEURAL NET BASED PERFORMANCE PREDICTION

Artificial Neural Networks (ANN) can be effectively used to predict the performance of planing hulls, provided sufficient examples of the behavior that is intended to be captured exist. ANNs have found extensive applications in the marine industry in general, and in ship design specifically. For example, Ray et.al.[13], suggested application of ANNs with examples that included the prediction of the container capacity of a ship. Bertram and Mesbahi[14] derived formulae for resistance and power prediction for fast semi-displacement monohulls using ANNs. Koushan[15] utilized ANNs for automatic optimization of hull lines to reduce the ship resistance. Inzunza et. al.[16] presented an empirical formula for viscous roll damping of ships.

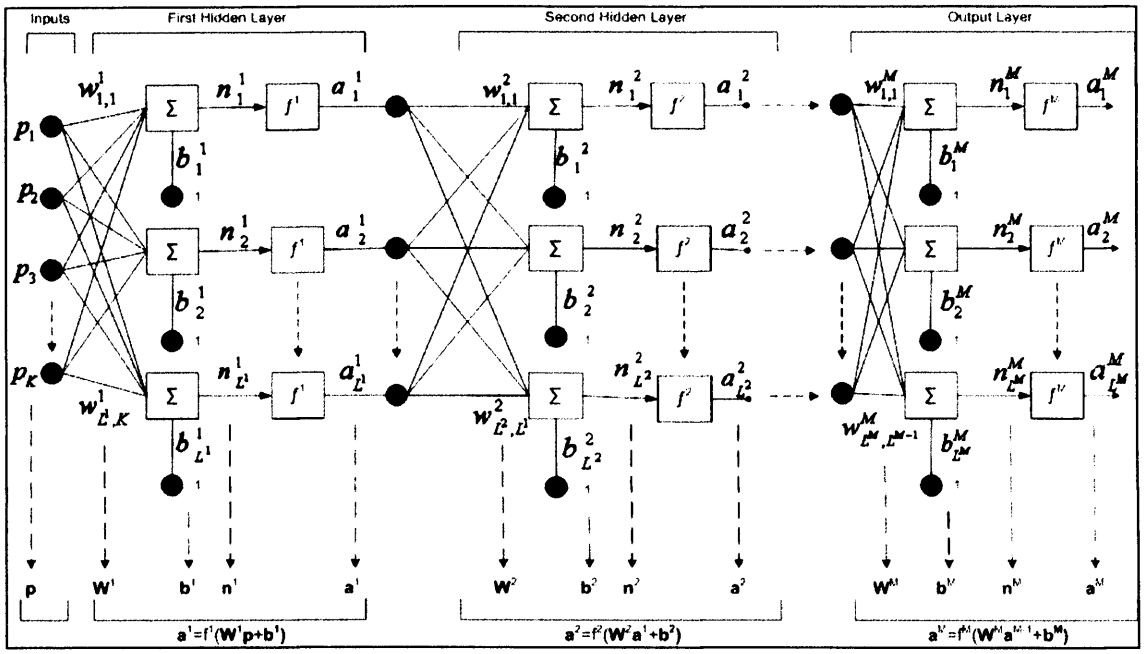

Fig.2 Neural Network architecture

An Artificial Neural Network (ANN) is a system (Fig.2) composed of many simple processing elements operating in parallel which can acquire, store and utilize experiential knowledge. Therefore, the ANN needs examples of proper behavior - examples of inputs and their respective outputs. The processing ability of the network is stored in the inter unit connection strengths, or weights. These weights and biases are continually adjusted over several iterations until the output error converges to a global minimum. This process is achieved by minimizing the network performance function i.e., the ANN output and the target output. ANNs can thus extract any regularities or patterns that may exist and can be used to predict the outputs of a new set of inputs.

Neural Networks

The choice of network, algorithm, transfer functions, number of layers and number of neurons depend on the type of problem that is to be solved. A multilayer perceptron network can be used as a universal function approximator[17]. It has been shown[17] that a multilayer network of two or more layers with enough neurons and nonlinear transfer functions will allow the network to learn nonlinear and linear relationships between input and output vectors. For ANNs in general larger networks tend to over fit, while smaller networks are inadequate to provide a proper fit of the data. The network that gives the closest output to the target or the lowest performance index, determined through experimentation, should be selected.

For the current research the Levenberg-Marquardt (LM) algorithm, which is an approximate steepest descent algorithm that minimizes squared error (performance index), was chosen. The LM has the advantage that the network solution will not be trapped at a local minima[17]; it is possible to get the correct weights for the optimum solution without reinitializing the network and retraining several times. The optimum number of layers and the number of neurons was determined by experimentation.

GENETIC OPTIMIZATION

Genetic Algorithms (General Description/advantages/disadvantages)

Genetic Algorithms (GA) are search and optimization techniques based on natural evolution. They are increasingly being used in a wide variety of applications in engineering design. They work on a large population of designs and iteratively modify the population using genetic operators. As iterations progress, the fitness of the population in terms of the design objective improves, eventually leading to optimal solutions.

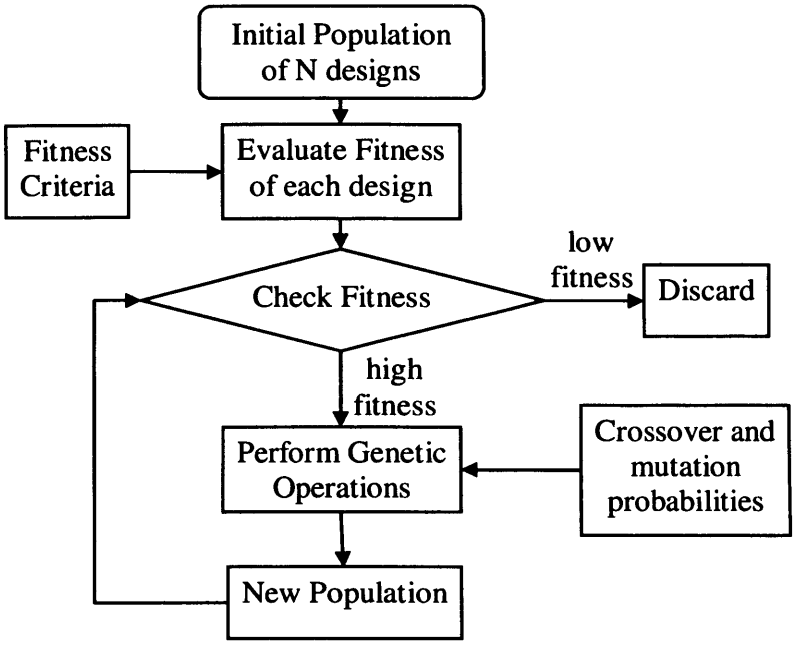

Fig 3. Schematic of a genetic algorithm based optimization

Genetic algorithms offer a number of advantages over traditional methods used in engineering optimization. They perform well in multimodal search spaces with multiple local optima. They do not require computationally expensive derivative information during the optimization process. They can also be hybridized with traditional search techniques to give any desired balance between local and global optimization. However, GAs have some disadvantages. Globally optimal solutions cannot be guaranteed, though a near-optimal solution with high accuracy can be ensured. Most GA applications need a lot of computational time even with parallel processing.

GA Applications in Ship Design

Several researchers have applied GA-based optimization techniques in ship design. Some of them have used a single objective for optimization. For hydrodynamic optimization, this is generally wave resistance [18-20]. In other cases this may be construction cost [21], weight [22], payload weight fraction [23]etc. Some authors consider multiple objectives, but combine them to form a single objective called Overall Measure of Effectiveness (OMOE) using weighted sum techniques [10, 24-33]. This greatly simplifies the problem, with no complexity of multiobjective optimization. Preferences among objectives are to be given by the decision maker before starting the optimization process. True multi-objective optimization considers all objectives simultaneously [34-39]. The decision makers need not give a priori preferences among objectives. After the optimization, they are presented with a number of optimal solutions of equal merit.

THE PRESENT STUDY

Most of the studies so far have used GA for demonstrating its use in optimization. They have not been tailored to the need of a ship designer and are not directly useful in the design office. The present study is focused towards this need. Further enhancements such as decision modeling under uncertainty using influence diagrams [40], when integrated with the current model, will enable optimization when the design parameters are best modeled as probabilistic variables. Examples of such variables could be for instance - displacement of a naval ship, which is expected to vary as the ship is upgraded and refitted with various subsystems over its lifecycle.

The present study vs. current ship design tools

Currently there are no optimization tools accepted by commercial ship designers. The proposed tool is tailored towards use in a design office, and has the potential to be the industry standard when fully developed. A design synthesis procedure can be built within the GA-based optimization program. One of the drawbacks of GA-based optimization programs is that they need to have reliable analysis routines that are generally computationally expensive considering the large number of iterations involved. The present tool proposes to use ANN for analysis, which will be considerably faster after the network is fully trained.

The proposed tool is tailored towards modification to true multi-objective optimization. This will enhance designer-customer interaction by presenting the customer with a wide variety of choices and corresponding cost/performance implications. This is advantageous compared to the present design tools that allow the designer to present only a few alternatives to the customer at a time.

DEMONSTRATION OF CONCEPT

In order to demonstrate the working of the concept, a limited model was built using MATLAB software with the objective of choosing the optimal hull form parameters. MATLAB was used to construct the value functions, neural nets and finally to optimize the design space in terms of the coded values and the predicted responses. The primary trade-off space consisted of resistances at top speed and cruise speed. The design space was limited to planing monohulls for the purpose of demonstration. It was assumed that ship would have a displacement of around 95000 lbs. Additionally, it was assumed that the uncertainty related to the development of the concept made it preferable to have greater displacement capability. It was also decided that the ship would have a cruise speed of 20 knots and a top speed of 50 knots. The value functions for resistance at cruise speed and top speed was constructed in part by examining the resistance values for existing designs. This permitted determination of the location parameters for the value function. Similarly the bounds for displacement were set as 70000 lbs and 120000 lbs to ensure the design space was sufficiently expansive.

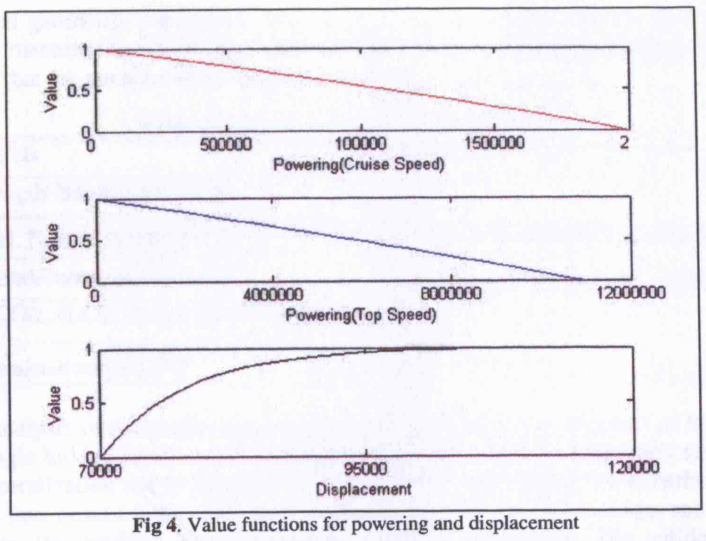

Fig 4. Value functions for powering and displacement

The value functions for powering at cruise speed and the top speed were modeled as linear functions by choosing large values for ρ. The preference function for displacement was fitted by having a large penalty for falling below 95000 lbs. The exact value for ρ was calculated by assuming $V_{dis}(95000) = 0.96$. The value functions are depicted graphically in Fig 4. The swing weights were calculated as 0.4, 0.5 and 0.1 for resistance (cruise & top speed) and displacement respectively using the balance beam method[1].

Data for training artificial neural nets

Data for the current research is derived from ACCeSS database[41], a comprehensive electronic database of experimental model tests conducted at the Davidson Laboratory, Series-62 (Naval Ship Research and Development Center) and SNAME Small Craft Data Sheets (The Society of Naval Architects and Marine Engineers, NY).

A brief description of the procedure adopted to estimate the resistance for a planing hull is presented. The tasks involved can be outlined in the following manner

1. Select the inputs that would be critical in predicting the output
2. Data cleaning and manipulation
3. Identifying suitable neural network architecture.
4. Training, validation and prediction

Inputs and desired outputs

This paper restricts itself to predicting the resistance of planing hulls. Conclusions drawn from Hubble[42] suggest that resistance characteristics of any planing hull are a function of speed, load displacement, longitudinal center of gravity and the absolute size of the hull which can be related to projected length and beam. Once the variables involved were identified, data were gathered and cleaned while ensuring that no significant gaps remained in the dataset

Table I. Distribution of data from each source.

Source	Reports/Hulls	No. of Examples for training
Davidson Laboratory	47 Reports	2250
Series 62	6 Hulls	1030
SNAME Small Craft report	11 Hulls	157
Series 65 (Only considered for early prediction)	4 Hulls	100

Since the individual geometric parameters, test conditions and resultant data do not lend themselves to direct comparison, meaningful non-dimensional coefficients were considered instead. Table II shows the inputs and outputs that are considered as most useful for the current research.

Table II. Inputs to and outputs from the neural nets

Inputs	Outputs
Length-Beam ratio (L/B)	Resistance-Weight ratio (R/Δ)
Vol. Froude Number ($F_{n\nabla}$)	
Slenderness ratio ($L/\Delta^{1/3}$)	
LCG/L (LCG measured from transom)	
Deadrise angle (β)	

After systematic analysis of the performance of networks with different number of layers and neurons, a network with a single hidden layer and 29 neurons was chosen. A method for early stopping was adopted to improve the generalization and to prevent the network from over fitting. This method involves dividing the available data into three subsets namely- training set, validation set and test set. The training set is used for computing the gradient and updating the weights and biases. The validation set is used to monitor the error during the training process. The test set error is used to compare different models and is not used during the training. The trained neural network was tested on several hull forms. The results of resistance –weight ratios over a range of Froude numbers from Neural Networks at different L-B ratios and slenderness ratios were compared to those of the experimental results. (Fig 5).

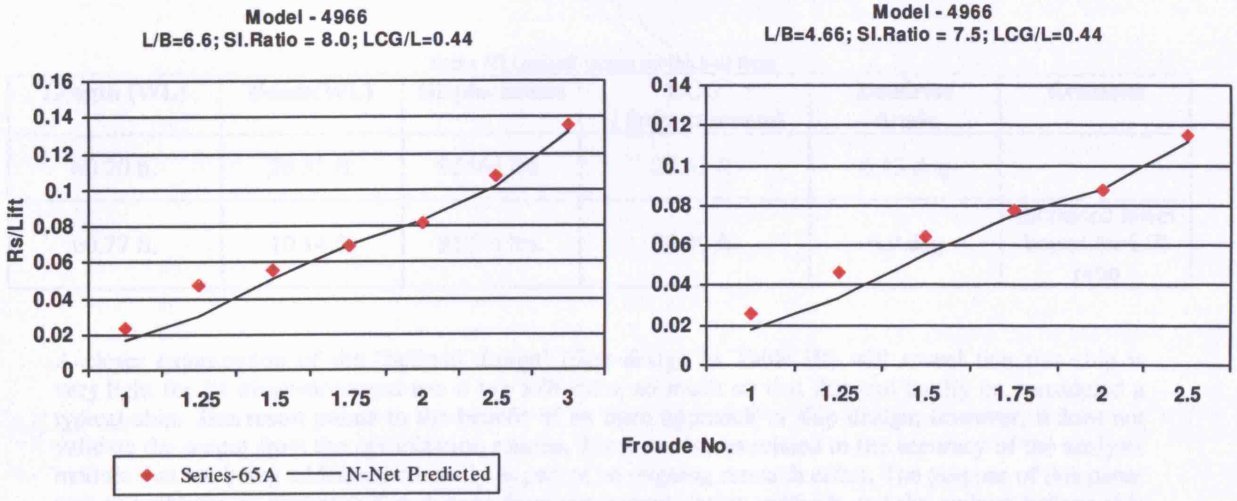

Fig.5 Series-65: Resistance-Weight ratio with respect to; $F_{n\nabla}$

Once the neural net was sufficiently trained, it was integrated with the value function module. This enabled the execution of the genetic optimization algorithm. The Results are discussed below

RESULTS

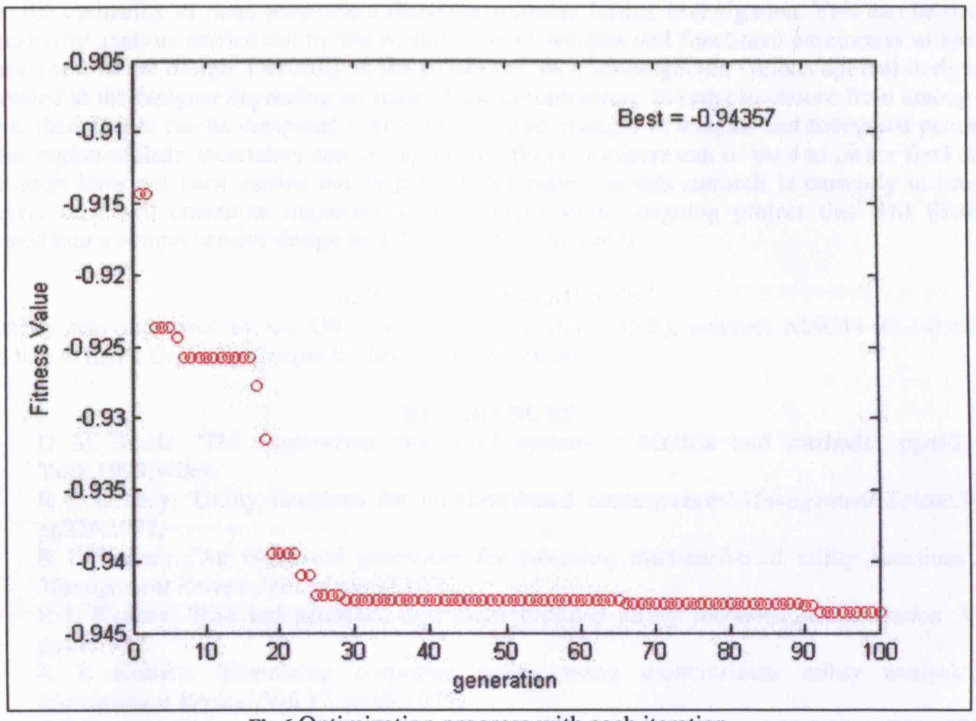

Fig 6 Optimization progress with each iteration

The optimization was carried out in MATLAB using genetic algorithms. Results of a sample GA run are shown in Fig.6 showing improvement in fitness as generations progress. Multiple GA runs seemed to produce slightly different optimal ships in terms of design variables (Length, Beam, Displacement, LCG, Deadrise) though their fitness values were comparable, indicating that further research is needed to validate the GA results. Besides, sensitivity studies need to be carried out for the GA parameters (population size, number of generations, probabilities of crossover and mutation etc). A design synthesis module also needs to be incorporated to ensure that the optimum ship found by the GA module satisfies the payload and other requirements as well as stability and other constraints. A typical output from the optimization module is presented in Table III.

Table III Optimal values for the hull form

Length (WL)	Beam(WL)	Displacement	LCG (from transom)	Deadrise Angle	Remarks
60.20 ft.	28.55 ft.	95464 lbs.	23.63 ft.	6.13 deg	
60.77 ft.	10.14 ft.	95724 lbs.	30.80 ft.	6.0 deg	Increased lower bound for L/B ratio

A closer examination of the 'optimal design' (first design in Table III) will reveal that this ship is very light for its dimensions and has a low L/B ratio, so much so that this can hardly be considered a typical ship. This result points to the benefit of an open approach to ship design; however, it does not validate the output from the optimization routine. There are issues related to the accuracy of the analysis module that are being addressed currently as part of an ongoing research effort. The purpose of this paper was to highlight an approach that departs from the current design methods and the authors believe that

this goal has been achieved. In comparison, constraining the design space by having a lower bound of 4 for the L/B ratio resulted in a more 'conventional' ship as seen in Table III (second design). The performance prediction for this design was validated by comparing to existing designs in the database[41].

Additionally, the fitness values associated with each design are sensitive to the weights and the parameters of the value function. As the weights and function parameters are themselves subjective in nature, the optimality of these parameters therefore warrants further investigation. This can be resolved via sensitivity analysis carried out by the perturbation of weights and functional parameters to ascertain the robustness of the design. Normally in the process of such investigation, various optimal designs will be revealed to the designer depending on scale of the perturbations. In order to choose from among these designs, their fitness can be compared over evenly spaced changes to weights and functional parameters over the region of their uncertainty and an aggregated fitness measure can be used to pick a final design. These steps have not been carried out as part of this paper, as this research is currently in progress. However, they will constitute important improvements to an ongoing project that will finally be integrated into a comprehensive design tool developed by ACCeSS.

ACKNOWLEDGEMENTS

This study was supported by US Office of Naval Research (ONR), contract N00014-03-1-0160. We would like to thank Dr. Kelly Cooper for her continued support.

REFERENCES

1. D M Buede. 'The engineering design of systems : Models and methods', pp462, New York,1999,Wiley.
2. R L Keeney. 'Utility functions for multiattributed consequences',*Management Scienc,*Vol.18, pp276,1972,
3. R L Keeney. 'An illustrated procedure for assessing multiattributed utility functions',*Sloan Management Review* ,Vol.14, pp37,1972,
4. R L Keeney. 'Risk independence and multiattributed utility functions',*Econometrica* ,Vol.41, pp27,1973,
5. R L Keeney. 'Examining corporate policy using multiattribute utility analysis',*Sloan Management Review* ,Vol.17, pp63,1975,
6. R L Keeney. 'Using values in operations research',*Operations Research,*Vol.42, pp793,1994,
7. R L Keeney. 'Creativity in decision making with value-focused thinking',*Sloan Management Review,*Vol.35, pp33,1994,
8. E H Forman and S I Gass. 'The analytic hierarchy process - an exposition',*Operations Research,*Vol.49, pp469,2001,
9. Saaty and T L. 'How to make a decision: The analytic hierarchy process',*European Journal of Operational Research,*Vol.48, pp9,1990,
10. A Brown and T Mierzwicki. 'Risk metric for multi-objective design of naval ships',*Nav.Eng.J.,* pp55-71,2004,
11. C W Kirkwood. 'Strategic decision making : Multiobjective decision analysis with spreadsheets', pp345, Belmont,1997,Duxbury Press.
12. R L Keeney, v Winterfeldt, Detlof, Eppel and Thomas. 'Eliciting public values for complex policy decisions',*Management Science,*Vol.36, pp1011,1990,
13. T Ray, R P Gokarn and O P Sha. 'Neural network applications in naval architecture and marine engineering',*Artificial Intelligence in Engineering,*Vol.1, pp213-226,1996,
14. F Bertram and E Mesbahi. 'Simple design formulae for fast monohulls',*Ship Technology Research,*Vol.51, pp146-148,2004,
15. K Koushan. 'Automatic hull form optimization towards lower resistance and wash using artificial intelligence',*FAST,*Vol.7,2003,FAST.
16. M S Inzunza, E Mesbahi, K E Brink and V Bertram. 'Empirical roll damping formula derived by artificial neural network applications',*Jahrbuch Der Schiffbautechnischen Gesellschaft,*2001,Springer.
17. M T Hagan, H B Demuth and M H Beale. 'Neural network design', Boston,1996,PWS Pub.
18. R Dejhalla, Z Mrsa and S Vukovic. 'A genetic algorithm approach to the problem of minimum ship wave resistance',*Marine Technology,*Vol.39, pp187-195,2002,
19. L J Doctors, A H Day and S Node. 'Hydrodynamically optimal hull forms for river ferries',1995, Intl Symposium on High Speed Vessels for Transport and Defence; 23 & 24 Nov 1995; London, UK. Procs. Publ by RINA, London, UK. Ppr 5

20. M A Gammon and A Alkan. 'Initial vessel design by evolutionary optimisation', pp77-87,2003, IMDC '03, 8th Intl Marine Design Conf; 5-8 May 2003; Athens, Greece. Proceedings. Vol I
21. G Zhou, H Nobukawa and F Yang. 'Discrete optimization of cargo ship with large hatch opening by genetic algorithms', pp231-246,1997, ICCAS `97, 9th Intl Conf on Computer Applications in Shipbuilding; 13-17 Oct 1997; Yokohama, Japan, Vol 1
22. K Lee and M Roh. 'An efficient genetic algorithm using gradient information for ship structural design optimization',*Ship Technol Res,*Vol.48, pp161-170,2001,
23. S Shahak. 'Naval ship concept design: An evolutionary approach',1998,Master's Thesis, Department of Ocean Engineering, Massachusetts Institute of Technology.
24. A Brown and M Thomas. 'Reengineering the naval ship concept design process',1998, From Research to Reality in Ship Systems Engineering Symposium, ASNE, September 1998
25. A Brown and J Salcedo. 'Multiple-objective optimization in naval ship design',*Nav.Eng.J.,* pp49-61,2003,
26. R W Birmingham and T A G Smith. 'Automatic hull form generation: A practical tool for design and research', pp281-288,1998,Elsevier Science B.V., Proc. of 7th Intl Symposium on Practical Design of Ships and Mobile Units (PRADS 98); 20-25 Sept 1998; The Hague, The Netherlands.
27. G Zaraphonitis, A Papanikolaou and D Mourkoyannis. 'Hull-form optimisation of high speed vessels with respect to wash and powering', pp43-54,2003, IMDC `03, 8th Intl Marine Design Conf; 5-8 May 2003; Athens, Greece., Proceedings. Vol II
28. K Lee, S Han and M Roh. 'Optimal compartment layout design for a naval ship using an improved genetic algorithm',*Marine Technology,*Vol.39, pp159-169,2002,
29. G E Hearn and P N H Wright. 'Seakeeping for design: Optimisation of motion responses and wave making resistance of catamarans via the application of a genetic algorithm', pp231-240,1997, Fast `97, 4th Intl Conf on Fast Sea Transportation, 21-23 July, 1997; Sydney, Australia. Vol 1
30. R Wolf, J Dickmann and R Boas. 'Ship design using heuristic optimization methods',2004, http://www.twocw.net/mit/NR/rdonlyres/Aeronautics-and-Astronautics/16-888Spring-2004/BADEDA1F-754C-463A-B77E-80C116A21D28/0/finrep_wofdickbos.pdf
31. S N Neti. 'Ship design optimization using ASSET',2005,Master's Thesis, Ocean Engineering, Virginia Polytechnic.
32. A H Day and L J Doctors. 'Design of fast ships for minimal resistance and motions', pp569-583,1997, IMDC '97, 6th Intl Marine Design Conf; 23-25 June 1997, Newcastle upon Tyne, U.K. Vol I
33. A H Day, L J Doctors and N A Armstrong. 'Concept evaluation for large very-high-speed vessels', pp65-84,1997, Fast '97, 4th Intl Conf on Fast Sea Transportation, 21-23 July, 1997; Sydney, Australia. Vol 1
34. D Peri and E F Campana. 'Multidisciplinary design optimization of a naval combatant',*J.Ship Res.,*Vol.47, pp1-12, 1,2003,
35. D Todd. 'Multiple criteria genetic algorithms in engineering design and operation',1997,Doctoral Thesis, Department of Marine Technology, University of Newcastle, U.K.
36. A I Olcer, C Tuzcu and O Turan. 'Internal hull subdivision optimisation of ro-ro vessels in multiple criteria decision making environment', pp339-351,2003, IMDC `03, 8th Intl Marine Design Conf; 5-8 May 2003; Athens, Greece. Proceedings. Vol I
37. G Zaraphonitis, E Boulougouris and A Papanikolaou. 'An integrated optimization procedure for the design of ro-ro passenger ships of enhanced safety and efficiency', pp313-324,2003, IMDC `03, 8th Intl Marine Design Conf; 5-8 May 2003; Athens, Greece. Proceedings. Vol I
38. E Boulougouris and A Papanikolaou. 'Optimisation of naval ships with genetic algorithms for enhanced survivability', pp727-740,2003, IMDC `03, 8th Intl Marine Design Conf; 5-8 May 2003; Athens, Greece. Proceedings. Vol II
39. K W Hutchison and P Sen. 'Multiple criteria design optimisation of ro-ro passenger ferries with consideration of recently proposed probabilistic stability standards', pp303-312,1998, PRADS 98, 7th Intl Symposium on Practical Design of Ships and Mobile Units; 20-25 Sept 1998; The Hague, The Netherlands.
40. J.a Tatman, Shachter and R.D. 'Dynamic programming and influence diagrams',*Systems, Man and Cybernetics, IEEE Transactions on,*Vol.20, pp365-379,1990,
41. S Maroju, M DeLorme, R Datla and M Bruno. 'ACCeSS ship design database',.2002, Hoboken,NJ,2005, http://access.dl.stevens-tech.edu/access, The Atlantic Center for the Innovative Design and Control of Small ships. Stevens Institute of Technology.

42. N E Hubble. 'Resistance of hard-chine, stepless planing craft with systematic variation of hull form, longitudinal center of gravity, and loading',Vol.TR 4307, Bethesda, MD,1974,Naval Ship Research and Development Centre.

Appendix B. Chronological literature review - optimisation in ship design (using traditional algorithms)

This appendix discusses the literature on ship design optimisation using traditional gradient-based and direct search algorithms (non-heuristic techniques).

1. Mandel, P. & Leopold, R. 1966 [82]

   This is a seminal paper on optimisation in ship design. A convergent random search technique is used in conjunction with a weighted multi-parameter objective function. The technique is demonstrated for a cargo ship optimisation problem. The objective function is a weighted sum of cost, payload weight requirement and payload volume requirement. Weights, volumes, freeboard, stability, costs, power etc are estimated using empirical equations. Considering that this is one of the first attempts on ship design optimisation, the treatment has been quite elaborate. However, the objective function necessarily is rather simplistic.

2. Moe, J. & Lund, S. 1968 [83]

   Optimisation of the midship section of tankers with the objective of cost minimisation satisfying longitudinal strength constraints based on classification society rules. Non-linear programming using direct search and sequential unconstrained minimisation technique is used. The authors acknowledge the possibility of local optima, but claim that this has not caused trouble in practical applications to structural problems. Even if several optima exist, it is suggested that the process can be repeated from several starting points to locate the global optimum. Another difficulty is that the design variables are to be continuous for applying the optimisation techniques used, whereas in practice there are a number of variables with discrete integer values (number of stiffeners, plate thicknesses etc). Also the designs are at constant displacement, rather than constant payload weight or volume.

3. Nowacki, H., Brusis, F., & Swift, P. M. 1970 [84]

   The preliminary design of tankers has been treated as a constrained optimisation problem. Two optimisation techniques have been demonstrated – an adaptive direct search and sequential unconstrained minimisation technique. The required freight rate is used as the measure of merit. Empirical formulations are used in the design model, along with constraints on dimensional ratios and stability. As seen in the earlier papers, the major limitations are the use of single objective and the possibility of local optima.

4. Keane, A. J., Price, W. G., & Schachter, R. D. 1991 [24]

   Keane describes a computer-based modular concept design system using optimisation techniques. A single objective optimisation has been attempted, with constraints imposed for stability, L/D ratio, minimum enclosed volume etc. Various optimisation techniques have been explored, including gradient-based as well as direct search methods. The system is demonstrated for a simple frigate design problem. The main achievement is that the synthesis process could be automated (though for constant displacement, rather than constant payload), in addition to analysis of competing designs. The choice of a single objective function for optimisation seems to be a major limitation, even though it has been suggested that weighted sum of various objectives is possible.

5. Ray, T. & Sha, O. P. 1994 [86]

   Ray and Sha discuss a nonlinear optimisation tool with multiple objectives combined into a single measure of merit using multi-attribute decision making methods (MADM). Simple estimation tools are used for stability, weight, power, cost etc. A decision system using MADM is used to identify the weightings for various objectives based on their relative importance. This allows the use of incommensurate objectives and subjective constraints. However, the optimisation tools used is not capable of ensuring the global optimum; hence without a good initial guess, the result may be a local optimum.

6. Whitfield, R. I., Duffy, A. H. B., Wu, Z., & Meehan, J. 2001 [141]

   This demonstrates the application of the theory of Design of Experiments (DOE) to enable the design space to be explored efficiently. The DOE stage produces response surfaces that can be used by the optimisation module to search the design space. A catamaran design with seakeeping parameters forming the response surfaces is illustrated. In the present research, it is proposed to demonstrate the use of artificial neural networks for performance analyses. Effectively, ANNs create response surfaces similar to those mentioned in this paper.

7. Percival, S., Hendrix, D., & Noblesse, F. 2001 [142]

   Optimisation of total resistance with constant displacement and waterplane moment of inertia is attempted. A simple CFD tool based on slender-ship approximation is used for wave resistance calculation, which can rank different hulls accurately though the absolute values of wave resistance may not be very accurate. The simplicity of the tool makes it relatively fast compared to other CFD methods. Optimisation of a Wigley hull is demonstrated with hull definition using NURBS surfaces, though it is not clear how or on what basis the modifications are carried out. Also, the optimisation is based solely on underwater volume identity, thus neglecting practical design issues.

8. CCDoTT 2003 [143,144]

   A method based on artificial neural networks is developed for hydrodynamic shape optimisation with the objective of minimising drag and maximising lift-to-drag ratios. All that is done is to replace the CFD tool with an ANN tool to reduce computational time. The optimisation is managed using the commercial software iSIGHT.

9. Marzi, J. 2003 [145]

   A hull form optimisation environment in an automated scheme including form modification, analysis and optimisation is developed at HSVA, Haslar. NAPA is

used to define hull geometry and generate the panel mesh. A non-linear free surface potential flow code and a RANSE viscous flow code are used for analysis. Hull modifications are carried out using an in-house tool which has various modification functions like global parameters B/T, local modification of bulb etc. The commercial software modeFrontier is used for optimisation. An example is given which minimises the wave resistance. The methodology shows good potential, though in the present form there is no design synthesis module and the optimisation consists of a single objective only.

10. Grigoropoulos, G. J. 2004 [146]

Constrained optimisation of seakeeping qualities (weighted sum) is carried out on a parent ship by variations in Cw, C_B, C_P, LCF, LCB and KB. The optimised ship is then locally refined to achieve minimum resistance, without considerably worsening the seakeeping characteristics achieved. The Hooke and Jeeve's algorithm is used for optimisation. Strip theory is used for seakeeping analysis and the wave resistance is calculated using a CFD tool (SHIPFLOW). The optimisation is done keeping the displacement constant, thus disregarding the deadweight and other design requirements.

Appendix C. Multi-objective optimisation techniques

Several methods are available for multi-objective optimisation (MOO) especially suited to engineering applications. These methods are briefly discussed here. The most promising among these methods is identified as genetic algorithms, which is implemented in the current thesis.

Traditional methods for optimisation are based on pattern search or gradient methods. Hooke & Jeeve's [147] and Powell's direction set [148] are well-known examples of pattern search methods. Such methods have a high probability of getting trapped in local optima unless the starting point is located near the global optimum. Fletcher-Reeves' conjugate approach [149] is an example of gradient methods. Gradient methods require derivative information for each point in the search space. Moreover, numerical evaluation of partial derivatives of the objective with respect to each design variable can be very time consuming. These characteristics of the traditional optimisation techniques make them unattractive especially in the case of MOO.

Several heuristic methods for optimisation have been developed in recent years. These methods are useful to solve problems that were difficult or impossible to solve previously using traditional methods. The majority of these techniques are based on analogy with natural evolution and are collectively known as 'Evolutionary Algorithms' (EA). Veldhuizen [114] examines the history of EA and its use in multi-objective optimisation. Other popular heuristic optimisation methods include Particle Swarm Optimisation (PSO), Simulated Annealing (SA), Tabu Search (TS) etc. Such methods have been demonstrated to be better than traditional methods in many respects. For example, Hirata [140] compares a gradient-based method with genetic algorithms (which is a type of EA) for minimising total resistance of ships. It is found that the gradient-based method frequently gets trapped in local optima whereas genetic algorithms easily locate the global optima. Besides, the computational times taken by both methods are found to be similar, indicating that genetic algorithms are superior to gradient-based methods.

The popular heuristic methods are briefly described in the following sections.

C.1. Evolutionary algorithms (EA)

There are mainly four methods that fall under the umbrella of EA. They are:

- Genetic Algorithms (GA) [112,113,129,150]
- Evolution Strategies (ES) [112,113,129]
- Genetic Programming (GP) [112,113,129]
- Evolutionary Programming (EP) [112,113,129]

These techniques are similar to one another in principle, but differ in details of their implementation. The common underlying idea is that the environmental pressure on a population of individuals causes natural selection ('survival of the fittest') causing an increase in fitness of the population with time. The evolution is characterised by genetic operators such as selection, crossover and mutation. An overview of the range of engineering applications using EA can be found in [151].

Genetic Algorithms are the most popular type of Evolutionary Algorithms. The main genetic operator used is crossover, in addition to selection and mutation. Traditionally, the variables in the problem are represented as strings of binary numbers, in combination with bit-exchange crossover, bit-flip mutation, and roulette-wheel selection. Modern GAs are much more versatile – they can use binary / integer / real variables in combination with a wide variety of genetic operators. Traditional GAs are ideal to tackle combinatorial optimisation problems such as timetabling and scheduling problems. Modern GAs have been found useful in engineering fields to solve global optimisation problems. They are especially useful in problem domains that have a complex fitness landscape, where traditional hill climbing algorithms usually get stuck in local optima.

Evolution strategies are based on ideas of adaptation and evolution. Traditionally, it relied on real-vector coding, mutation as the search operator, and a population size

of one. Modern ES uses mutation, crossover, and selection as genetic operators. Mutation is performed by adding a Gaussian distributed random value. The mutation rate is often self-adaptive such that larger mutation at the start of the optimisation allows wider search of the design space, and lower mutation towards the end of the optimisation allows exploitation of the optimal region. Modern ES and GA are similar in many ways; however, they do differ in the reproduction mechanisms, and the size of the parents and offspring.

Evolutionary Programming is similar to ES though the two were developed independently. Traditional EP was concerned with machine learning tasks. Variable representation and operators were specialised for this application. EP never uses any crossover; mutation is the primary operator. Both EP and ES use self-adaptation of Gaussian mutation in the case of real-valued variables.

Genetic Programming is a similar technique, in which computer programs, instead of function parameters, are optimised. GP uses tree-based internal data structures to represent the computer programs for adaptation instead of the 'string' structures typical of GAs. GP typically requires running time that is orders of magnitude greater than that for GAs, but they may be suitable for problems that are intractable with genetic algorithms. They are useful for creating commercially usable new inventions in areas such as quantum computing, electronic design and game playing.

C.2. Particle swarm optimisation (PSO)

Particle swarm optimisation has been developed based on social interactive and co-operative behaviour of groups of organisms, like flocking birds [115,149]. PSO is similar to GA in that they both are initialised with a set of random solutions. However, unlike GA, each potential solution ('particle') is also assigned a random velocity and then 'flown' through the problem hyperspace. The particles interact and co-operate by exchanging information. PSO has been found to be effective in solving a wide range of engineering problems [116]. However, it was developed for unconstrained optimization problems only; research for developing effective methods in handling constraints is under progress.

C.3. Simulated annealing (SA)

Simulated Annealing is a global optimisation technique based on analogy with statistical mechanics [44]. In statistical mechanics, annealing is often performed to relax the system to a state with minimum free energy. In this process, a solid is heated until it melts and then the temperature is lowered slowly. The ground state with minimum system energy can be achieved if the maximum temperature is sufficiently high and the cooling is done sufficiently slowly. A similar effect is achieved in SA by testing random mutations on a single individual. A mutation that improves fitness is always accepted. A mutation which worsens fitness is accepted probabilistically based on the difference in fitness and a decreasing temperature parameter. SA is found useful for large combinatorial problems like network configuration. There have been a few instances of its application in ship design as well [117,152].

C.4. Tabu search (TS)

Tabu Search is basically a gradient search with memory [44]. It is similar to Simulated Annealing, in that both traverse the solution space by testing mutations of an individual solution. While SA generates only one mutated solution, TS generates many mutated solutions and moves to the solution with the lowest fitness. In order to prevent cycling and encourage greater movement through the solution space, a tabu list is maintained of partial or complete solutions. It is forbidden to move to a solution that contains elements of the tabu list, which is updated as the solution traverses the solution space. TS has been found useful in a wide variety of applications including engineering [153,154].

C.5. Comparison of the MOO methods

From the literature, it is seen that most of the methods discussed above can successfully be used for multi-objective optimisation. Among the EA methods, those most suitable for engineering optimisation seem to be GA and ES. Recently there has been extensive research on the use of GAs in naval architecture [5,10-

12,14,16,17,64,67,88,89,100,102,123,130,131,136,145,155-188]. EP and ES have been less popular [189,190].

Among the other methods, both SA and TS are widely used for optimisation, including engineering applications. There have been a few examples of the use of SA in naval architecture [117,152,190]. However, no application of TS in naval architecture could be found.

PSO is another promising method [186,191]. In [186], a version of PSO for ship design is compared with various GAs and it is concluded that PSO is computationally more efficient. This is supported by Mouser [192] for structural dynamics problems. However, in [193], comparison between GA and PSO in the context of control systems indicates that GA is superior to PSO in terms of computational time as well as the quality of the results. Moreover, constraint handling seems to be easier with GAs.

In terms of optimisation performance, there seems to be little difference among GA, EP, ES, SA and TS, especially once the parameters are tuned for a specific application [117,189]. Nevertheless, the most popular method for ship design optimisation was found to be GA. This is probably because GA has proved successful in many other fields including engineering. Besides, GA is relatively easy to implement. Hence it was decided to use GA for the proposed research.

The main disadvantage of GA is the long computational time required. However, this problem is common for all heuristic optimisation methods including EP, ES, SA and TS. The excessive computational time arises because of the large number of objective function evaluations. Apart from adopting parallel processing [194], the only way to reduce the computational time is to use faster performance analysis routines as objective functions. The importance of this can be seen from simplified analysis routines used in most GA applications (for example, resistance calculation: [9-11,15,100,102,136,141,173,178,187,195,196]).

Appendix D. Chronological literature review – heuristic algorithms and their application in ship design

The following sections describe the development of heuristic algorithms (with particular emphasis on genetic algorithms) and their application in ship design optimisation.

D.1. Development of genetic and other heuristic algorithms

This section monitors the development of heuristic algorithms for optimisation, with primary focus on genetic algorithms.

1. Mitchell, M. & Forrest, S. 1994 [197]

   Review of the history and scope of research on genetic algorithms. Sample application areas are listed.

2. Srinivas, N. & Deb, K. 1994 [97]

   Nondominated Sorting Genetic Algorithm (NSGA) has been developed to form the Pareto-front. This is better than Schaffer's Vector Evaluated Genetic Algorithm (VEGA), as demonstrated for a few test problems with two objectives.

3. Keane, A. J. 1996 [189]

   Review of four evolutionary optimisation methods – Genetic Algorithm, Evolutionary Programming, Evolution Strategies and Simulated Annealing. Keane concludes that GAs are better than the other three methods for the two test functions used; however, the GA implementation used is rather advanced while the others are quite simplistic, which means more sophisticated implementations of EP / ES / SA could out-perform GA in specific applications.

4. Mitchell, M. 1996 [150]

   A basic text book on GA, explaining terminology, operators, basic steps in the GA process etc.

5. Camponogara, E. & Talukdar, S. N. 1997 [164]

   Reviews the use of GA for nonlinear programming problems. Most of the current methods use penalty functions in combination with objective functions to formulate the fitness measure of the population. The proposed method instead uses the concept of dominance.

6. Todd, D. 1997 [111]

   This PhD thesis has developed a general purpose GA-based tool for handling large combinatorial multiple criteria problems. (Note: only combinatorial problems have been tackled, i.e., the ordering of numbers, such as the Travelling Salesman Problem. Parametric problems, under which ship design should come, are not considered. However, most of the principles would remain the same for parametric problems as well). Multi-Criteria Genetic Algorithm (MCGA) has been developed, including implementation and testing of various techniques. Presentation of results / visualisation of high dimensional spaces is indicated as an interesting area for further research.

7. Coello, C. A. C. 1999 [94,95]

   Review of the available techniques for multi-objective optimisation based on evolutionary principles. The most popular techniques include weighted sum methods, and different applications of GA (VEGA, MOGA, NSGA, NPGA). The strengths and weaknesses of each are described, along with practical applications.

8. Lampinen, J. 2000 [96]

   A survey of research on multi-objective nonlinear Pareto-optimisation focussing on evolutionary algorithms. A number of references and sources are listed.

11. Yang, B. S., Yeun, Y.-S., & Ruy, Y.-S. 2002 [198]

    A model management framework is presented for single and multi-objective optimisation by using approximate models instead of high-fidelity computationally expensive techniques in order to reduce total computational time. For single objective problems, this is achieved by using the high fidelity model to evaluate a few points, fitting an approximate function through those points, executing optimisation with this approximate function, evaluating the optimum obtained with the high fidelity model, updating the approximation model with this optimum obtained, and repeating these steps. Multi-objective problems are approached in a similar manner by starting with a few points in the Pareto set as calculated by the high fidelity model. This methodology could be quite useful to us if the proposed optimisation tool takes too long for performance analysis: empirical equations can be used as the low-fidelity model, and more complicated analysis can be used as the high-fidelity model.

D.2. Application of genetic and other heuristic algorithms in ship design

This section tracks the application of heuristic algorithms for optimisation, with primary focus on genetic algorithms. A few relevant papers on the application of multiple criteria decision making (MCDM) are also included.

1. Sen, P. 1992 [22]

    Sen proposes MCDM methods for marine design. MCDM allows multiple conflicting goals to co-exist, thus such techniques are more representative of the real-life design problems as opposed to classical optimisation techniques that are essentially rather simplistic in assuming that all design goals and constraints are mutually consistent. Various multi-objective and multi-attribute techniques have been described for use in design synthesis and design selection. A generalised goal programming approach is demonstrated for optimisation.

2. Robertson, A. J. S., Buxton, I. L., Sen, P., & Hills, W. 1992 [85]

   This report demonstrates the use of MADM techniques for OPV selection, taking into account both objective and subjective factors. The final ranking is based on cost-effectiveness.

3. Doctors, L. J., Day, A. H., & Node, S. 1995; Day, A. H., Doctors, L. J., & Armstrong, N. A. 1997 [136,195]

   Minimisation of wave resistance at one speed using GA. A parametric representation of hull surface is used (with B-spline control vertices). Thin ship theory is used for wave resistance estimation. A few constraints have been included like fixed displacement, L/T and interior space.

4. Ray, T., Gokarn, R. P., & Sha, O. P. 1995 [117]

   This is an extension of Ray & Sha 1994 [86]for global optimisation using simulated annealing. Solutions from SA lie close to the global optimum predicted by random search methods and genetic algorithms. The results indicate that SA is as good as GA for optimisation.

5. Day, A. H. & Doctors, L. J. 1997 [161]

   Minimisation of total calm-water resistance and maximisation of passenger comfort in a seaway for a catamaran. Only underwater geometry is considered. A parametric hull definition is used with 15 design variables. Wave resistance is calculated using Mitchell's thin ship theory modified to include transom stern effects. Ship motions are calculated using strip theory. The frequency-weighted root mean square vertical acceleration on the passenger deck level is the parameter used to indicate passenger comfort. A weighted sum is used as the objective function. Optimisation is achieved using GA combined with a hill-climbing technique to speed up convergence near optimum.

6. Hearn, G. E. & Wright, P. N. H. 1997 [162]

   Various combinations of resistance and seakeeping are used as objective functions. L, B/T, Cwp, LCF & LCB are the design variables. Variations in these are limited to ±10%, ±10%, ±0.5, ±1.0%, ±1.0% in that order (compared to a parent demihull). As with many other papers, this lacks a design synthesis module. Besides, weighted sum approach is used for the objective function.

7. Jang, C. D. & Shin, S. H. 1997 [190]

   Use of GA, SA & ES for optimisation is discussed.

8. Sommersel, T. 1997 [199]

   This application is somewhat different from the usual "minimisation of resistance" etc. The aim is "given the required values for the relevant functional parameters, the program should be able to design a ship satisfying it". In addition, it should also be possible to optimise a particular requirement. The approach is demonstrated using the example of a supply ship. A number of characteristics important for a supply ship are considered as the objectives (functional parameters). These are tank capacities, freeboard, displacement, deck area, stability, cabin facilities etc. A weighted sum is used as objective function. The author suggests that the program can be trained using existing "best" ships to tune the weighting factors. The ship is divided into various zones, depending on space utilisation. The dimensions and utility factor of each form the main design variables. Parametric equations are developed to relate the design variables to the objective function. In summary, this looks like a good "black box" for designing a particular type of ship, utilising past design knowledge.

9. Trincas, G., Zotti, I., Kahu, O., & Totolici, S. 1997 [88]

   MCDM for concept design of monohulls. Robustness is evaluated by combining MADM and risk analysis. Sample designs are generated using an adaptive Monte Carlo method. Soft constraints are handled using fuzzy functions. Designs are

refined around preferred non-dominated designs to establish robustness of the preferred solutions.

10. Zhou, G., Nobukawa, H., & Yang, F. 1997 [163]

    This is a single objective optimisation, structural construction cost being the sole objective. Plate thickness, stiffener dimensions etc are the design variables. The optimal design problem is treated as a constrained minimisation with transverse, longitudinal and torsional strength acting as the constraints. The GA procedure requires unconstrained maximisation of fitness function; hence a transformation is carried out, applying a penalty term depending on the degree of constraint violation.

11. Birmingham, R. W. & Smith, T. A. G. 1998 [168]

    This paper demonstrates the automatic generation of preliminary hull forms using GA-based optimisation techniques. Inputs are the required form parameters (e.g.: B, Δ, LCB, LCF, C_P, Cwp). A hull modeller using a number of B-spline surfaces is designed to create a hull geometry and evaluate it. A GA-based search strategy is used for improving the current design. Design variables for GA are the control points of the B-spline control surfaces. Two examples are given: to recover the original form from a random population by specifying the known form parameters, and to fit a faired surface through given offset data.

12. Hutchison, K. W. & Sen, P. 1998 [89]

    The use of multi-criteria genetic algorithms for damage stability requirements is discussed. The recent probabilistic standards for damage stability are ideal for GA exploration because of the absence of legacy information due to lack of experience.

13. Scott, J. A., Todd, D. S., & Sen, P. 1998 [169]

    Discussion on multi-criteria genetic algorithms and its application to a scheduling problem. This is discussed in more detail in Todd's PhD [111].

14. Shahak, S. 1998 [98]

This dissertation is one of the first major attempts at using evolutionary algorithms in ship concept design optimisation. The U.S Naval ship DDG51 is used as a case study. A simple objective function is used – minimisation of the payload-weight fraction. This is a rather unusual choice of objective function, the aim being to design a ship that can carry the same payload as DDG51 but with a lower displacement. A design synthesis module (ASSET) is included within the optimisation. It is claimed that 10% reduction in displacement could be achieved by the optimisation, though the accuracy of performance prediction methods has not been validated.

15. Day, A. H. & Doctors, L. J. 2000 [173]

This paper reviews the current optimisation techniques, modelling of the hull geometry, and the choice of analysis methods in hydrodynamic design of hull forms. The advantages and disadvantages of various traditional optimisation methods are described and compared with GA. It is concluded that the effective use of GA relies upon the appropriate selection of geometric representation, and effective implementation of the hydrodynamic analysis and the optimisation strategy. The practical limitations of the technique principally relate to the range of applicability of the analysis methods.

16. Lee, K.-Y. & Roh, M.-I. 2001 [176]

A new crossover operator using the gradient information is introduced. This is claimed to ensure that crossover always generates better offspring. A few examples are given which seem to substantiate the claim, with little penalty in computational time. However, it is felt that the usual simple crossover, combined with local optimisation, would perform equally well without much difference in CPU time.

17. Dejhalla, R., Mrsa, Z., & Vukovic, S. 2002 [178]

    Single objective optimisation based on GA, with wave resistance at one speed as the objective function. A linearised three-dimensional potential flow solver based on Dawson method is used for analysis. The method is demonstrated for a series 60 hull by allowing up to 5% breadth variations at each station. No geometric constraints are imposed, not even displacement identity.

18. Lee, K.-Y., Han, S.-N., & Roh, M.-I. 2002 [130]

    A GA with a modified crossover operator is demonstrated for optimal compartment layout. The objective function used is a combination of the total transport cost and adjacency requirements between various compartments. It is concluded that the proposed algorithm is superior to an existing algorithm. The interesting part is a modified crossover operator which ensures that between the two parents, the one having higher fitness value provides more genes to the child. An inversion operator is also used after crossover, which is rather rare among the GA papers examined.

19. Brown, A. & Salcedo, J. 2003; Brown, A. & Thomas, M. 1998 [10,11]

    This demonstrates the application of GA in ship concept design optimisation. Two objectives are considered: maximisation of the Overall Measure of Merit (OMOE) and minimisation of life cycle cost. OMOE vs. life cycle cost forms the Pareto-front. OMOE comprises a number of parameters on mission effectiveness. The formulation is rather detailed using AHP and MAVT. Simple regression equations are used for performance analysis.

20. Gammon, M. A. & Alkan, A. 2003 [183]

    Single objective optimisation (resistance) with various constraints. The novelty in this paper is that two types of chromosomes are used: principal parameters (L, B, T) as real variables, and hull offsets in the form of matrices. This is referred to as concurrent global and local optimisation. Offsets are allowed to vary between 50% and 150% of their original values.

21. Lowe, T. W. & Steel, J. 2003 [182]

    This is a rather different application of GA. Given a set of required geometric parameters (displacement, L, B, T, LCF, LCB etc), GA is used to generate a number of suitable hull forms. These are meant to be used by the designer for analysis and evaluation. No optimisation is attempted for. The fitness function for the GA is how closely the generated form satisfies each design requirement. One limitation of such an approach is that there may exist other points in the design space that satisfy the requirements but were not discovered by the GA.

22. Peri, D. & Campana, E. F. 2003 [15]

    This is a true multi-objective optimisation – three objectives (minimisation of resistance, heave and pitch) are optimised simultaneously without the use of weighted sums. CFD is used for analysis. Evaluation of objective function is done using variable fidelity modelling. A set of Pareto-optimal solutions is generated. Then, an automated decision maker ranks the designs based on their Euclidean distance from the ideal solution. The approach is similar to the proposed research, except for the absence of the design synthesis module.

23. Zaraphonitis, G., Boulougouris, E., & Papanikolaou, A. 2003; Boulougouris, E. & Papanikolaou, A. 2003 [12,16]

    The objectives are to maximise ship's survivability after damage (modelled as attained subdivision index), and efficiency (transport capacity and building cost). NAPA is used for naval architectural calculations and modeFrontier for optimisation. L, B, T and Δ are fixed; hence only the internal arrangement is modified, causing changes in deadweight.

24. Zaraphonitis, G., Papanikolaou, A., & Mourkoyannis, D. 2003 [100]

    The objectives are the minimisation of wash and powering. NAPA is used for hull form generation, SHIPFLOW for hydrodynamic evaluation and modeFrontier for optimisation. Two example applications are given: a monohull and a catamaran. SHIPFLOW Analysis is limited to potential flow only, to

reduce computational time. Details of the optimisation procedure have not been included. Results are shown as resistance vs. wash scatter plots indicating the Pareto-optimal frontier.

25. Olcer, A. I., Tuzcu, C., & Turan, O. 2003 [14]

    Three objectives are to be maximised: KG limiting value satisfying damage stability criteria, maximum allowable wave height satisfying damage stability criteria, and Cargo capacity. Design variables are deck heights, bulkhead positions etc. Constraints are various SOLAS 90 requirements. GA-based optimisation is done using modeFrontier software, and parametric hull modelling is achieved in NAPA. The Pareto-optimal solutions are treated as an MADM problem, and ranked using the TOPSIS technique.

26. Yu, L. & Tan, J. 2003 [91]

    The Interval AHP (IAHP) method is introduced as a better alternative to AHP. In AHP, weights are determined using expert opinion, and small changes in weights can cause large changes in results. In IAHP, experts give a range (e.g. 0.6 to 0.65) instead of a single value as weight. A pairwise comparison matrix with intervals as individual elements is formed. This matrix can be reduced to the weights as obtained by AHP. Such weights are more consistent and stable compared to the weights obtained in AHP.

27. Mierzwicki, T. S. 2003; Brown, A. & Mierzwicki, T. 2004 [17,99]

    An Overall Measure of Risk (OMOR) is proposed, similar to Overall Measure of Effectiveness (OMOE). This results in multiple Pareto-fronts (OMOE vs. Cost) for various values of OMOR.

28. Wolf, R., Dickmann, J., & Boas, R. 2004 [123]

    The GA performance is compared with gradient search optimisation. Maximisation of speed, range and combat capability (combined into OMOE) and minimisation of cost are the two objectives. An empirical model (MIT Math

Model) is used for design synthesis. The ship design landscape is explored using combinatorial and DOE methods. Sensitivity study for variations in weightings in the formulation of OMOE indicates that different weightings can have significant influence on the results of the optimisation. It is concluded that GA is a promising method for effective exploration of the complex design space; however, the use of OMOE as the objective can mask potentially useful areas of the design space.

29. LOGBASED Methodology Toolkit. 2005 [200]

This EU-funded project was aimed at developing an integrated ship design methodology through the integration of design / operation issues, and making the overall transport system competitive, involving Owner, Market and Ship. It is suggested that the optimisation of the three players together is undertaken using GA.

30. Neti, S. N. 2005. [5]

This dissertation reports the implementation of GA-based optimisation, and its demonstration for two naval ships DDG51 & LHA(R). Objectives are OMOE and cost, with a rather elaborate formulation for OMOE. Design variables are also rather elaborate, based on trade studies identifying various areas of improvements for the two ships. Combination of three software tools is used: DARWIN (GA-based optimisation tool), ASSET (to evaluate the feasibility of a given design) and Model Centre (to integrate DARWIN and ASSET, calculate OMOE and cost, and send them to DARWIN for generating better designs).

31. Whitfield, R. I., Hills, B., & Coates, G. 2005 [103]

The Design of Experiments method is used to generate points for exploring the design space. This is used to form a response surface as second order regression equations. GA module uses this response surface to quickly explore the design space and produce the Pareto-front. It is claimed that this method produces faster and more robust ships; however, it is not clear how much time the DOE

would take to generate the response surface; nor is it clear how the response surface based on regression equations ensure robustness of design.

32. Mason, A. & Couser, P. 2005 [187]

This paper demonstrates the method that is being used in ACCeSS – ANN is used for resistance prediction, and GA is used for optimisation. The difference is that, this paper is limited to single-objective optimisation only. The concept is demonstrated for a catamaran hull form. It is not clear what constraints were used; in any case there is no design synthesis incorporated.

33. Peri, D. & Campana, E. 2005 [201]

This paper demonstrates the use of high and low fidelity analysis models for reducing the total computational time in multi-objective optimisation. The optimisation process is divided into global and local phases. In the global phase, a few computationally expensive simulations are carried out for creating analytical approximations (surrogate models) of the objective functions. Global optimisation is done using these surrogate models, and the promising solutions are then locally refined using high-fidelity simulations. The new results of the high-fidelity analyses are used to improve the surrogate models. This process reduces the overall computational time. The interesting aspect is the dynamic refinement of the surrogate models using high-fidelity models. The method is demonstrated for a destroyer ship. One limitation is that it is not clear how much computational time can be saved by using the surrogate model. In the context of the proposed research, the combination of high and low fidelity models may not be necessary if ANNs are used for performance analysis. This is because ANNs are effectively polynomial equations representing the response surface; thus they can achieve high accuracy at a low computational time. However, there may be cases when alternative analysis methods may have to be used. In such cases computational time may become an issue, and surrogate models as demonstrated in this paper seem to be a viable option in tackling the problem.

34. Lowe, T. W. 2005. [188]

This paper presents the automatic generation of hull forms as surface meshes based on partial differential equations (PDEs) with appropriate boundary conditions. Various equality and inequality constraints can be handled (like B/T range, C_B range etc). Automation is achieved using GA to search the design space, resulting in a number of designs satisfying the constraints. The use of PDEs ensures surface fairness. The methodology is very similar to [168], the main difference being that Lowe uses PDE instead of B-spline curves. This method has the potential to generate hull surfaces easily once the ship particulars are known. For example, in the proposed research, GA-based optimisation will result in a number of optimum ships specified in terms of their design variables. Lowe's method (a "nested" GA inside the optimisation GA) can be used to fit hull surfaces satisfying these design variables.

35. Peri, D. & Campana, E. 2005. [202]

Four novel global optimisation methods are illustrated: Genetic Algorithm (GA), Multistart Gradient Method (MsGM), Particle Swarm Optimisation (PSO) and Diagonal Rectangular Algorithm for Global Optimisation (DRAGO). These methods are compared on the basis of whipping of a cruise ship. No clear conclusions on the relative merits of the four methods can be derived. The merits depend on a number of parameters used within each algorithm, as well as on the shape of the performance space. For example, if the peak of the performance space is rather flat, the MsGM will find it very difficult to find a suitable direction of improvement. However, this paper shows that other novel optimisation tools can out-perform GAs in terms of both effectiveness and computational time.

36. Pinto, A. & Campana, E. F. 2005. [186]

Multi-Objective Deterministic Particle Swarm Optimisation Algorithm (MODPSO) is demonstrated and compared with Nondominated Sorting Genetic Algorithm (NSGA) and Strength Pareto Evolutionary Algorithm

(SPEA). MODPSO accuracy in finding Pareto solutions is comparable to that of SPEA and higher than that of NSGA. Also, MODPSO is computationally an order of magnitude more efficient than NSGA and SPEA.

Appendix F. Genetic algorithms – background information

Genetic algorithms are computational techniques based on natural evolution, and they have become very popular for optimisation in various fields. They work on a large population of designs and iteratively modify the population using genetic operators. As iterations progress, the fitness of the population in terms of the design objectives improves, eventually leading to optimal solutions.

F.1. Genetic algorithms for optimisation – advantages

As opposed to most traditional optimisation methods, GAs are very generic: there are no restrictions of linearity, convexity, size of search space, multimodal spaces etc. They can achieve near-global optimum, rather than local optimum.

GAs work on a large population of potential solutions. Hence, in the case of multi-objective optimisation, the whole set of optimal solutions is obtained instead of a single optimum, as would be the case with traditional optimisation techniques.

GAs will not run into difficulties if regions of the design space are encountered where solutions of the objective function can not be found (this can cause difficulties for traditional search techniques)

Most of the traditional optimisation methods have difficulty in handling discrete variables. For GAs, the variables may be of mixed types (e.g.: real: L, B, T; integer: number of hulls, for multihull ships; Boolean: presence / absence of bulbous bow).

GAs do not require derivative information during the optimisation process, as opposed to traditional methods. Derivatives become computationally expensive as the number of design variables increases.

GAs can be hybridised with local search techniques to give any desired balance between local and global optimisation.

F.2. Genetic algorithms for optimisation – disadvantages

GA-based optimisation can not guarantee achieving globally optimal solutions, though a near-optimal solution with high accuracy can be ensured within reasonable computational time.

It is a comparatively slow technique when the design space is relatively simple, and the number of design variables is small. Traditional search methods can be faster.

GA applications take a lot of computational time, even with parallel processing.

GAs require the setting of a number of parameters. A little experimentation is necessary to establish suitable values for these parameters in a given problem.

As the number of design variables increases, the population size needs to be increased, requiring more computational time.

F.3. GA-based optimisation: outline of the process

Genetic algorithms start with an initial random population of designs. Each design is represented by means of its design variables. Then the required objective functions of each design are evaluated. Fitness of each design is calculated based on the values of these objective functions. Low fitness individuals are discarded, and high fitness individuals are used to perform genetic operations resulting in the formation of offspring. The offspring and the parents are combined in some manner to create the new generation. Then the process is repeated with this new generation, until there is little improvement in the fitness levels as generations progress. An outline of this process is shown in Figure F-1. The basic GA terminology is given in Appendix G.

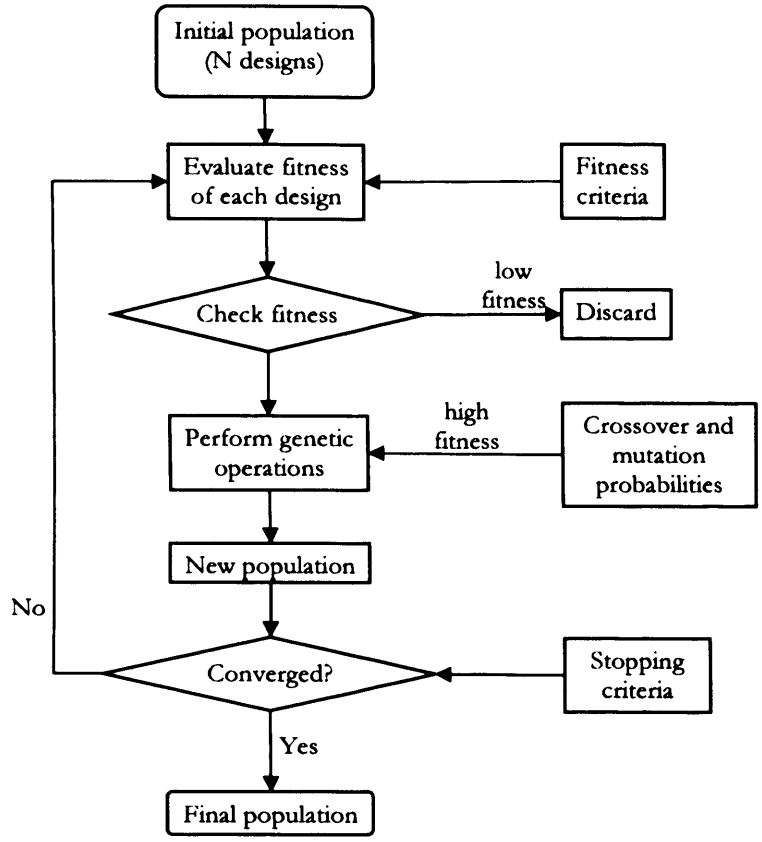

Figure F-1: GA Flowchart

The main functional elements of a GA-based optimisation program are:

1. GA coding schemes - representation of the design variables (the chromosome)
2. Objective function / fitness function (one or more objectives)
3. Basic GA operators (selection, crossover and mutation)
4. Formulation of the new generation
5. Checking for convergence

Each of these is discussed in detail in the following subsections, followed by other important aspects of GA implementation.

F.3.1. GA coding schemes

The first task in a GA-based optimisation is the encoding of design variables (i.e., the formulation of the "chromosome"). There are four coding schemes available:

- Binary
- Gray-coded
- Integer
- Real

The earliest GAs used binary coding. That is, all design variables were converted to binary format and stored together as a single long string.

Gray-coding is a modification of the binary coding scheme to improve computational efficiency. It is a one-to-one mapping of a standard binary coding that minimises the Hamming Distance of adjacent numbers, which means that the numbers N and N+1 differ by only a single bit flip.

Integer coding is useful for combinatorial problems, which requires node numbers as genes; for example, the Travelling Salesman Problem.

Most of the newer applications use real number coding, and others use binary coding. Gray-coding appears rare, and integer coding can be used only in certain specialised applications.

F.3.2. Objective function / fitness function

The objective function evaluates all the objectives under consideration, such as calculation of resistance and seakeeping characteristics. The calculated values are termed the 'fitness' of the individual. The term 'fitness function' is often used to mean 'objective function'; however, the two are not equivalent - the fitness function scales the values output by the objective function depending on the ranking scheme adopted (see Appendix F.3.6).

F.3.3. Basic GA operators

The GA achieves its functionality using just three basic operators: selection, crossover and mutation. Selection, as the name implies, selects the most suitable chromosomes from the current population, forming the "reproduction pool". Crossover creates the offspring population by suitably combining parent chromosomes chosen from the reproduction pool. Mutation applies random modifications in genes. These operators are described below.

Selection

This operator is used to form the reproduction pool from the current population. The probability of selecting a particular chromosome is decided in accordance with its fitness. The raw fitness values are often scaled depending on various ranking schemes before applying the selection operator. A variety of selection methods are available:

1. Roulette wheel [111]

   This is the simplest selection method. An imaginary roulette wheel is divided into N segments (N is the population size). The size of each segment is proportional to the fitness of each individual. The wheel is "spun" N-times, and during each spin, the segment where the marker falls is selected and the corresponding individual is included in the reproduction pool. Note that multiple selection of the same individual is possible. Since the size of the segment is proportional to its fitness, individuals with higher fitness have a better probability of selection than low-fitness individuals during each wheel-spin.

   There seem to be a few disadvantages for roulette wheel selection. It is not suitable for minimisation problems. Moreover, it suffers from loss of selection pressure as the population converges, when all individuals have similar fitness values. In addition, it is susceptible to super-individuals (i.e., one or two individuals with much higher fitness than the rest of the

population) that will soon dominate the population causing premature convergence.

2. Baker's selection [98]

   This is similar to the roulette wheel, except that there are N equally-spaced markers is present (instead of one marker), hence N individuals can be selected in one spin of the wheel (instead of N spins). The uniformly distributed markers ensure diverse selection; high fitness individuals still have a higher chance to get more copies.

3. Tournament [111]

   A few individuals (known as "tournament size") are randomly selected; the best among them (in terms of fitness) is considered as the "winner of the tournament", and is selected as a parent. This process is repeated N times. Note that selection pressure increases as the number of individuals in the tournament increases. Tournament size can be as small as 2 in typical applications.

4. Elitist [111]

   This ensures that the best one or more individuals are taken into the next generation, without going through selection, crossover or mutation – they are virtually copied through. The rest of the individuals are selected using another selection mechanism (like roulette wheel).

5. Sigma truncation [111]

   In this method, the weakest individuals in the population, lying more than 's' standard deviations away from the average individual, are simply removed. Selection is then carried out by any of the earlier-mentioned methods. Typically s = 1 to 3.

Crossover

This is the operator fundamental to the success of GA in promoting high-fitness individuals and discarding low-fitness individuals as generations progress. Two parents are chosen from the reproduction pool. Parts of the chromosomes are interchanged to produce two offspring.

Crossover starts with matching of two individuals from the reproduction pool as parents. Usually the two parents are chosen randomly. Sometimes certain niching schemes are employed to match up similar parents.

Once two parents are chosen, crossover between them takes place. There are a number of crossover operators found in the literature [111,129,150].

1. Single-point crossover: This will generate a cut-point in the two parent chromosomes. Then the first part of the first parent is re-combined with the second part of the second parent, and vice versa, to form two offspring.

   e.g.: Parent 1 : X X|X X X X X X

   Parent 2 : Y Y|Y Y Y Y Y Y

   Child 1 : X X Y Y Y Y Y Y

   Child 2 : Y Y X X X X X X

2. Two-point crossover: This is similar to single-point crossover, except that two cut-points are generated, instead of a single cut-point.

   e.g.: Parent 1 : X X|X X X|X X X

   Parent 2 : Y Y|Y Y Y|Y Y Y

   Child 1 : X X Y Y Y X X X

   Child 2 : Y Y X X X Y Y Y

3. Multi-point crossover: This is similar to the two-point crossover, except that more than two cut-points are generated, instead of two cut-points.

4. Uniform crossover: For each gene, one of the two parents chosen with a probability of 0.5, and its value of that gene is given to the first offspring; and the other parent gives its value of the gene to the second offspring. This process is repeated for all genes in the chromosome.

   e.g.: Parent 1 : **X** X **X** X X **X** X X

   Parent 2 : Y **Y** Y **Y** **Y** Y **Y** **Y**

   Child 1 : **X Y X Y Y X Y Y**

   Child 2 : Y X Y X X Y X X

The classical single-point crossover is the most common, though multi-point crossover has been suggested by some authors as having more potential.

The above crossover operators are applicable to both binary-coded and real-coded GA. There are a few others applicable to real-coded GA only. These are described below (with X and Y being two genes from the two parents, represented as real numbers):

1. Mid-point crossover: The gene of the offspring = (X+Y)/2. This is repeated for each gene with a chosen probability.

2. Flat crossover (BLX-0.0): In this case the gene of the offspring is taken as a random number between X and Y. The operator is repeated for each gene with a chosen probability.

3. BLX-alpha: This is similar to the flat crossover, except that the random number is generated between (X-delta and Y+delta) where delta = alpha * (Y-X). (It is assumed that X < Y).

4. Arithmetic crossover:

Child 1 = a X + (1-a) Y

Child 2 = a Y + (1-a) X

where the value of 'a' varies from 1 to 0.1 as the search advances, as per the equation: a = 1 – 0.9 gen / gen_max (where gen = current generation; gen_max = maximum number of generations)

Note that the arithmetic crossover is equivalent to flat crossover when a = 0.5.

Mutation

Mutation helps in simulating random infrequent changes that occur in genes of natural organisms. It ensures exploration of the whole design space and maintains diversity of the population.

Mutation is a random change in one or more genes of a chromosome. Probability of mutation is generally much smaller than the crossover probability. Very low mutation may cause premature convergence to local optimum.

If the GA uses binary representation, mutation is quite simple – flip 1 to 0 or vice versa, depending on the probability of mutation.

For real coding, generally Gaussian mutation is used by adding a random value based on Gaussian distribution. Low variance is specified for high fitness individuals, and vice versa.

Constant probability of mutation throughout all generations generally causes problems for GA. Hence, modern GAs use a relatively high mutation probability at the start to promote diversity, and this probability is gradually reduced as generations progress.

F.3.4. Formulation of new generation

The offspring formed after applying the genetic operators can be used in various ways to form the next generation. In some schemes, the offspring always replace the

parents; in others, they compete with the parents in a variety of ways. The fraction of the population that is replaced in each cycle is known as "generation gap". A generation gap of 1.0 means that the whole population is replaced by the offspring. Sometimes, a fraction of the population is directly copied to the next cycle. This is known as "elitism", and it ensures that the best fitness does not deteriorate as generations progress.

F.3.5. Checking for convergence

In practice, there are no agreed tests for convergence. One popular test is the absolute and relative improvement of the fitness values over the last few generations.

Similarly, there seems to be no method to identify premature convergence. Some authors simply specify a minimum number of generations, before which if convergence occurs, it is assumed to have converged prematurely. Premature convergence is usually tackled by "cataclysmic restarts", in which the best individual out of a population is kept, and all others are replaced by newly initialised individuals. (e.g.: [173]).

F.3.6. Ranking and fitness scaling

The selection operator uses the fitness of individuals as the selection criterion. There are some mechanisms to improve selection by adopting various ranking schemes before selection.

1. Linear rank and scaled fitness

   This method ranks the population in terms of fitness, and assigns new linear fitness values in the order of rank. It effectively scales the fitness values of the individuals to increase or decrease the discrimination between good and bad strings.

2. Non-dominated sorting [97]

   This method involves first finding the Pareto optimal points, giving them a rank of one and removing them. Then the Pareto optimal points in the remaining population members are given a rank of two and removed. This process is repeated until the whole population has been ranked.

3. Multi-objective ranking [as seen in 111,203]

   In this scheme, each individual is given a rank according to how many individuals dominate it. If an individual is nondominated, it is given a rank of 1. This method gives a greater range of ranks, and also penalises areas of high density solutions.

F.3.7. Fitness sharing (niching)

The GA-based optimisation should result in individuals widely distributed along the Pareto front, instead of concentrating on a few areas. The concept of fitness sharing (niching) is used to generate and maintain a diverse range of Pareto optimal points. In other words, niching is required in order to distribute the points evenly along the Pareto-front. In principle, this is achieved by encouraging individuals to move away from crowded areas by somehow penalising the individuals in such areas. Various algorithms have been developed for niching. They include Multiple Objective GA (MOGA) [as seen in 111,203,204], Niched Pareto GA (NPGA) [as seen in 111,156,205], Nondominated Sorting GA (NSGA) [97], Cluster-Oriented Genetic Algorithms (COGA) [206] etc.

F.3.8. Restricted crossover (mating restriction):

This is used to ensure that individuals far away from each other do not mate, to avoid the formation of low-fitness individuals with completely dissimilar properties.

F.3.9. Local search schemes

The results of a search can be considerably improved if the offspring (and initial population if necessary) are subjected to some kind of optimisation. Possible

operators include a local search, or non-local search methods like simulated annealing. A few instances of this approach are seen in the literature [161,195] where GA has been combined with a hill-climbing technique for optimisation to speed up convergence near the optimum.

F.3.10. Pareto selection mechanisms

After generating the Pareto-front using GA, various techniques can be used to help decision makers quantify their preferences among the Pareto-optimal solutions, thus helping them to make an informed choice. Commonly used techniques are based on Multiple Criteria Decision Making (see Section 2.6.7).

F.4. Choice of the GA parameters

The last section showed that a number of parameters are to be chosen before executing genetic algorithms. The choice of the parameters influences the efficiency of genetic algorithms. Grefenstette [207] shows that the optimum values of the GA parameters largely depend on the problem under consideration; i.e., the parameters have to be tuned for each application. Nevertheless, good performance can usually be ensured with a range of parameter settings, and hence the exact optimum values may not be significant. An alternative approach for the optimisation of the GA parameters is to enable the GA to modify its own parameters dynamically, though this may involve an increase in computational time.

F.5. Summary - GA-based optimisation

GA is a promising method for multi-objective optimisation; however, its efficiency and effectiveness largely depends upon the choice of various parameters. Tuning of these parameters in the context of a particular application may be important. Moreover, there are many variations of the basic GA seen in the literature, especially for fitness sharing. They also need to be investigated for the current application.

Appendix G. GA terminology

Objective Function: The objective function is the function one wants to optimise. It gives the values of all objectives under consideration.

Fitness Function: The fitness function generates fitness values by scaling the output of the objective function depending on the ranking scheme adopted.

Fitness Values: The numerical values for the objectives to be optimised. The fitness values may be the same as the values of the objectives under consideration; however, they are often scaled or modified depending on the type of GA implementation.

Population and Individuals: The population consists of all individuals in one generation. In the present context, the population is the collection of all ships considered in one generation.

Population size: number of individuals in a population.

Genome / Chromosome and Genes: Representation of an individual in terms of its design parameters is referred to as a genome / chromosome and the discrete entries as genes. For instance, in the context of ship design, the genome consists of the design variables that define the ship (L, B, T, C_B etc). It is the genome of an individual that determines the value(s) of its objective function.

Genotype and Phenotype: The code devised to convert the parameters of the problem to a chromosome is called the genotype and the uncoded version is the phenotype. The distinction arises only when some coding scheme (for example binary coding) is used to represent the design variables. The analogy in nature is that, for example, the colour of the eye is the phenotype, and the corresponding set of genes is the genotype.

Diversity: Diversity refers to the average distance between individuals in a population. Diversity is essential to the genetic algorithm because it enables the algorithm to search a larger region of the design space.

Generation: At each iteration of the GA, a series of computations on the current population produces a new population. Each such successive population is called a new generation.

Parents and Children/Offspring: To create the next generation, the genetic algorithm selects certain individuals in the current population, called parents, and uses them to create individuals in the next generation, called children (offspring).

Reproduction: Production of a new member of the population from existing members; may be used to make an exact copy of the original member.

Reproduction pool: The set of genes available for reproduction.

Genetic operator: Operators that act upon the chromosome to produce a new individual. They are used to maintain diversity and improve the fitness of the individuals across generations. Genetic operators include selection, crossover, mutation etc.

Selection: The stage in which parent chromosomes are chosen from a population for reproduction using crossover, mutation etc. Typically, the algorithm is more likely to select parents that have better fitness values.

Crossover / Recombination: Creating a new individual's chromosome from parts of its parents' chromosome by exchange of genes. Crossover swaps genetic information between parents, shuffling the genes in a population, but it does not produce any new genetic information. (This is not strictly true for some advanced crossover operators acting on real variables).

Mutation: Arbitrary change to a chromosome, often at random. Mutation is the primary source of introducing "new" genetic information to a population.

Migration: An operator used in parallel or distributed GA, to exchange genetic information between subpopulations.

Elitism: A property of selection methods that guarantees the survival of the best individual(s) to the next generation. Elitism ensures that one or more individuals

with the highest fitness in the current generation are directly copied to the next generation without using crossover or mutation.

Premature Convergence: When a genetic algorithm's population converges to something which other than the global optimal solution.

Generation gap: The ratio of the number of offspring to the size of the parent population. For example, a generation gap of 1.0 means that the whole population is replaced by the offspring.

Pareto optimality: Optimality criterion for problems with multiple objectives. A state 'A' (a set of objective parameters) is said to be Pareto optimal, if there is no other state 'B' dominating the state 'A' with respect to the set of objective functions under consideration. A state dominates another state, if the former is better than the latter in at least one objective function and not worse with respect to all other objective functions.

Pareto front / Pareto set: a set of states of objective parameters satisfying the criterion of Pareto optimality.

Niching: Mechanism for maintenance of diversity in the population by appropriate techniques. Niching ensures that the Pareto-front is evenly populated.

Memetic Algorithm: When GA is combined with some local optimisation procedure to speed up convergence near the optimum (local or global), the resulting hybrid algorithm is called a memetic algorithm.

Appendix H. GA Tool – implementation details

This appendix briefly explains the implementation details of the GA Tool, such as the choice of the software platform, description of the input and output files, the procedure for executing the GA Tool, the performance analysis modules currently implemented, and the calculation of fitness values. Flow charts explaining the functioning of the tool are also included.

The GA Tool User Guide [125], along with the accompanying CD containing source code and examples, provides further guidance on using the GA Tool. It also includes tutorials on how to run the GA Tool and visualise the results. For more details on individual functions and files used within the GA Tool, explanatory comments are provided within the source code of each function.

H.1. General considerations

At the start of the development of the GA Tool, a literature survey was carried out to investigate the software tools available for GA-based optimisation. The most commonly used software tools are:

1) ModeFrontier [208]

   ModeFrontier is a commercial optimisation software package incorporating various optimisation techniques. Several authors have used this for their research [12,14,100].

2) iSIGHT [209]

   iSIGHT is another commercial software package for integration of multiple software tools and design optimisation. There are only a few instances of this found in ship design [210].

3) Genetic Algorithm and Direct Search Toolbox in Matlab [211]

   GA Toolbox is part of the standard Matlab suite of programs. It has got a powerful library of GA tools, but is limited to single-objective optimisation [123].

4) DARWIN [212]

   DARWIN is a general purpose optimisation software. It is currently limited to single-objective optimisations [5].

The only tool among the above that can handle multi-objective optimisation is ModeFrontier, which is an expensive commercial software package. For this reason, it was decided to look for multi-objective routines in the public domain. Numerous optimisation routines were found on the Internet, available free of cost [213-216]. Among these, the MOEA Toolbox developed by Tan [214] was found to provide maximum functionality in terms of the different types of optimisation algorithms. However, the source code for this was not available, and hence it was discarded. From a few initial trials using the remaining routines, a set of programs developed by Andrey Popov was found most satisfactory [215] for implementation in Matlab. It was decided that these routines would be sufficient for the proposed research, and additional functionality could be added when required. This approach turned out to be successful.

For ship design synthesis, researchers seem to use in-house programs. Wolf [123] uses an empirical Matlab-based synthesis tool called MIT Math Model. The Advanced Surface Ship Evaluation Tool (ASSET) for naval ships is used in [5]. Most other literature do not include a design synthesis tool; they simply use a standard naval architectural software like NAPA for generating and evaluating the designs based mainly on the underwater volume, without going into actual design synthesis. For the present research, a design synthesis module based on the UCL Ship Design Process [35] was developed in Matlab. This synthesis procedure is shown in Figure H-1.

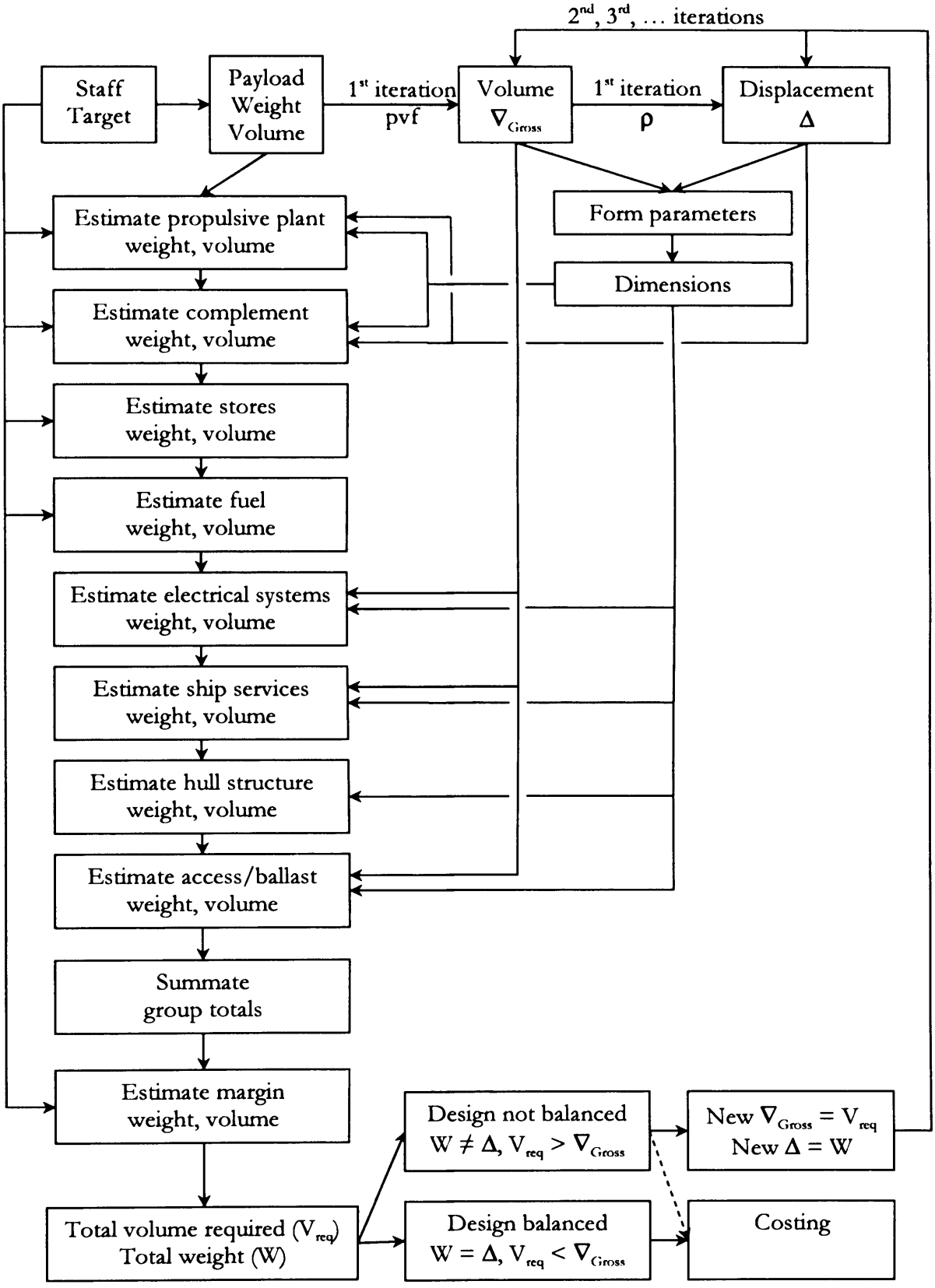

Figure H-1: UCL design synthesis procedure for a surface monohull

H.2. Input files

There are two sets of input files needed while running the GA Tool. The first set includes the design inputs and GA parameters that generally need to be modified before executing the GA Tool. The second set includes constant input data that do not need modification unless the GA Tool itself is modified.

H.2.1. Input files that need to be modified before executing the GA Tool

There are four files that fall within this category: input.mat, GAParams.mat, TargetFitnessValues.mat and coeffs.mat.

1. **input.mat** specifies customer inputs as well as the ranges for the design variables and soft constraints. These include:

   (i.) B_T_min & B_T_max : the lower and upper bounds of B/T

   (ii.) circM_min & circM_max : the lower and upper bounds of Ⓜ

   (iii.) Fndisp_min & Fndisp_max : the lower and upper bounds of Froude displacement number

   (iv.) L_B_min & L_B_max : the lower and upper bounds of L/B

   (v.) L_D_min & L_D_max : the lower and upper bounds of L/D

   (vi.) ObjName : the names of the objectives

   (vii.) V_kn : the top speed of the ship, in knots

   (viii.) V_endur : the speed for endurance calculation, in knots

   (ix.) range_nm : the range to be achieved at the endurance speed, in nautical miles

   (x.) Ncrew : number of crew

(xi.) bounds_orig: matrix of size [num_desvar, 2] where num_desvar is the number of design variables. Each row of bounds_orig represents one design variable, and the two columns represent the minimum and maximum value of the corresponding design variable. For the present implementation of the GA Tool, num_desvar=9. These nine design variables are:

- D (depth) [m]
- pvf (payload/volume factor) [-]
- ρ (overall density of the ship - i.e., displacement / gross enclosed volume) [t/m^3]
- ss (superstructure ratio) [-]
- C_B [-]
- C_P [-]
- GM [-]
- Payload weight [t]
- Payload volume [m^3]

The values of pvf and ρ are only used for starting the design synthesis process. Their values after the synthesis process may fall outside the specified ranges.

The value of GM may be either specified or estimated during the design synthesis process. If it is to be estimated, its lower and upper bounds are to be specified as -999. All the results presented in this report use the estimated value for GM.

2. **GAParams.mat** specifies the values of the GA parameters (see Appendix F.3). These are listed below. The default values for each parameter is mentioned; these taken together form the standard set of GA parameters that have been used for the demonstration runs presented in this thesis.

   (i.) AlphaCrossover

   In the case of binary crossover, AlphaCrossover represents the probability of crossover. In the case of 'BLX-alpha' crossover, it represents the crossover factor (see Appendix F.3.3). The current GA implementation uses 'BLX-alpha' as the type of crossover, except when OptSelect=4 (see below), which uses simulated binary crossover. For the GA runs demonstrated in this thesis AlphaCrossover = 0, so that the values of the offspring genes will fall within the bounds of the parent genes.

   (ii.) MutRate

   Mutation rate. For the GA runs demonstrated in this thesis MutRate = 0.1.

   (iii.) NumGen

   Number of generations for each GA run. For the GA runs demonstrated in this thesis, unless mentioned otherwise, NumGen=100. Note that extended runs can be used to increase the number of generations as multiples of NumGen. For example, 6 extended runs with NumGen=100 (and other GA parameters remaining the same) would mean a total number of generations = 600.

   (iv.) NumObj

   Number of objectives

(v.) OptSelect

Selection of the type of GA to be used for fitness scaling and ranking, resulting in the reproduction pool. Assign a value from 1 to 5 where:

1 → NSGA (Nondominated Sorting Genetic Algorithm - fitness scaling and ranking based on [97])

2 → Pareto Optimal (parents are selected randomly from among the Pareto-set of the current generation)

3 → Random (pure random selection of parents, equivalent to simulating random synthesis of designs at every generation)

4 → NSGA-II, which is a modified version of NSGA, as given in [217], using the GA operators used by the authors. They include binary tournament selection, simulated binary crossover (SBX) with probability 0.9, and polynomial mutation with probability 1/PopSize.

5 → NSGA-II mentioned above, but with modified GA operators, including 'BLX-alpha' crossover and user-specified values for AlphaCrossover and MutRate.

For the GA runs used in this thesis OptSelect=5. According to Zitzler [135], NSGA-II is the best choice among all types of genetic algorithms currently available. Besides, from a number of GA runs, NSGA-II was found to give the best performance among the five methods considered, in terms of the quality of the Pareto-front generated as well as fast convergence.

(vi.) PopSize

Population size. For the GA runs demonstrated in this thesis, unless mentioned otherwise, PopSize=100.

(vii.) NumRuns

Number of multiple runs for a fixed set of GA parameters mentioned above. The results of multiple runs can be examined to check if the GA has converged to the same Pareto-front. For the GA runs demonstrated in this thesis, unless mentioned otherwise, NumRuns=5.

3. **TargetFitnessValues.mat** represent the target values of Fitness (if applicable). See Section 5.3 for the use of assigning target values for fitness.

4. **coeffs.mat** include the coefficients for adjusting the estimated weight, volume, GM and cost within the SynthesisModule. The aim of using these coefficients is is to match the estimated values with the known values of a parent vessel, when available.

H.2.2. Files that remain constant for the current version of the GA Tool

There are two input files that require no changes before executing the current implementation of the GA Tool. These are:

1. GAopt.mat, which defines various default values of parameters required during the GA run (such as on-screen display of numerical/graphical results), to complement the user-defined parameters defined in GAParams.mat.

2. globals_numdesvar_numshippart.mat, which defines the number of design variables and the number of ship particulars (9 and 11 for the current implementation of the GA Tool).

H.3. Output files

There are two sets of output files that are generated by the GA Tool. The first set includes the standard numerical and graphical results that are automatically output during each run of the GA Tool. The second set includes additional graphical results that can be generated using post-processing functions after the GA Tool is finished.

H.3.1. Standard output files

The standard output files store and display the information about the Pareto-front in numerical and graphical formats. These files include:

1. PF_O*,P*,G*,S*,M*,C*,R*.mat

   Includes fitness values, genes and ship particulars of the Pareto-front, saved in a format that can be read by Matlab. The name of the file indicates the values of various GA parameters used in forming the Pareto-front. In the name template shown above:

   O* → number of objectives (e.g.: O2 → two objectives)

   P* → PopSize (e.g.: P100 → 100 ships in each generation)

   G* → NumGen (e.g.: G100 → the GA was run for 100 generations)

   S* → type of GA used, as indicated by digits 1 to 5 (e.g. S5 → NSGA II)

   M* → mutation ratio (e.g.: M0.1 → mutation ratio = 0.1)

   C* → crossover factor (e.g.: C0 → crossover factor = 0)

   R* → run number (e.g.: R1 → results of the first run with a given set of GA parameters. R_All is a special value that indicates the combine Pareto-front formed by multiple runs of the GA with the same set of other GA parameters)

e.g.: "PF_O3,P100,G100,S5,M0.1,C0,R3.mat" → the Pareto-front of the third run of the GA Tool for a three-objective problem with PopSize=100 and NumGen=100. The type of GA used was NSGA II, with mutation ratio = 0.1 and crossover factor = 0.

2. PF_*.fig → the Pareto-front as mentioned above, but shown in a graph. The graph is generated only when NumObj=2 or 3.

3. PF_*.txt → the same data contained in PF_*.mat, but saved as a text file so that it can be opened outside Matlab.

4. FP_O*,P*,G*,S*,M*,C*,R*.mat

   "Final Population" that includes the genes and ship particulars of all ships in the last generation during a GA run. This is used as the initial population if further extended runs are required. Note that the information stored in this file is about the whole population rather than just the Pareto-front.

5. WP_O*,P*,G*,S*,M*,C*,R*.fig

   Graph showing the fitness values of all designs during all generations of a GA run. This graph is created only when NumObj=2 or 3. It is usually used only to check that most of the individuals during a GA run are concentrated near the Pareto-front.

6. FF_O*,P*,G*,S*,M*,C*,R*.txt

   Text file that stores the history of all individuals across all generations (including fitness data, genes and ship particulars).

7. CP_O*,P*,G*,S*,M*,C*,R*.fig

   Shows the values of the constraints of the designs on the Pareto-front along with the lower and upper bounds of those constraints. The default plot would include the standard constraints L/B, L/D, B/T, Ⓜ, Fn_V, D, ss, C_B

and C_P. It is possible to generate a single plot for any of these constraints. If there are additional constraints, they will have to be plotted separately.

H.3.2. Output plots that can be generated additionally

The GA Tool can generate various types of plots, which are useful at different stages of the design process (see Appendix J). These are listed below (the name of the Matlab function to be used is given in parentheses).

1. 3D plot as 2D plus colour (Plot3dAs2dPlusColour.m)
2. Matrix of 2D plots (PlotMatrix2D.m)
3. Parallel coordinates (MultiPlot_ParallelCoords.m)
4. Star plots (StarPlotPF.m)
5. Constraints plots (PlotConstraints.m)
6. Sensitivity plots for design space exploration (Sensitivity_DesignVar.m)
7. Local slopes plots for performance space exploration - (LocalSlopes_ParetoFront.m)
8. Colour diagram - This is created in Microsoft Excel using a macro kept in the template file "ColourTableTemplate.xls"

H.4. How to run the GA Tool

The GA Tool is executed using the function "BatchRun_ExtendedRuns":

function [] = BatchRun_ExtendedRuns(NewOrExtend, NumExtendedRuns, StartingSubFolderSuffix)

"NewOrExtend" should be either 1 or 2, with 1 indicating a new GA run starting with a random population of ships, while 2 would indicate the extension of a previous GA run. In the latter case, the final population of the previous run is considered as the initial population for the second run.

"NumExtendedRuns" → the number of extended runs of the GA Tool. The results at the end of each extended run are stored in separate subfolders, such as "E0", "E1" etc.

"StartingSubFolderSuffix" → used to name the subfolders mentioned above. For example, if StartingSubFolderSuffix is defined as 4, the first subfolder created will be named "E4", and subsequent extended runs will be stored n "E5", "E6" etc.

Extended runs are useful to store intermediate results from the GA Tool. For example, a single GA run with NumGen=1000 will store the results after the 1000th generation. In contrast, 10 extended runs with NumGen=100 will store the results at the end of 100th, 200th, ..., 900th and 1000th generation.

Extended runs also useful when the Pareto-front obtained from the GA Tool has not reached convergence. In this case, the final population from the earlier run can be used as the initial population for the new GA run.

e.g.:

BatchRun_ExtendedRuns(1,6,0)

This will start a new set of GA runs. The GA will be executed 6 times; the first run will use a random initial population, and the other runs will use the final population of the previous run as the initial population. The subfolders for storing the results will be E0, E1, E2, ..., E5).

BatchRun_ExtendedRuns(2,4,6)

This will extend the results of a previous GA run. The GA will be executed 4 times. The results will be stored in subfolders "E6", "E7", "E8" and "E9".

H.5. Program flow diagrams

As mentioned in the last section, the starting function for executing the GA Tool is (usually) "BatchRun_ExtendedRuns". The flow chart for this function is shown in Figure H-2. The important function calls are expanded in additional flow charts, as indicated.

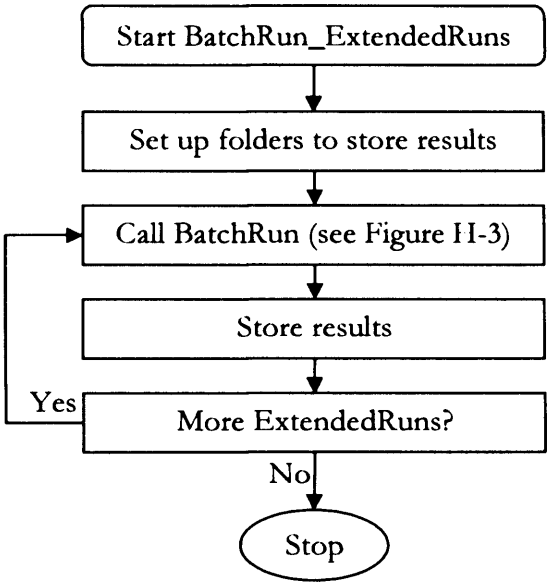

Figure H-2: Flow chart - BatchRun_ExtendedRuns

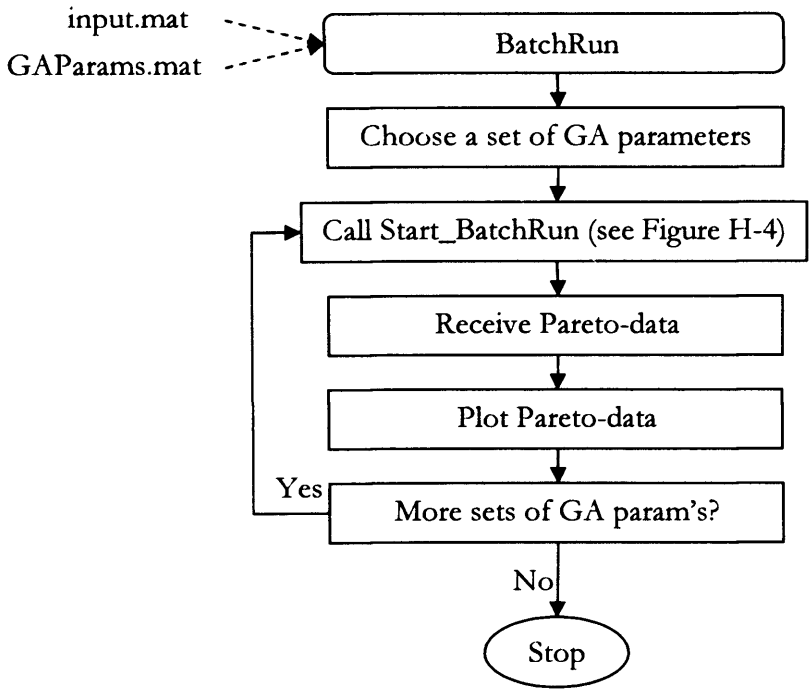

Figure H-3: Flow chart – BatchRun

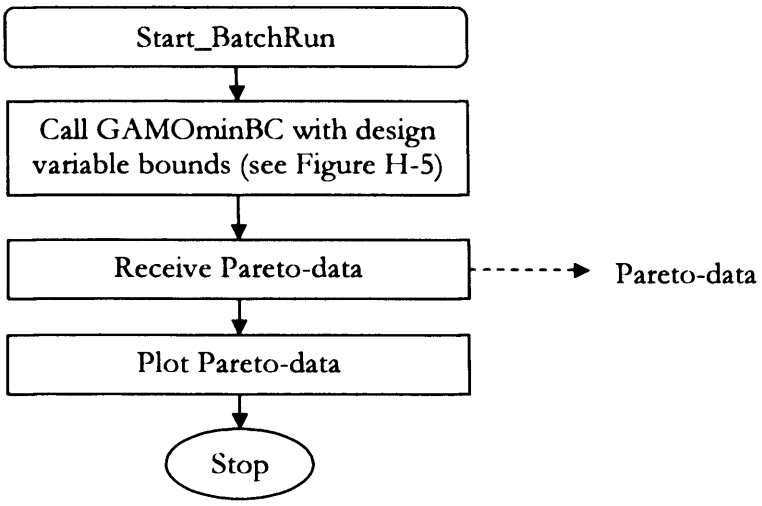

Figure H-4: Flow chart – Start_BatchRun

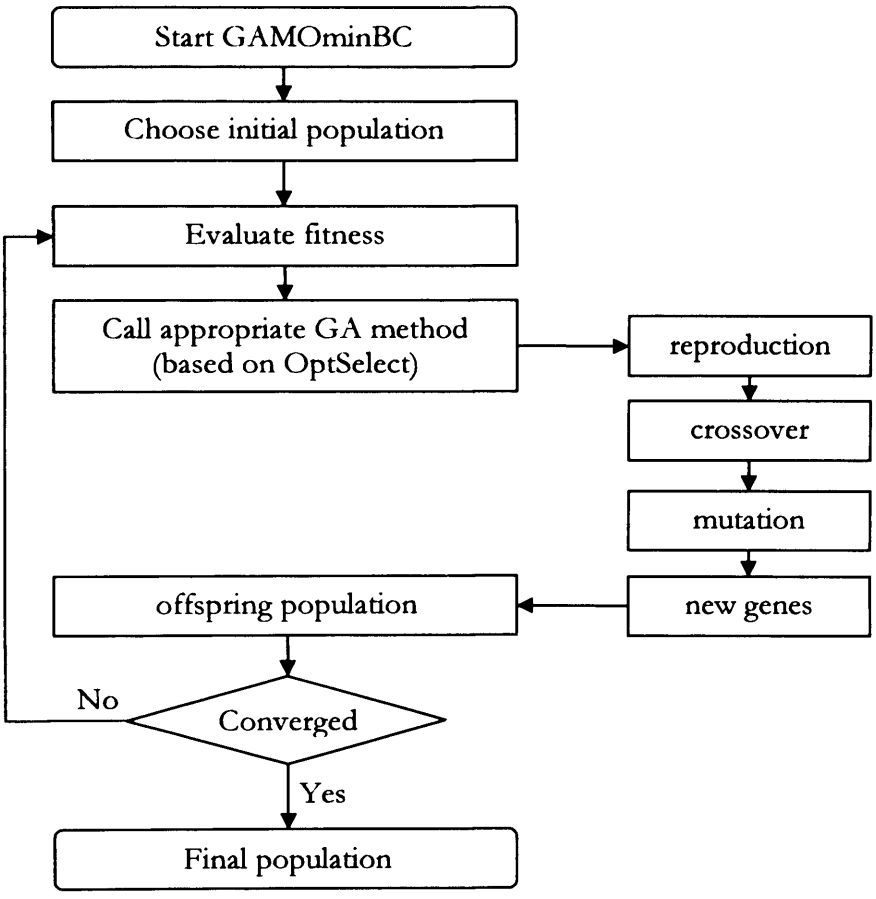

Figure H-5: Flow chart – GAMOminBC

H.6. Performance analysis modules

The performance analysis modules currently implemented in the GA Tool are somewhat simplistic in view of computational time. These are described below. The corresponding source file names in Matlab are given in parentheses.

H.6.1. Resistance calculation (CalcResistance.m)

A simple regression method based on Holtrop [29] has been implemented.

H.6.2. Weight estimate (WeightEstimate.m)

The GA Tool has implemented two sets of algorithms. The first one is based on the detailed weight groupings for warships, as given in [28]. There are seven weight groups: Hull, Personnel, Ship Systems, Main Propulsion, Electric Power, Payload, Variable. The weights of the components in each group are separately estimated, usually based on regression equations for type ships. Further details can be found in [28]. The regression equations have been implemented in the GA Tool. Where such equations are not available, appropriate assumptions are made, which are stated in the source file.

The second set of algorithms is based on a simpler calculation for merchant ships. The total weight is calculated as the sum of structural weight, outfit weight and machinery weight, apart from the weight of fuel, freshwater, personnel and payload. For structural weight, outfit weight and machinery weight, simple regression equations / graphs taken from [28] has been used. Where coefficients are needed, appropriate values for a typical frigate have been used. Weight of fuel and fresh water are estimated based on endurance requirements.

Note: All examples presented in this thesis, except those in Section 5.2, are based on the detailed warship groups.

H.6.3. Volume estimate (VolumeEstimate.m)

Similar to the weight estimate, two sets of algorithms have been implemented for volume estimate. The first one is based on the detailed warship groupings, as mentioned earlier [28].

The second one is based on a simpler formulation for merchant ships. Gross enclosed volume of the ship is estimated as the sum of the volumes for machinery, fuel, fresh water, personnel, payload and remainder. The machinery volume is estimated based on the machinery weight, as given in page 194 of [28]. The rest of the volumes are estimated with coefficients calibrated suitably to match with a typical frigate.

Note: All examples presented in this thesis, except those in Section 5.2, are based on the detailed warship groups.

H.6.4. Build cost (CalcBuildCost.m)

Similar to the case of weight and volume estimates, two sets of algorithms are implemented for cost estimate. The first one is based on the detailed warship groupings [28]. The second one, based on merchant ships, is a simpler calculation as the sum of the costs for structure, machinery and outfit [27].

Note: All examples presented in this thesis, except those in Section 5.2, are based on the detailed warship groups.

H.6.5. Bales Rank (Fitness_BalesRank.m)

This is based on Bales [30,31]. The formula used is:

$R = 8.422 + 45.104\ Cwf + 10.078\ Cwa - 378.465\ T/L + 1.273\ c/L - 23.501\ Cvpf - 15.875\ Cvpa + 12.9*(\Delta-4300)/4300$

Where:

R Bales Rank

Cwf forward waterplane area coefficient

Cwa aft waterplane area coefficient

T draught

L length (waterline)

c aft cut-up length

Cvpf forward vertical prismatic coefficient

Cvpa aft vertical prismatic coefficient

Δ displacement

Typical values for Bales Rank, as given in [31], range from 1 to 20 approximately for destroyer-type hull forms with displacement varying from 3000t to 9000t.

H.6.6. Large angle stability (StabilityUniechowski.m)

Based on Uniechowski [218] method for estimating large angle stability from parent ship data. It is assumed that the new ship is obtained from the parent ship by scaling in the X, Y and Z directions (the scale need not be the same for the three directions). Note that large angle stability has not been included in the examples demonstrated in this thesis.

H.7. Calculating fitness values – the penalty approach

For a set of design variables, the synthesis module produces a numerically balanced design in terms of weight and volume, such that the summation of the estimated weights and volumes of ship components equal the estimated displacement and gross enclosed volume respectively. Such a design may not satisfy all design constraints, such as the bounds of L/D. A design that violates one or more design constraints may be called an 'infeasible design'.

A method is necessary to feasibility of the designs in the Pareto-front. Two ways of implementing this in the GA Tool were tried before choosing one of them. These are described below.

The first method to handle infeasible designs is to evaluate each synthesised design against constraints and discard all infeasible designs. This method is simple to

implement; however, it is found to suffer from two drawbacks. Firstly, even a slight violation of a soft design constraint, such as the upper bound of L/D, would result in an otherwise good design being discarded. Besides, each design thus discarded would mean another execution of the synthesis module to generate a feasible design. This is found to cause a significant increase in computational time.

The second method is to make use of the "penalty approach", as done in [11]. In this approach, an infeasible design is not discarded: instead, its fitness values are appropriately penalised depending on the level of constraint violation. For a feasible design that violates no constraints, the fitness values are the same as the objectives under consideration. However, for an infeasible design, the fitness values are the penalised values of these objectives. For example, consider a design having UPC and -Bales Rank as objectives, their values being £150M and -10. Assume it has an L/D of 14.1 while the upper bound of L/D has been specified as 14, making it slightly infeasible. This would result in its fitness values being increased, for example, to £160M and -9. If the design were highly infeasible (say, L/D=30), it might result in a much larger penalty (say, £10000M and +999). Since genetic algorithms look for solutions with low fitness values to form the Pareto-front, highly infeasible solutions with high fitness values are unlikely to survive across many generations. This approach is found to work very well in practice. There are two main advantages for this approach. Firstly, it permits good designs to survive if the level of constraint violation is small, which ensures that superior genetic material is kept in the reproduction pool for crossover with other chromosomes. Secondly, it does not involve additional execution of the synthesis module, resulting in significant savings in computational time.

Because of its significant advantages, the penalty approach has been implemented in the current version of the GA Tool to deal with infeasible designs. A parameter 'dofinf' ("degree of infeasibility") has been defined to indicate the level of constraint violation of a design. For a feasible design that violates no constraints, dofinf=0. For infeasible designs that violate one or more constraints, dofinf>0. The higher the value of dofinf, the greater the level of constraint violation, and the greater the

penalty applied to the fitness values. For example, the dofinf for violating the upper bound of L/D is currently calculated as follows:

$$dofinf\left(\frac{L}{D}\right)_{max} = \frac{\frac{L}{D} - \left(\frac{L}{D}\right)_{max}}{\left(\frac{L}{D}\right)_{max} - \left(\frac{L}{D}\right)_{min}} \text{ ---------- (1)}$$

The values of dofinf for violating other constraints are calculated in a similar manner. The sum of all such values gives the total dofinf. This value is used to penalise the objectives in the calculation of fitness values. For example, the fitness value corresponding to the objective 'UPC' is calculated as follows:

$$fitness(UPC) = UPC \times (1 + dofinf^3) \text{ ---------- (2)}$$

This representation ensures that the fitness value of UPC will be greater than or equal to the value of the UPC itself, since dofinf is a non-negative number.

The calculation of dofinf and fitness is somewhat arbitrary, since there is no precise way of determining the optimum penalty. This is the main difficulty in the implementation of the penalty approach. If the penalty is very low, many infeasible designs may appear in the Pareto-front. Very high penalties will avoid this problem and ensure that the Pareto-front will contain only feasible designs; however, this has another difficulty: when the optimal design parameters correspond to a constraint boundary, too high a penalty for crossing that boundary will 'confuse' the GA. This is because designs on one side of the boundary will have very good fitness, while designs on the other side, though having similar design parameters, will have rather bad fitness (as a result of the large penalty). This will effectively drive the designs away from the constraint boundary, i.e., away from the optimal region. In the present case, the calculation of fitness values as done in equations (1) and (2) above has been arrived at after some trial and error to ensure that they give good convergence without too many infeasible designs on the Pareto-front.

Appendix I. Validation of the GA Tool

The GA Tool was validated in two ways. Firstly, it was used in conjunction with complex mathematical test functions selected from the literature. Secondly, it was compared with random synthesis of a number of ships. The quality of the Pareto-front generated as well as the computational time taken was examined.

I.1. Comparison for a mathematical test function

The first test function (from [217]) considered is as follows:

Minimise $f_1(x)$ and $f_2(x)$, where:

$$f_1(x) = \sum_{i=1}^{n-1} -10e^{-0.2\sqrt{x_i^2 + x_{i+1}^2}} \quad \text{---------- (1)}$$

$$f_2(x) = \sum_{i=1}^{i=n} \left(|x_i|^{0.8} + 5\sin x_i^3 \right) \quad \text{---------- (2)}$$

in the interval x_i = [-5,5] and n = 3

The expected Pareto-front, as given in Fig.6 of [217] is reproduced in Figure I-1.

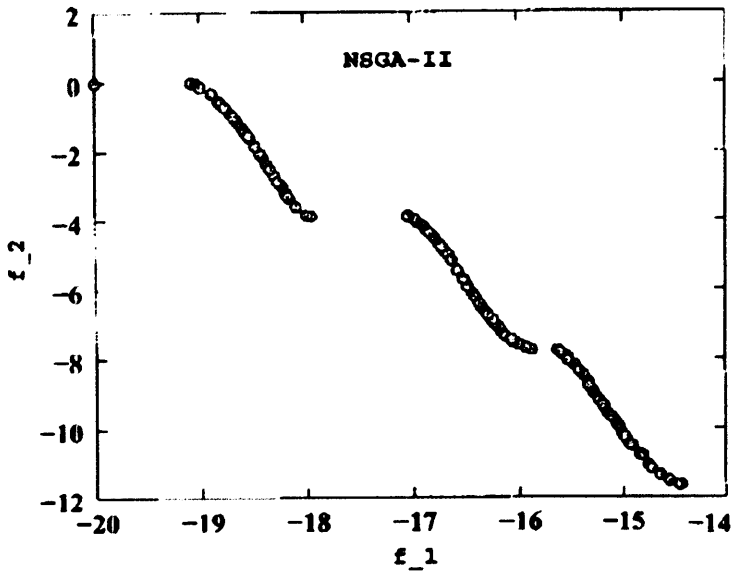

Figure I-1: Pareto-front for the test problem, as reproduced from [217]

The corresponding Pareto-front obtained from the GA Tool is shown in Figure I-2. It looks very similar to the expected Pareto-front.

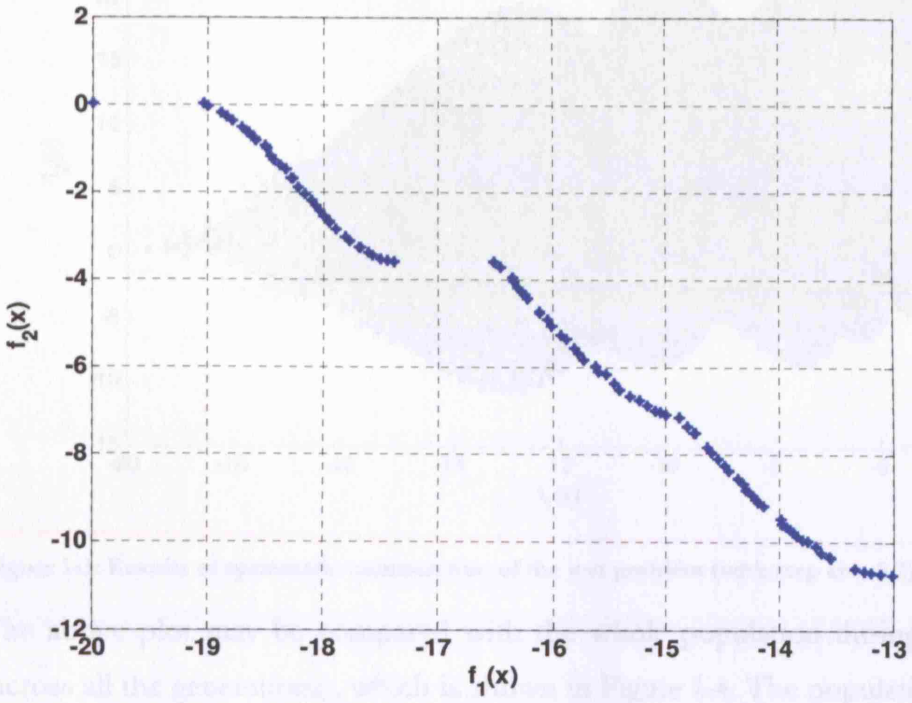

Figure I-2: Pareto-front for the test problem, as generated by the GA Tool

Now let us compare the Pareto-front obtained by the GA Tool against the results of a systematic search of the design space. This is done by calculating the values of $f_1(x)$ and $f_2(x)$ for every value of x in the interval [-5,5] at a step size of 0.2. The results are shown in Figure I-3. The plot appears very different from the Pareto-front obtained by the GA Tool. This is mainly because the systematic search produces a much larger range of $f_1(x)$ and $f_2(x)$. Most values of produced points by the systematic search are far away from the Pareto-front. In fact, there are very few designs lying close to the Pareto-front.

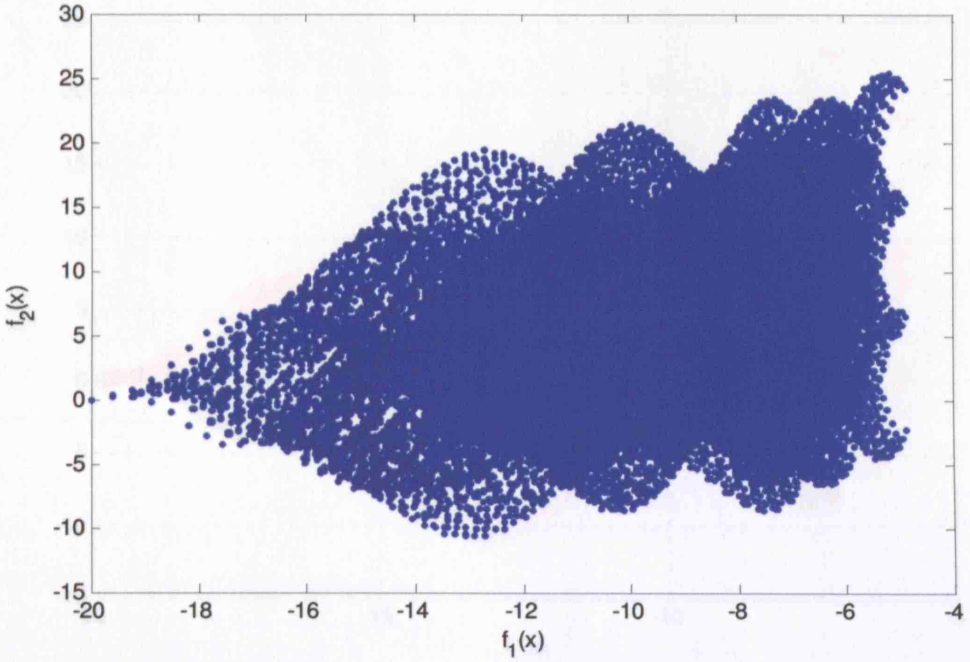

Figure I-3: Results of systematic enumeration of the test problem (with step size 0.2)

The above plot may be compared with the whole population during the GA run (across all the generations), which is shown in Figure I-4. The population during the GA run is clearly focussed near the Pareto-front region, as opposed to the very few individuals on the Pareto-front during brute force enumeration. This demonstrates the ability of the GA to concentrate on the region of the performance space that has good fitness values.

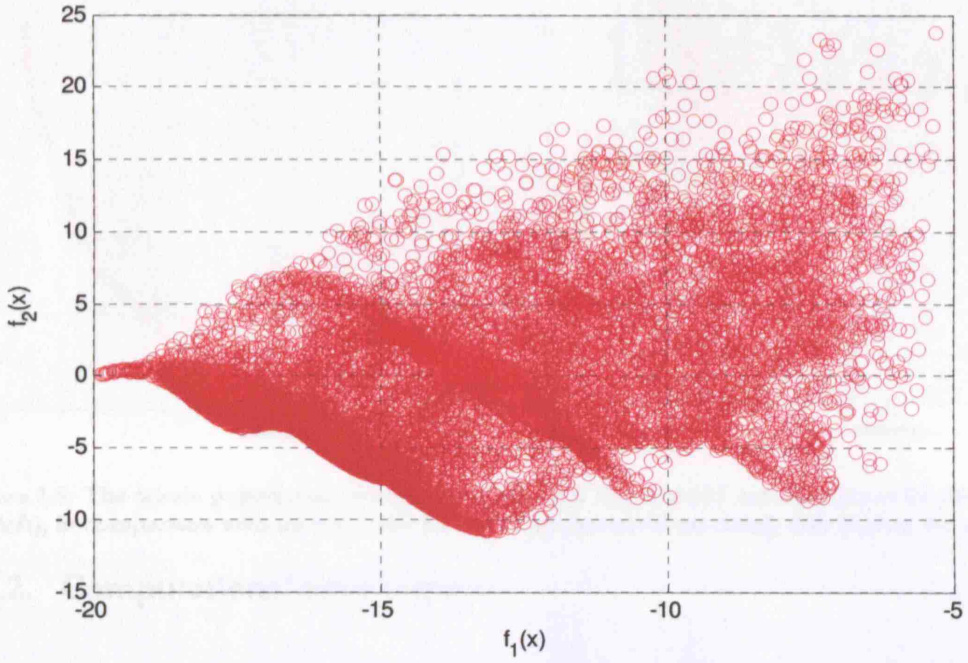

Figure I-4: Test problem - whole population during the GA run (PopSize=100, NumGen=250)

In summary, tests with special mathematical test problems demonstrated the capability of the GA Tool in effectively and efficiently forming the Pareto-front.

I.2. GA Tool vs random synthesis

The GA tool was run with various combinations of PopSize and NumGen. For each run, the total number of ships synthesised was recorded. The same number of ships were synthesised randomly. The graphical results produced from these two sets were compared with regard to the quality of the Pareto-front generated. The corresponding CPU times were also tabulated.

I.2.1. Quality of the Pareto-front

A sample plot comparing the quality of the Pareto-front between GA and random synthesis is shown in Figure I-5. The plot on the left side shows the results from the GA and the right side plot shows the results of random synthesis. Clearly, most designs from the GA lie near the Pareto-front, whereas very few designs from random synthesis are near the Pareto-front. This demonstrates the ability of the GA to quickly identify good solutions and eliminate bad solutions.

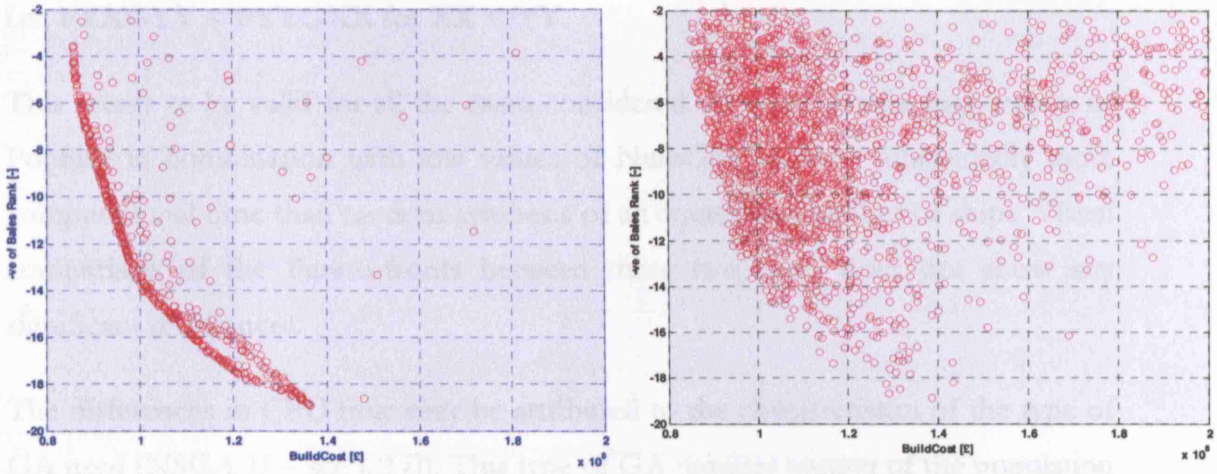

Figure I-5: The whole population during a GA Run with PopSize=50 and NumGen=50 (the plot on the left), in comparison with an equal number of ships generated randomly (the plot on the right)

I.2.2. Computational time required

Calculation of the computational time required for the GA (with various combinations of PopSize 'P' and NumGen 'G') was compared with random synthesis of an equal number of ships. The summary of average CPU Times for various P and G combinations is given below:

	G					
P	20	50	100	150	200	300
20	-	4.46	8.79	-	19.90	-
50	5.81	-	31.18	55.31	86.80	-
100	16.03	43.70	-	-	309.06	619.73
150	-	86.42	-	-	-	-
200	49.86	147.30	388.91	-	-	-
300	-	-	855.47	-	-	-

From this table, it is clear that CPU Time for PXXGYY < PYYGXX for XX < YY.

Example: XX = 50, YY = 100

PXXGYY → P50G100 → CPU Time = 31.18

PYYGXX → P100G50 → CPU Time = 43.70

→ P50G100 < P100G50

i.e., PXXGYY < PYYGXX for XX < YY

This seems to be valid for all the cases considered. In other words, high values of PopSize in combination with low values of NumGen requires substantially more computational time than random synthesis of an equivalent number of ships. Visual comparison of the Pareto-fronts between these two cases does not show any significant differences.

The differences in CPU time may be attributed to the characteristics of the type of GA used (NSGA II – see [217]). This type of GA requires sorting of the population at every generation to identify individuals with good fitness characteristics ("nondominated sorting"). The higher the PopSize, the more the time taken for nondominated sorting. Thus, lower PopSize values in conjunction with higher NumGen values may be preferred to higher PopSize values and lower NumGen.

I.2.3. Summary – GA vs random synthesis

From the comparison between the results from the GA and the RS for the same number of ships synthesised, the following conclusions can be derived:

1. The Pareto-front generated by the GA is qualitatively better. At the end of the GA process most of the designs lie on the Pareto-front, whereas in the case of RS a large percentage of the designs lie far away from the Pareto-front. However, RS is capable of generating a reasonable outline of the Pareto-front within the same time as the GA.

2. At higher PopSize values, the GA tends to take much higher CPU time than the RS (for equal number of ships synthesised). This is because of the overheads involved in nondominated sorting. Thus, for the GA Tool it is recommended that lower PopSize values be used in conjunction with higher NumGen, rather than vice versa.

Appendix J. Visualisation of the Pareto-front generated by the GA Tool

Once the Pareto-front is generated, how it is used and analysed would depend on the current application of the GA Tool. Irrespective of the application, different ways of visualising the Pareto-front will be needed. The methods implemented with the GA Tool are discussed in the following subsections.

J.1. 2D plots

These are simple 2-dimensional graphs that are useful to display the Pareto-front in the performance space when there are just two objectives to consider. A sample plot is shown in Figure J-1.

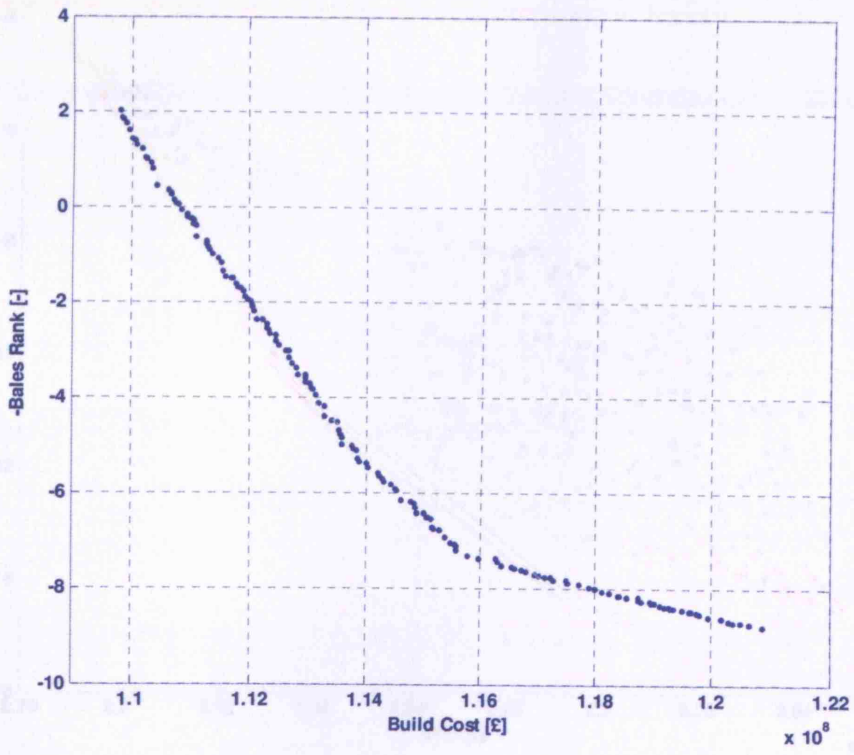

Figure J-1: A sample 2D plot of the Pareto-front

J.2. 3D data as 2D plots plus colour variation

When there are three objectives, it is possible to plot them along three axes; however, 3D plots are not easy to interpret. They are somewhat useful on the

computer screen, where the user can rotate the plot interactively, thus examining different views; however, when plotted on paper, they become rather difficult to comprehend. One way to overcome this difficulty is to plot two of the three objectives as a 2D plot, and show the value of the third objective qualitatively by varying the colour of each data point.

To make this clear, consider the plot given in Figure J-2. The two axes represent two of the three objectives (UPC and -Bales Rank). The third objective (P_s in this case) is shown as varying colours of the data points – blue dots represent low values and red dots correspond to high values. This helps in understanding the trade-off among the three objectives: for example, at a given UPC, there are a number of solutions with varying -Bales Rank, among which the ones with low -Bales Rank have rather high P_s and vice versa.

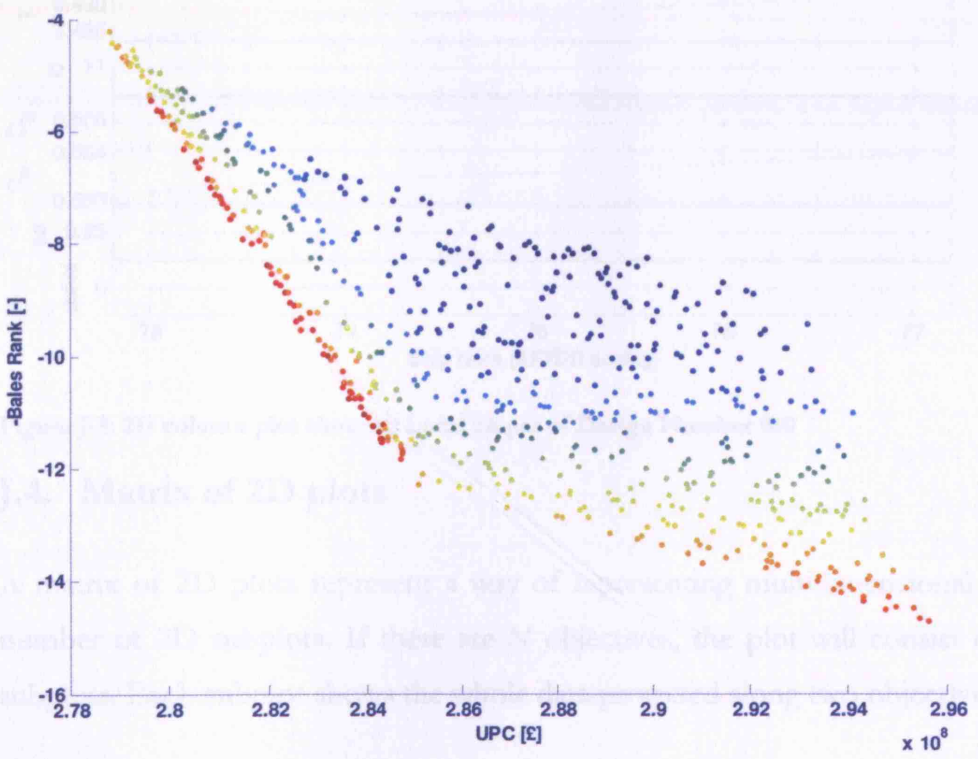

Figure J-2: Three objectives shown as a 2D plot with the third objective represented by colour variations

J.3. Column of 2D plots

These consist of many 2D-plots sharing the same x-axis. The plot shows the design parameters and performance characteristics of a few designs of interest. The chosen

designs need not be related in any way; however, in practice, they are meant to be adjacent designs, either in design space (while exploring the design space) or in performance space (while exploring the performance space), as discussed in Section 5.1.3.

A sample plot is shown in Figure J-3. It shows five designs (numbered 73 to 77 in the x-axis). The y-axis shows the performance characteristics (the top two subplots) and the design parameters (the remaining subplots) for these five designs.

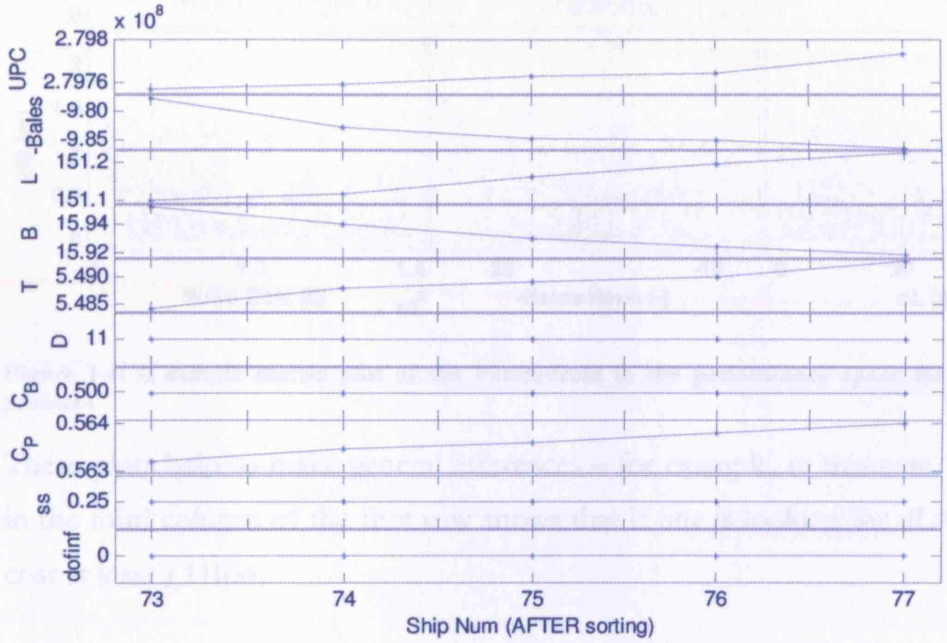

Figure J-3: 2D column plot showing Local Slopes of Design Number S60

J.4. Matrix of 2D plots

A matrix of 2D plots represent a way of representing multidimensional data as a number of 2D subplots. If there are N objectives, the plot will consist of N x N subplots. Each subplot shows the whole data projected along two objectives.

The matrix of 2D plots is useful to display the Pareto-front in the performance space when there are more than two objectives to consider. They can also be used to display the design space. A sample plot showing the performance space in a 4-objective problem is shown in Figure J-4.

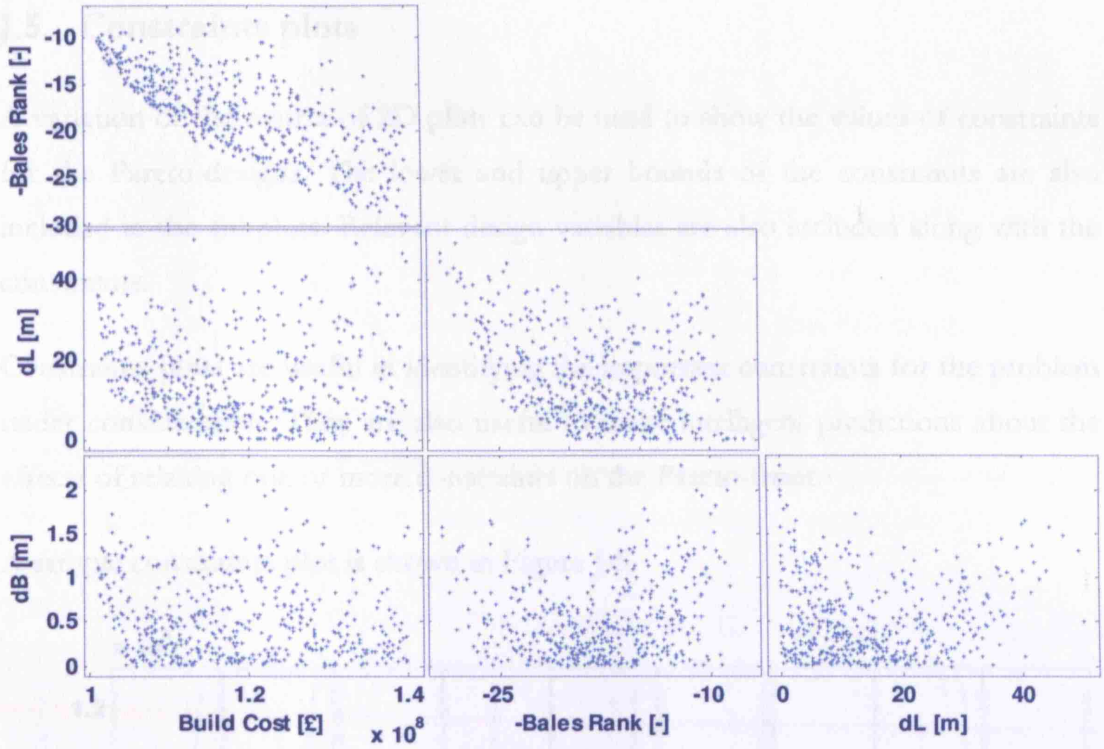

Figure J-4: A sample matrix plot of the Pareto-front in the performance space for a 4-objective problem

These plots help to make general inferences – for example, in this case, the subplot in the third column of the first row shows that if one is looking for dL≈0, it would cost at least £110M.

When a point is selected in one subplot, the corresponding design should get highlighted in the other subplots. This would help to examine how good a design is with respect to all the objectives. However, this functionality is not currently available.

J.5. Constraints plots

A variation of the matrix of 2D plots can be used to show the values of constraints for the Pareto-designs. The lower and upper bounds of the constraints are also included in the subplots. Relevant design variables are also included along with the constraints.

Constraints plots are useful in identifying the important constraints for the problem under consideration. They are also useful to make intelligent predictions about the effects of relaxing one or more constraints on the Pareto-front.

A sample constraints plot is shown in Figure J-5.

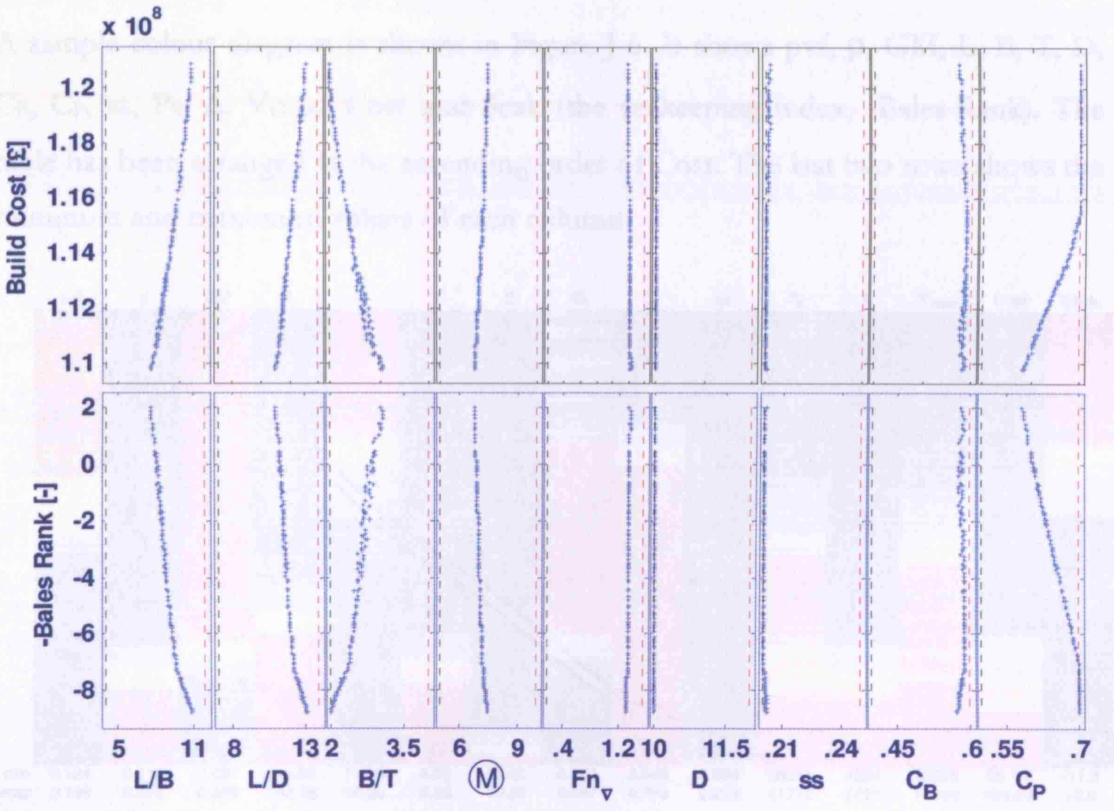

Figure J-5: A sample constraints plot with two objectives

From this plot, it is seen that the lower bounds of D and ss are important throughout the Pareto-front; relaxing them should improve the quality of the whole Pareto-front. In comparison, Ⓜ (circular M) stays well within its bounds, indicating that relaxing them may not affect the Pareto-front in any way.

J.6. Colour diagrams

Colour diagrams show design parameters and objectives as a table of colours. Each column of the colour diagram represents one design parameter or objective, and each row corresponds to one ship. Different colours represent different bands of values of the parameter. The lowest values are shown in blue and the highest values in red. Intermediate values are given appropriate colours within this range.

Colour diagrams are useful in spotting the trends between design variables and objectives, and in identifying any designs that have very different design parameters from the surrounding designs. This helps in short-listing designs from the Pareto-front for further analysis (see Appendix K).

A sample colour diagram is shown in Figure J-6. It shows pvf, ρ, GM, L, B, T, D, C_B, C_P, ss, P_S, Δ, ∇_{Gross}, Cost and Seak (the seakeeping index, -Bales Rank). The table has been arranged in the ascending order of Cost. The last two rows shows the minimum and maximum values of each column.

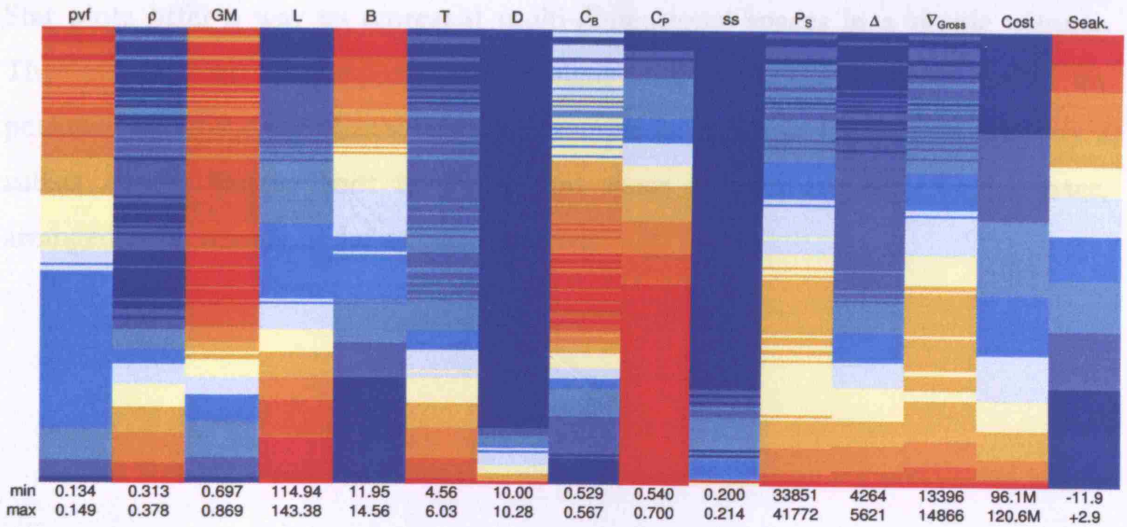

Figure J-6: Colour diagram showing trends of design parameters and performance characteristics

Many trends can be inferred from the plot. For example, by examining the last four columns (Δ, ∇_{Gross}, Cost and Seak), it is clear that as seakeeping decreases (i.e., improves), Δ, ∇_{Gross} and Cost increase.

J.7. Star plots

Star plots represent relevant design or performance parameters of one ship in a single shape such as the one shown in Figure J-7. Each "spoke" of the plot represents one variable (design or performance parameter). The length of the spoke is proportional to the value of the parameter: the longer a spoke the larger the parameter it represents.

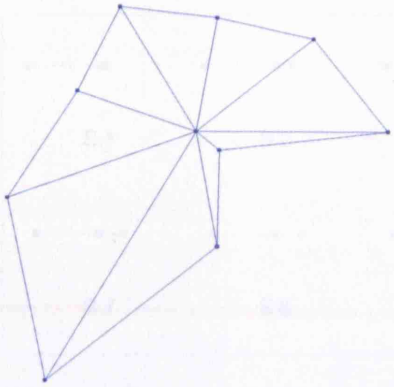

Figure J-7: A sample generic star plot

Star plots offer a way to represent multi-dimensional spaces in a simple manner. They can be used to compare a few designs both in the design space and in the performance space simultaneously. An example is shown in Figure J-8. It shows a subset of the Pareto-front in the design space as well as performance space, arranged in increasing order of one objective.

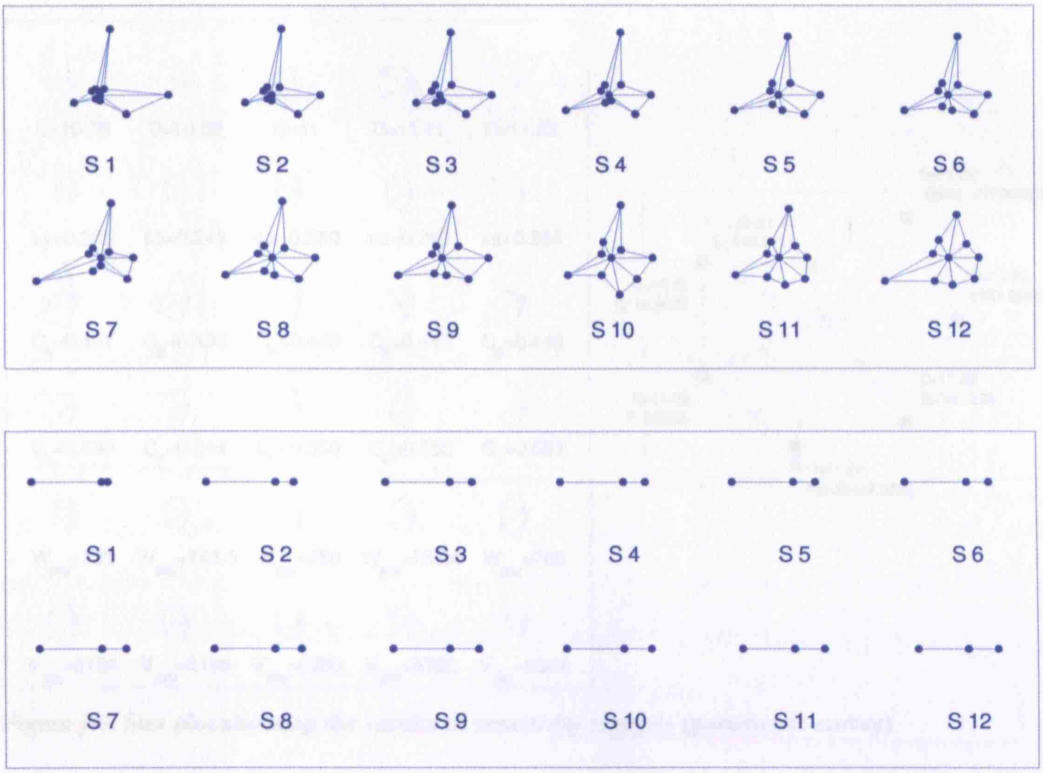

Figure J-8: Design parameters and performance characteristics presented as star plots

One use of star plots is to identify any designs that have design parameters significantly different from nearby designs in the performance space. This helps while short-listing designs for further analysis (Section 4.3.2 and Appendix K) and during design space exploration (Section 4.3.3).

The second use of star plots is while exploring the design space (sensitivity analysis). Here it is used to display how changes in one design variable affect other design parameters and objectives. An example for this is shown in Figure J-9. Here, each row corresponds to the variations in one design variable. A single 'star' is shown separately to indicate which parameter each spoke represents. For instance, the first row corresponds to the design variable D, and shows how changes in D would affect design parameters such as L, B, T, P_s, dofinf (a parameter used by genetic algorithms – see Appendix H.7), UPC, and the seakeeping measure of merit (-Bales Rank). Similarly, the remaining rows represent other design variables.

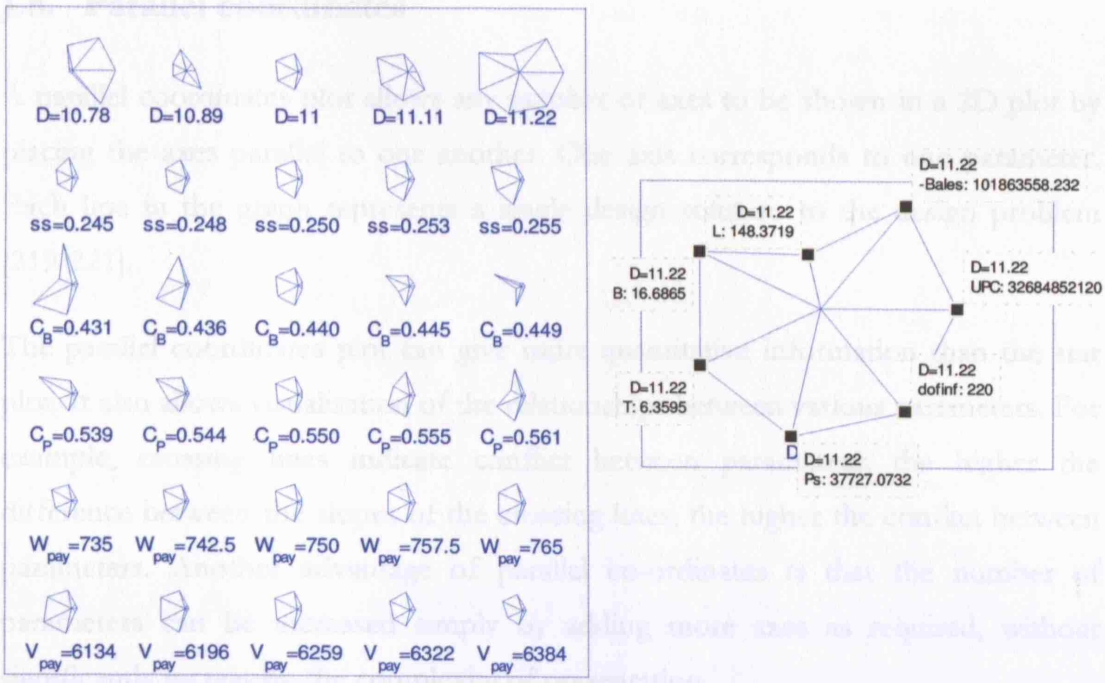

Figure J-9: Star plot showing the results of sensitivity analysis (parametric survey)

The third use of star plots is to compare the performance characteristics of one or more designs with the performance requirements. This would be useful in visually selecting designs that closely match the performance requirements. For example, Figure J-10 shows the actual performance in blue and the required performance in red; it is easy to spot the designs that most closely match the required performance.

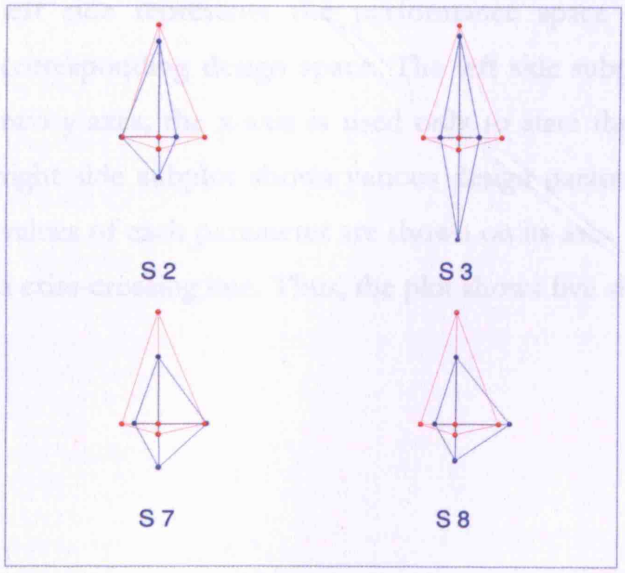

Figure J-10: Star plots showing the required performance (in red) superimposed on the actual performance (in blue)

J.8. Parallel coordinates

A parallel coordinates plot allows any number of axes to be shown in a 2D plot by placing the axes parallel to one another. One axis corresponds to one parameter. Each line in the graph represents a single design solution to the design problem [219-221].

The parallel coordinates plot can give more quantitative information than the star plot. It also allows visualisation of the relationships between various parameters. For example, crossing lines indicate conflict between parameters; the higher the difference between the slopes of the crossing lines, the higher the conflict between parameters. Another advantage of parallel co-ordinates is that the number of parameters can be increased simply by adding more axes as required, without significantly increasing the complexity of presentation.

However, in practice, these plots might appear rather cluttered with too many lines crossing one another, especially when there are many ships to compare. Moreover, multiple ordering of axes may be necessary to spot different trends among the parameters.

A sample parallel coordinates plot is shown in Figure J-11. Here, the subplot on the left side represents the performance space and the right side represents the corresponding design space. The left side subplot shows two objectives along the two y-axes; the x-axis is used only to state the names of the two objectives. The right side subplot shows various design parameters. The minimum and maximum values of each parameter are shown on its axis. Each ship is shown in one colour as a criss-crossing line. Thus, the plot shows five ships.

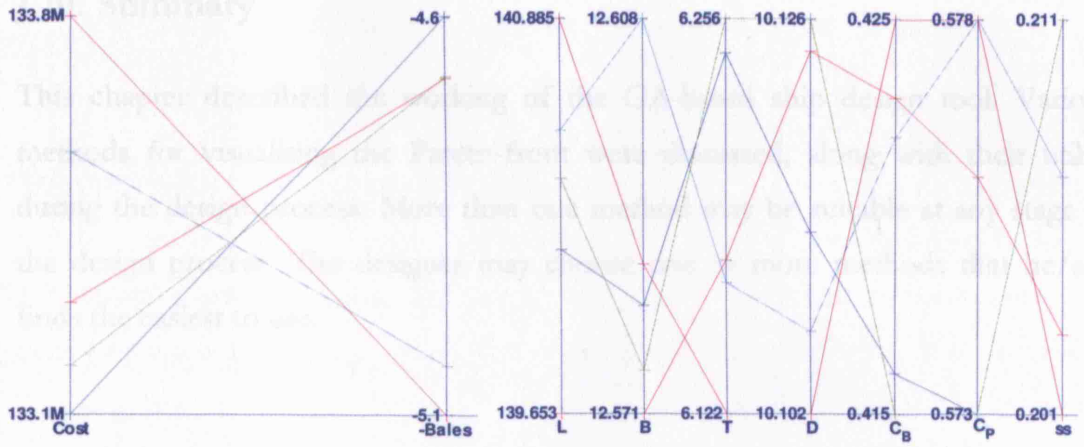

Figure J-11: Parallel plots showing the results of sensitivity analysis

From the subplot on the left, the conflicting nature of the two objectives is clear. The plot on the right showing the design parameters appears rather cluttered.

J.9. Uses for various types of plots

Various types of plots are useful in various stages of analysing the Pareto-front. Table J-1 summarises the uses of each plot and gives references to sections where more information can be found.

Table J-1: Uses of various types of plots for various stages of Pareto-front analysis

	2D plots	3D data as 2D plot plus colour	Column of 2D plots	Matrix of 2D plots	Constr's plots	Colour diagrams	Star plots	Parallel coord's	Reference (Section)
Visualising the whole design space				√	√	√		√	
Visualising the whole performance space	√	√		√		√		√	
Short-listing designs for further analysis	√	√		√	√	√	√		4.3.2
Design space exploration for each short-listed design			√				√	√	4.3.3
Performance space exploration for each short-listed design			√				√	√	4.3.4

J.10. Summary

This chapter described the working of the GA-based ship design tool. Various methods for visualising the Pareto-front were discussed, along with their utility during the design process. More than one method may be suitable at any stage of the design process. The designer may choose one or more methods that he/she finds the easiest to use.

Appendix K. How to short-list a few designs from the Pareto-front

The Pareto-front may contain a hundreds of designs, from which a subset needs to be chosen for detailed design and analysis. This may be done by comparing the performance characteristics of each design on the Pareto-front with the performance constraints to select the most suitable ones. However, this process of deciding how many designs are to be short-listed and choosing them from the Pareto-front may not always be straightforward. It is rather subjective and dependent on the designer's judgement; however, different ways to visualise and examine the Pareto-front can help the designer in this process.

K.1. Selection based on 2D-plots of the Pareto-front

Consider a design problem with two objectives – minimisation of build cost and minimisation of acceleration at the bridge. As an example, suppose there is a customer constraint on build cost (say, max build cost = £50m), and another one on absolute vertical acceleration at the bridge (max acceleration = 0.4g). Application of these constraints would cut off the tails of the Pareto-front (in the performance space), as shown in Figure K-1.

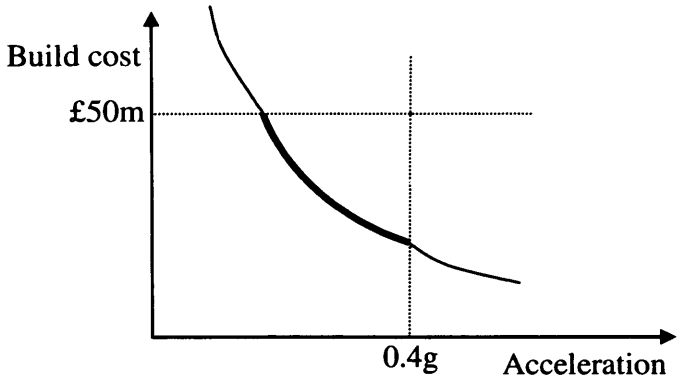

Figure K-1: Example Pareto-front highlighting the feasible region that satisfies performance constraints

The thick curve represents the designs that satisfy the performance constraints. Ideally, all these designs need to be presented to the customer; however, depending on the number of such designs, it may not be practical to analyse all of them and

present the results to the customer. Therefore, some means of filtering the designs is necessary. In this example, a few designs evenly spaced along the Pareto-front may be chosen arbitrarily by the designer.

Consider another scenario where there are no designs that simultaneously satisfy both the performance constraints. For example, suppose the constraint on acceleration was 0.2g (Figure K-2):

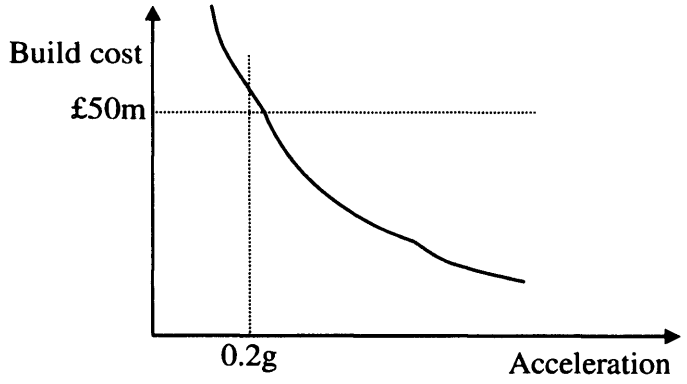

Figure K-2: Example Pareto-front – no feasible region that satisfies performance constraints

In this case, the customer's performance constraints are unrealistic, and the designer will have to select some compromise designs. One way to do this is to relax the performance constraints (rather arbitrarily!) and then look for designs that satisfy these relaxed constraints. For example, with relaxed constraints, the above case may appear as shown in Figure K-3.

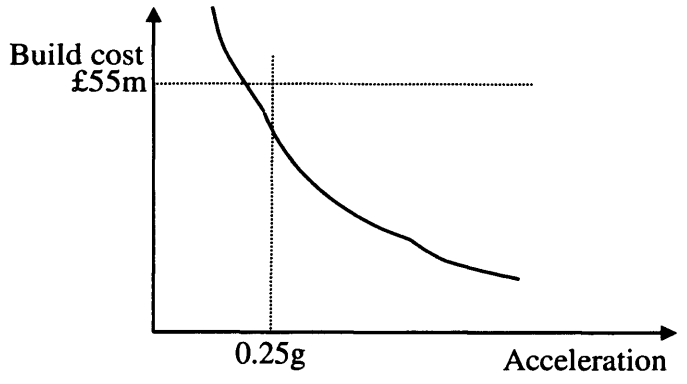

Figure K-3: Example Pareto-front – relaxing performance constraints to get feasible designs

Now there are a few designs that satisfy the relaxed performance constraints, and they can be included in the short-list for further analysis.

K.2. Selection based on star plots of the Pareto-front

When there are more than two objectives, the designer will not be able to visually select designs equally spaced on the Pareto-front. In this case, all the results can be simultaneously viewed as star-plots (in the performance space); however, selection of suitable designs using star-plots (by examining EACH design on the Pareto-front) is more difficult and time-consuming compared to the two-objective case (where ALL designs on the Pareto-front can be simultaneously compared with the performance constraints in one 2D-plot). To reduce this difficulty, the designer can filter the Pareto-front with appropriate lower and/or upper bounds for each objective (based on the performance constraints) and view the filtered designs in the form of star-plots. This is shown in Figure K-4. The filtering can be varied to obtain a reasonable number of designs.

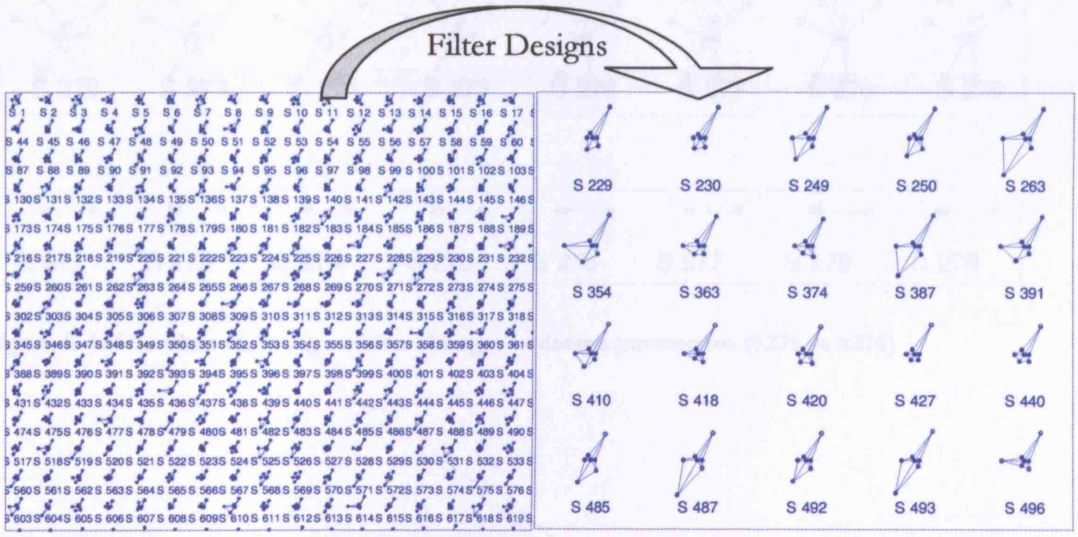

Figure K-4: Filtering the multi-objective performance space based on performance constraints

Each filtered design can then be compared with the performance constraints, as shown in Figure K-5, and the most suitable ones may be included in the short-list for further analysis.

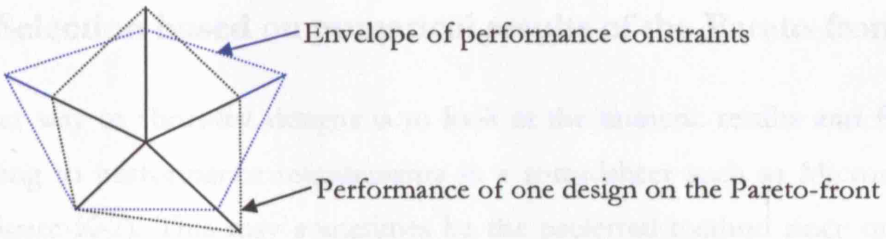

Figure K-5: Star plot showing actual performance vs required performance

Star plots can also help in identifying any designs that have design parameters significantly different from nearby designs in the performance space. For example, see Figure K-6. It is clear that designs S254 to S275 have similar design parameters, which change suddenly at S276. In other words, designs S275 and S276 are widely separated in the design space, though they are close together in the performance space. Both of them may then be included in the short-list for further analysis.

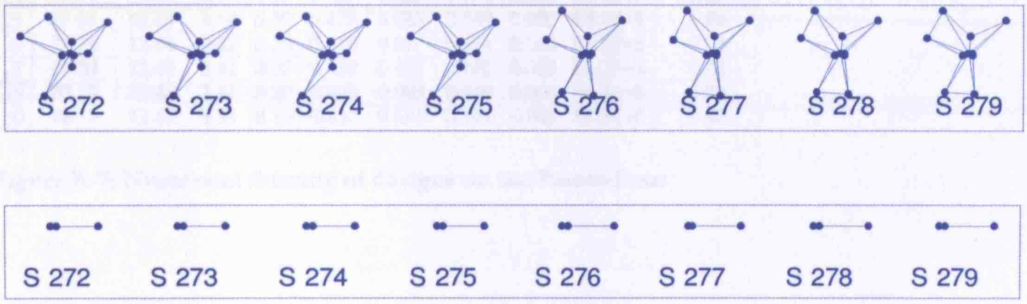

Figure K-6: Star plots showing sudden changes in design parameters (S275 vs S276)

K.3. Selection based on numerical results of the Pareto-front

Another way to short-list designs is to look at the numeric results and filter them according to performance requirements in a spreadsheet such as Microsoft Excel (see Figure K-7). This may sometimes be the preferred method since quantitative information on each objective is directly available. Besides, the design space can also be examined simultaneously with the performance space.

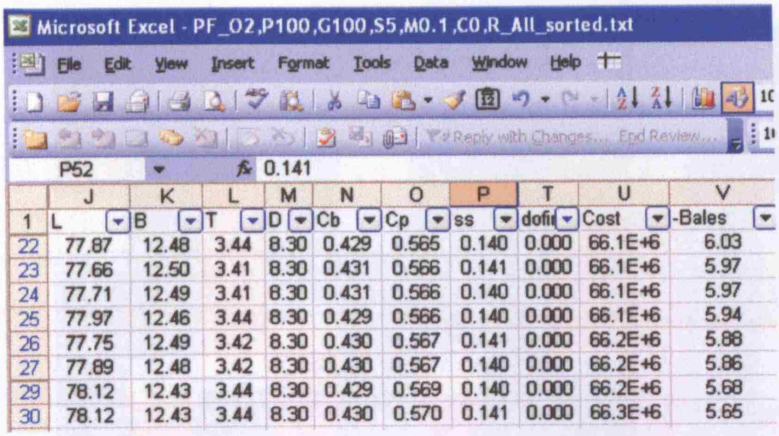

	J	K	L	M	N	O	P	T	U	V
1	L	B	T	D	Cb	Cp	ss	dofi	Cost	-Bales
22	77.87	12.48	3.44	8.30	0.429	0.565	0.140	0.000	66.1E+6	6.03
23	77.66	12.50	3.41	8.30	0.431	0.566	0.141	0.000	66.1E+6	5.97
24	77.71	12.49	3.41	8.30	0.431	0.566	0.140	0.000	66.1E+6	5.97
25	77.97	12.46	3.44	8.30	0.429	0.566	0.140	0.000	66.1E+6	5.94
26	77.75	12.49	3.42	8.30	0.430	0.567	0.141	0.000	66.2E+6	5.88
27	77.89	12.48	3.42	8.30	0.430	0.567	0.140	0.000	66.2E+6	5.86
29	78.12	12.43	3.44	8.30	0.429	0.569	0.140	0.000	66.2E+6	5.68
30	78.12	12.43	3.44	8.30	0.430	0.570	0.141	0.000	66.3E+6	5.65

Figure K-7: Numerical filtering of designs on the Pareto-front

K.4. Selection based on colour diagram

A colour diagram can be a useful alternative in visualising the Pareto-front. Its main advantage is that it can qualitatively display the trends of design parameters and objectives simultaneously. It is useful to spot any 'odd' designs, i.e., those with design parameters very different from nearby designs. A sample colour plot is shown in Figure K-8.

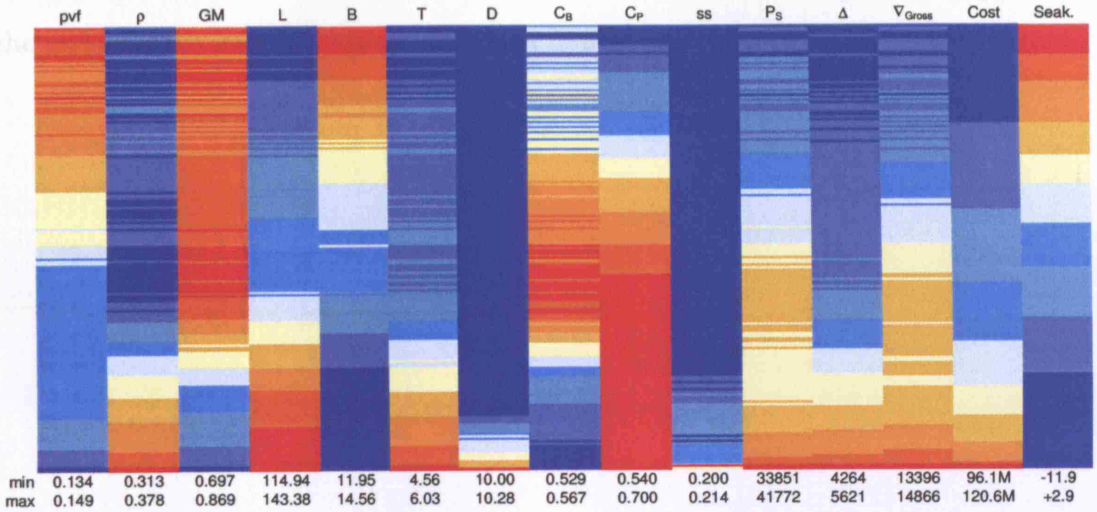

Figure K-8: Colour diagram representation of the Pareto-front

From this colour diagram, looking at the last four columns, it is clear that ships with good seakeeping values (blue colour) have high cost, displacement and enclosed volume (red colour).

Besides the variation of colours, one also needs to look at the minimum and maximum values of a parameter before interpreting the colour diagram. For example, suppose the GA Tool was run with the lower and upper bounds of D specified as [10.0,12.0]. Further, suppose that all designs on the Pareto-front have values of D near the lower bound, say in the range [10.00, 10.01]. This means all the designs on the Pareto-front have virtually the same D value; however, the colour plot would represent 10.00 in blue colour and 10.01 in red colour, giving a false impression of the trends of D against other design parameters and objectives.

The limitation of colour diagrams is that it becomes difficult to spot any odd designs when there are more than two objectives. This is because in the case of two objectives, it is possible to visually sort the data with respect to one objective, which automatically ensures that the data would be in the reverse order for the second objective. However, when there are more than two objectives, this sorting is not so obvious, and the resulting trends may not be very clear. One way to get around this problem is to filter the objectives appropriately so that the remaining Pareto data effectively becomes a 2D Pareto-front. Different sets of filtering can be applied to the same Pareto data to examine different combinations of two objectives.

K.5. Selection based on constraints plots

The constraints plot may sometimes be used for guidance while short-listing designs. For example, consider the constraints plot shown in Figure K-9. Suppose the designer is looking for a design not close to D=11m. Then, from the constraints plot, it can be seen that the better seakeeping designs will all have to be discarded because their D values are close to 12m. The designer will have to choose a lower cost design, with not-so-good seakeeping.

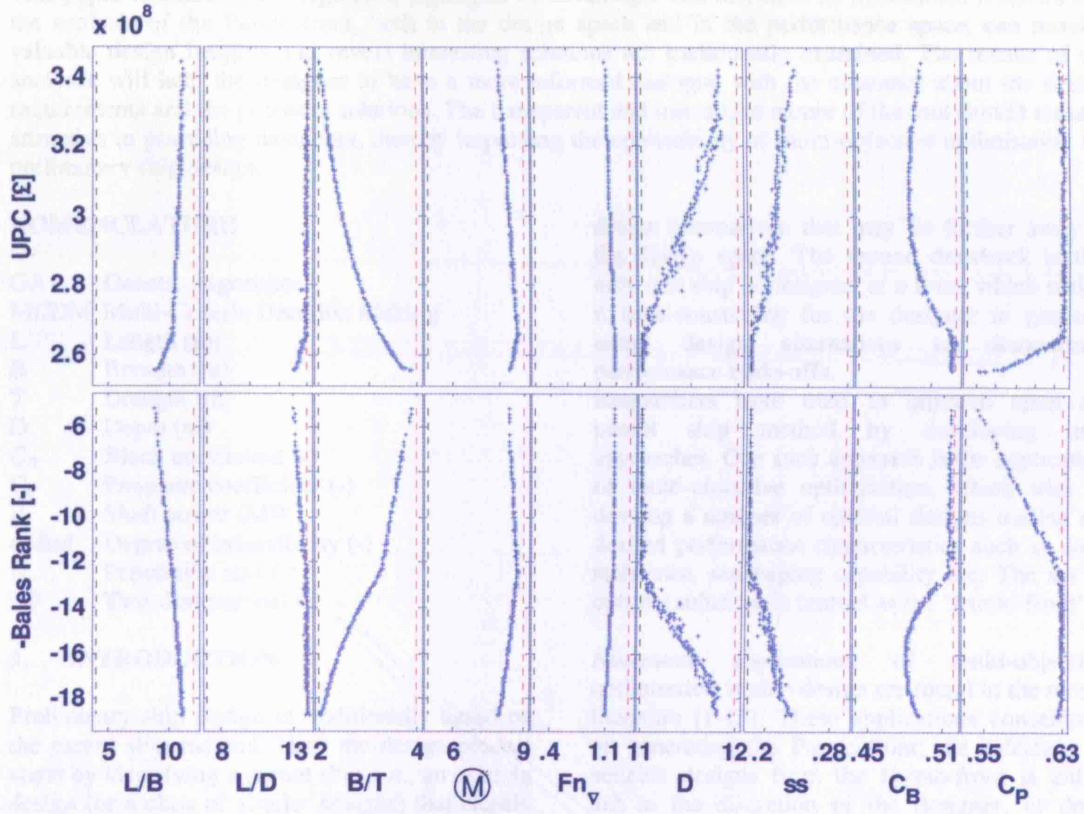

Figure K-9: A sample constraints plot for a Pareto-front

K.6. Conclusion

To conclude, filtering the Pareto-front to short-list a few designs for further analysis is not a straightforward process. Appropriate numeric / graphical representation of results and good judgement by the designer are equally important.